Cyclic di-AMP homeostasis and osmoregulation in *Listeria monocytogenes*

Dissertation

for the award of the degree

„Doctor rerum naturalium“ (Dr. rer. nat.)

of the Georg-August-Universität Göttingen

within the doctoral program „Microbiology and Biochemistry “

of the Georg-August University School of Science (GAUSS)

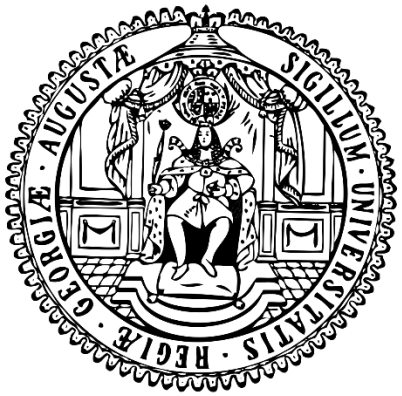

submitted by

Johannes Gibhardt

from Kassel

Göttingen, 2019

Examination board

Thesis advisory committee

apl. Prof. Dr. Fabian M. Commichau

Institute of Microbiology and Genetics; Department of General Microbiology

Prof. Dr. Jörg Stülke

Institute of Microbiology and Genetics; Department of General Microbiology

Prof. Dr. Carsten Lüder

University Medical Center Göttingen; Department of Medical Microbiology

Additional members of the examination board

Referee:

Prof. Dr. Stefanie Pöggeler

Institute of Microbiology and Genetics; Department of Genetics of Eukaryotic Microorganisms

Co-referee:

Prof. Dr. Henning Urlaub

Max-Planck-Institute for Biophysical Chemistry; Bioanalytical Mass Spectrometry Group

2nd Co-referee:

Prof. Dr. Rolf Daniel

Institute of Microbiology and Genetics; Department of Genomic and Applied Microbiology

Date of oral examination: 2nd of April 2019

Statement of authorship

I hereby declare that the doctoral thesis entitled **"**Cyclic di-AMP homeostasis and osmoregulation in *Listeria monocytogenes***"** has been written independently and with no other sources and aids than quoted.

Johannes Gibhardt Göttingen, the 15th of February 2019

Danksagung

Zu aller erst möchte ich mich bei Dir bedanken, Fabian. Danke für inzwischen gute 7 Jahre der Unterstützung, dem Anhören meiner, oft um drei Ecken gedachten, Ideen und all dem, was ich in der Zeit von dir lernen durfte! Danke auch für den ein oder anderen unterhaltsamen Kneipenabend, mit dem doch häufig vorgekommenen „last call“ und allgemein der äußerst exzellenten Arbeitsatmosphäre in der HIF. Als nächstes möchte ich mich bei Jörg bedanken. Danke auch Dir für die Unterstützung in all den Jahren, den zahlreichen Tipps und auch den kritischen Fragen und Vorschlägen. Vielen Dank an dieser Stelle auch an euch beide für die Möglichkeit nicht nur meine Zeit als Doktorand, sondern bereits meine Zeit im Bachelor und Masterstudium in dieser außergewöhnlichen Abteilung zu verbringen! Ich möchte mich auch bei Dir, Carsten, bedanken, dass Du Teil meines Thesis Committee warst und dir die Zeit genommen hast meinen Fortschritt zu begutachten und mich zu beraten. An dieser Stelle möchte ich mich auch bei Stefanie Pöggeler, Henning Urlaub und Rolf Daniel für die Mitwirkung in meinem Prüfungskomitee bedanken.

Weiterhin möchte ich mich bei allen Kooperationspartnern bedanken die an den Projekten mitgewirkt haben. Allen voran Sven, Samuel, Jana, Alex, Anna-Lena, Annette, Vincent T. Lee, Volkhard Kaever, Uwe Völker und dem SPP1879 (hier vor allen Sebastian und Gerd für die unterhaltsamen Abende bei den Konferenzen).

Nun zu euch liebe AGS und AGC: Ich würde gerne zu jedem etwas schreiben, aber dies würde den Rahmen der Danksagung sprengen. Danke für die unglaublich geile Zeit! Wenn ich an meine Zeit als Bachelor, Master und anfänglicher PhD Student zurück denke muss ich sicherlich den „alten Hasen“ Katrin, Steffi, Joni, Miriam, Dodo, Chris, den Jans, Daniel, Lorena, Nora, Ingrid, Raphael und Bingyao für alles danken! An dieser Stelle darf natürlich auch Christina, Sabine, Silvia, Julia und Andrea nicht vergessen werden. Ohne euch würde mit Sicherheit nicht viel in der Abteilung passieren. Vor allem der hilfreiche Input von Christina und Sabine waren eine große Hilfe, sowie die angedrohten „Peitschenhiebe“ von Silvia ;-). Natürlich darf man auch die „jungen Küken“, vor allem Larissa, Martin B&W, Neil, Björn, Patrick und Mengyi nicht vergessen. Nicht nur ihr habt, hoffentlich, etwas von mir gelernt, sondern ich auch von euch und ihr alle habt auf unterschiedliche Art zu dieser Arbeit beigetragen und auch dafür gesorgt, dass man immer wieder gerne zur Arbeit gekommen ist! Ach Leute, wir hatten schon eine überragende Zeit! Wenn ich nur an den ein oder anderen „Pizza & Fußballabend“ zurückdenke, der traditionell aus dem Ruder gelaufen ist oder manch böses Erwachen, dann vermisse ich die Zeit schon jetzt! Ich werde euch alle vermissen oder tue dies bereits. Danke für alles!

Anika und Cedric, wir haben damals, vor bereits sieben Jahren, zusammen unsere Bachelorarbeit angefangen. Später kam dann die Master und nun schließlich die Doktorarbeit… wer hätte das gedacht? Danke euch für die überragende Zeit! Ich bin sicher wir bringen das Ganze zu einem erinnerungswürdigen Abschluss!

Natürlich möchte ich auch meinen ganzen Studenten danken, denen ich die Ehre hatte in den Jahren (hoffentlich) das ein oder andere beizubringen. Danke Gregor, Ole, Julian, Jasmin, Birthe, Lisa, Veronika, Sandra, Judith, Tariq und Lars! Ich habe auch etwas an Erfahrung von euch mitgenommen. Vor allem euch, Gregor, Ole und Julian möchte ich für die sehr unterhaltsame Zeit in- und außerhalb des Labors danken. Ob Kneipenabend, dass ein oder andere Bier in der Abteilung oder der spontane Alpenmax besuch nachts um halb 2, ich hatte viel Spaß euch „zu betreuen“ ;-).

Zu guter Letzt möchte ich den Menschen danken die mir am meisten am Herzen liegen, meinen Freunden und meiner Familie. Worte können nicht beschreiben, was ihr mir bedeutet!

Mädels und Jungs, ich danke euch für die geilen Jahre, sei es die inzwischen weit zurückliegende Schulabschlusszeit, die Zeit als frisch gebackener Student oder den ein oder anderen Urlaub. All diese Erinnerungen sind nur besonders, weil wir sie zusammen erlebt haben! An dieser Stelle einen besonderen Dank auch an all die Leute mit denen ich das Vergnügen hatte das ein oder andere Abenteuer an fremden Orten zu erleben oder Sie dort kennen zu lernen!

Wie sagte sogar Erich Kästner? „Toren bereisen in fremden Ländern die Museen, Weise gehen in die Tavernen“.

Seien es Kurztrips nach Hamburg, Frankfurt, Leipzig oder Städtetrips nach Barcelona (mit nassen Füßen), Madrid, Prag (noch nie so viel Spaß beim „Fahrradfahren“ gehabt), Mailand (immer diese Stadiontouren…), Turin, Zürich (die spinnen doch, was die Bierpreise angeht…), St. Petersburg (verrückte Iren und die weiße Nächte, прекрасно!), Moskau (Old School Pub und очень вкусный хачапури!), Susdal (dieser Met (медовуха) und dieser Ausblick, unbeschreiblich!), New York, Boston, Miami (27°C im November und ein kühles IPA, was will man mehr?), Key West (ein Wort, paradiesisch!), Orlando, Brügge, Brüssel (und die tausend Biere), London (und die verrückte Dart WM), und, und, und… Wir hatten eine geile Zeit und ich freue mich schon auf das nächste Abenteuer ;-). Danke Katha und Kaddah, Johannes und David, Mike, Hoffi, Anja, Annika, Chris, Marcel, Nils, Stephan, geborener Stelmecke ;-), Martin, Micha, Paddy, Robin, Borschti, Kevin, Sabrina, Daniel, Bierwirth, Kimi, Guilia, Nadine und der kleine Stubsi Jr., äh Mika ;-), … Danke für alles!

Nein euch habe ich nicht vergessen ;-) Mein besonderer Dank gilt euch, liebes Wolfrudel! Kalle & Tobi, danke! Danke für einfach so viele geile Augenblicke und Erinnerungen! Ich wüsste nicht wo ich heute ohne euch wäre und ich hoffe diese Freundschaft wird ein Leben lang halten! Ich höre hier jetzt lieber auf, sonst schreibe ich weitere 170 Seiten…

Zu guter Letzt möchte ich euch danken, liebe Familie! Danke euch allen, Martin, Florian, Pate Carsten, Godi Karin, Luis & Paul, Silvia, Ludmilla, Heinz-Jürgen, Dieter, Christa, Juliane, Katrin, Lena, Merle, Rudi, Anchen, Stephan, Simone, Daniela, Tom, … Danke!

Omas Elisabeth und Erika, Opas Heinrich und Henner, ich danke euch für alles was ihr in den 28 Jahren für mich gemacht habt. „Öpchen“ Henner, du wirst sehr vermisst! Mama, Papa und Christine, Worte können nicht ausdrücken wie dankbar ich euch bin und wie wichtig ihr mir seid! Danke für alles!

Diese Arbeit widme ich euch!

Table of contents

Examination board *I*

Thesis advisory committee **I**

Additional members of the examination board **I**

Statement of authorship *III*

Danksagung *V*

Table of contents *VII*

Summary *IX*

Lists of abbreviations *XI*

1. Introduction *1*

Osmoregulation in bacteria **1**

Sensing of changes in osmolarity by bacteria **3**

The nucleotide second messenger c-di-AMP **5**

Synthesis and degradation of c-di-AMP **6**

The signaling network of c-di-AMP **8**

***Listeria monocytogenes* and c-di-AMP** **11**

Objective of this thesis **14**

2. The YbbR domain-containing protein CdaR regulates diadenylate cyclase activity of CdaA *15*

Abstract **15**

Introduction **16**

Experimental procedures **17**

Results **23**

Discussion **30**

3. Characterization of c-di-AMP-controlled potassium transporters of Listeria monocytogenes *35*

Abstract **35**

Introduction **36**

Experimental procedures **37**

Results **41**

Discussion **48**

4. Global effects of c-di-AMP on gene expression and protein biosynthesis in Listeria monocytogenes *51*

Abstract **51**

Introduction **52**

Experimental procedures **53**

Results **57**

Discussion 62

5. The inhibitory effect of DNA on the activity of the diadenylate cyclase DisA of Bacillus subtilis is relieved by ions ***67***

Abstract 67

Introduction 68

Experimental Procedures 69

Results 73

Discussion 78

6. The sRNA rli31 affects lysozyme resistance, motility and gene expression in Listeria monocytogenes ***81***

Abstract 81

Introduction 82

Experimental Procedures 83

Results 86

Discussion 92

7. Discussion ***97***

Regulation of diadenylate cyclase activity 97

Regulation of CdaA by CdaR 98

The role of the YbbR domains of the diadenylate cyclase regulator CdaR 100

Regulation of other diadenylate cyclases 103

c-di-AMP-regulated osmotic homeostasis in *Listeria monocytogenes* 104

c-di-AMP affects global gene expression and protein biosynthesis 106

Outlook 109

8. Supplementary Data ***i***

Chapter 2 i

Chapter 4 iv

Chapter 5 xii

Chapter 6 xiv

9. References ***xix***

10. Appendix ***xxxv***

11. Curriculum vitae ***xxxix***

List of publications xl

Summary

The second messenger cyclic diadenosine monophosphate (c-di-AMP) is essential for most of the bacteria synthesizing the nucleotide. c-di-AMP is produced by diadenylate cyclases (DACs) and degraded by specific phosphodiesterases (PDEs). c-di-AMP is involved in the control of different cellular processes, such as cell wall metabolism, carbon metabolism and osmoregulation. Osmoregulation is the cause for the essentiality of c-di-AMP, because regulation of osmolyte uptake systems has been shown to be affected by the second messenger. Hence, c-di-AMP is a major regulator of osmotic homeostasis in bacteria. The Gram-positive human pathogen *Listeria monocytogenes* possesses the DAC CdaA and the PDEs PdeA and PgpH for c-di-AMP synthesis and degradation, respectively. The CdaA-type of DAC is widespread in firmicute pathogenic bacteria and therefore a prime target for the development of novel antibiotics. The gene encoding CdaA is conserved with the genes *cdaR* and *glmM*, encoding the protein CdaR and the phosphoglucosamine mutase GlmM, respectively. It is however unclear, how bacteria modulate c-di-AMP concentrations in response to osmotic changes and how c di AMP affects important osmotic adaptation processes, such as potassium transport, in *L. monocytogenes*. Here, novel insights on the regulation of DAC activity and the impact of c-di-AMP on cellular processes are elucidated. Synthesis and degradation of c-di-AMP have to be tightly adjusted, in dependency of the external osmolarity to maintain an isosmotic intracellular environment. In concert with modulations of the cell wall metabolism this subsequently results in maintaining a balanced turgor pressure. Hence, the proteins CdaR and GlmM are prime targets to modulate CdaA activity. CdaR consists of an N-terminal transmembrane domain and four YbbR domains of unknown function. It is shown that CdaR, like CdaA, is a membrane protein, with the four YbbR domains located outside of the cell. Moreover, a Δ*cdaR* mutant shows defects in the adaptation to osmotic stress and an altered intracellular c-di-AMP concentration. For normal regulation of CdaA activity upon osmotic shock, both, the membrane localization and the presence of the YbbR domains are required. It is furthermore shown that both CdaR and GlmM are able to interact with CdaA and inhibit its activity *in vivo*. This highlights that CdaA probably integrates clues, signaling changes in osmolarity and cell wall biosynthesis, *via* its two regulators CdaR and GlmM, respectively. Additionally, protein-protein interaction studies, show possible interactions between CdaAR and the PDEs, indicating cross-talk of synthesis and degradation machineries and local signaling of c-di-AMP. Moreover, using directed and undirected approaches, novel targets in *L. monocytogenes* that might be regulated by c-di-AMP are investigated. The proteins KtrCD and KimA of *L. monocytogenes* are shown to possess potassium transporter activity and both, KtrCD and KimA are demonstrated to be inhibited by c-di-AMP *in vivo*. KtrC, furthermore, binds the nucleotide *in vitro*. The analysis of changes in global gene expression and protein synthesis demonstrates a broad impact of c-di-AMP on *L. monocytogenes*. Important cellular processes, such as the central metabolism, the regulation of transport processes and motility, as well as cell wall remodeling are implicated. Investigations of the connection between c-di-AMP signaling and alterations of the cell wall, additionally, demonstrated that *L. monocytogenes* rapidly adapts to the muralytic enzyme lysozyme by acquiring mutations in the promoter of the sRNA *rli31*, which has been shown to affect expression of cell wall modifying enzymes. To conclude, in the present study regulatory processes affecting c-di-AMP synthesis by changes in the osmolarity and the impact of c-di-AMP on global gene expression, protein biosynthesis, cell wall modifications and especially its impact on osmohomeostasis in the human pathogen *L. monocytogenes*, are investigated. The gained knowledge will help to understand the mechanisms Firmicutes use to sense changes in osmolarity and highlights mechanisms they use to adapt. Understanding regulation of DAC activity eventually can lead to the development of novel antibiotic to treat infections by these increasingly multi antibiotic resistant pathogens.

Lists of abbreviations

Abbreviation	Meaning
% (*v/v*)	% (volume/volume)
% (*w/v*)	& (weight/volume)
(p)ppGpp	guanosine penta -/ tetraphosphate
ad	up to
ADP	adenosine diphosphate
amp	ampicillin
AMP	adenosine monophosphate
AP	alkaline phosphatase
ATP	adenosine triphosphate
B.	*Bacillus*
BHI	Brain Heart Infusion
C	carbon
CAA	casamino acids
cAMP	cyclic adenosine monophosphate
CdaA / *cdaA*	cyclic di-AMP synthase A / -gene
CdaR / *cdaR*	cyclic di-AMP synthase regulator / -gene
CdaS / *cdaS*	*B. subtilis* sporulation specific cyclic di-AMP synthase / -gene
c-di-AMP	cyclic di-adenosine monophosphate
c-di-GMP	cyclic di-guanosine monophosphate
cDNA	chromosomal DNA
DAC	diadenylate cyclase
cm	chloramphenicol
DarA / *darA*	c-di-AMP receptor A
DisA / *disA*	*B. subtilis* DNA integrity scanning protein A / -gene
DNA	desoxyribonucleic acid
dNTP	desoxyribonucleotide
E.	*Escherichia*
e.g.	exempli gratia
EDTA	ethylenediaminetetraacetic acid
erm	erythromycin
et al.	*et alia*; and others
Fig.	figure
Fwd.	forward
GlmM / *glmM*	phosphoglucosamine mutase / -gene
HhH	helix-hairpin-helix
HIF	high impact factory
IPTG	isopropyl β-D-1-thiogalactopyranoside
K	potassium
kan	kanamycin
Ktr / *ktr*	potassium transporter / -gene
L.	*Listeria* or in some cases *Lactococcus*
LB	lysogeny broth
L-form	cell wall less form
LSM	*Listeria* synthetic medium
MCS	multiple cloning site

Abbreviation	Meaning
MDR	multi drug resistance
mGfp / *mgfp*	monomeric green fluorescent protein / -gene
MOPS	3-(N-morpholino)propanesulfonic acid
mRNA	messenger RNA
N	nitrogen
Na	sodium
NAG	N-acetylglucosamine
NAM	N-acetylmuramic acid
OD_x	optical density at a wavelength of λ=x nm
ORF	open reading frame
P	promoter
p	plasmid
pApA	phosphoadenylyl adenosine
PASTA	PBP and serine/threonine kinase associated
PCR	polymerase chain reaction
PDE	phosphodiesterase
PdeA / *pdeA*	phosphodiesterase A / -gene
penG	penicillin G
PG	peptidoglycan
PgpH / *pgpH*	HD-domain phosphodiesterase / -gene
pH	power of hydrogen
P_{ii}	inorganic pyrophosphate
PrfA / *prfA*	positive regulatory factor A / -gene
primer	oligonucleotide
RBS	ribosomal binding site / Shine-Dalgarno sequence
Rev.	reverse
RNA	ribonucleic acid
RNase	ribonuclease
S	supplementary
S.	*Staphylococcus* or *Streptococcus*
SDS	sodium dodecyl sulfate
SOE	splicing by overhang extension
T4	T4 phage
Tab.	table
TM	transmembrane
TRIS	Tris(hydroxymethyl)aminomethane
tRNA	transfer RNA
UTR	untranslated region
WGS	whole genome sequencing (illumina sequencing)
wt	wild type
X-Gal	5-bromo-4-chloro-3-indolyl-β-D-galactopyranoside
λ	lambda / wavelength

Abbreviation	Meaning
°C	degree Celsius
A	ampere
b	base

Abbreviation	Meaning
bar	bar (100 kPa)
bp	base pair
g	gram
h	hour
Hz	hertz (cycle per second)
kb	kilo base pair (10^3 bases)
l	liter
M	molar (mole/l)
min	minute
rpm	round per minute
sec	second
U	units
V	volt
W	watt
mole	number of atoms in 12 g carbon
x g	x g-forces

One letter code	Three letter code	Meaning
A	Ala	alanine
C	Cys	cysteine
D	Asp	aspartic acid
E	Glu	glutamic acid
F	Phe	phenylalanine
G	Gly	glycine
H	His	histidine
I	Ile	isoleucine
K	Lys	lysine
L	Leu	leucine
M	Met	methionine
N	Asn	asparagine
P	Pro	proline
Q	Gln	glutamine
R	Arg	arginine
S	Ser	serine
T	Thr	threonine
Y	Thy	tyrosine
V	Val	valine
W	Trp	tryptophan

Abbreviation	Meaning	Abbreviation	Meaning
k	kilo (10^3)	A	adenine
m	milli (10^{-3})	C	cytosine
µ	micro (10^{-6})	G	guanine
n	nano (10^{-9})	T	thymine
p	pico (10^{-12})	U	uracil

1. Introduction

The 17th and 18th centuries were a time full of new scientific discoveries, with observations that seemed rather unexplainable for the people of the era. Not only did Antonie van Leeuwenhoek observe microorganisms for the first time and thereby opened the door to a strange and unknown world, but also the first description of osmosis was recorded in this period (van Leeuwenhoek, 1677). The French physicist Jean-Antoine Nollet noticed that an alcohol filled cylinder that was sealed with a gallbladder increased in volume in a water bath (Nollet, 1748). The volume increased to such an extent that pressure built up and the alcohol would shoot out if the gallbladder is pricked with a needle. This is not only the first observation of osmosis, the directed flow of particles across-a semipermeable membrane, but also the first description of the resulting turgor pressure.

The next chapters will highlight the importance for bacteria to maintain a normal turgor pressure by osmoregulation, mechanisms they employ therefore and tools bacteria have developed to sense and regulate these mechanisms, including the second messenger c-di-AMP.

Osmoregulation in bacteria

Bacteria have to cope with various environmental conditions and their changes. Due to their confinement to an imminent location, bacteria have evolved a multitude of mechanisms to sense and cope with changes in environmental conditions, like the regulation of osmotic homeostasis (Sleator & Hill, 2002; Wood, 1999). Osmotic homeostasis is the maintenance of a gradient of osmolytes across-the cell envelope. For bacteria and plants, which have a rigid cell wall, in contrast to animal cells, the difference between internal and external osmolarity is not isotone, but higher inside the cells. For Gram-negative bacteria, like *Escherichia coli*, an internal pressure (turgor) of about 0.3-3 bar has been reported, while for Gram-positive bacteria, like *Bacillus subtilis*, a pressure of about 10 bar has been reported (Rojas & Huang, 2018). The osmotic pressure on a cell is determined by the concentration of osmolytes that are not able to diffuse through the cell membrane and therefore able to generate concentration gradients. Their ability to cross-the cell envelope is controlled by regulated transport mechanisms. An osmolyte is a substance that influences osmosis by its ability to bind water molecules; also called osmotic active substance. Prime examples are ions, amino acids, sugars and peptides and other charged molecules (Wood, 1999). Bacterial cells that live in dynamic environments have therefore evolved mechanism to cope with changes in external osmolarity – counteracting osmotic stress.

There are two kinds of osmotic stress: hypoosmotic stress, induced by a downshift (decrease) of external osmolytes and hyperosmotic stress, induced by an upshift (increase) of external osmolytes. During hypoosmotic stress, water follows the gradient of osmolytes and thereby increases the cellular volume, leading to a higher intracellular pressure and osmotic swelling. The opposite happens during hyperosmotic stress: cells release water, undergo a loss of turgor pressure, causing an invagination of the membrane. Bacteria have to cope with these two antagonistic stresses in different ways. To cope with a hypoosmotic stress it is important to prevent the additional import of osmolytes and to reestablish the natural concentration gradient by exporting osmolytes in the surrounding. Furthermore, mechanosensitive water channels, aquaporins, open rapidly and function as a kind of emergency pressure valve by releasing cytoplasmic content in the

surrounding (Hoffmann *et al.*, 2008) During hyperosmotic stress, the cell needs to import additional osmolytes and prevent secretion of cytosolic osmolytes to lower the concentration gradient between the high external and low internal osmolarity. The basic changes and reactions of bacterial cells to osmotic stress are illustrated in **Fig. 1.1**.

As reviewed by Jane M. Wood the effects of an osmotic upshift on structure and physiology of *E. coli* cells can be summarized in three main phases (Wood, 1999). An osmotic upshift leads to a rapid dehydration of the cell, accompanied with a shrinkage of the cytoplasmic water content, increased cytoplasmic crowding and altered strain on the cell envelope. These structural changes are accompanied by inhibition of respiration and many transport processes, activation of potassium and osmolyte import, a transient increase in pH difference and also a transient increase in the ATP concentration. After this initial period, which happens in the first one to two minutes, nucleic acid counterions are replaced and the cell rehydrates, potassium glutamate and compatible solutes accumulate, cell processes are resumed and pH and ATP levels normalize. This period takes up 20 to 60 minutes and is followed by the last phase that involves remodeling of the cell envelope and nucleoid, the resume of cellular functions and re-establishment of physiological gradients of osmolytes by expression of compatible solute import and/or export systems.

It is interesting to note that the first response bacteria employ to cope with a hyperosmotic stress usually is the rapid uptake of potassium ions (Kempf & Bremer, 1998). The intracellular concentration of ions, including potassium, is crucial for the survival of cells. On the one hand it is necessary for proper ribosome and on the other hand to buffer the negative charge of the phosphate backbone of the DNA. Furthermore, it is essential for maintaining cellular turgor (Nierhaus, 2014; Pasi *et al.*, 2015; Sleator & Hill, 2002; Wood, 1999). Another osmolyte that is important in the first response is the negative charged amino acid glutamate. Glutamate is often designated as a counterion to potassium and its intracellular concentration, by synthesis and/or uptake, usually rises together with the potassium concentration (Yan *et al.*, 1996). Since an excess of potassium would also be detrimental for the cell if exposed to too high concentrations or for a too long time, potassium is usually replaced by other low molecular weight compounds that can accumulate in the cell without disturbing cellular functions; also known as compatible solutes. Examples for compatible solutes are amino acids (e.g. proline or carnitine), oligopeptides, carbohydrates (e.g. trehalose) and other molecules such as glycine betaine (Wood *et al.*, 2001). Maintaining cellular turgor is not only important for maintaining cellular shape and integrity, it is also a driving force of bacterial cell growth and an important factor influencing division (Rojas & Huang, 2018). Moreover, it is not enough for the cells to accumulate osmolytes and compatible solutes, the cell also has to sense when the osmotic concentration gradients are again acceptable for the cell again and therefore when to stop synthesis or uptake of osmolytes.

The opposite case, a hypoosmotic shock, has to be counteracted by the cell in the opposite direction and can again be separated in three phases: the cell has to get rid of internal osmolytes and prevent the further influx of water molecules and osmotic swelling. In less than a minute after decreasing the external concentration of osmolytes, water flows into the cell, leading to a rapid hydration and swelling, a decrease in cytoplasmic crowding and also alterations of cell envelope strain. These effects are rapidly counteracted by the opening of mechanosensitive aquaporin channels that allow a rapid release of pressure by releasing cytoplasmic material and water molecules into the surrounding (Hoffmann *et al.*, 2008). This first phase is followed by the shrinkage of the cell and a re-increase in cytoplasmic crowding and extrusion of water and co-solvents. In these few minutes, proton motive force probably also collapses. The effects in the third phase,

which lasts only 10 to 20 minutes are mainly the closing of mechanosensitive channels, restoration of proton motive force and re-accumulation of osmolytes (Wood, 1999).

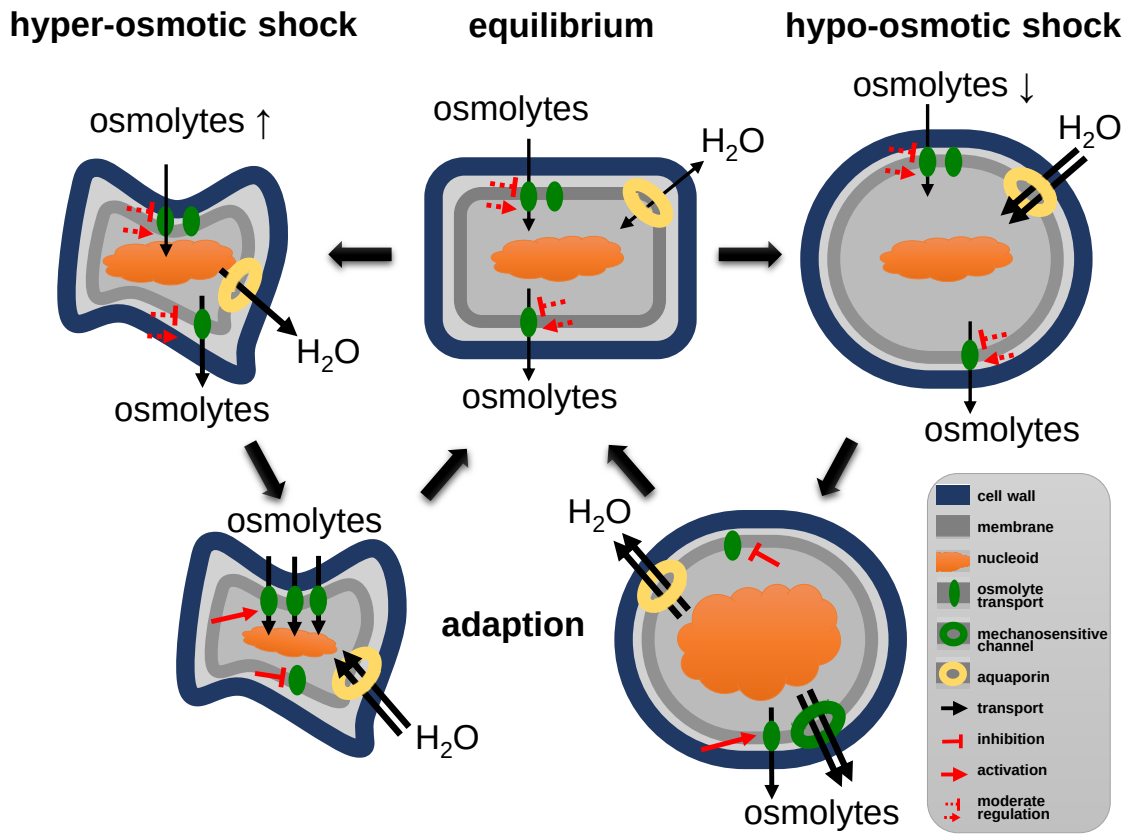

Fig. 1.1 Model depicting the effects of a hyper- and a hypoosmotic shock on bacterial cells and how they adapt. During a hyperosmotic shock, the external osmolyte concentration suddenly increases. This causes a rapid efflux of water, a shrinkage of the cellular volume and is accompanied by strain on the cell envelope. The cell adapts by increasing the intracellular osmolyte concentration through increased uptake and decreased export. There are secondary effects in this stage, e.g. shrinkage of the nucleoid due to influx of potassium ions and increased molecular crowding. In the end it promotes an influx of water and import and/or synthesis of compatible solutes that restore the equilibrium. The opposite, a hypoosmotic shock is triggered by a rapid decrease of external osmolytes. This leads to a rapid swelling of the cellular volume, accompanied by strain on the cell envelope. The cell adapts by decreasing the intracellular concentration of osmolytes by decreasing import and facilitating efflux through transporters and mechanosensitive channels. The decreased molecular crowding induces a de-condensation of the nucleoid and efflux of water. In the end the equilibrium is reconstituted. For further details see the text (modified from Commichau *et al.*, 2018).

To summarize, a bacterial cell faces a variety of changes in cellular structure and physiology upon osmotic stress that have to be counteracted appropriately. It is therefore crucial for the cell to sense their internal and external osmotic state and to adjust accordingly to changes.

Sensing of changes in osmolarity by bacteria

As discussed above, the cell has to adjust to changes in extracellular osmolarity in an appropriate and timely manner. For this purpose, cells have evolved a variety of mechanisms to sense external and internal concentrations of osmolytes and changes in cellular turgor. One of those mechanisms that may be less straight forward are interactions between DNA and proteins. Despite its rather compact packaging, which reduces the space about four to ten times compared to free DNA (Martínez-Antonio *et al.*, 2004), the nucleoid is estimated to have a DNA concentration of about 50-

100 µg/µl and an occupational space of about 12.5 to 20% of the total cytoplasmic lumen, which is highly dependent on the macromolecular crowding (Wood, 1999). The study by Gray *et al.* suggests a correlation between the nucleoid filled spaces and cell size that is independent of replication but species dependent; meaning that the nucleoid filled space increases with an increased cell size (Gray *et al.*, 2018). For *B. subtilis* the average nucleoid area was reported to be to be around 3 μm^2 with an average cell area of 10 μm^2, resulting in a ratio of nucleoid to cell area of 0.3. *E. coli* on the other hand has an average nucleoid are of 2 μm^2, and an average cell area of 4.5 μm^2, resulting in a nucleoid to cell area ratio of about 0.45. This demonstrates that protein-DNA interactions might have developed species specific, regarding protein amount and binding affinities (Gray *et al.*, 2018). Their study also suggests no correlation between growth under different osmolarities and nucleoid to cell area ratio. However, transient effects that occur in a very short timeframe after an osmotic stress have not been investigated in this study. Other studies show a transient effect of osmotic stress on nucleoid size and structure (Cagliero & Jin, 2013). Interestingly, osmotic stress seems to also alter the general packaging structure of DNA. Initial osmotic stress leads to an increase in supercoiling and the subsequent increased potassium transporter activity leads again to a relaxation (Meury & Kohiyama, 1992). A DNA-based osmotic stress sensor therefore has to be adapted to the DNA concentration, the nucleoid to cellular area ratio and osmotic stress induced changes in cellular size; all of these alterations are species specific. Therefore, the expression and DNA-binding affinities as well as other factors like ion binding have evolved to allow a specific and timely response. Examples for osmotic-stress controlled DNA-binding are the RNA polymerase (RNAP) or the transcriptional regulator BusR. A study by Cagliero & Jin demonstrates the rapid dissociation of the RNAP from the nucleoid after hyperosmotic stress. This is caused by condensation of the nucleoid due to increased molecular crowding after the initial import of potassium ions. Eventually, the RNAP re-associates again when osmoprotectants accumulate and the potassium concentration decreases (Cagliero & Jin, 2013). BusR on the other hand is the transcriptional repressor of the *busAA-busAB* operon in *Lactococcus lactis* that encodes a glycine betaine importer (consisting of BusAA and BusAB). Romeo *et al.* found that BusR interaction with the complex of RNAP and the *busA* promoter is released in dependency of the ionic strength *in vitro* (Romeo *et al.*, 2007). Therefore, after the initial osmotic stress phase, once the RNAP re-associates with the nucleoid and binds the *busA* promoter. The increase in ionic strength would prevent interaction of BusR, thereby allowing elevated expression of the BusA glycine betaine importer to import additional compatible solutes. This simplified model is of course not the complete story. In case of BusR additional regulatory mechanism have been identified, which are highlighted in the following chapters.

Interestingly, the most responsive systems allowing adaption to osmotic stress are localized in the plasma membrane. This is the case for both, potassium and osmolyte transporter that counteract an osmotic upshift and for mechanosensitive channels that counteract an osmotic downshift (Wood, 2011). One important determinant for transporter activity is the effect of solvents on the membrane. Similar as positive charged ions like magnesium, calcium, sodium or potassium mitigate the negative charge of the DNA backbone; ions also interact strongly with the charged headgroups of phospholipids, like phosphatidylglycerol or phosphatidylethanolamine (Roux & Bloom, 1990). Alterations in surface charge due to an in- or decrease in local ion concentrations have therefore the power to impact protein-membrane and protein-protein interactions at the membrane. They can also affect protein activity and are therefore a potential signal that can be measured by the cell. More obvious than alterations in charge distributions, however, are the physical changes that osmotic up and downshifts pose on the lipid bilayer of cell membranes. Although the membrane is fluid, it is rather inelastic and strains through alteration of cellular turgor influence

the lateral pressure on transmembrane (TM) domains of proteins and can thereby alter protein activity or lead to opening or closing of mechanosensitive channels (Sleator & Hill, 2002; Wood, 2011). An interesting example for a mechanosensitive measuring system is the PhoQ/PhoP two-component system from *E. coli*. Interestingly, this system senses a whole variety of different stimuli, e.g. the extracellular magnesium concentration, low pH and the presence of antimicrobial peptides. Thereby it plays a crucial role for enterobacterial infection. In addition to those stimuli, it has also been shown that the system is able to sense an osmotic upshift by integrating the thickness and lateral pressure of the membrane on the TM helices of PhoQ. The conformational changes in the membrane are then passed on to the cytosolic kinase domain and thereby lead to an altered signal transduction (Yuan *et al.*, 2017). Intriguingly, a variety of osmolyte transporters, such as OpuA from *B. subtilis* (glycine betaine transporter consisting of OpuAA-OpuAC), BetP from *Corynebacterium glutamicum* (glycine betaine) or ProP from *E. coli* (glycine betaine and proline) seem react to changes in osmolarity. Reconstitution experiments in proteoliposomes suggest that they react to changes in ion concentrations independent of changes in turgor (Poolman *et al.*, 2004). However, the situation *in vivo* might be more complex and the transporter might integrate more than one stimulus and it is not yet fully understood if sensing is achieved by ligand binding, alterations in charges or ion distribution, hydration or changes in membrane strain, tension or curvature or a combination of them and might vary from transporter to transporter (Wood, 2011). One way the cell can integrate such a variety of different stimuli in a unified cell-wide answer is the use of second messenger signaling pathways. In those an environmental stimulus, such as changes in osmolarity, is sensed by different mechanisms and subsequently changes the concentration of a second messenger by altering synthesis, degradation and/or export. The osmolyte transporter of OpuCA of *Listeria monocytogenes* and *Staphylococcus aureus*, which are homologs of the above discussed OpuAA from *B. subtilis* have recently been identified to bind and be inhibited by the nucleotide second messenger cyclic di-AMP (c-di-AMP) that plays a major role in osmoregulation of Firmicutes (Huynh *et al.*, 2016; Schuster *et al.*, 2016).

The nucleotide second messenger c-di-AMP

Bacteria sense a multitude of different environmental changes with the corresponding signals sensed outside, inside the cell, in the cell envelope, through communication with other bacteria and many more. The bacteria have to integrate all these signals and respond appropriately. In this sensing process, so called, second messenger molecules play an important role. They function as an integrator, which controls biological processes upon changes in concentration. Signal input can modulate free second messenger concentration by synthesis, degradation, export or binding to target structures. Second messengers are furthermore known to bind and modulate very different target structures, such as RNAs or proteins (Newton *et al.*, 2016).

Nucleotide second messenger have now been known since the discovery of cyclic adenosine monophosphate (cAMP) by the later Nobel laureate Earl Wilbur Sutherland, Jr. and colleagues in the 1950's (Rall *et al.*, 1957; Rall & Sutherland 1958). cAMP plays an important role in eukaryotes and in prokaryotes, ranging from regulation of sugar metabolism, over gene expression, to neuronal functions; highlighting the importance and diversity of second messenger signaling (Newton *et al.*, 2016). Since the discovery of cAMP, a variety of nucleotide second messenger molecules has been identified and studied: cyclic di-guanosine monophosphate (c-di-GMP), cyclic guanosine monophosphate (cGMP), guanosine tetra- and pentaphosphate; ((p)ppGpp), cyclic guanosine

monophosphate-adenosine monophosphate (cGAMP) or cyclic di-adenosine monophosphate (c-di-AMP) (Corrigan & Gründling, 2013; Gomelsky, 2011; Kalia *et al.*, 2013; Wu *et al.*, 2012).

c-di-AMP is a quiet special nucleotide second messenger: it is the only known one that is essential in many c-di-AMP synthesizing bacteria, it is produced by many pathogenic Gram-positive bacteria, it is absent in humans and it is the first discovered second messenger that governs a biological process on two distinct levels – Regulation of gene expression and protein activity. For all these reasons is c-di-AMP a prime target for the development of novel antibiotics, which are desperately needed in a time of increased multiple antibiotic resistance in many clinically relevant Gram-positive bacteria, like *S. aureus* or *Streptococcus pneumoniae* (Laxminarayan *et al.*, 2013; Rosenberg *et al.*, 2015; WHO, 2014). c-di-AMP, together with two molecules of pyrophosphate (PP_i), is synthesized by the diadenylate cyclase (DAC) domain containing proteins from two molecules of adenosine triphosphate (ATP). The synthesis of c-di-AMP, however, has also been reported from one molecule of ATP and one molecule of adenosine diphosphate (ADP) in *Mycobacterium tuberculosis* (Manikandan *et al.*, 2014; Witte *et al.*, 2008). Degradation of c-di-AMP is facilitated by specific phosphodiesterases (PDEs) into the linear phosphoadenylyl adenosine (pApA) that can be further hydrolyzed to AMP. The known PDEs contain either DHH/DHHA1 or HD domains, like PdeA (GdpP in *B. subtilis*) or PgpH, respectively (Huynh *et al.*, 2015; Rao *et al.*, 2010).

Synthesis and degradation of c-di-AMP

While many pathogenic firmicutes, like *L. monocytogenes*, *S. aureus* or *S. pneumoniae* only harbor one DAC domain containing enzyme of the CdaA/DacA-type, *B. subtilis* contains three different type of DACs: the DNA-binding protein DisA, the membrane bound CdaA and the sporulation specific CdaS. Interestingly, *B. subtilis* is able to survive if only one cyclase is expressed, highlighting that c-di-AMP is essential independent of the producing enzyme (Mehne *et al.*, 2013). The DisA-type (DNA integrity scanning protein A) of DAC is present in spore-forming firmicutes, like *Clostridium difficile*, in actinobacteria, like *C. glutamicum*, in *M. tuberculosis*, in the hyperthermophilic bacterium *Thermotoga maritima* and has even been described in archaea, like *Methanocaldococcus jannaschii* (Bai *et al.*, 2012; Commichau *et al.*, 2019; Kellenberger *et al.*, 2015; Witte *et al.*, 2008). DisA, which forms homooctamers, has been shown to bind DNA, moving along it and being stalled upon DNA damages that lead to an inhibition of cyclase activity. Furthermore, it interacts with other proteins of DNA repair pathways such as the branch migration transferase RadA (Oppenheimer-Shaanan *et al.*, 2011; Witte *et al.*, 2008; Zhang & He, 2013). The function and regulation of the CdaS-type (sporulation-specific cyclic di-AMP synthase) DAC is less well studied. It is known to play a role in sporulation initiation and/or efficient germination and that it forms hexamers that consists of three homodimers by interaction of the two N-terminal domains of CdaS, which if truncated lead to hyperactivity (Mehne *et al.*, 2014; Zheng *et al.*, 2015). The most widespread kind of DAC is of the CdaA-type (cyclic di-AMP synthase A). CdaA, which is also called DacA (Corrigan *et al.*, 2011; Mehne *et al.*, 2013; Rismondo *et al.*, 2016; Rosenberg *et al.*, 2015; Woodward *et al.*, 2010), is a membrane bound protein. It consists of three N-terminal TM domains and the DAC domain, which is flanked by two coiled-coil domains. The gene encoding for CdaA is conserved together with the *cdaR* gene, encoding a protein of unknown function and the gene encoding the essential glucosamine mutase GlmM. In *B. subtilis* they are encoded in one operon, while in *L. monocytogenes* for example *cdaA* and *cdaR* are in one operon followed by *glmM* with its own promoter (Mehne *et al.*, 2013; Rismondo *et al.*, 2016). CdaA is active *in vitro* with the metal ions Mn^{2+} or Co^{2+}, in contrast to DisA, which is active with Mg^{2+} as a cofactor. It furthermore forms

homodimers, which are important for its activity. Depletion of CdaA and thereby c-di-AMP has been linked to alterations in the cell wall metabolism and increased susceptibility to cell wall-acting antibiotics (Rismondo *et al.*, 2016; Witte *et al.*, 2013). The CdaR protein consists of an N-terminal TM domain and four YbbR domains of unknown function. It has been demonstrated to self-interact *via* the YbbR domains and to interact only in its full-length variant with the full-length CdaA protein. Moreover, a deletion of *cdaR* leads to altered c-di-AMP levels in *B. subtilis*, *L. monocytogenes* and *S. aureus* and is able to influence CdaA activity if co-expressed in *E. coli*, suggesting that CdaR is a modulator of CdaA activity (Bowman *et al.*, 2016; Gundlach *et al.*, 2015b; Mehne *et al.*, 2013; Rismondo *et al.*, 2016). Although protein crystallographic structures of the YbbR domains are available, which show some structural homology to domains of unknown function from L25 and TL5 ribosomal binding protein, their function as putative sensory domains is not yet elucidated (Barb *et al.*, 2010). The second protein, which has been shown to play a role in regulating CdaA activity is GlmM. GlmM converts glucosamine-6-phosphate to glucosamine-1-phosphate, which is one of the first reactions for the synthesis of N-acetylglucosamine, an important building block of the bacterial peptidoglycan (Barreteau *et al.*, 2008; Mengin-Lecreulx & van Heijenoort, 1996). GlmM has been shown to interact with CdaA in *B. subtilis* and is hypothesized to affect its activity (Gundlach *et al.*, 2015b). Moreover, in *L. lactis* an osmoresistant suppressor mutant with a mutation in GlmM was identified that lead to a decrease in the intracellular c-di-AMP concentration, demonstrating a functional link between GlmM and CdaA activity (Zhu *et al.*, 2016). Intriguingly, today a novel study was published by the Gründling lab, demonstrating an inhibitory effect of GlmM on CdaA activity in *S. aureus in vitro* and *in vivo*. They propose a model, were interaction of GlmM with the DAC domain perturbs CdaA self-interaction and therefore catalytic activity (Tosi *et al.*, 2019).

c-di-AMP has just been identified about 10 years ago and as shown above, novel discoveries and hypothesis are very frequent. Another recent example is the discovery of a founding member of a novel DAC class. In the minimal and cell wall-less human pathogen *Mycoplasma pneumoniae* an enzyme that produces c-di-AMP was discovered, designated CdaM, while both CdaR and GlmM homologs are not present in this organism (Blötz *et al.*, 2017). Recent discoveries, furthermore, demonstrate the presence of even more classes of DAC domain containing enzymes in different organisms, reviewed elsewhere (Commichau *et al.*, 2019).

Additionally, another important part of the c-di-AMP metabolism is to regulate the concentration by degradation or export. In studies with *L. monocytogenes*, multidrug resistance transporters (Mdr) where identified to export c-di-AMP. As a consequence, c-di-AMP triggers a type I interferon response in human cells by activation of the innate immune sensor STING. Furthermore, it also leads to inhibition of the oxidoreductase RECON, resulting in anti-inflammatory responses and intriguingly increased cell-to-cell spread of *L. monocytogenes*, highlighting c-di-AMPs effect in virulence (Archer *et al.*, 2014; Kaplan Zeevi *et al.*, 2013; McFarland *et al.*, 2017; McFarland *et al.*, 2018). Efflux of c-di-AMP may also be a fast way to decrease the intracellular concentration independent of degradation. Degradation occurs *via* hydrolyzation by c-di-AMP-specific PDEs. In *B. subtilis* and *L. monocytogenes* two different PDEs are synthesized, GdpP (PdeA in *L. monocytogenes*) and PgpH. GdpP is of the DHH/DHHA1 type an consists of two TM domains, followed by a PAS, a GGDEF domain and the catalytic DHH/DHHA1 domain. GdpP is competitive inhibited by ppGpp another second messenger that is important in regulating the stringent response during nutrient starvation, suggesting cross-talk between the c-di-AMP and ppGpp regulatory networks (Rao *et al.*, 2010). Furthermore, the PAS domain of GdpP has been shown to inhibit catalytic activity of GdpP upon binding of heme, suggesting a link between c-di-AMP and the redox state of the cell (Rao *et al.*, 2011). PgpH, a member of the second major class of c-di-AMP hydrolyzing

enzymes consists of an extracellular 7TMR HDED domain, followed by seven TM helices and the catalytic HD domain. As for GdpP, PgpH was also found to be inhibited by ppGpp, again suggesting a cross-talk between c-di-AMP signaling and the stringent response (Huynh *et al.*, 2015). PgpH was furthermore identified to be the major c-di-AMP degrading enzyme in *B. subtilis*, with its deletion leading to an accumulation of c-di-AMP. Interestingly, a *gdpP pgpH* double mutant lead to toxic accumulation, which is why c-di-AMP is also termed "essential poison", highlighting the importance to maintain adequate levels of this second messenger (Gundlach *et al.*, 2015b). Accumulation of c-di-AMP by PDE deletion was furthermore found to deregulate expression of about 700 genes and in consequence lead to defects in biofilm formation and plant attachment of *B. subtilis* (Gundlach *et al.*, 2016; Townsley *et al.*, 2018). There are also other classes of PDEs, degrading c-di-AMP to pApA and further to AMP, nano-RNases that degrade pApA to AMP or PDEs that degrade c-di-AMP extracellular, which are covered in a recent review by Commichau and colleagues (Commichau *et al.*, 2019).

The study by Gundlach and colleagues also demonstrates why the essential function of c-di-AMP has eluded discovery for almost a decade (Gundlach *et al.*, 2016): the plethora of different phenotypes and intertwines of different signaling pathway, ranging from cell wall phenotypes, over lifestyle changes, DNA damage responses to the discovery of c-di-AMPs involvement in osmoregulation (Corrigan *et al.*, 2011; Commichau *et al.*, 2015; Dengler *et al.*, 2013; Gundlach *et al.*, 2017; Luo & Helmann, 2012; Rismondo *et al.*, 2016; Whiteley *et al.*, 2015; Whiteley *et al.*, 2017; Witte *et al.*, 2013).

The signaling network of c-di-AMP

The first identified bacterial c-di-AMP-regulated protein was the TetR-like transcriptional factor DarR in *Mycobacterium smegmatis* (Zhang *et al.*, 2013). Binding of c-di-AMP has been shown to stimulate DNA-binding of DarR that in consequence negatively regulates expression of an operon coding for three genes, including a major facilitator family transporter, a medium chain fatty acyl-CoA ligase and a homolog of the cold shock protein CspA. Since this study, c-di-AMP was found to regulate a variety of cellular targets in bacteria, of, which many are highlighted in **Fig. 1.2**. c-di-AMP was identified to bind and regulate the potassium import system KtrAB by binding to the RCK_C domain of the cytosolic KtrA and cation/proton antiporter CpaA in *S. aureus* that putatively functions as a potassium export system, which were also subjects of further studies illuminating the molecular mechanisms (Chin *et al.*, 2015; Corrigan *et al.*, 2013; Kim *et al.*, 2015). Interestingly, c-di-AMP would thereby control potassium homeostasis in *S. aureus* by inhibiting import and stimulating export. In the same study, the PII-like protein PstA of unknown function and the histidine kinase KdpD of the KdpDE two component system were identified as c-di-AMP binding proteins (Corrigan *et al.*, 2013). While the function of PstA is unknown, KdpDE regulated expression of the Kdp(F)ABC potassium import system, indicating again an important role for c-di-AMP in potassium homeostasis. Intriguingly, translation of KtrAB and YdaO (which was later identified as a high-affinity potassium importer in *B. subtilis* and renamed KimA) are regulated by a c-di-AMP responsive riboswitch. Binding of c-di-AMP to the *ydaO* (*kimA*) riboswitch prevents translation of the potassium importers. This makes c-di-AMP a special regulator and the first of its kind by regulating a biological process by controlling synthesis and activity (Gao & Serganov, 2014; Gundlach *et al.*, 2017; Moscoso *et al.*, 2015; Nelson *et al.*, 2013).

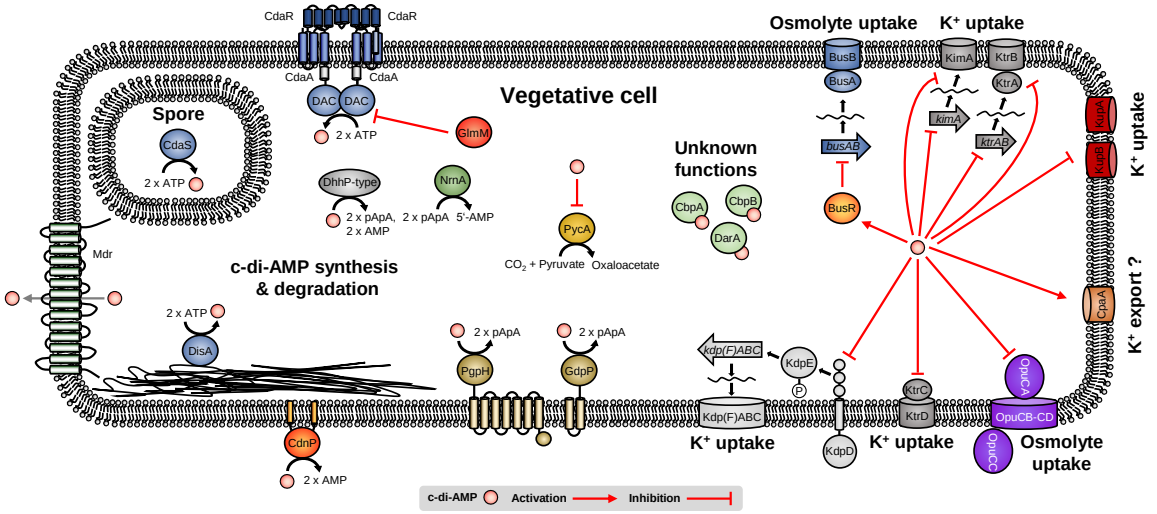

Fig. 1.2 Synthesis and degradation of the essential second messenger c-di-AMP and its cellular targets. c-di-AMP is synthesized by DACs. Shown are members of the main three types of DACs: CdaA, DisA and CdaS. CdaA activity is modulated by the YbbR-domain containing protein CdaR by the cell wall precursor synthesizing glucosamine mutase GlmM. c-di-AMP is degraded by PDEs to pApA. Shown are members of the main types of PDEs, GdpP and PgpH and also of the DhhP- (that can also degrade pApA further to AMP) and the CdnP-type, (that degrades c-di-AMP to AMP) as well as the pApA to AMP degrading nano-RNase NrnA. Shown is also MdrT, a member of c-di-AMP secreting multidrug resistance transporters. Furthermore, targets that have been shown to bind c-di-AMP are depicted: the pyruvate carboxylase PycA, which is allosterically inhibited by c-di-AMP and the proteins of unknown function: DarA, CbpA and CbpB of *L. monocytogenes*. Moreover, the known c-di-AMP-controlled osmolyte transporters are shown: The high-affinity potassium uptake systems KtrAB and KimA that are controlled on protein level and via a c-di-AMP-binding riboswitch in *B. subtilis*, the Kdp(F)ABC high-affinity potassium transporter, whose transcription is regulated via the c-di-AMP inhibited two component system KdpDE in *S. aureus* and the low-affinity potassium transporter KtrCD. Two novel high-affinity potassium transporters, KupA and KupB, which were recently identified as c-di-AMP regulated in *L. lactis* are depicted, as well. c-di-AMP, moreover, regulates the putative potassium exporter CpaA in *S. aureus* and binds the BusR transcription factor that inhibits expression of the glycine betaine importer BusAB in *L. lactis* and *S. agalactiae*. Finally, the OpuC glycine betaine transporter from *B. subtilis* is depicted, too (modified from Commichau *et al.*, 2018).

To emphasize the importance of c-di-AMP on potassium homeostasis, it should be noted that it was identified to regulate potassium import in a whole variety of different bacteria. It was found to inhibit uptake in *S. pneumoniae via* binding to the CabP protein that interacts with the potassium importer TrkH and thereby inhibits import (Bai *et al.*, 2014). Interestingly, a later study showed that CabP deletion leads to reduced c-di-AMP concentrations in *S. pneumoniae*, indicating that either CabP or the resulting altered potassium homeostasis is able to be senses and thereby to modulate c-di-AMP homeostasis (Zarrella *et al.*, 2018). Moreover, c-di-AMP concentrations were recently identified to be light-dependent in the cyanobacterium *Synechococcus elongatus* and a *cdaA* deletion mutant was more susceptible to oxidative stress during the nighttime part of a day-night cycle. Interestingly, *S. elongatus* encodes several putative c-di-AMP regulated potassium importers and an impairment in potassium transport leads to a similar susceptibility to oxidative stress, as it was shown for the *cdaA* mutant (Rubin *et al.*, 2018). In *L. lactis*, c-di-AMP has been shown to inhibit potassium uptake *via* KupA and KupB of the Kup family potassium importer and even in the minimal organism *M. pneumoniae*, c-di-AMP was identified as a regulator of potassium uptake (Blötz *et al.*, 2017; Quintana *et al.*, 2019). Eventually, c-di-AMP was shown to be essential due to its central role in regulating potassium homeostasis in *B. subtilis* (Gundlach *et al.*,2017). Taken together this demonstrates the critical role of c-di-AMP in potassium homeostasis in a broad spectrum of different bacteria.

c-di-AMP was also found to regulate other cellular processes or bind to proteins whose function is not yet elucidated. It was shown to allosterically inhibit the pyruvate carboxylase PycA in

L. monocytogenes and *L. lactis* or bind to the *S. aureus* PstA homologs in *B. subtilis* (DarA) or *L. monocytogenes* (PstA). The same is also true for two other proteins of unknown function, CbpA and CbpB in *L. monocytogenes* and NrdR, the negative regulator of the ribonucleotide reductase operon *nrd* (Campeotto *et al.*, 2015; Choi *et al.*, 2015; Choi *et al.*, 2017; Gundlach *et al.*, 2015a; Müller *et al.*, 2015a; Sureka *et al.*, 2014). While the function of PstA/DarA or the c-di-AMP binding proteins CbpA or CbpB is not yet understood, recent studies identifying novel binding proteins or genetic linkages *via* c-di-AMP dependent suppressor mutations demonstrate that c-di-AMP is not only regulating potassium homeostasis, but homeostasis of osmolytes in general. c-di-AMP can therefore be described as a major regulator for osmoregulation in Firmicutes. Whiteley *et al.* identified the growth of *L. monocytogenes* in a defined minimal medium as the first reported condition where c-di-AMP was non-essential (Whiteley *et al.*, 2015). They could show that the limitation of osmolytes allows deletion of *cdaA* and that accumulation of suppressor mutations in genes encoding oligopeptide uptake systems (OppABCDF), the PII-like protein PstA, the alarmone synthase/hydrolase RelA, a glycine betaine importer (GbuABC), the pyruvate carboxylase, the potassium importer homolog Lmo0993 (KtrD) or the CbpB protein contributed, among others, to suppression of c-di-AMP essentiality on complex media. In their second study they could, furthermore, show that the mutations in the *opp* and *gbu* genes are sufficient to allow *cdaA* deletion mutants to grow on complex medium, resulting in the hypothesis that uncontrolled accumulations of oligopeptides and glycine betaine under these conditions is detrimental for growth of *L. monocytogenes*. Interestingly, they could further show that c-di-AMP impacts regulation of the flux in the citric acid cycle, an import cross-section between carbon and nitrogen metabolism and therefore also biosynthesis of amino acids that also act as osmolytes (Whiteley *et al.*, 2017). c-di-AMP, furthermore, has been identified to regulate uptake of the osmolyte carnitine in *L. monocytogenes* by binding to the CBS domain of OpuCA of the OpuC transporter but not to the CBS domain in GbuA of the GbuABC glycine betaine importer or the CBS domain of BilEA, of the bile salt specific exporter BilE (Huynh, *et al.*, 2016). Binding of c-di-AMP to OpuCA was also confirmed for *S. aureus* but again other CBS domain containing proteins, including the magnesium transporter MgtE and the transcription factor CcpN, where not identified as c-di-AMP binding proteins (Schuster *et al.*, 2016). Interestingly, although c-di-AMP has been established as a major determinant for osmotic regulation in *S. aureus*, due to its effect on osmolyte (glycine betaine *via* OpuD) and amino acid uptake (AlsT), it also seems to have a great impact on cell respiration and is dispensable under anaerobic conditions in this bacterium, highlighting that the complex regulatory effects of c-di-AMP are even with the increased knowledge not yet fully understood (Zeden *et al.*, 2018). c-di-AMP has furthermore been identified to regulate osmotic homeostasis in *Streptococcus agalactiae* and *L. lactis,* by binding to BusR, that upon binding negatively regulates expression of the genes encoding BusAB, a glycine betaine importer (Devaux *et al.*, 2018; Pham *et al.*, 2018). Interestingly, in the study of Pham and colleagues, impact of osmotic up- and downshifts on c-di-AMP concentrations in different bacteria and mutants was investigated, too. They could show, that upon osmotic upshift (hyperosmotic shock) c-di-AMP levels rapidly decrease and *vice versa* increase upon hypoosmotic shock. Intriguingly, energizing of the cells that is required for ATP synthesis and presence of the DAC CdaA and the PDE GdpP/PdeA seemed to have the greatest influence on the bacteria to adapt their c-di-AMP concentration accordingly (Pham *et al.*, 2018). Taken together, c-di-AMP has been shown to influence many cellular processes, predominantly osmotic homeostasis, in many bacteria that produce this nucleotide second messenger, with *L. monocytogenes* being a prominent bacterium of c-di-AMP research (Commichau *et al.*, 2015; Commichau *et al.*, 2018).

Listeria monocytogenes and c-di-AMP

The bacterium *L. monocytogenes* has been the subject of many c-di-AMP related studies: the first crystal structure of a CdaA-type DAC, the most abundant one, was obtained from a truncated *L. monocytogenes* enzyme (Rosenberg *et al.*, 2015), many c-di-AMP binding proteins, such as CbpA, CbpB, PycA or OpuCA were first identified in this bacterium (Huynh *et al.*, 2016; Sureka *et al.*, 2017). Moreover, *L. monocytogenes* was the first bacterium were conditions were identified under which c-di-AMP is dispensable (Whiteley *et al.*, 2015).

L. monocytogenes is closely related to *B. subtilis*, belonging also to the phylum of the Firmicutes. It was first described in 1926 by Everitt George Dunne Murray as *Bacterium monocytogenes* and later on named in honor of the British surgeon Joseph Lister and the upon infection occurring monocytosis (Gray & Killinger, 1966; Murray *et al.*, 1926; Pirie, 1940). One interesting aspect of *L. monocytogenes* is its lifestyle change. On the one hand, the bacterium can be found ubiquitous in nature as a saprophyte and on the other hand it is a facultative foodborne human pathogen (Farber & Peterkin, 1991; Freitag *et al.*, 2009). *L. monocytogenes* therefore needs to precisely sense its environment to adapt accordingly. Here, the transcription factor PrfA (positive regulator of listeriolysin A), the master regulator of the virulence of *L. monocytogenes* is the key player. Upon changes in temperature, nutrient conditions, components of stress response pathways, like the metabolic regulator CodY and effector molecules, such as glutathione, amount and activity state of PrfA is altered (de las Heras *et al.*, 2011; Lobel *et al.*, 2015; Reniere *et al.*, 2015). In turn, PrfA-dependent genes that are important for triggering endocytosis (esp. internalins InlA and InlB), intracellular vacuolar escape (specific lipases PC-PLC, PI-PLC and the lytic enzyme LLO), uptake of nutrients (hexosephosphate transporter Hpt), intracellular traversation (actin polymerization by ActA) and infection of neighboring cells are expressed (Chico-Calero *et al.*, 2002; Scortti *et al.*, 2007). Another key feature of *L. monocytogenes* is its ability to actively cross-protection barriers inside humans, such as the blood-brain or blood-placenta barrier, making it a dangerous bug for immunocompromised persons with the possibility of high mortality rates after encephalitis or meningitis and for pregnant women with the danger of prenatal infections, leading to severe consequences for the fetus, including disabilities, stillbirths or miscarriages (Low and Donachie, 1997; Vázquez-boland *et al.*, 2001).

The adaptation of *L. monocytogenes* to such different environmental niches makes it a very interesting candidate to study osmohomeostasis. The bacteria must on the one hand be able to withstand changes in solute concentrations by environmental events such as changes in humidity and on the other hand be able to survive the transition to the intracellular life style, featuring passage through the stomach, exposure to bile salts in the gut and transition from a natrium rich to a potassium rich environment. One big difference between *B. subtilis* and *L. monocytogenes* is the inability of *L. monocytogenes* to form spores as a persistence state that is resistance against many environmental stresses and its ability despite that to be resistant against various pH, temperature or salt stresses (Farber & Peterkin, 1991). The main strategy for *L. monocytogenes* is hereby the accumulation of the compatible solutes glycine betaine, carnitine, glutamate and oligopeptides with some indications that glycine betaine uptake is also triggered upon cold stress in *L. monocytogenes* (Ko *et al.*, 1994; Smith, 1996; Whiteley *et al.*, 2017). Interestingly, glycine betaine is co-transported with sodium ions, which in turn have to be exported by putative cation-proton antiporter systems, leading to an increase in internal protons that in turn could be exported again by electron transport system, thereby linking osmolyte uptake to generation of proton motive force that has also been linked to c-di-AMP itself (Wood, *et al.*, 2001; Zeden *et al.*, 2018). **Fig. 1.3** shows an overview of the most prominent systems or putative homologs of *L. monocytogenes* to known

systems of *B. subtilis* (MrpA-G, NhaK, KimA, KtrCD, MscL, MscS and NrnA) or *S. aureus* (KdpFABCDE) that are involved in osmoregulation and/or c-di-AMP metabolism.

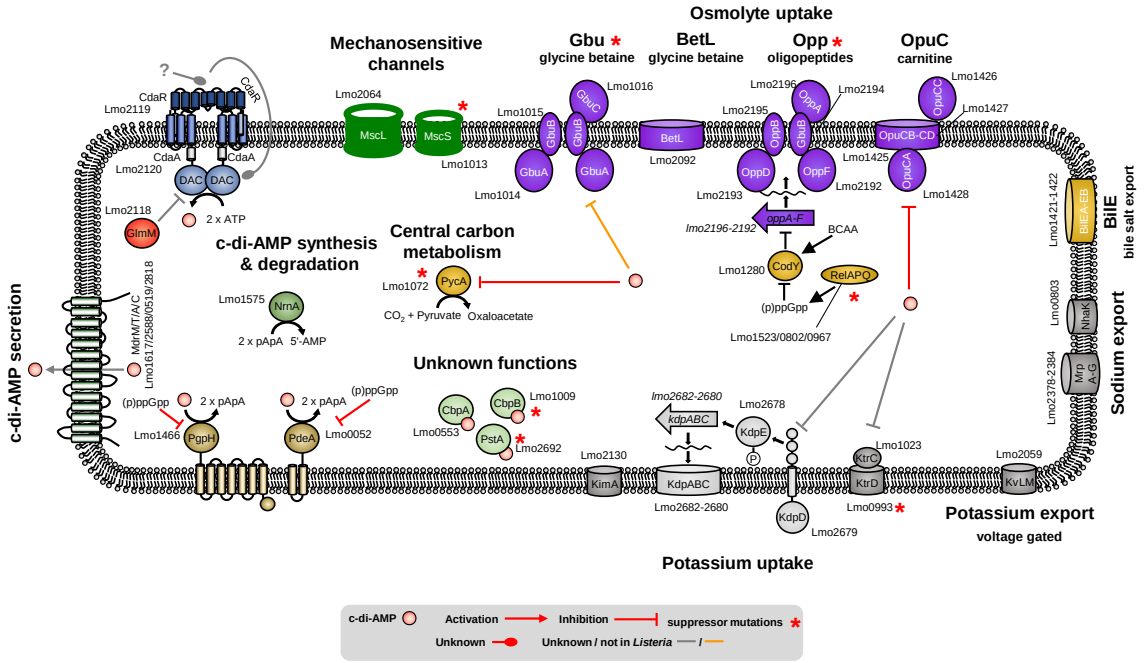

Fig. 1.3 c-di-AMP signaling and osmoregulation in *L. monocytogenes*. c-di-AMP is synthesized in *L. monocytogenes* by the sole DAC CdaA that is regulated by CdaR and GlmM in *L. monocytogenes*. c-di-AMP has been shown to be secreted by the multidrug resistance transporters and degraded by the PDE PdeA (GdpP) and PgpH. *L. monocytogenes* also harbors a homolog of the nano-RNase NrnA that has been shown to degrade pApA further to AMP. c-di-AMP binds to the proteins of unknown function CbpA, CbpB and PstA (DarA). It has also been shown to inhibit the pyruvate carboxylase PycA and the osmolyte (carnitine) uptake system OpuC in *L. monocytogenes*. c-di-AMP has also been shown to inhibit uptake of glycine betaine in other organisms via homologs of the Gbu osmolyte transporter, but no binding could be identified for *L. monocytogenes*. In other bacteria, c-di-AMP has been shown to inhibit potassium uptake of the KtrCD low affinity potassium transporter and to inhibit transcription of the KdpABC high affinity transporter by binding to KdpD of the KdpDE two-component system. Despite those c-di-AMP-related systems, *L. monocytogenes* possesses other proteins that have been shown to play a role in un- or specific osmoregulation. Those are the mechanosensitive channels MscL and MscS (large and small conductance, respectively), the glycine betaine uptake system BetL, the voltage gated potassium exporter Lmo2059 (KvLm), homologs of the *B. subtilis* sodium exporter NhaK and MrpA-G. *L. monocytogenes* also expressed a bile salt specific exporter that is important in virulence (BilE) and an oligopeptide transporter, whose expression is regulated by CodY and the stringent response. In *L. monocytogenes* c-di-AMP signaling related suppressor mutations have been found in CbpB, PstA, KtrD, RelA, Gbu system, Opp system and PycA, indicating a functional relationship between them and c-di-AMP signaling (based on Commichau *et al.*, 2018).

As depicted, *L. monocytogenes* encodes homologs of two high-affinity potassium uptake systems, KimA and KdpABC, that are translational or transcriptional controlled by c-di-AMP in *B. subtilis* and *S. aureus* respectively. Interestingly, the *kimA* riboswitch seems to be absent in *L. monocytogenes* (Nelson *et al.*, 2013). *L. monocytogenes* also encodes a voltage gated potassium transporter KvLm (Lmo2059; Santos *et al.*, 2008; Santos *et al.*, 2012) and homologs of two potential sodium export system Lmo0803 (NhaK) and Lmo2378-2374 (MrpA-G). Furthermore, *L. monocytogenes* possesses two uptake system for glycine betaine, GbuABC and BetL, an uptake system for oligopeptides (OppABCDF), an uptake system for carnitine (OpuC) and a bile salt specific exporter (BilE), demonstrating a broad set of different osmolyte transport systems (for further details see chapters above). Of those Gbu, Opp and Opu have been directly or indirectly implicated to be regulated by c-di-AMP (**Fig. 1.3**). Genes for homologs of two mechanosensitive channels Lmo2064 and Lmo1013 (MscL and MscS, respectively) and the c-di-AMP binding proteins, PycA, CbpA, CbpB and PstA (DarA) are also present. Several c-di-AMP secreting multi drug efflux systems (MdrMTAC) and two PDEs PdeA (GdpP) and PgpH and a potential homolog of the nano-RNase NrnA (Lmo1575) are

present, as well. Concerning the synthesis of c-di-AMP, *L. monocytogenes* harbors only on DAC domain containing enzyme, CdaA, or also called DacA, encoded together with its regulator CdaR and also the GlmM enzyme (Commichau *et al.*, 2018; Kaplan Zeevi *et al.*, 2013; Rismondo *et al.*, 2016; Rosenberg *et al.*, 2015; Sureka *et al.*, 2014; Whiteley *et al.*, 2015; Whiteley *et al.*, 2017; Woodward *et al.*, 2010).

L. monocytogenes has a broad set-up of osmolyte transport systems, interesting life-style changes and is known for its adaptiveness. The bacterium encodes only one DAC, of the most abundant CdaA-type that is a prime target for finding novel antibiotics. These characteristics make *L. monocytogenes* an interesting subject to study c-di-AMP and its effect on osmoregulation and especially how synthesis of c-di-AMP might be regulated and coupled to sensing alterations in the osmotic state of the environment.

Objective of this thesis

One of the major open questions about c-di-AMP signaling is how the cell senses changes in osmolarity to modulate DAC activity. The DAC CdaA is the most abundant type of c-di-AMP synthesizing enzyme, present in a lot of firmicute pathogens and hence an interesting target for novel antibiotics. It was hypothesized that CdaA activity is modulated by the CdaR and the GlmM protein. The YbbR domains of CdaR have an unknown function and are a potential sensory domain that allow CdaR to sense changes in osmolarity and convey the signal input to CdaA. GlmM in contrast could serve to connect cell wall biosynthesis to osmoregulation that need to be intertwined to allow adaption of the cell to turgor changes. We therefore aimed to deepen the knowledge of the role of CdaR and GlmM in regulation of CdaA activity.

Furthermore, the identifications of novel c-di-AMP regulated processes in *L. monocytogenes* is crucial to elucidate the signaling network. Therefore, the identification of c-di-AMP binding proteins in *L. monocytogenes*, the investigation of their function and regulation is another focus of this study. The main interest in this context were proteins, like potassium transporter, that play important roles in osmoregulation.

c-di-AMP has been shown to impact a variety of cellular functions, ranging from osmoregulation, cell wall biosynthesis to DNA damage repair. To broaden the understanding of the c-di-AMP signaling network, we analyzed the effects of a *cdaA* deletion mutant in *L. monocytogenes*. The aim was to find novel pathways that are transcriptional or translational regulated by c-di-AMP using a transcriptomic and proteomic approach.

Finally, c-di-AMP is synthesized by other types of DACs. The second most abundant class is of the DNA-binding DisA type. Hence, we wanted to investigate the regulation of DisA from *B. subtilis* in the context of osmoregulation. We hypothesized that DNA-binding of DisA might be regulated by macromolecular crowding upon osmotic stress, as it has been shown for other DNA-binding proteins that are involved in osmoregulation.

Summarizing, the main goal of the following work was to expand the current knowledge about the fascinating second messenger c-di-AMP and its important regulatory functions in *L. monocytogenes*.

2. The YbbR domain-containing protein CdaR regulates di-adenylate cyclase activity of CdaA

Johannes Gibhardt, Ole Hinrichs, Volkhard Kaever, and Fabian M. Commichau

Author contribution:
JG and OH performed the experiments. VK performed the c-di-AMP measurements. JG and FMC wrote the manuscript.

Abstract

The regulation of osmotic homeostasis in Firmicutes is regulated by the second messenger c-di-AMP. This signal molecule has been shown to regulate various osmolyte transport systems for the uptake of potassium or glycine betaine in important bacteria, like *Bacillus subtilis*, *Listeria monocytogenes* or *Staphylococcus aureus*. One of the most important open questions is still the regulation of synthesis and degradation of c-di-AMP, by diadenylate cyclases (DACs) and phosphodiesterases (PDEs), respectively. Here, we show that *cdaR*, which is located in an operon with *cdaA*, is involved in osmotic regulation of *L. monocytogenes*. A Δ*cdaR* mutant was identified in a phenotype microarray to have an altered metabolic activity under osmotic stress conditions and shows a decreased growth rate if grown with the osmolytes NaCl, KCl, or sorbitol. Furthermore, we show that the YbbR domains of CdaR are involved in regulation of c-di-AMP levels and osmotic adaptation. Topology determinations show that these domains are located towards the outside, potentially sensing mechanic forces in the bacterial cell wall due to turgor changes. In addition, we demonstrate in an *E. coli*-based screening system the ability of CdaR and of the phosphoglucosamine mutase GlmM to influence DAC activity of CdaA. Additionally, we show that both, membrane localization and the YbbR domains of CdaR are important for proper function of the regulatory process. Moreover, suppressor mutants that show increased resistance to osmotic stress impact the stress sigma Factor SigB, leading to its inactivation. Finally, we show a potential interaction network between synthesis and degradation systems of the *L. monocytogenes* c-di-AMP metabolic network.

Introduction

The second messenger c-di-AMP has been discovered a decade ago in the crystal structure of the DNA-integrity scanning protein DisA (Witte *et al.*, 2008). Interestingly, it is the first second messenger that is both, essential and toxic at the same time (Corrigan *et al.*, 2011; Gundlach *et al.*, 2015b; Mehne *et al.*, 2013; Woodward *et al.*, 2010). c-di-AMP is also a special second messenger, since it has been shown to regulate a biological process on more than one level – by regulating the expression of a gene and the activity of the protein. It binds to the *kimA* riboswitch, preventing gene expression of the *ktrAB* genes that encode for the high affinity potassium transporter KtrAB and it also binds KtrA directly, inhibiting the potassium import (Corrigan *et al.*, 2013; Gundlach *et al.*, 2017; Kim *et al.*, 2015; Nelson *et al.*, 2013). This two-level regulation, demonstrates that regulation of potassium import needs to be tightly controlled, because it is one of the most important tools bacteria have to adapt to changes in extracellular osmolarity as a first response (Sleator & Hill, 2002). Adaptation to changes in osmolarity is a complex process involving not only regulated uptake of potassium but furthermore the later replacement of potassium with more compatible solutes, such as glycine betaine and also the adaption of cell wall and membrane to allow the bacterial cell envelope to adapt accordingly to the changes in turgor (Misra *et al.*, 2013; Rojas *et al.*, 2014; Sévin & Sauer, 2014; Wood *et al.*, 2001). Uptake or synthesis of compatible solutes is a widespread tool and bacteria, as *Escherichia coli*, *B. subtilis*, *L. monocytogenes*, *S. aureus*, *Salmonella typhimurium* or *Streptococcus pneumoniae* all developed mechanisms for synthesis or uptake of different compatible solutes (Sleator & Hill, 2002). Interestingly, c-di-AMP does not only regulate potassium import systems, but also the import of compatible solutes like glycine betaine or carnitine (Huynh *et al.*, 2016; Schuster *et al.*, 2016; Zeden *et al.*, 2018). c-di-AMP can therefore be described as the major regulator of osmotic homeostasis in Firmicutes. Despite the increasing knowledge about its function and target proteins, a lot is still unknown. Recently, conditions were found, under which c-di-AMP is dispensable (Gundlach *et al.*, 2017; Whiteley *et al.*, 2015; Whiteley *et al.*, 2017; Zeden *et al.*, 2018). Intriguingly, those conditions are defined growth conditions, under which osmolyte availability is limited. Gundlach *et al.* could show that c-di-AMP levels in *B. subtilis* concord with the external concentrations of potassium and also the nitrogen source (Gundlach *et al.*, 2015b; Gundlach *et al.*, 2017). The bacteria must therefore have systems in place that can detect the osmotic state they are living in and adjust synthesis and degradation of c-di-AMP accordingly. This is also one of the major open questions: how do bacteria sense changes in osmolarity and how do they confer these stimuli to altered activity or expression of the DACs and PDEs. For the DisA-type cyclase, it has been shown that binding of DNA, especially complex holiday junction structure inhibits its enzymatic function (Bejerano-Sagie *et al.*, 2006; Witte *et al.*, 2008). It is unclear though, how this might be connected to changes in osmolarity. *B. subtilis* is of special interest for c-di-AMP research, since it is the only bacterium that has three DACs, DisA, CdaA and the sporulation specific CdaS (Mehne *et al.*, 2014). CdaS is only highly expressed after sporulation initiation (Nicolas *et al.*, 2012). It features a C-terminal DAC domain and two N-terminal helices. Truncation of those helices leads to hyperactivity of the catalytic domain and they are therefore designated as autoinhibitory domains (Mehne *et al.*, 2014). The regulatory effect of these N-terminal helices *in vivo* is unknown and remains to be elucidated. The CdaA type of DACs, which is also referred to DacA, is a membrane bound enzyme (Corrigan *et al.*, 2011; Mehne *et al.*, 2013; Rosenberg *et al.*, 2015; Woodward *et al.*, 2010). It consists of three N-terminal transmembrane (TM) domains, a coiled-coiled domain, followed by the DAC domain and another C-terminal coiled-coiled domain. *cdaA* is genetically conserved with *cdaR*, the gene encoding the CdaR protein and *glmM* encoding the phosphoglucosamine mutase GlmM. CdaR has an N-terminal domain, designated as signal peptide and four YbbR domains of unknown function. GlmM on the other

side is a cytosolic protein that catalyzes the conversion of glucosamine-6-phosphate to glucosamine-1-phosphate and is therefore one of the early enzymes for peptidoglycan synthesis and essential (Mehne *et al.*, 2013; Rismondo *et al.*, 2016; Tosi *et al.*, 2019). Interestingly, it has been shown that GlmM affects CdaA activity in *Lactococcus lactis* (Zhu *et al.*, 2016), demonstrating a regulatory cross-talk between c-di-AMP metabolism (and therefore osmotic regulation) and cell wall biosynthesis. In the present study, we show that both the CdaR and GlmM proteins are able to modulate CdaA activity *in vivo*. Furthermore, we show that the YbbR domains of CdaR are important for the regulation of CdaA activity. They are located outside of the cell and might act as a sensor for turgor changes in the cell envelope. We furthermore show interactions between multiple parts of the c-di-AMP metabolic network, demonstrating potential cross-talk between the synthesis and degradation machineries.

Experimental procedures

Bacterial strains and growth conditions – *L. monocytogenes* EGD-e and its derivatives were cultivated in BHI medium (Sigma-Aldrich) at 37°C and 220 rpm if not specified otherwise. *E. coli* was grown in LB medium at 37°C and 220 rpm (strains **see Tab. 2.1**). For agar plates, medium was supplemented with 15 g/l Bacto Agar (Difco). Antibiotics and medium supplements were used with the following concentrations, if indicated: erythromycin (5 µg/ml), kanamycin (50 µg/ml), ampicillin (100 µg/ml), chloramphenicol (30 µg/ml), streptomycin (100 µg/ml), X-Gal (100 µg/ml; 5-bromo-4-chloro-3-indolyl-β-D-galactopyranoside; Sigma-Aldrich), IPTG (1 mM or 50 µM; Isopropyl β-D-1-thiogalactopyranoside; Sigma-Aldrich), L-arabinose (0.005% (*w/v*)). For *E. coli* experiments under defined conditions, a modified, potassium defined M9 medium was used, as described elsewhere (**see chapter 3**). As a minimal medium for *L. monocytogenes* the LSM medium (Whiteley *et al.*, 2017) was used with the following minor changes (equimolar substitutions): riboflavin-5'-monophosphate instead of Riboflavin, L-isoleucine, L-methionine and L-valine instead of the DL-enantiomers and L-cysteine · HCL · H_2O instead of L-cysteine · 2 HCL. For pouring minimal medium agar plates, 2 X concentrated medium was pre-warmed to 37°C and mixed with to 70°C pre-warmed 2 X Bacto agar, directly before pouring the plates.

DNA manipulation – DNA amplification *via* PCR and transformation of *E. coli* was performed using standard procedures (Sambrook *et al.*, 1989). DNA fragments were purified using the PCR purification kit (Qiagen) and plasmid DNA was extracted using the NucleoSpin Plasmid Kit (Macherey and Nagel). Commercially available restriction enzymes, T4 DNA ligase and DNA polymerases were used as recommended by the manufacturers. DNA sequences were determined by the dideoxy chain termination method (Microsynth, Göttingen, Germany). Chromosomal DNA of *L. monocytogenes* was isolated using the NucleoSpin Microbial DNA Kit (Macherey and Nagel). Oligonucleotides were purchased from Sigma-Aldrich (Germany).

Tab. 2.1 Strains

Name	Genotype	Description/Construction	Reference
E. coli			
BL21(DE3)	F^- *ompT gal dcm lon hsdS*$_B$($r_B^-m_B^-$) λ(DE3 [*lacI lacUV5-T7p07 ind*1 *sam*7 *nin*5]) [*malB*$^+$]$_{K-12}$(λ^S)	Protein expression	Stratagene
BTH101	F^- *cya*99 *araD*139 *galE*15 *galK*16 *rpsL*1 (Str^R) *hsdR*2 *mcrA*1 *mcrB*1	BACTH assays	Karimova *et al.*, 1998

Name	Genotype	Description/Construction	Reference
DH5α	F$^-$ ϕ80*lacZ*ΔM15 Δ(*lacZYA-argF*) U169*rec*A1 *end*A1 *hsd*R17 (r_k^-, m_k+) *gal*$^-$ *phoA supE*44 λ$^-$ *thi*$^-$1 *gyrA*96 *relA*1	PhoA and LacZ assays	Sambrook *et al.*, 1989
LB2003	F$^-$ *aroE rpsL metE thi gal rha kup1* (*trkD1*) Δ*kdpABC*5 Δ*trkA aroE*$^+$	Potassium importer deficient strain	Stumpe & Bakker, 1997
XL1-Blue	*rec*A1 *end*A1 *gyr*A96 *thi*$^-$1 *hsdR*17 *supE*44 *relA*1 *lac* [F' *proAB lacI*^{q} ZΔM15 Tn*10* (*Tet*^{R})]	Cloning	Stratagene
L. monocytogenes			
EGD-e	Wild type	Serotype 1/2a strain	Laboratory collection
LMJR45	Δ*cdaR*	Chromosomal deletion of *cdaR*	Rismondo *et al.*, 2016
BPL16	Δ*cdaR attB*::P$_{help}$-*lacO-cdaR lacI neo*	IPTG-dependent *cdaR* expression	Rismondo *et al.*, 2016
BPL45	*attB*::P$_{help}$-*lacO*-MCS *lacI neo*	pIMK3 → EGD-e	This work
BPL46	Δ*cdaR attB*::P$_{help}$-*lacO*-MCS *lacI neo*	pIMK3 → LMJR45	This work
BPL47	Δ*cdaR attB*::P$_{help}$-*lacO-cdaR* (*aa* 32-452; ΔTM) *lacI neo*	pBP255 → LMJR45	This work
BPL48	Δ*cdaR attB*::P$_{help}$-*lacO-cdaR* (*aa* 1-320; ΔYbbR domain 4) *lacI neo*	pBP256 → LMJR45	This work
BPL49	Δ*cdaR attB*::P$_{help}$-*lacO-cdaR* (*aa* 1-230; ΔYbbR domain 3-4) *lacI neo*	pBP257 → LMJR45	This work
BPL50	Δ*cdaR attB*::P$_{help}$-*lacO-cdaR* (*aa* 1-130; ΔYbbR domain 2-4) *lacI neo*	pBP258 → LMJR45	This work
BPL51	Δ*cdaR attB*::P$_{help}$-*lacO-cdaR* (*aa* 1-33; ΔYbbR domain 1-4) *lacI neo*	pBP259 → LMJR45	This work
BPL52	*rsbU* 128G>T (E116X)	EGD-e suppressor mutant, isolated on LSM + 0.5 M D-sorbitol	This work
BPL53	*sigB* 178GT>CC 171_175delCAAGT (I71X)	EGD-e suppressor mutant, isolated on LSM + 0.5 M D-sorbitol	This work
BPL55	Δ*cdaR* pIMK3 *rsbU* 665C>T (A222V) *pdeA* 1698C>T	BPL46 suppressor mutant, isolated on LSM + 0.25 M NaCl	This work
BPL56	Δ*cdaR* pIMK3 *lmo1515* 261delC (L115X)	BPL46 suppressor mutant, isolated on LSM + 0.25 M NaCl	This work
BPL57	Δ*cdaR* pIMK3 *rsbU* 532delG (L189X)	BPL46 suppressor mutant, isolated on LSM + 0.25 M NaCl	This work
BPL58	Δ*cdaR* pIMK3 *lmo0892*/*lmo0893* intergenic (929,827A>G; 929,831_929,832insAA; 929,832T>A; 929,836A>G; 929,842T>A; 929,845GT>TA; 929,854AA>GT; 929,857T>A; 929,861C>T; 929,866T>A; 929,868C>A; 929,870TA>AG; 929,879A>G; 929,881GG>TT) *lmo1432*/*lmo1433* intergenic (1,464,183C>T)	BPL46 suppressor mutant, isolated on LSM + 0.25 M KCl	This work
BPL59	Δ*cdaR* pIMK3 *lmo1515* 412_422dupTTTTATATTTA; 423delA (X141fs173)	BPL46 suppressor mutant, isolated on LSM + 0.25 M KCl	This work
BPL77	Δ*cdaA*	pBP352 →→EGD-e	This work

neo = kan^R (50 µg/ml kanamycin); → transformation; →→ transformation and gene deletion; aa = amino acids, :: = insertion

Plasmid construction – For the determination of the membrane topology of the CdaR protein, plasmids pBP250 (*cdaR*), pBP251 (*cdaR* aa 1-33; ΔYbbR domains), pBP252 (*cdaR* aa 34-452; ΔTM domain), pBP253 (*prkA*; *lmo1820*) and pBP254 (*prfA*; *lmo0200*) were constructed on the base of the pKTop plasmid (Karimova *et al.*, 2009; plasmids are listed in **Tab. S2.1**). This plasmid allows the IPTG-dependent expression of fusion proteins with a C-terminal *phoA* gene and the *lacZ* α-

fragment. The genes were amplified using oligonucleotide pairs JH121/122, JH121/124, JH123/JH122, JH126/127 and JH128/JH129, respectively (oligonucleotides are listed in **Tab. S2.2**). The resulting DNA fragments were digested with *Bam*HI/*Kpn*I and ligated to pKTop, digested with the same enzymes. To analyze the effect of the membrane localization and the role of the YbbR domains *in vivo*, plasmids pBP255 (*cdaR* aa 32-452; ΔTM), pBP256 (*cdaR*; aa 1-320; ΔYbbR 4), pBP257 (*cdaR*; aa 1-230; ΔYbbR 3-4), pBP258 (*cdaR*; aa 1-130; ΔYbbR 2-4), pBP259 (*cdaR*; aa 1-33; ΔYbbR 1-4) were constructed on the base of the pIMK3 plasmid (Monk *et al.*, 2008). The pIMK3 plasmid allows for IPTG-dependent, ectopic expression of genes in *L. monocytogenes* EGD-e by integration of the whole plasmid in the $tRNA^{Arg}$ locus (*lmot17*). The genes were amplified using the oligonucleotide pairs JH130/JH22, JH21/JH132, JH21/JH133, JH21/JH134 and JH21/JH131, respectively. The resulting DNA fragments were digested using *Nco*I/*Sal*I and ligated to pIMK3, digested with the same enzymes. For the analysis of CdaA activity in *E. coli* and the impact of GlmM, CdaR and CdaR variants on its activity, plasmids pBP387 (*cdaA-cdaR*), pBP388 (*cdaA-cdaR-glmM*), pBP389 (*cdaA-glmM*), pBP260 (*cdaA-cdaR* aa 34-452; ΔTM), pBP261 (*cdaA-cdaR* aa 1-320; ΔYbbR 4), pBP262 (*cdaA-cdaR* aa 1-230; ΔYbbR 3-4), pBP263 (*cdaA-cdaR* aa 1-130; ΔYbbR 2-4) and pBP264 (*cdaA-cdaR* aa 1-33; ΔTM) were constructed based on the pBAD33 plasmid (Guzman *et al.*, 1995). The genes for pBP387, pBP261, pBP262, pBP263 and pBP264 were amplified using oligonucleotide pairs JH51/JH103, JH51/JH138, JH51/JH139, JH51/JH140 and JH51/JH137, respectively. The resulting DNA fragments were digested with *Xba*I/*Pst*I and ligated to pBAD33, digested with the same enzymes. For pBP388 and pBP389, the *glmM* gene was amplified with the oligonucleotides JH104 and JH105 and the resulting DNA fragments digested with *Pst*I/*Hind*III. They were ligated to pBP387 (pBAD33-*cdaAR*) or pBP370 (pBAD33-*cdaA*) digested with the same enzymes, respectively (Quintana *et al.*, 2019). For the construction of plasmid pBP260, the *cdaA* gene and the *cdaR* gene - lacking the first 33 amino acids - were amplified using oligonucleotide pairs JH51/JH135 and JH136/JH103, respectively. The two products were fused *via* splicing by overlap extension PCR (Horton *et al.*, 1990) using oligonucleotides JH51 and JH103. The resulting DNA fragment was digested with *Xba*I/*Pst*I and ligated to pBAD33, digested with the same enzymes. To analyze the protein-protein interaction of different proteins of the c-di-AMP metabolism, plasmids pBP359 to pBP362 (*glmM*; *lmo2118*), pBP269 to pBP272 (*pdeA*; *lmo0052*), pBP273 to pBP276 (*pgpH*; *lm1466*) and pBP277 to pBP280 (*kimA*; *lmo2130*) were constructed on basis of the BACTH plasmids pUT18, pUT18C, p25-N and pKT25, respectively (Claessen *et al.*, 2008; Karimova *et al.*, 1998). These plasmids allow the construction of either C- or N-terminal T18 or T25 domains of the cAMP adenylate cyclase to investigate protein-protein interactions in *E. coli* strains with *cya* mutations, lacking the native cAMP AC gene, like the BTH101 strain (Karimova *et al.*, 1998). The genes for *glmM*, *pdeA*, *pgpH* and *kimA* were amplified using oligonucleotide pairs FC336/FC337, JH160/JH161, JH162/JH163 and JH164/JH165, respectively. Resulting DNA fragments were digested with *Xba*I/*Kpn*I and ligates to pUT18, pUT18C, p25-N or pKT25, which were digested with the same enzymes, respectively. For the chromosomal deletion of the *cdaA* gene, pBP352 was constructed. The up- and downstream regions of *cdaA*, while sparring the *cdaA* ORF out, were amplified using oligonucleotide pairs JH05/JH06 and JH07/JH08, respectively. The resulting PCR products were fused by SOE PCR using oligonucleotides JH05 and JH08, digested with *Eco*RI and *Bam*HI and ligated to pMAD (Arnaud *et al.*, 2004; Horton *et al.*, 1990), which was digested using the same enzymes. Plasmids pBP223 and pBP131 were constructed for overexpression of N-terminal-Strep-tagged CdaR (Δaa 1-28) and PrfA, respectively. The *cdaR* and *prfA* genes were amplified using oligonucleotide pairs JR56/JR28 and FC206/FC205, respectively. The resulting DNA fragments were digested using *Sac*I/*Bam*HI and *Sac*I/*Bgl*II, respectively and ligated to pGP172, digested with *Sac*I/*Bam*HI (Merzbacher *et al.*, 2004).

L. monocytogenes *strain construction* – For the investigation of the impact of CdaR on c-di-AMP synthesis and adaptation to osmotic stress *in vivo*, *L. monocytogenes* mutants were constructed as follows. Electrocompetent cells were prepared as described elsewhere (Monk *et al.*, 2008). Shortly, the EGD-e wt or the Δ*cdaR* mutant (LMJR45) were cultured in BHI until early exponential phase, the cell wall synthesis was at this point inhibited by 10 µg/ml ampicillin for two hours at 37°C and 220 rpm. Afterwards, the cells were washed in decreasing amounts of SGW buffer (10% (*w/v*) glycerol, 500 mM sucrose, pH7) and incubated with10 µg/ml of lysozyme for 30 minutes at 37°C. The cells were washed one more time and frozen as aliquots in liquid nitrogen. For the electroporation of plasmid DNA, 50 µl of electrocompetent cells were added on 1-5 µg precipitated DNA, incubated for 10 min on ice and transferred to a chilled 0.1 cm gap electroporation cuvette (BioRad). Electroporation was performed at 18 kV/cm using the MicroPulser electroporator (BioRad). Immediately after the electroporation, 1 ml of to 37°C pre-warmed medium was added and the cells incubated for 1.5 h at 30°C without agitation. Eventually, bacteria were plated on selective media and correct chromosomal integration of the pIMK3 derivatives was confirmed *via* PCR and integrity of the MCS by Sanger sequencing. With this protocol, the following strains were constructed: BPL45 (EGD-e + pIMK3 empty plasmid), BPL46 (Δ*cdaR* + pIMK3 empty plasmid), BPL47 (Δ*cdaR* + pBP255 (pIMK3-*cdaR* ΔTM)), BPL48 (Δ*cdaR* + pBP256 (pIMK3-*cdaR* ΔYbbR 4)), BPL49 (Δ*cdaR* + pBP257 (pIMK3-*cdaR* ΔYbbR 3-4)), BPL50 (Δ*cdaR* + pBP258 (pIMK3-*cdaR* ΔYbbR 2-4)), BPL51 (Δ*cdaR* + pBP259 (pIMK3-*cdaR* ΔYbbR 1-4)). For the chromosomal deletion of the *cdaA* gene, strain BPL77 was constructed as follows. The EGD-e wt was electroporated with plasmid pBP352 (pMAD-Δ*cdaA*) and plated on LSM medium with erythromycin and X-Gal at 30°C for up to 72 h. Single, blue colonies were streaked on the same medium and incubated for up to 72 h at 42°C to force integration into the *cdaA* locus. Several blue colonies were used to inoculate 5 ml of LSM without antibiotics at 30°C for 4 h, temperature was shifted to 42°C for 6 h, after which serial dilutions were plated on LSM medium with X-Gal and incubated at 37°C for up to 72 h. Erythromycin-sensitive, X-Gal negative bacteria that did grow on LSM medium but not on BHI were subjected to colony PCR as described elsewhere (Dussurget *et al.*, 2002). *cdaA* deletion and absence of ectopic suppressor mutations was confirmed by whole genome sequencing (WGS) and Sanger sequencing and the strain designated BPL77.

Phenotypic microarray screening – To screen for a phenotype of the Δ*cdaR* mutant (LMJR45), a Phenotype MicroArray (PM; Biolog Inc.; Bochner *et al.*, 2001) was employed. The *L. monocytogenes* wt or the Δ*cdaR* mutant were streaked to single colonies on BHI agar plates (37°C overnight). 10 ml of BHI were incubated from a single colony at 37°C and 220 rpm to an OD_{600} of 0.4-0.5. 9 ml of those cultures were harvested by centrifugation at 3300 g for 10 min at 4°C and the pellet resuspended in 1 ml BHI with 25% (*w/v*) glycerol, frozen in liquid nitrogen and stored at -80°C. A 10 µl inoculation loop was used to freshly re-streak the bacteria from cryo cultures on BHI agar plates to a bacterial lawn, prior to each PM and incubated for 20 h at 37°C. The cells were scratched evenly from the bacterial lawn, resuspended in the manufactures inoculation fluid and adjusted to an OD_{600} of 0.3 in 1 ml of the inoculation fluid. The remaining treatment was performed according to the recommendations of the manufacturer. The cells were incubated on the different PM 96-well plates (Microtest Plate 96-Well,F, Sarstedt) with 100 µl of cells per well for 48 hours at 37°C with orbital shaking (237 cpm, 4 mm) and the OD_{590} was measured in 30 min intervals using an Epoch2 multiwell reader, equipped with the Gen5 software (02.09.2001; BioTek Instruments).

Osmotic stress and bacterial growth – To evaluate the osmotic phenotype of the Δ*cdaR* mutant (LMJR45), seen in the Biolog PM, the growth of the mutant was compared to the EGD-e wt under osmotic stress. Bacteria were pre-cultured overnight from single colonies in 5 ml BHI medium at

37°C and 220 rpm. 10 ml BHI were inoculated from the pre-cultures to an OD_{600} of 0.1 and grown at 37°C and 220 rpm until they reached an OD_{600} of 0.4-0.8. The optical density was adjusted to 0.2 and 100 µl of the cell suspension was pipetted into 96-well plates, containing 100 µl BHI medium with or without various concentrations of NaCl, KCl, or D-sorbitol. The final concentrations were 0, 0.25, 0.5, 0.75, 1, 1.5 and 2 M of the different osmolytes. Bacteria were grown at 37°C and 237 cpm (4 mm) agitation using an Epoch2 multiwell platereader, equipped with the Gen5 software (02.09.2001; BioTek Instruments) and the optical density was determined in 15 min intervals at 600 nm. Growth rates of the exponential phases were determined as described elsewhere (**see chapter 3**) and plotted against the osmolyte concentration.

Protein purification and generation of an anti-CdaR and anti-PrfA antiserum – Plasmids pBP223 and pBP131 were used to overexpress the N-terminally Strep-tagged CdaR (Δaa 1-28) and PrfA from *L. monocytogenes*, respectively, using BL21(DE3) as described previously for CdaA (Rosenberg *et al.*, 2015). The proteins were purified with the Strep-tag II–Strep-Tactin purification system (IBA, Göttingen, Germany) and used for the generation of polyclonal antibodies in rabbits (Seqlab, Göttingen, Germany). The antibodies were diluted 1:1000 for Western blot analyses.

Western blot analysis of CdaR localization – Strains EGD-e (wt), BPL77 (Δ*cdaA*) and LMJR45 (Δ*cdaR*) were cultivated in 100 ml LSM at 37°C and 220 rpm from an OD_{600} of 0.05 to about 0.5 and harvested by centrifugation for 10 min at 3300 g and 4°C. Pellets were washed once in 10 ml ZAP (50 mM Tris-HCl, pH 7.5, 200 mM NaCl). Pellets were resuspended in 400 µl ZAP with DNase I (0.5 U/ml; Sigma-Aldrich) and cOmplete EDTA-free Protease Inhibitor Cocktail (1 tablet/50 ml; Sigma-Aldrich). 200 µl of cell suspension were added to 0.5 g glass beads (0.1 mm diameter; Carl Roth) and disrupted using a TissueLyserII (Qiagen) for 15 min at 30 Hz at 4°C. 600 µl of the buffer was added to the tubes and incubated for 10 min on ice. Samples were centrifuged for 2 min at 20000 g and 4°C and the supernatant transferred to a new tube (whole cell lysate). 1 ml was subjected to ultracentrifugation at 235000 g for 1 h at 4°C. The supernatant was transferred to a new tube (cytosolic fraction) and the pellet resuspended in 1 ml of buffer. After a second ultracentrifugation for 30 min, the supernatant was transferred to a new tube and the pellet resuspended (membrane fraction) in 100 µl of the buffer with 17 mM CHAPS (3-[(3-Cholamidopropyl)dimethylammonio]-1-propanesulfonate hydrate; Sigma-Aldrich). Protein concentrations were determined by Bradford assay (Sambrook *et al.*, 1989) and 10 µg of protein extracts separated on 12% SDS polyacrylamide gels. Proteins were transferred on a polyvinylidene difluoride membrane (Bio-Rad) by electroblotting. Proteins were detected by specific antibodies against CdaA (Rosenberg *et al.*, 2015), CdaR or PrfA, respectively. The primary antibodies were visualized by using anti-rabbit IgG (immunoglobulin G) AP (alkaline phosphatase) secondary antibodies (Promega) and the CDP* detection system (Roche Diagnostics).

Determination of CdaR membrane topology – To determine the location of the YbbR domains of the CdaR regulatory protein, plasmids pBP250, pBP251, pBP252, pBP253, pBP254 and the pKTop empty plasmid. *E. coli* DH5α was subsequently transformed with the constructed plasmids. This strain has a deletion of the *phoA* gene, encoding the alkaline phosphatase PhoA and the Δ(*lacZ*)M15 mutation that allows complementation of the β-galactosidase with the LacZ α-fragment. The bacteria were grown in LB supplemented with kanamycin from an OD_{600} of 0.1 to 0.3-0.6 from overnight cultures. The OD_{600} was adjusted to 0.1 and 5 µl of the cell suspension was streaked out on LB plates containing kanamycin, 1 mM IPTG, 80 µg/ml X-phosphate (5-Bromo-4-chloro-3-indolyl phosphate disodium salt; Sigma-Aldrich), 100 µg/ml RedGal (6-Chloro-3-indolyl-β-D-galactopyranoside; Sigma-Aldrich) and 50 mM sodium phosphate buffer (pH 7). The plates were incubated overnight at 37°C (Karimova *et al.*, 2009). For the quantification of the alkaline

phosphatase and β-galactosidase activity a slightly modified procedure as described by (Thongsomboon *et al.*, 2018) was applied. DH5α cells, containing the afore mentioned plasmids, were grown in LB medium containing kanamycin from overnight cultures from an OD_{600} of 0.1 to 0.5-0.6 at 37°C and 220 rpm. Four times 1.5 ml cell culture were harvested by centrifugation at 20000 g, 4°C for 2 min, two of them were washed in 1 ml Z buffer (60 mM Na_2HPO_4, 40 mM NaH_2PO_4, 10 mM KCl, 1 mM $MgSO_4$) and the other two in 1 ml 10 mM Tris (pH 8). Cell pellets were resuspended in 1ml of the same buffers and lysed by addition of 50 µl 0.1% (*w/v*) SDS, 50 µl chloroform, vortexing for 10 s and incubation at room temperature for 10 min. To determine the β-galactosidase activity, 200 µl of a 4 mg/ml ONPG (o-Nitrophenyl-β-D-galactopyranosid; Sigma-Aldrich) in Z buffer solution was added. Reactions were stopped by addition of 500 µl 1 M Na_2CO_3 when samples turned yellow, the time difference was noted and the OD_{415} of the supernatant was measured after 10 min of centrifugation at 20000 g. Afterwards the specific β-galactosidase activity [µmol/min/mg] was calculated using the following formula: $(3.38 \cdot OD_{415})/(OD_{600} \cdot V\ (1.5) \cdot \Delta t$ [min]). For the determination of the alkaline phosphatase activity, 800 µl of lysed cells in 10 mM Tris (pH8) were added to 100 µl pNPP solution (SigmaFast solution 1 mg/ml -Nitrophenyl phosphate in 200 mM Tris pH 8; Sigma-Aldrich). The samples were incubated at 37°C until they turned yellow. Reactions were stopped by addition of 100 µl 3 M NaOH, the time was noted and the OD_{415} of the supernatant after 10 min of centrifugation (20000 g) was measured. Specific alkaline phosphatase activity [µmol/min/mg] was calculated using the following formula: $(6.46 \cdot OD_{415})/(OD_{600} \cdot V\ (1.5) \cdot \Delta t$ [min]).

Analysis of the role of CdaR in osmotic adaptation – To assess the role of CdaR and the YbbR domains on adaptation of *L. monocytogenes* to osmotic stress, drop dilution experiments were performed. Strains BPL45, BPL46, BPL47, BPL48, BPL49, BPL50, BPL51 and BPL16 (Δ*cdaR* + pIMK3-*cdaR*) were streaked out on BHI agar plates containing kanamycin and incubated overnight at 37°C. Single colonies were used to inoculate 5 ml of LSM medium with kanamycin overnight at 37°C and 220 rpm. These cultures were used to inoculate 5 ml LSM medium with kanamycin to an OD_{600} of 0.1. The bacteria were grown to an OD_{600} of 0.3-0.8, adjusted to 0.1 and 10 µl of serial dilutions were drop spotted on LSM agar plates with or without 0.25 M of NaCl, KCl or D-sorbitol. The plates were incubated at 37°C and photos taken every 24 h.

Isolation of suppressor mutants and WGS – Emerging suppressor mutants were re-streaked twice on the same medium as isolated, cultured overnight and chromosomal DNA isolated as stated above. WG illumina sequencing was performed by the G2L Göttingen, the resulting reads analyzed using the Geneious software (Geneious Prime 2019.0.4 (https://www.geneious.com)) and potential mutations re-sequenced by Sanger Sequencing (Microsynth, Göttingen). The phenotypes of the mutants were confirmed by additional drop dilution assays.

Determination of intracellular c-di-AMP concentration – Strains BPL45, BPL46, BPL16, BPL47 and BPL51 were cultivated from single colonies overnight in 10 LSM with kanamycin. These pre-cultures were used to inoculate 75 ml LSM medium with kanamycin and 1 mM IPTG to an OD_{600} of 0.1. Bacteria were incubated at 37°C with agitation (220 rpm) until they reached an OD_{600} of 0.5-0.6. At this time point (t_0) two times 10 ml samples for the determination of the c-di-AMP concentration and two times 1 ml samples for the determination of the protein concentration were taken (see below). Two times 27 ml of each culture was transferred into new flasks with either 3 ml of LSM or 3 ml of LSM with 2.5 M NaCl (- and + 250 mM NaCl, respectively). Cultures were incubated for another 25 minutes and once more samples were taken for c-di-AMP and protein amount determination. The 1 ml samples for protein concentration determination were harvested by centrifugation at 20000 g for 1 min at 4°C and further processed as described earlier (Rismondo *et al.*,

2016). The 10 ml samples for determination of the c-di-AMP concentration, were rapidly cooled by swirling in liquid nitrogen, centrifuged for 5 min at 3300 g and 4°C and the pellets frozen in liquid nitrogen. Samples were further processed, as described elsewhere (Rismondo *et al.*, 2016).

Bacterial two hybrid (BACTH) assay – To investigate possible protein-protein interactions between different enzymes of the c-di-AMP regulatory network, a BACTH assay was employed. Therefore, *E. coli* BTH101 was transformed with the plasmids pBP232-pBP235 (*cdaA*), pBP224-pBP227 (*cdaR*), pBP359-pBP362 (*glmM*), pBP269-pBP272 (*pdeA*), pBP273-pBP276 (*pgpH*), pBP277-pBP280 (*kimA*) and pGP976-pGP979 (rny^{Bsu}), which all are derivatives of plasmids pUT18, pUT18C, p25-N and pKT25. pUT18C-zip and pKT25-zip served as controls. *E. coli* was co-transformed with the plasmids in combinations that always a plasmid harboring the T18 and the T25 domain of the cAMP adenylate cyclase were together. As described in more detail elsewhere (Claessen *et al.*, 2008; Karimova *et al.*, 1998), 5 µl of bacteria were drop spotted on LB medium with kanamycin, ampicillin, streptomycin, 1 mM IPTG and X-Gal for 24-48 h at 30°C.

Impact of GlmM, CdaR and variants on CdaA activity in E. coli – Plasmid pBP384 (pWH844-*kimA*) allows the IPTG dependent expression of the *L. monocytogenes* potassium transporter KimA (**see chapter 3**). *E. coli* LB2003 was co transformed with the plasmid together with the pBAD33-based and plasmids pBP370 (*cdaA*) or pBP373 (*cdaA**) that allow the L-arabinose-inducible expression of the *L. monocytogenes* DAC CdaA or an inactive mutant CdaA* (D171N; Quintana *et al.*, 2019; Rosenberg *et al.*, 2015). This strain is deficient for potassium transport due to deletions in genes encoding for the three major potassium uptake systems of *E. coli* and is only viable in medium with sufficient potassium or if a potassium transporter is expressed in it (Stumpe & Bakker, 1997; **see chapter 3**). The plasmids pBP370 and pBP373 served hereby as controls for c-di-AMP production and no c-di-AMP production. In the same manner, *E. coli* LB2003 was co-transformed with the plasmids pBP387 (*cdaA-cdaR*), pBP388 (*cdaA-cdaR-glmM*), pBP389 (*cdaA-glmM*), pBP260 (*cdaA-cdaR* aa 34-452; ΔTM), pBP261 (*cdaA-cdaR* aa 1-320; ΔYbbR 4), pBP262 (*cdaA-cdaR* aa 1-230; ΔYbbR 3-4), pBP263 (*cdaA-cdaR* aa 1-130; ΔYbbR 2-4) or pBP264 (*cdaA-cdaR* aa 1-33; ΔTM) together with pBP384, respectively. For growth of LB2003, the NaCl was replaced with 1% (*w/v*) KCl in the LB medium to allow growth. Strains were cultivated in M9 minimal medium with 0.35 mM KCl, 50 µM IPTG and 0.005% (*w/v*) L-arabinose in an Epoch2 Multiwell reader, equipped with the Gen5 software (02.09.2001; BioTek Instruments), as described in more detail elsewhere (**see chapter 3**). Growth rates of the exponential phases were calculated to depict the impact of the different constructs on CdaA activity and therefore also the potassium import *via* the c-di-AMP-regulated KimA transporter.

Results

CdaR is membrane-localized and involved in adaptation to osmotic stress – As previously reported, a *L. monocytogenes* Δ*cdaR* (*lmo2119*) mutant shows elevated intracellular c-di-AMP concentrations, while expression and localization of the DAC CdaA - with which CdaR interacts - is not influenced (Rismondo *et al.*, 2016). CdaR has therefore been postulated to modulate CdaA activity by unknown environmental stimuli. To identify the triggers that are sensed by the CdaR protein, a phenotype microarray was employed. The Biolog PM plates PM1-10 and PM13B were used to investigate the influence of different carbon sources, nitrogen sources, antibiotics, pH and osmolytes on the metabolic activity of the *L. monocytogenes* wild type (wt) and the Δ*cdaR* mutant (Bochner *et al.*, 2001). The Δ*cdaR* mutant showed an altered metabolic activity with some carbon and nitrogen sources such as α-D-lactose or L-phenylalanine, respectively and with di- or tri-peptides – especially if they contain aromatic amino acids (**Fig. S2.1**), but most strikingly was the

altered metabolic activity on plate PM9, that contains different osmolytes. The Δ*cdaR* mutant shows an altered metabolic activity if challenged with osmolytes, such as increasing amounts of NaCl (**Fig. 2.1, A**). To test whether the changes in metabolic activity of a Δ*cdaR* mutant also reflect in a growth phenotype, the mutant and the *L. monocytogenes* wt were grown in BHI medium with increasing concentrations of the osmolytes NaCl, KCl or sorbitol. As shown in **Fig. 2.1, B**. The altered metabolic activity on plate pM8, containing different osmolytes, was most remarkable. The Δ*cdaR* mutant shows a decreased growth rate in the presence of osmolytes, independent of the nature of the osmolyte (ionic, non-ionic). Since CdaA and CdaR showed protein-protein interaction, we also tested if CdaR is like CdaA membrane-localized and if both are expressed in minimal medium, a condition under which the *cdaA* gene is non-essential (Whiteley *et al.*, 2015, Whiteley *et al.*, 2017).

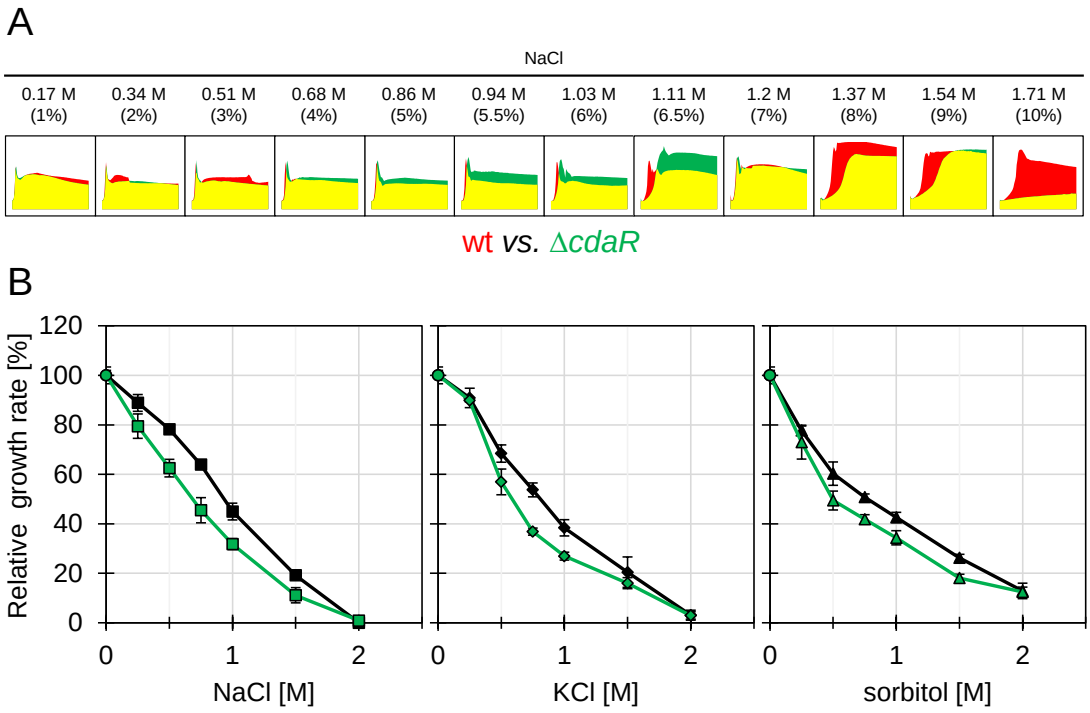

Fig. 2.1 CdaR is important for osmotic adaptation. (A) Phenotype Microarray (PM) of plate PM9 wells A1-A12 of the *L. monocytogenes* wild type (wt) vs. Δ*cdaR* mutant with increasing concentrations of NaCl, shows altered metabolic activity of the Δ*cdaR* mutant. (B) A Δ*cdaR* mutant shows a decreased growth rate if grown in the presence of osmolytes. The wt and Δ*cdaR* mutant were grown in BHI medium with increasing concentrations of either NaCl, KCl or sorbitol. The relative growth rates of exponentially growing bacteria are plotted against the different osmolyte concentrations. Means of biological triplicates and the standard derivations are shown. *vs.*, *versus*.

The wt, a Δ*cdaA* (*lmo2120*) mutant and a Δ*cdaR* mutant were grown in LSM medium. Exponentially growing cells were harvested and lysed. Proteins of whole cell extracts, as well as cytosolic and membrane fractions were separated by SDS-PAGE and protein expression and localization of CdaA, CdaR and the cytosolic transcription factor PrfA (Lmo0200, Mengaud *et al.*, 1991) were investigated by Western blotting, using specific polyclonal antibodies to detect the respective proteins. PrfA is found in the cytosolic fraction and both CdaA and CdaR are enriched in the membrane fraction (**Fig. 2.2**). CdaR does not impact CdaA expression or localization, as previously reported (Rismondo *et al.*, 2016) and neither CdaA, nor CdaR have an influence on PrfA expression or localization. Furthermore, CdaR is similar as CdaA enriched in the membrane fraction, but in contrast to CdaA, the expression of CdaR seems to be decreased in the Δ*cdaA* mutant, probably due to

secondary effects of the truncated polycistronic *cdaA-cdaR* mRNA, but once more, localization is not influenced.

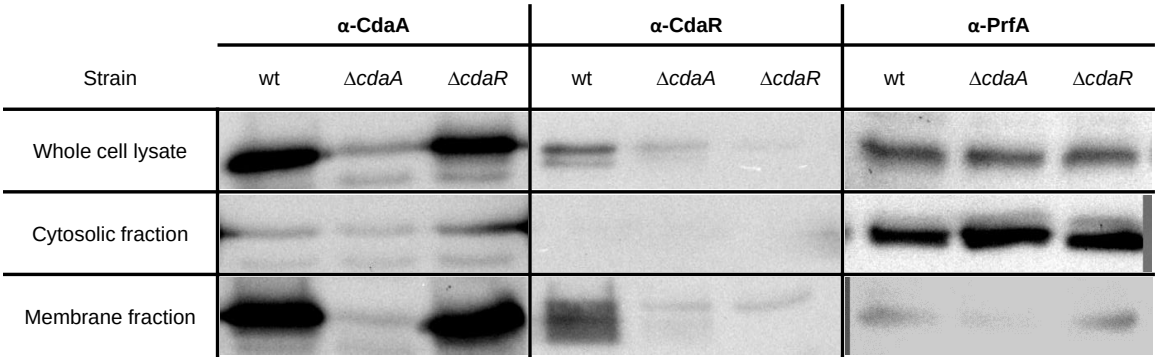

Fig. 2.2 Synthesis and localization of the DAC CdaA and the effector protein CdaR. Expression of *cdaA*, *cdaR* and *prfA* in the *L. monocytogenes* wild type (wt), a Δ*cdaA* mutant and a Δ*cdaR* mutant. Bacteria were grown in LSM and expression and localization of the different proteins was investigated for exponential growing cells. Cytosolic and membrane proteins were separated by centrifugation. 10 µg of the different protein fractions were separated by SDS-PAGE (12%) and analysed by Western blotting using CdaA, CdaR or PrfA polyclonal antibodies, respectively.

The YbbR domains are surface exposed – CdaR impacts both, intracellular c-di-AMP concentration and metabolic activity of *L. monocytogenes*. It is therefore tempting to hypothesis that CdaR senses changes in osmolarity and modulates CdaA activity accordingly. The CdaR protein consists of an N-terminal TM domain and four YbbR domains of unknown function (**Fig. 2.3, A**). It has been shown previously that the membrane domain of both, CdaA and CdaR are important for their direct protein-protein interaction (Rismondo *et al.*, 2016), but it is unclear in which part of the cell the YbbR domains are localized and therefore also the signal that might be sensed by them. To analyze the orientation of the CdaR protein in the cell envelope, fusion proteins with C-terminal alkaline phosphatase PhoA and the α-fragment of the β-galactosidase LacZ were constructed using the pKTop vector (Karimova *et al.*, 2009). *E. coli* DH5α was transformed with the pKTop empty vector and derivatives for the expression of CdaR, CdaR without the N-terminal TM domain (ΔTM, aa 34-452), CdaR without the YbbR domains (ΔYbbR, aa 1-33), PrfA as a control for a cytosolic protein and PrkA (Lmo1820, Lima *et al.*, 2011) as a control for a membrane protein. Both, *E. coli* harboring the pKTop empty vector or the *prfA* containing derivative show a red coloration on indicator plates and therefore high β-galactosidase activity and a cytosolic localization of the C-terminal part, containing the PhoA and LacZ fusion proteins (**Fig. 2.3, B**). In contrast, *E. coli* expressing the PrkA fusion protein show a blue coloration, indicating high alkaline phosphatase activity and therefore a periplasmic localization of the C-terminal PhoA and LacZ fusion proteins. The same is true for full length CdaR, demonstrating an outward localization of the C-terminal YbbR domains. *E. coli* expressing the *cdaR* ΔTM and ΔYbbR domain constructs show red and blue colored colonies, respectively, demonstrating that the N-terminal TM domain is both, necessary and sufficient for correct localization of the C-terminal fusion part. To further assess the localization of the YbbR domains and the role of the TM domain for the localization of the CdaR protein, enzymatic assays to determine the alkaline phosphatase and β-galactosidase activity of the different constructs were performed (**Fig. 2.3, C**). The enzymatic assays confirm the phenotype of the *E. coli* plate assay, CdaR is membrane localized in dependency of the TM domain and the YbbR domains are surface exposed.

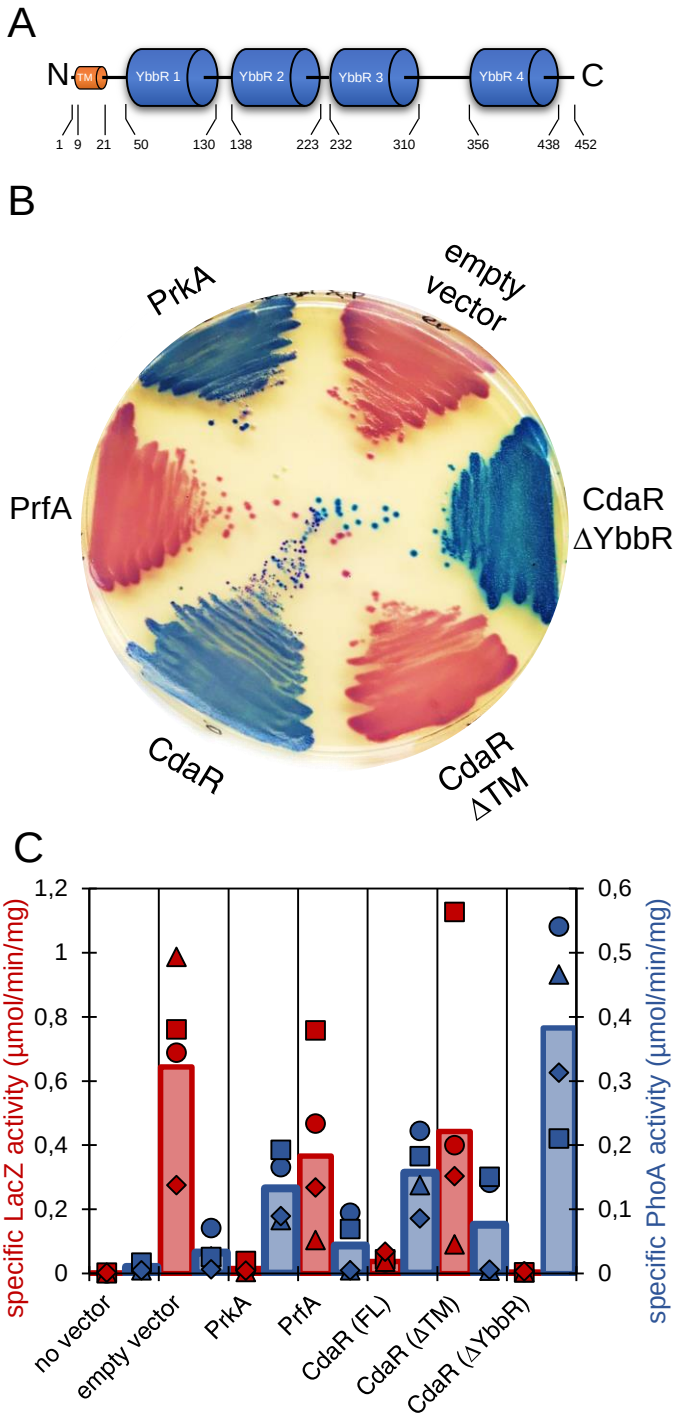

Fig. 2.3 CdaR topology analysis. (A) Domain architecture of the CdaR protein. CdaR consists of four YbbR domains and an N-terminal transmembrane (TM) domain. (B) Determination of the topology of CdaR. *E. coli* DH5α cells expressing CdaR, CdaR ΔTM (aa 34-452), CdaR ΔYbbR (aa 1-33), PrfA (cytosolic control), or PrkA (membrane control) with PhoA and the LacZ alpha fragment fused to the C-terminus or harboring the pKTop empty vector were plated on LB plates with Red-Gal (for β-galactosidase activity) and X-Pho (for phosphatase activity). Blue colored colonies (phosphatase activity) indicates a periplasmic localization of the C-terminus, while a red coloration (β-galactosidase activity) indicates a cytosolic localization. (C) Quantification of PhoA and LacZ activities of protein extracts of *E. coli* DH5α and DH5α harboring the same fusion proteins as described above. Cells were grown in LB medium and logarithmic growing bacteria were harvested. Cells were lysed and alkaline phosphatase and β-galactosidase activity of whole cell lysates determined using pNPP and ONPG as substrates, respectively. Specific enzymatic activities of four biological replicates are shown.

CdaR is important for survival of L. monocytogenes *upon continuous exposure to increased osmolarity* – To further assess the role of CdaR, its membrane localization and the role of the YbbR domains on the ability of *L. monocytogenes* to adapt to osmotic stress, several mutants were constructed. Using the integrative pIMK3 vector that allows IPTG-dependent expression, *L. monocytogenes* strains were constructed, in the background of the *cdaR* deletion, to express CdaR without its membrane localization (ΔTM, aa 32-452) and consecutive truncations of the YbbR domains (ΔYbbR 4, aa 1-320; ΔYbbR 3-4, aa 1-230; ΔYbbR 2-4, aa 1-130; ΔYbbR 1-4, aa 1-33). As controls the pIMK3 empty vector (ev) was integrated into the EGD-e wt chromosome and into that of the Δ*cdaR* mutant and investigated together with a CdaR full-length expressing complementation

strain (Rismondo *et al.*, 2016). The strains were cultivated in LSM medium and ten-fold serial dilutions drop spotted on LSM agar plates with or without addition of osmolytes. The Δ*cdaR* mutant and to a lesser extend the Δ*cdaR* mutant expressing CdaR ΔTM showed slightly decreased growth if challenged with osmolytes (data not shown). After prolonged incubation the Δ*cdaR* mutant starts to lyse and suppressor mutants appear (to a lesser extend also in the wt background; **Fig. 2.4**). In contrast, consecutive truncations of the YbbR domains led to more robust growth of *L. monocytogenes*. The phenotypes were equally for NaCl and KCl as osmolytes and less pronounced with sorbitol (data not shown). Two suppressor mutants of the wt strain, isolated from LSM plates supplemented with 0.5 M sorbitol and 5 suppressor mutants in the Δ*cdaR* pIMK3 background from LSM plates supplemented with 0.25 M NaCl (three) or 0.25 M KCl (two) were isolated and subjected to WGS. Interestingly, mutations were found in the genes *rbsU* and *rbsV* that are involved in the regulatory network leading to inactivation of the stress sigma factor SigB and a mutation was found directly in the *sigB* gene. Further mutations were identified in *pdeA* (silent mutation), *lmo1515*, encoding a homolog to *B. subtilis* CymR that is a pleiotropic regulator of sulfur metabolism and in *lmo1432* that encodes for a protein of unknown function that was also identified in a transposon study searching for salt sensitive *L. monocytogenes* mutants (Evens *et al.*, 2006; Gardan *et al.*, 2003; **see Tab. 2.1**).

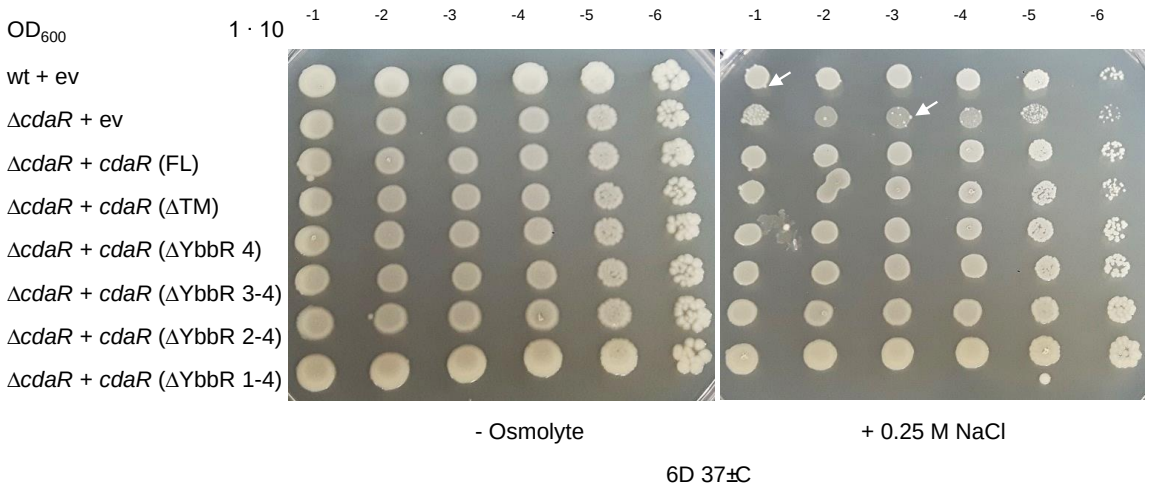

Fig. 2.4 Impact of CdaR, its membrane domain and the YbbR domains on growth under increased osmolarity. The *L. monocytogenes* wild type (wt) harboring the pIMK3 empty vector (ev), the Δ*cdaR* mutant harboring the ev or pIMK3 derivatives for the expression of the full length (FL) CdaR protein, CdaR without the transmembrane domain (ΔTM, aa 32-452) or consecutive truncations of the YbbR domains (ΔYbbR 4, aa 1-320; ΔYbbR 3-4, aa 1-230; ΔYbbR 2-4, aa 1-130; ΔYbbR 1-4, aa 1-33) were analyzed for their growth and long term adaptation under increased osmolarity. Bacteria were grown in LSM and ten-fold serial dilutions plated on LSM plates with or without 0.25 M NaCl at 37°C growth was observed every 24 hours. Image shows plate after six days (6D). Arrows indicate appearance of suppressor mutants in the Δ*cdaR* mutant and to a lesser extend also in the wt background.

Impact of CdaR on the intracellular c-di-AMP concentration upon osmotic stress – To assess the impact of CdaR, its membrane localization and the YbbR domains on the concentration of c-di-AMP inside *L. monocytogenes* cells, the wt and the Δ*cdaR* mutant (harboring the pIMK3 ev) and Δ*cdaR* mutants harboring pIMK3 derivatives for the expression of full-length CdaR and CdaR without the membrane localization (ΔTM) or without the YbbR domains (ΔYbbR) were investigated. Bacteria were grown in LSM media and the bacteria stressed by the addition of 0.25 M NaCl. Samples before and 25 min after osmotic challenge (as well as control samples without addition of osmolytes) were analyzed. In all cases, c-di-AMP concentrations decreased after osmotic stress. In the Δ*cdaR* mutant and the strain expressing CdaR without the TM domain, c-di-AMP concentrations were lower than in the wild type and c-di-AMP changes less pronounced (**Fig. 2.5**).

In contrast, the complementation strain expressing the *cdaR* gene from an IPTG-dependent promoter, showed increased c-di-AMP concentrations and a greater range of change. Interestingly, the Δ*cdaR* complemented with CdaR without the YbbR domains, showed very low c-di-AMP concentrations.

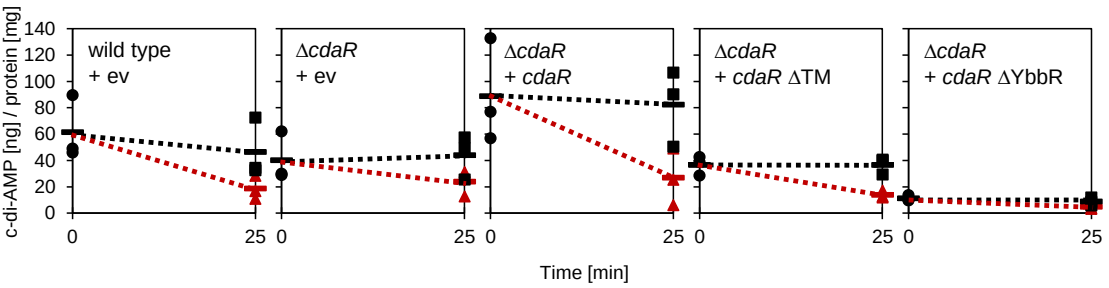

Fig. 2.5 Roles of CdaR, its transmembrane domain and the YbbR domains on intracellular c-di-AMP concentrations during osmotic stress. *L. monocytogenes* wild type (wt), harboring the pIMK3 empty vector (ev), the Δ*cdaR* mutant harboring the ev or derivatives for the expression of full-length CdaR, CdaR without the transmembrane domain (ΔTM, aa 32-452) or without the YbbR domains (ΔYbbR, aa 1-33) was grown in LSM at 37°C. Samples of logarithmic growing cells were taken (t_0; black circles) and the cultures split. Half was subjected to osmotic stress, by the addition of 0.25 M NaCl, while the other half was treated with the same volume of LSM without salt addition. After 25 minutes, additional samples (t_{25}) of osmotic stressed (red triangles) and non-stressed cells (black squares) were taken. Intracellular c-di-AMP levels were determined and normalized to the cellular protein amounts. Data of biological triplicates are shown.

Analysis of protein-protein interactions of components involved in c-di-AMP signaling – To investigate interactions between different parts of the c-di-AMP regulatory network, the DAC CdaA and its two effector proteins (CdaR and the phosphoglucosamine mutase GlmM), the two PDEs PdeA and PgpH and the c-di-AMP regulated potassium transporter KimA (**see chapter 3**) bacterial two hybrid (BACTH) assays were employed (Karimova *et al.*, 1998). The leucine zipper protein Zip served as a control and additionally the 5'→3'-exoribonuclease RNase Y from *B. subtilis* was employed as an additional control (Commichau *et al.*, 2009). The BACTH analysis (**Fig. 2.6**) shows interactions between CdaA and CdaR, GlmM, PdeA and PgpH and between CdaR and CdaA, CdaR, PdeA, PgpH and KimA, demonstrating protein-protein interactions between synthesis and degradation machinery. Strong self-interaction of the GlmM protein, the PdeA and the PgpH PDEs is seen, additionally. Interestingly, also strong interactions between the two PDEs. Furthermore, interactions between the PDEs and KimA, as well as self-interactions of KimA can be seen. None of the proteins interacts with the Zip control, but the second control protein, RNase Y, seems to interact with every protein, including the cytosolic GlmM and the Zip control.

CdaR and GlmM influence CdaA activity – Two investigate the impact of CdaR and CdaR variants lacking membrane localization or YbbR domains and the influence of the GlmM enzyme on CdaA activity, a previously established reporter system was used (**see chapter 3**). Hence, the potassium transporter deficient *E. coli* strain LB2003 (Stumpe and Bakker, 1997) harboring the pWH844-based plasmid for expression of the c-di-AMP inhibited KimA potassium transporter was used. The strain was transformed with pBAD33 plasmids for the expression of CdaA or an inactive mutant (D171N; Rosenberg *et al.*, 2015) as controls for c-di-AMP synthesis and non-synthesis (Quintana *et al.*, 2019). Synthesis of c-di-AMP leads to inhibition of KimA, a decrease in potassium import and therefore reduced growth of the bacteria. To investigate the influence of the effector proteins on CdaA activity, independent of other proteins of the c-di-AMP metabolism, the genes encoding the CdaR protein, the GlmM protein or both, were cloned together with CdaA into the pBAD33 vector. In a similar approach, co-expression vectors of CdaA together with CdaR ΔTM (aa 34-452) or CdaR with consecutive truncations of the YbbR domains (ΔYbbR 4, aa1-320; ΔYbbR 3-4, aa 1-

230; ΔYbbR 2-4, aa 1-130; ΔYbbR 1-4, aa 1-33) were constructed. The cells were grown in M9 minimal medium with a defined potassium concentration of 0.35 mM (K_M of KimA), expression of the CdaA operons was induced and growth monitored. High activity of CdaA leads to a decrease in growth, while inhibition of CdaA leads to an increase in growth.

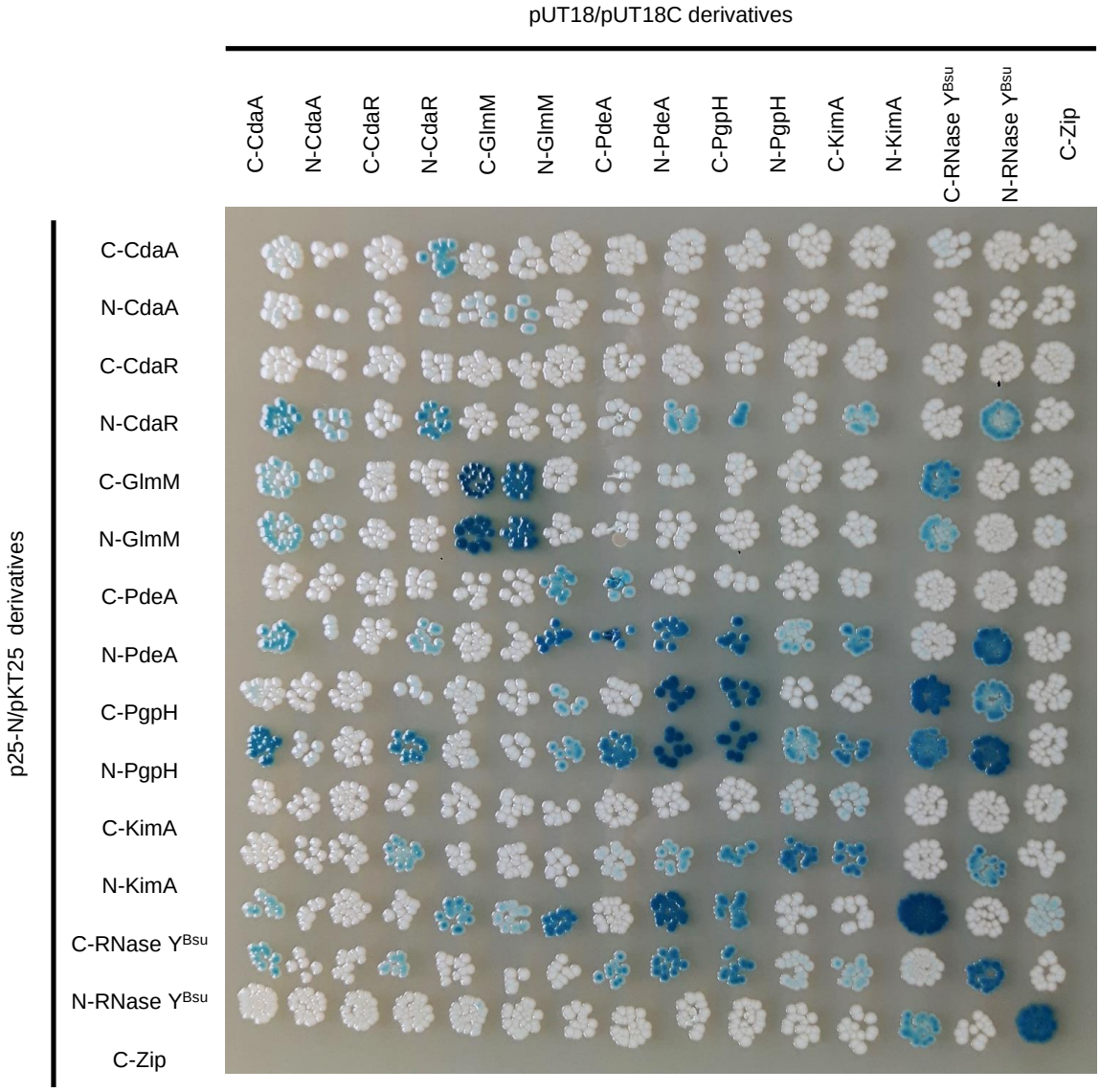

Fig. 2.6 Analysis of protein-protein interactions between proteins of the c-di-AMP synthesis and degradation machinery and the KimA potassium transporter. *E. coli* BTH101 cells were co-transformed with pUT18/pUT18C derivatives and p25-N/pKT25 derivatives for the expression of fusion proteins of CdaA, CdaR, GlmM, PdeA, PgpH or KimA from *L. monocytogenes*, as indicated. The leucine zipper protein (Zip) served as a control. As an additional control the RNase Y protein from *B. subtilis* was included. Cells were plated on selective LB agar plates supplemented with 1 mM IPTG for induction of protein expression and 100 µg/ml X-Gal as a colorimetric substrate for visualization of β-galactosidase activity and incubated at 30°C for 36 hours.

Growth rates of the different strains were determined and as shown in **Fig. 2.7**, CdaR and to a lesser extend GlmM restore the growth rate, compared to the strain synthesizing CdaA alone. If both are present, growth is also substantially restored. Expression of CdaR lacking the TM domain shows the most similar growth rate compared to CdaA alone, indicating that membrane localization is important for CdaR to act on CdaA. Interestingly, the truncations of the YbbR domains have no impact on the growth rate, compared to the full-length variant, as long as one domain is still

present. The strain expressing only the TM domain of CdaR shows an intermediate phenotype, indicating that the TM domain alone is able to influence CdaA activity to some degree.

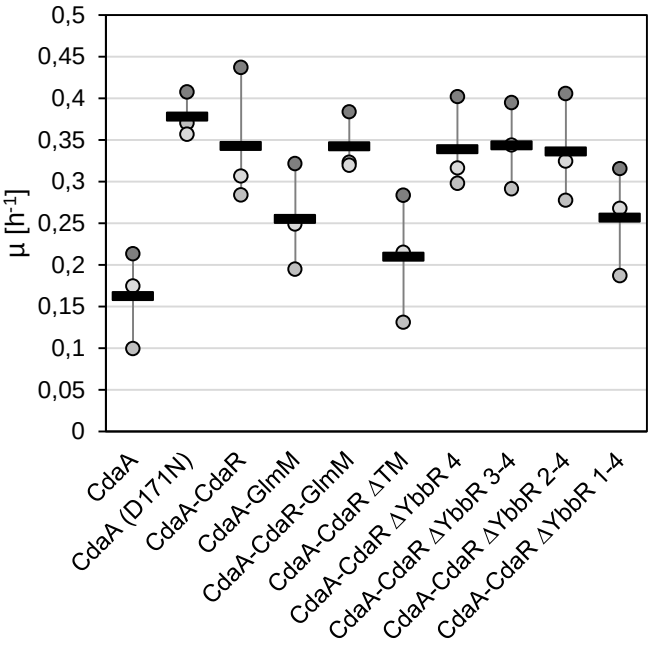

Fig. 2.7 Effect of CdaA and the effector proteins GlmM and CdaR growth of *E. coli* expressing the c-di-AMP regulated KimA potassium transporter. The potassium transporter deficient *E. coli* strain LB2003 was transformed with a plasmid for the expression of the c-di-AMP-inhibited potassium transporter KimA from *L. monocytogenes*. Using pBAD33 derivatives, CdaA, an inactive mutant (D171N), CdaA together with either CdaR, GlmM or both, or CdaA together with CdaR variants (ΔTM, aa 34-452; ΔYbbR 4, aa 1-320; ΔYbbR 3-4, aa 1-230; ΔYbbR 2-4, aa 1-130; ΔYbbR 1-4, aa 1-33) were co-expressed together with KimA. Cells were grown in M9 minimal medium with a defined potassium concentration of 0.35 mM (K_M of KimA), 50 µM IPTG for KimA induction and 0.005% (*w/v*) L-arabinose for induction of the different CdaA operons. Growth rates (µ) of three biological replicates and means (black bars) are shown.

Discussion

CdaR impacts osmoregulation in L. monocytogenes – It has been previously reported that CdaR impacts the intracellular c-di-AMP concentration for different bacteria, such as *B. subtilis*, *L. monocytogenes* or *S. aureus* (Bowman *et al.*, 2016; Mehne *et al.*, 2013; Rismondo *et al.*, 2016; Zhu *et al.*, 2016). Interestingly, in *S. aureus* a Δ*cdaR* (*ybbR*) mutant was also more susceptible to acidic stress and required suppressor mutations that increased the c-di-AMP concentration, among others in the DAC encoding gene *dacA* (Bowman *et al.*, 2016). Due to the genetic conservation of *cdaR* with the CdaA-type encoding genes and direct protein-protein interactions and the influence of CdaR on CdaA activity, CdaR has been proposed to be a modulator of CdaR activity with the YbbR domains of unknown function as sensory domains (Mehne *et al.*, 2013; Rismondo *et al.*, 2016). Here, we show that the sensing of changes in osmolarity might be the trigger that CdaR senses to modulate CdaA activity. CdaR influences the metabolic activity of *L. monocytogenes* in the presence of osmolytes and leads to a decreased growth rate (**Fig. 2.1**).

The outwards localized YbbR domains and the membrane localization are important for the function of CdaR – The next question we asked was whether CdaR is like CdaA also a membrane-bound protein and if the putative sensory YbbR domains are located in the cytoplasm or outside of the cell. Western blot analysis of CdaR expression and localization shows that CdaR is enriched in the membrane fraction. In the Δ*cdaA* mutant, CdaR seems to be less abundant than in the wt, but this effect might be due to secondary effects of the truncation of the polycistronic *cdaA-cdaR* mRNA (**Fig. 2.2**; Mehne *et al.*, 2013). To address the questions of the localization of the YbbR domains and the role of the N-terminal TM domain (**Fig. 2.3, A**), the pKTop system, described by Karimova *et al.*, was used (Karimova *et al.*, 2009). One hypothesis was that the YbbR domains might sense the intracellular concentration of osmolytes, such as potassium ions, and confer that information directly to the cytoplasmic DAC domain of CdaA. The YbbR domains share some structural

similarity with the C-terminal domains of TL5 and L25 ribosomal proteins (Barb *et al.*, 2010; Fedorov *et al.*, 2001; Lu & Steitz, 2000). Even though the role of those proteins is not yet fully understood, potassium and magnesium ions are crucial for proper function of the ribosome and T25 of *E. coli* has been crystallized binding RNA and five magnesium ions (Lu & Steitz, 2000). The second hypothesis was that the YbbR domains are located in the extracellular space and sense either integrity or composition of the bacterial cell wall, interact with other proteins or ligands, sense the extracellular osmolarity or sense turgor changes by self-interaction of the YbbR domains (Rismondo *et al.*, 2016). The sensing of turgor changes would thereby be sensed as changes in the YbbR domain self-interactions through lateral forces when the turgor changes. In this case, the only interaction surface between CdaR and CdaA would be the TM domains. In the past, c-di-AMP and cell wall biosynthesis have been linked by many observations (Kaplan Zeevi *et al.*, 2013; Luo & Helmann, 2012). Many of the reported phenotypes could however be indirect phenotypes due to the effects of c-di-AMP on osmotic homeostasis (Commichau *et al.*, 2018). The PhoA and LacZ activity assays (**Fig. 2.3, B & C**) demonstrate that the TM domain is both, necessary and sufficient for periplasmic localization of the C-terminus in *E. coli* and the YbbR domains are located at the cell surface. Following the closer analysis of the membrane topology of CdaR, we wanted to analyze the effect of localization and presence of the YbbR domains on the ability of *L. monocytogenes* to adapt to osmotic stress and their role in adapting the c-di-AMP concentration upon osmotic stress. As shown in **Fig. 2.4**, deletion of *cdaR* or lack of the TM domain, leads to lysis of bacteria after prolonged growth on LSM plates supplemented with osmolytes. CdaR seems to be important for survival under osmotic stress. Interestingly, truncations of the YbbR domains increased *L. monocytogenes* capability to thrive under the same conditions. Analyzing the c-di-AMP concentration in these mutants, the Δ*cdaR* mutant and the mutant lacking the TM domain showed a decreased c-di-AMP content and a decreased range comparing the changes of osmotic stressed and unstressed cells (**Fig. 2.5**). In contrast, the complementation mutant, in which the *cdaR* full-length gene is expressed under a strong IPTG-dependent promoter (Monk *et al.*, 2008), shows elevated c-di-AMP concentration and an increased range between stressed and unstressed cells. This demonstrates the role of CdaR in sensing osmotic changes and conferring those on the intracellular c-di-AMP concentration. The strain expressing CdaR without the TM domain behaved most similar to the Δ*cdaR* mutant, while the mutant lacking all four YbbR domains showed in general very low concentrations of c-di-AMP. This demonstrates that the YbbR domains – their proper localization and presence – are crucial for the correct function of CdaR. To isolate potential effects of other parts of the c-di-AMP metabolic network, such as degradation by PDEs, or efflux by multi drug efflux system, the effect of CdaR and CdaR mutants, as well as the GlmM enzyme was investigated in *E. coli* (Kaplan Zeevi *et al.*, 2013; Mehne *et al.*, 2013). Using the growth dependency of an *E. coli* strain lacking native potassium transporter on the activity of the c-di-AMP regulated potassium transporter KimA from *L. monocytogenes* as a readout, we investigated the direct effect on the ability of CdaA to produce c-di-AMP as a screening system for DAC function (**see chapter 3**). The growth phenotypes demonstrate that CdaR and to a lesser extend GlmM can inhibit CdaA activity *in vivo*. While the TM domain for CdaR seems to be important for CdaR function, only one YbbR domain seems to be required for proper function. CdaR consisting only of the TM domain, however, still seems to have some impact on CdaA activity (**Fig. 2.7**). Intriguingly, the effect of CdaR lacking all YbbR domains is the opposite in *E. coli* for what we observe in *L. monocytogenes* (**Fig. 2.5**). The reason for this remains elusive, but it could either be a consequence of the different structure of the Gram-positive and Gram-negative cell envelope or a possible crosstalk between synthesis and degradation machinery in *L. monocytogenes*. To investigate this possibility, a BACTH assay was employed to analyze protein-protein interactions between different components of the c-di-AMP metabolic network. The assay demonstrated potential interactions

between CdaA and CdaR and the PDEs. A possible influence of CdaA or CdaR on PDE activity could be the reason for the phenotype discrepancy between *E. coli* and *L. monocytogenes* and should be the subject of future studies. A recent publication by Pham *et al.* demonstrates the effects of osmotic up- and downshifts on the c-di-AMP concentration of various bacteria, including *L. monocytogenes* (Pham *et al.*, 2018). They demonstrated that an osmotic downshift, a hypoosmotic shock, leads to a rapid increase of the c-di-AMP concentration, while an osmotic upshift, a hyperosmotic shock, leads to a rapid decrease. As depicted in the model in **Fig. 2.8**, the regulation of synthesis and degradation have to be coordinated to increase the c-di-AMP concentration for preventing further increase of osmolytes during a hypoosmotic stress and to decrease the c-di-AMP concentration to allow influx of osmolytes during a hyperosmotic stress. The CdaR protein might regulate CdaA activity, as depicted, by interacting with itself *via* the YbbR domains and with CdaA *via* the TM domains of the two proteins, acting as a buffer for CdaA self-interaction and therefore activity in a positive or negative manner, depending on the forces in the cell envelope during osmotic driven turgor changes (**Fig. 2.8**).

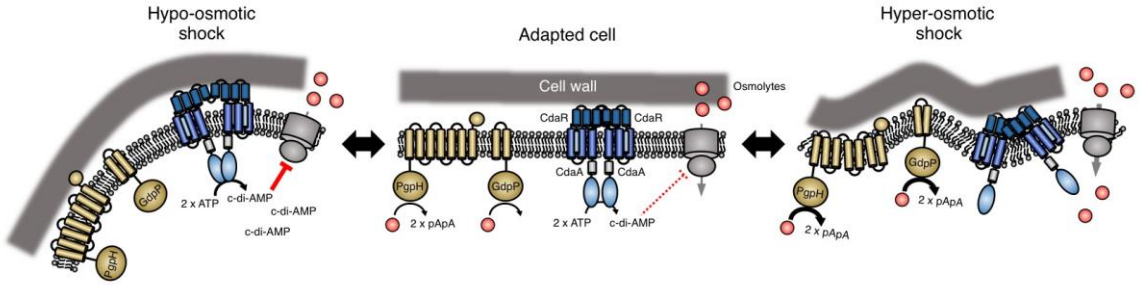

Fig. 2.8 Model depicting the control of c-di-AMP synthesis and degradation in dependence of the external osmolarity. Bacteria that are adapted to the osmotic state in the environment live in an equilibrium of c-di-AMP synthesis and degradation and osmolyte import and export to maintain the cellular turgor. Sudden changes in external osmolarity change this equilibrium. A decrease in external osmolarity, a hypoosmotic shock, leads to rapid influx of water and osmotic swelling. Under these conditions, c-di-AMP has to be synthesized to prevent excess accumulation of osmolytes. Hence, PDE activity has to decreases, while DAC activity has to be increased. The CdaR protein could function as a stabilator of CdaA interaction. The opposite, a hyperosmotic shock, e.g. rapid efflux of water to dilute an outside excess of osmolytes and shrinkage of cellular volume leads to membrane invaginations. To counteract, c-di-AMP synthesis has to be de- and PDE activity increased. The CdaR protein could function in this context as a buffer to decrease CdaA self-interaction.

The c-di-AMP synthesis and degradation machineries might build up interacting networks – *L. monocytogenes* Δ*cdaR* mutant colonies on minimal media (LSM) agar plates supplemented with osmolytes became translucent after prolonged incubation and suppressor mutants appeared. To a lesser extent, suppressor mutants also appeared in the wt background without changes in colony morphology. Five mutants in the *cdaR* background and two mutants in the wt background were subsequent subjected to WGS. The majority of mutations were found in the regulatory pathway, regulating activity of the stress sigma factor SigB. There also mutations were found in genes of unknown function, involved in regulation of cysteine metabolism, a silent mutation in the PDE encoding gene *pdeA*, mutations in genes regulating activity of the sigma factor SigB and in the gene *sigB* itself (**see Tab. 2.1**). The mutations affecting SigB, either truncated SigB directly or affected genes necessary for activation of SigB, all presumably inactivating SigB. Interestingly, it has been previously reported for *L. monocytogenes* that inactivation of SigB leads to hyperresistance against oxidative stress (Boura *et al.*, 2016). The reason why inactivation of SigB, which should activate expression of genes to cope with various stresses, such as oxidative or osmotic stress, causes an increased resistance of *L. monocytogenes* is fascinating but needs further investigations. It seems, however, be independent of the c-di-AMP metabolism, since similar mutations were

identified in both, the wt and the Δ*cdaR* mutant. To conclude, we could show that CdaR is important for adaptation to osmotic stress, by regulating CdaA activity. Localization and presence of the outwards and self-interacting YbbR domains (Rismondo *et al.*, 2016) is important for proper CdaR function. Another way for *L. monocytogenes* to cope with osmotic stress is the inactivation of SigB that leads to increased resistance against osmotic stress. Finally, we showed that components of the synthesis and degradation machinery interact with each other, demonstrating potential regulatory cross-talk inside the c-di-AMP regulatory network.

Acknowledgements

We are grateful to Jonathan Rosenberg, Lisa Maria Schulz, Sandra Klama and Veronika Lutz for help with some experiments and for Anna-Lena Hagemann and Annette Garbe for technical assistance This work was supported by the grant CO 1139/2-1 from the Deutsche Forschungsgemeinschaft *via* the Priority Program SPP1879, the Fonds der Chemischen Industrie and the Max-Buchner-Forschungsstiftung (MBFSt-Kennziffer 3381) to FMC.

3. Characterization of c-di-AMP-controlled potassium transporters of *Listeria monocytogenes*

Johannes Gibhardt, Gregor Hoffmann, Vincent T. Lee, and Fabian M. Commichau

Author contribution:

JG and GH performed the experiments. VTL performed the DRaCALA binding experiments. JG and FMC wrote the manuscript.

Abstract

Many bacteria and some archaea produce the second messenger cyclic diadenosine monophosphate (c-di-AMP). c-di-AMP was shown to be essential for growth of Firmicutes, including the human pathogen *Listeria monocytogenes* because it controls the uptake of osmolytes such as glycine betaine and potassium ions. The cellular c-di-AMP levels have to be tightly regulated for optimal growth in environments with changing osmolarities. Here, we have identified and characterized the high- and low-affinity potassium transporters KimA and KtrCD of *L. monocytogenes*, respectively. We also show that *Staphylococcus aureus* contains a homolog of KimA, which mediates potassium transport. The KimA and KtrCD transporters from *L. monocytogenes* are both inhibited by c-di-AMP *in vivo*. The C-terminal domain of KimA seems to be involved in the c-di-AMP-dependent regulation of the transporter. The nucleotide also binds to the cytoplasmatic regulatory subunit KtrC of the KtrCD potassium transporter *in vitro*. Thus, many phylogenetically related bacteria use c-di-AMP for controlling the uptake of osmolytes such as potassium, which is essential to adjust the cellular turgor to the environment.

Introduction

Bacteria use complex signal transduction systems to adjust the cellular turgor to the environmental osmolarity (Sleator and Hill, 2002; Wood, 1999; Wood, 2011). Under hyperosmotic growth conditions, potassium ions are imported to prevent water efflux from the cytosol and to increase the cellular turgor (Kempf and Bremer, 1998). The potassium ions are thereupon often replaced by compatible solutes such as glycine betaine and ectoine; osmolytes that do not disturb essential cellular processes (Kempf and Bremer, 1998). Depending on the external osmolarity, the import and export of osmolytes have to be tightly controlled to prevent osmotic swelling and shrinking of the cell, respectively (Commichau *et al.*, 2018; Gundlach *et al.*, 2017; Wood, 1999). Although osmoregulation has been intensively studied, it is still rather unclear how cell sense the environmental osmolarity to adjust the turgor accordingly. The second messenger c-di-AMP, which is produced by specific diadenylate cyclases (DACs), plays a key role in regulating the turgor in Firmicute bacteria because it controls the uptake and export of osmolytes including potassium (see below; Bai *et al.*, 2014; Chin *et al.*, 2015; Corrigan *et al.*, 2013; Gundlach *et al.*, 2017; Huynh *et al.*, 2016; Pham *et al.*, 2018; Schuster *et al.*, 2016; Whiteley *et al.*, 2015; Whiteley *et al.*, 2017; Zeden *et al.*, 2018).

c-di-AMP was discovered during the structural characterization of DNA integrity scanning protein DisA, which is involved in DNA damage response and in controlling sporulation initiation in the Gram-positive bacterium *Bacillus subtilis* (Bejerano-Sagie *et al.*, 2006; Gándara and Alonso, 2015; Raguse *et al.*, 2017; Valenzuela-García *et al.*,2018; Witte *et al.*, 2008). DisA is present in spore-forming Firmicutes, in actinobacteria (Corrigan and Gründling, 2013) and in hyperthermophilic bacteria (Witte *et al.*, 2008). While DisA is the only c-di-AMP-producing enzyme in actinobacteria, bacteria like *B. subtilis* also contain the DACs CdaA and CdaS, of which the latter is required for efficient spore germination (Mehne *et al.*, 2013; Commichau *et al.*, 2019). CdaA is attached to the membrane and DisA and CdaS are soluble proteins (Mehne *et al.*, 2013; Rismondo *et al.*, 2016; Witte *et al.*, 2008). CdaA is the most abundant DAC and many prominent apathogenic and pathogenic Gram-positive bacteria, such as *Lactococcus lactis*, *L. monocytogenes*, *S. aureus*, *Streptococcus agalactiae*, rely only on this DAC for c-di-AMP synthesis (Corrigan and Gründling, 2013). Since c-di-AMP is essential for growth of these bacteria (Devaux *et al.*, 2018; Woodward *et al.*, 2010; Zeden *et al.*, 2018), the DAC CdaA is an interesting target for novel antibiotics.

c-di-AMP is degraded intracellular by specific phosphodiesterases (PDEs), which can be assigned to three different groups (Commichau *et al.*, 2019; Huynh and Woodward, 2016). The GdpP- and PgpH-type PDEs consist of domains that are involved in signaling and enzyme catalysis. Both PDEs are attached to the membrane, suggesting that the enzymes may sense and respond to extracellular cues. The DhhP-type PDEs, which are located in the cytosol, form the third group of c-di-AMP-degrading enzymes (Huynh and Woodward, 2016). Since the DACs and the PDEs determine the cellular c-di-AMP levels that are required for optimal growth in environments with changing osmolarities (Gundlach *et al.*, 2017; Pham *et al.*, 2018), the activities of the enzymes have to be tightly regulated. Recently, it has been observed that the phosphoglucosamine mutase GlmM inhibits the DAC CdaA in *L. lactis*, suggesting a link between c-di-AMP metabolism and cell wall biosynthesis (Zhu *et al.*, 2016). However, the molecular mechanisms by which the DACs, the PDEs and GlmM sense the environmental osmolarity are unknown. Moreover, the sensing mechanisms may vary among the enzymes due to the different domain composition and cellular localization.

One important aspect of understanding c-di-AMP signaling was the identification of targets of c-di-AMP. Several have been identified, so far: c-di-AMP activates the DNA-binding activity of the

transcription factor DarR in *Mycobacterium smegmatis* (Zhang *et al.*, 2013). In *L. monocytogenes*, c-di-AMP inhibits the pyruvate carboxylase PycA (Choi *et al.*,2017; Sureka *et al.*,2014). c-di-AMP also binds to the cystathione-beta-synthase domain-containing (CBS) proteins CbpA and CbpB and the PII-like signal transduction DarA in this organism (Choi *et al.*,2015; Sureka *et al.*,2014). The DarA homologs from *B. subtilis* and *S. aureus* have also been structurally and biochemically characterized (Campeotto *et al.*, 2015; Gundlach *et al.*, 2015a; Müller *et al.*, 2015a). While the biological functions of CbpA, CbpB and DarA remain to be elucidated, several c-di-AMP targets are involved in the transport of osmolytes such as potassium, glycine betaine and carnitine (Corrigan *et al.*,2013; Huynh *et al.*,2016; Schuster *et al.*,2016; Whiteley *et al.*,2017; Zeden *et al.*,2018). c-di-AMP inhibits the KtrCD/KtrCB and CabP-TrkH potassium uptake systems from *S. aureus* and *S. pneumoniae*, respectively, by binding to the membrane-associated gating proteins (Bai *et al.*,2014; Corrigan *et al.*,2013; Kim *et al.*,2015). In *S. aureus*, the synthesis of the KdpFABC potassium transporter, is also inhibited by c-di-AMP (Moscoso *et al.*,2016). In the same organism, c-di-AMP stimulates the potassium and sodium transporter CpaA (Chin *et al.*,2015). In *B. subtilis*, the expression of the *ktrAB* and *kimA* genes, encoding the potassium transporters KtrAB and KimA, respectively, is negatively regulated by c-di-AMP (Gundlach *et al.*,2017). c-di-AMP also controls the uptake of the compatible solutes carnitine in *L. monocytogenes* and *S. aureus* (Schuster *et al.*,2016; Whiteley *et al.*,2017). Moreover, the DNA-binding transcription factor BusR represses the genes involved in glycine betaine uptake in *S. agalactiae* and *L. lactis* depending on the cellular c-di-AMP concentration (Devaux *et al.*,2018; Pham *et al.*,2018).

We are interested in the c-di-AMP-dependent control of osmolyte homeostasis in the food-borne pathogen *L. monocytogenes* (Rolhion and Cossart, 2017). The ability of *L. monocytogenes* to thrive under adverse conditions including high osmolarity depends on the c-di-AMP-dependent control of osmolyte transport such as carnitine (Whiteley *et al.*,2017). However, the involvement of c-di-AMP in potassium uptake or homeostasis in *L. monocytogenes* has remained elusive. Here, we show that the *L. monocytogenes* KimA (Lmo2130) and KtrCD (Lmo1023 and Lmo0993) proteins are high- and low-affinity potassium transporters, respectively. We also show that the transporters are inhibited by c-di-AMP and that unregulated activity leads to rapid osmotic swelling. The interaction between c-di-AMP and KtrC was also confirmed *in vitro.* Moreover, the C-terminal domain of KimA is important for the c-di-AMP-dependent regulation of potassium uptake.

Experimental procedures

Bacterial strains and growth conditions – The bacterial strains are listed in **Tab. 3.1**. The *Escherichia coli* strains XL1-Blue (Stratagene), Rosetta (DE3) (Novagen) and T7 Express I^q (NEB) were used for cloning and protein overproduction. *E. coli* was grown in LB medium and transformants were selected on LB plates (15 g/l Bacto agar (Difco)) containing kanamycin (50 µg/ml), ampicillin, carbenicillin (100 µg/ml) or chloramphenicol (30 µg/ml). The *L. monocytogenes* wild type strain EGD-e (laboratory strain collection) was cultivated in BHI medium (Sigma-Aldrich) The *B. subtilis* wild type strain 168 (laboratory strain collection) was cultivated in LB medium. Potassium transporter deficient *E. coli* strains LB650 and LB2003 were cultivated in LB-K medium (NaCl substituted by 1% KCl (*w/v*)) (Stumpe & Bakker, 1997). M9 medium was used for *E. coli* growth experiments with the following composition: 37.85 mM Na_2HPO_4, 22.05 mM KH_2PO_4, 18.75 mM NH_4Cl, 1 mM $MgSO_4$, 0.1 mM $CaCl_2$, 0.5 µM $FeCl_3$, 28 mM D-glucose or glycerol as sources of carbon. For the *E. coli* strain LB650 the M9 medium was supplemented with amino acids L-valine, L-isoleucine, L-methionine, L-proline, L-serine (each 0.02% (*w/v*)) and 3 µM Thiamine. For the *E. coli* strain

LB2003 the M9 medium was supplemented with 0.0066% (*w/v*) casein hydrolysate (acid) (Oxoid), 0.004% (*w/v*) L-proline and 3 µM Thiamine. For experiments with defined potassium concentrations, the KH_2PO_4 salt was replaced by NaH_2PO_4 and KCl was added as indicated. If not specified different, IPTG was used at a concentration of 50 µM and L-arabinose at 0.005% (*w/v*).

DNA manipulation – Transformation of *E. coli* was performed using standard procedures (Sambrook *et al.*, 1989). Plasmid DNA was extracted using the NucleoSpin Plasmid Kit (Macherey and Nagel). Commercially available restriction enzymes, T4 DNA ligase and DNA polymerases were used as recommended by the manufacturers. DNA fragments were purified using the PCR purification kit (Qiagen). DNA sequences were determined by the dideoxy chain termination method (Microsynth, Göttingen, Germany). Chromosomal DNA of *L. monocytogenes* or *B. subtilis* was isolated using the NucleoSpin Microbial DNA Kit (Macherey and Nagel). Chromosomal DNA of *S. aureus* COL was a kindly provided by Dr. Jan Pané-Farré (University of Greifswald, Germany). Oligonucleotides were purchased from Sigma-Aldrich (Germany).

Tab. 3.1 Strains

Name	Genotype	Description	Reference
E. coli			
LB2003	F⁻ *aroE rpsL metE thi gal rha kup1* (*trkD1*) Δ*kdpABC5* Δ*trkA aroE*⁺	Potassium uptake studies	Stumpe & Bakker, 1997
LB650	F⁻ *thi lacZ gal rha kup1* (*trkD1*) Δ*kdpABC5* Δ*trkH* (Cm^R) Δ*trkG* (Kan^R)	Potassium uptake studies	Stumpe & Bakker, 1997
NEB T7 Express I^q	MiniF *lacI*^{q}(Cm^R) */ fhuA2 lacZ::T7 gene1 [lon] ompT gal sulA11 R(mcr-73::miniTn10*--Tet^S*)2 [dcm] R(zgb-210::Tn10*--Tet^S*) endA1 Δ(mcrC-mrr)114::IS10*	Protein expression and DRaCALA	New England Biolabs
Rosetta (DE3)	F⁻ *ompT hsdS*$_B$(r_B^- m_B^-) *gal dcm* (DE3) pRARE (Cm^R)	Protein expression	Novagen
XL1-Blue	*recA1 endA1 gyrA96 thi-1 hsdR17 supE44 relA1 lac* [F′ *proAB lacI*^{q} *ZΔM15* Tn*10* (*Tet*^{r})]	Cloning	Stratagene
B. subtilis			
168	*trpC2*	Wild type	Laboratory collection
L. monocytogenes			
EGD-e	Wild type	Serotype 1/2a strain	Laboratory collection

:: = insertion

Plasmid construction – The genes encoding putative potassium transporters were introduced into the vector pWH844 allowing IPTG-dependent expression in *E. coli* (Schirmer *et al.*, 1997). The *kimA*^{Lmo} and *kimA*^{Sau} genes were amplified using the oligonucleotide pairs JH95/JH96 and JH97/JH98, respectively (**Tab. 3.2**). The PCR products were digested with *Eco*RI and *Bam*HI and ligated to pWH844 that was cut with the same enzymes. The resulting plasmids were designated as pBP384 and pBP385 (**Tab. 3.3**). To study the role of the C-terminal domain of KimA^{Lmo}, we generated the plasmid pBP396. The truncated *kimA*^{Lmo} gene was amplified using oligonucleotide pair JH95/JH120, digested with *Eco*RI and *Bam*HI and ligated to pWH844 cut with the same enzymes. The plasmid pBP371 for the expression of the *L. monocytogenes ktrCD* (*lmo1023* and *lmo0993*) genes was constructed as follows. The *ktrC* and *ktrD* genes were amplified using the oligonucleotide pairs JH59/JH60 and JH61/JH62, respectively and fused by Splicing by Overhang Extension (SOE) PCR using primer pair JH59/JH62 (Horton *et al.*, 1990). The resulting PCR product was digested with *Eco*RI and *Bam*HI and ligated to pWH844 cut with the same enzymes. The plasmids

pBP370 and pBP373 were constructed for producing the wild type CdaA enzyme and the inactive D171N variant (Rosenberg *et al.*, 2015). The *cdaA* gene was amplified using the oligonucleotide pair JH51/JH52 and introduced into the *Xba*I/*Pst*I sites of pBAD33 (Guzman *et al.*, 1995; Quintana *et al.*, 2019). For the construction of plasmid pBP373, we used the oligonucleotide pair JH51/JH52 together with the 5'-phosphorylated oligonucleotide JR18 to introduce the D171N mutation *via* the combined chain reaction (Bi & Stambrook, 1997; Quintana *et al.*, 2019). The pBAD33 and pWH844 expression vectors have compatible selection markers and origin of replications allowing the co-expression of potassium transporter genes (from pWH844) and *cdaA* variants (from pBAD33). The plasmids pBP345, pBP346 and pBP347 were constructed to study the binding of c-di-AMP to KtrC, the cytosolic domains of KimA^{Lmo} (aa 452-607) and KimA^{Sau} (aa 452-609). The respective genes were amplified using the oligonucleotide pairs GH5/GH6, GH7/GH8 and GH9/GH10, digested with *Bam*HI/*Sal*I and ligated to pWH844 cut with the same enzymes. The genes encoding the full-length KimA^{Lmo} and KimA^{Sau} proteins as well as the C-terminally truncated KimA^{Lmo} variant (aa 1-455) were amplified using oligonucleotide pairs JH142/JH96, JH143/JH98 and JH142/JH120, respectively. The PCR products were digested with *Sac*I/*Bam*HI and ligated to pGP172 (Merzbacher *et al.*, 2004) cut with the same enzymes. The resulting plasmids were designated as pBP265 (*kimA^{Lmo}*), pBP267 (*kimA^{Sau}*) and pBP266 (*kimA^{Lmo}* ΔC-terminus). The plasmids are suitable for the IPTG-dependent overproduction of the transporters with an N-terminal *Strep*-tag II in the *E. coli* strain Rosetta (DE3).

Tab. 3.2 Oligonucleotides

Name	Restriction sites are underlined, complementary regions are in bold, sequences 5'→3'	Purpose
GH5	AAAGGATCCATGAAAGAAGGATTTGCAGTCATCGGTCTTG	Fwd. *ktrC*^{Lmo} (*Bam*HI)
GH6	TTTGTCGACTTATTGAATTTTTTCTTGTAGTCGTTCAATGTCATCATCC	Rev. *ktrC*^{Lmo} (*Sal*I)
GH7	AAAGGATCCCATTACCGGAAAGTTGGACCACAACTTAG	Fwd. *kimA*^{Lmo} (aa 452-x) (*Bam*HI)
GH8	TTTGTCGACTTATTCTTTTAAATGATAAGGATATGTGGAAACTACTACATCC	Rev. *kimA*^{Lmo} (*Sal*I)
GH9	AAAGGATCCCATTATCGAGATATCGCAGAACAATTACGTTCTG	Fwd. *kimA*^{Sau} (aa 452-x) (*Bam*HI)
GH10	TTTGTCGACCTATTTTTTAAGTTTAAATGGAATTGTACAT-ACGTTAACATTCTTTTG	Rev. *kimA*^{Sau} (*Sal*I)
JH51	AAATCTAGACACGGAGGTGAAGTGATGGATTTTTCCAATATGTCGATATTGCAT	Fwd. *cdaA* (*Xba*I), Quintana *et al.*, 2019
JH52	TTTCTGCAGTCATTCGCTTTTGCCTCCTTTCCA	Rev. *cdaA* (*Pst*I), Quintana *et al.*, 2019
JH59	AAAGAATTCAAGGAGGTAACGTACACATGAAAGAAGG	Fwd. *ktrC*^{Lmo} (*Eco*RI)
JH60	**AATCTTCTGCTAAGTACGGCTTTTTATTG**AATTTTTTCTTGTAGTCGTTCAATG	Rev. *ktrC*^{Lmo}
JH61	**CAATAAAAAGCCGTACTTAGCAGAAGATT**AAAGCTTGTTTTGGCACG	Fwd. *ktrD*^{Lmo}
JH62	TTTGGATCCTTAACCAGTAATAATTTTCTCTTTTGGTAAACGAATC	Rev. *ktrD*^{Lmo} (*Bam*HI)
JH95	AAAGAATTCAAAGGTAGGGAATACAATGGCTTCGCC	Fwd. *kimA*^{Lmo} (*Eco*RI)
JH96	TTTGGATCCCTCTTGTTATTCTTTTAAATGATAAGGATATGTGGAAAC	Rev. *kimA*^{Lmo} (*Bam*HI)
JH97	AAAGAATTCAAAGGAATAGGAGATTATGTTCAATCAATTTAAAAGAC	Fwd. *kimA*^{Sau} (*Eco*RI)
JH98	TTTGGATCCGAATCTATTTTTTAAGTTTAAATGGAATTGTACATACGTTAAC	Rev. *kimA*^{Sau} (*Bam*HI)
JH120	TTTGGATCCTTATTTCCGGTAATGATGTCTTGTACGATGGAAAAC	Rev. *kimA*^{Lmo} (aa x-455) (*Bam*HI)
JH142	AAAGAGCTCGATGGCTTCGCCGCTAAAAAGACTATTAATCG	Fwd. *kimA*^{Lmo} (*Sac*I)
JH143	AAAGAGCTCGATGTTCAATCAATTTAAAAGACTTATTATAGGGCAACC	Fwd. *kimA*^{Sau} (*Sac*I)
JR18	P-GAATACACCGCTTCAT**A**ATGGAGCAGTTATTATTAA	5'-phosphorylated GAT→AAT (CdaA D171N), Rosenberg *et al.*, 2015

Fwd. = forward, Rev. = reverse, ^{Lmo} = *L. monocytogenes*, ^{Sau} = *S. aureus*, aa = amino acids, x = any

Drop dilution assay – Single colonies of the *E. coli* strain LB650 harboring the plasmids pWH844, pBP371, pBP372, pBP384, pBP385 or pBP396 were taken from LB-K plates and used to inoculate 4 ml LB-K medium supplemented with kanamycin, ampicillin and chloramphenicol. The cultures were incubated at 37°C and 220 rpm. The pre-cultures were used to inoculate 4 ml M9 medium supplemented with glucose, antibiotics and 50 mM KCl to an OD_{600} of 0.001. The cultures were incubated for about 16 h at 37°C. Next day, the cultures were used to inoculate 10 ml of the same medium to an OD_{600} of 0.1. At an OD_{600} between 0.3 and 0.5 the cells were harvested by centrifugation at 3300 g for 10 min at room temperature. The cell pellets were washed twice in 10 ml of M9 medium lacking KCl. The cell suspension was adjusted to an OD_{600} of 0.1 and 5 µl of the diluted cells were spotted onto M9 minimal media plates, which were incubated for 24 h at 37°C. M9 plates were prepared by mixing 2 X M9 medium (pre-warmed to 37°C) and 2 X Bacto agar (pre-warmed to 70°C before mixing). The finial medium contained glucose as a carbon source, 10 mM KCl, and 50 µM IPTG if required.

Tab. 3.3 Plasmids

Name	Insert/Features	Reference
pBAD33	P_{BAD} *cat araC*	Guzman *et al.*, 1995
pWH844	P_{T5} *bla*	Schirmer *et al.*, 1997
pGP172	P_{T7} *bla*	Merzbacher *et al.*, 2004
pBP265	pGP172-*Strep*-tag II-$kimA^{Lmo}$	This work
pBP266	pGP172-*Strep*-tag II- $kimA^{Lmo}$ ΔC-terminus	This work
pBP267	pGP172-*Strep*-tag II-$kimA^{Sau}$	This work
pBP345	pWH844-His_6-$ktrC^{Lmo}$	This work
pBP346	pWH844-His_{6}- $kimA^{Sau}$ C-terminal domain	This work
pBP347	pWH844-His_6-$kimA^{Sau}$ C-terminal domain	This work
pBP370	pBAD33-*cdaA*	Quintana *et al.*, 2019
pBP371	pWH844-$ktrC^{Lmo}$-$ktrD^{Lmo}$	This work
pBP372	pWH844-$ktrAB^{Bsu}$	Gundlach *et al.*, 2017
pBP373	pBAD33-*cdaA* (D171N)	Quintana *et al.*, 2019
pBP384	pWH844-$kimA^{Lmo}$	This work
pBP385	pWH844-$kimA^{Sau}$	This work
pBP396	pWH844-$kimA^{Lmo}$ (ΔC-terminus)	This work

cat = cm^R (30 µg/ml chloramphenicol), *bla* = amp^R (100 µg/ml ampicillin/carbenicillin),

Determination of kinetic parameters of the potassium transporters – To determine the growth characteristics of the *E. coli* strain LB650 synthesizing potassium transporters from *L. monocytogenes* and *S. aureus*, the bacteria were grown until the early exponential phase, harvested by centrifugation at 3300 g for 10 min. The pellet was resuspended in 10 ml M9 medium with glucose, ampicillin, 50 µM IPTG and without KCl. The cells were incubated for 1 h at 37°C, harvested by centrifugation and washed twice. The cultures were adjusted to an OD_{600} of 0.2 and 50 µl were used to inoculate a 96-well plate (Microtest Plate 96-Well,F, Sarstedt) containing 50 µl of M9 medium with glucose, ampicillin, 50 µM IPTG and KCl concentrations ranging from 0 to 100 mM. The 96-well plate was incubated at 37°C with medium orbital shaking at 237 cpm (4 mm) in an Epoch 2 Microplate Spectrophotometer, equipped with the Gen5 software (02.09.2001; BioTek Instruments) and growth (OD_{600}) measured in 15 min intervals. The growth rates were calculated ($\mu = (2.303 \cdot (\log(OD_2) - \log(OD_1))) / (t_2-t_1)$), plotted against the KCl concentrations and fitted to the Michaelis-Menten equation using the solver tool of Excel 2013 (Microsoft), to calculate V_{max} (µ [h^{-1}]) and the apparent K_M [mM KCl].

c-di-AMP in vivo *inhibition assay* – The potassium transporter deficient *E. coli* strain LB2003 was co-transformed with the plasmid pWH844 or derivatives (pBP371, pBP384, or pBP396) and the pBAD33 derivatives (pBP370 or pBP373) on LB-K plates containing 0.5% (*w/v*) glucose, ampicillin and chloramphenicol. Single colonies were used to inoculate 4 ml LB-K medium containing 0.2% (*w/v*) glucose, ampicillin and chloramphenicol and the exponentially growing cultures were used to inoculate M9 medium containing 0.2% (*w/v*) glycerol and 0.02% (*w/v*) glucose to an OD_{600} of 0.001. The cultures were incubated overnight at 37°C and used to re-inoculate the same medium (without glucose) to an OD_{600} of 0.1. After reaching early exponential phase (OD_{600} 0.3-0.5), the cells were washed and 100 µl of the suspensions were used to inoculate a 96-well plate. The M9 medium was supplemented with glycerol, 50 µM IPTG, ampicillin, chloramphenicol, KCl and with or without L-arabinose. Final concentrations of KCl were equal to the determined K_M values (**see Tab. 3.4**) and no or 0.005% (*w/v*) L-arabinose was present, as indicated. Growth was monitored in an Epoch 2 Microplate Spectrophotometer, equipped with the Gen5 software (02.09.2001; BioTek Instruments), as described above.

Protein expression and DRaCALA – The binding of c-di-AMP to the potassium transporters was analyzed using the *E. coli* strain Rosetta (DE3). Single colonies were used to inoculate 10 ml LB-K medium containing carbenicillin and chloramphenicol. After incubation overnight at 30°C, the pre-cultures were used to inoculate 1.5 ml of LB-K medium to an OD_{600} of 0.1. 1 mM IPTG was added at an OD_{600} of 1.0 - 1.5 to induce gene expression. After incubation for 4 h, the cultures were harvested by centrifugation (3300 g, 10 min, 4°C), the cell pellets were resuspended in 150 µl Tris-NaCl buffer (10 mM Tris, pH 8.0, 100 mM NaCl). Cells are lysed by three freeze-thaw cycles of -80˚C and room temperature. The Differential radial capillary action of ligand assay (DRaCALA) was performed by mixing 1 µL of ^{32}P-c-di-AMP with 20 µL of cell lysates. After an incubation for one minute, 2 µL of the mixture was spotted on dry nitrocellulose, dried, exposed to phosphorimager screen and imaged using FLA-7000 phosphorimager. The fraction bound was calculated using the inner and total areas and intensities as described previously (Roelofs *et al.*, 2011).

Microscopic analysis – Derivatives of the LB650 strain harboring the plasmids pWH844 (empty plasmid), pBP372, or pBP384 were cultivated in 4 ml LB-K medium containing ampicillin, kanamycin and chloramphenicol at 37°C. Next day, the cultures were washed twice and used to inoculate 10 ml M9 medium (containing 22.05 mM KH_2PO_4) with or without 1 mM IPTG to an OD_{600} of 0.1. Cells were transferred to standard microscope slides (Carl Roth) and examined using an Axioskop 40 FL fluorescence microscope, equipped with an Axio-Cam MRm digital camera, objectives of the Neofluar series at 1,000-fold magnification and the AxioVision Rel 4.8.2 software (Carl Zeiss). Images were later on equally processed using the ImageJ 1.48 software (Schneider *et al.*, 2012).

Results

In silico *identification of potassium transporters from* L. monocytogenes – Both, *B. subtilis* and *S. aureus* contain well-described potassium uptake systems. *B. subtilis* uses the high-affinity transporters KtrAB and KimA and the low-affinity transporter KtrCD (Gundlach *et al.*,2017; Holtman *et al.*,2003). By contrast, *S. aureus* relies on the high-affinity transporter KdpFABC, whose synthesis and activity is controlled by the two-component system KdpDE and c-di-AMP, respectively (Gründling, 2003; Moscoso *et al.*,2015; Price-Whelan *et al.*,2013). *S. aureus* also contains the low-affinity potassium transport systems KtrCB and KtrCD, sharing the accessory protein KtrC (Price-Whelan *et al.*,2013). A BLASTp sequence analysis revealed that the *L. monocytogenes* genome codes for the KdpABCDE (Lmo2682-Lmo2678) and KtrCD (Lmo1023, Lmo0993) proteins, which show about

31-56% and 51-64% overall amino acid identity, respectively, with the homologs from *S. aureus* and *B. subtilis*. The *kdpF* gene does not exist in the genome of *L. monocytogenes.* A homolog of the high-affinity potassium transporter KimA from *B. subtilis* is also present in *L. monocytogenes* and *S. aureus* (Gundlach *et al.*,2017). The KimA homologs from *B. subtilis*, *L. monocytogenes* and *S. aureus* are from now on designated as KimA^{Bsu}, KimA^{Lmo} (Lmo2130) and KimA^{Sau} (Sacol2443), respectively. KimA^{Lmo} and KimA^{Sau} show about 59% and 57% overall amino acid identity, respectively, with the *B. subtilis* homolog (**Fig. 3.1, A**). The membrane topology was illustrated using the web-based tool Protter (Gründling, 2013). Like KimA^{Bsu} also KimA^{Lmo} contains an N-terminal extracellular domain, 11 transmembrane (TM) helices and a C-terminal intracellular domain, which might be important for activity control of the transporter (**Fig. 3.1, B**). To conclude, although *B. subtilis*, *L. monocytogenes* and *S. aureus* are phylogenetically related, each species uses a different set of transporters for potassium uptake.

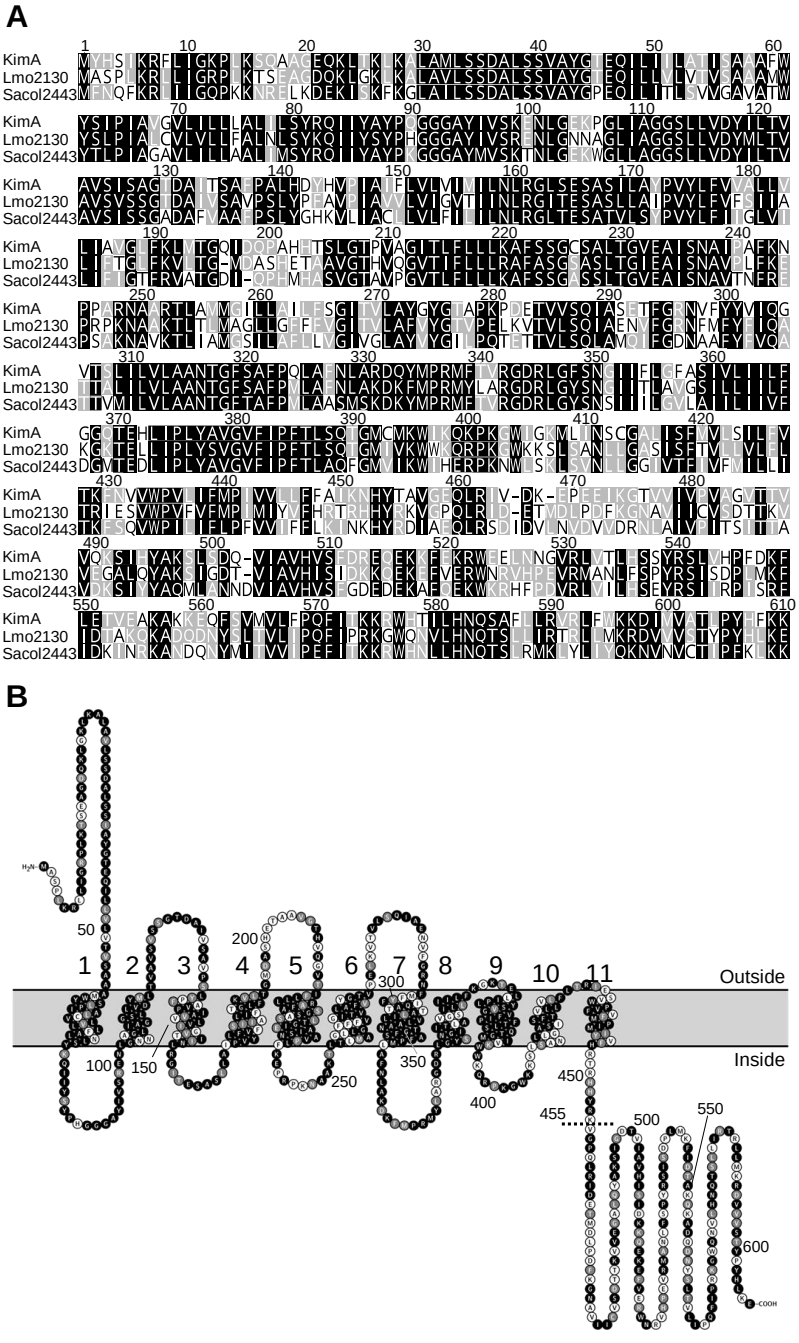

Fig. 3.1 Alignment of KimA homologs and domain organization of the KimA^{Lmo} protein. *A*, MUSCLE alignment of the KimA^{Bsu}, KimA^{Lmo} and KimA^{Sau} homologs from *B. subtilis*, *L. monocytogenes* (Lmo2130) and *S. aureus* (Sacol2443), respectively, generated with Geneious (46). Amino acids in black, grey and white have an amino acid similarity of over 80%, 60-80%, or less than 60%, respectively *B*, predicted membrane topology of KimA^{Lmo} overlaid with a MUSCLE alignment between KimA^{Bsu} and KimA^{Lmo}. The dashed line indicates the position at which the KimA^{Lmo} protein was truncated. Amino acids in black are identical; amino acids in grey are similar and amino acids in white are non-similar.

In vivo *activities of KimA and KtrCD potassium transporters* - To assess whether KimA^{Lmo} and KtrCD from *L. monocytogenes* are active in potassium transport, we cloned the *kimA* and *ktrCD* genes using the plasmid pWH844, which allows IPTG-dependent expression of heterologous genes in *E. coli* (Schirmer *et al.*,1997). We also cloned a truncated *kimA^{Lmo}* gene encoding the ΔC-KimA^{Lmo} variant lacking 152 amino acids of the C-terminal cytosolic domain. Furthermore, we cloned the *kimA^{Sau}* gene from *S. aureus*, to evaluate whether KimA homologs from other Firmicutes are involved in potassium uptake. The resulting plasmids were used to transform the *E. coli* strain LB650 that is unable to take up potassium *via* the native uptake systems Kup, KdpABC, TrkG and TrkH (Stumpe and Bakker, 1997). The strain is suitable to study potassium transporters because it is only viable in minimal medium supplemented with potassium concentrations above 15 mM KCl (**see Fig. 3.4**). The empty plasmid and a plasmid encoding the *B. subtilis ktrAB* genes, which were previously shown to mediate potassium transport in *E. coli* LB650 (Gundlach *et al.*, 2017), served as negative and positive controls, respectively. The cells were grown during the day in M9 medium with 50 mM KCl and without IPTG induction, collected by centrifugation, washed in potassium-free medium and propagated on M9 minimal medium plates without and with 10 mM IPTG. As shown in **Fig. 3.2**, with the exception of the strain harboring the plasmid for *kimA^{Sau}* expression, the bacteria could not grow in the absence of IPTG. The weak growth of the cells containing the *kimA^{Sau}* gene could be due to a leaky promoter, the high affinity of the encoded KimA^{Sau} transporter for potassium and perhaps a stronger translation due to using the natural ribosomal binding sites of the different transporter (see below). By contrast, the strains carrying the *ktrAB^{Bsu}*, *kimA^{Lmo}*, *ktrCD^{Lmo}*, could grow with low amounts of K^+ when these genes were induced with IPTG (**Fig. 3.2**).

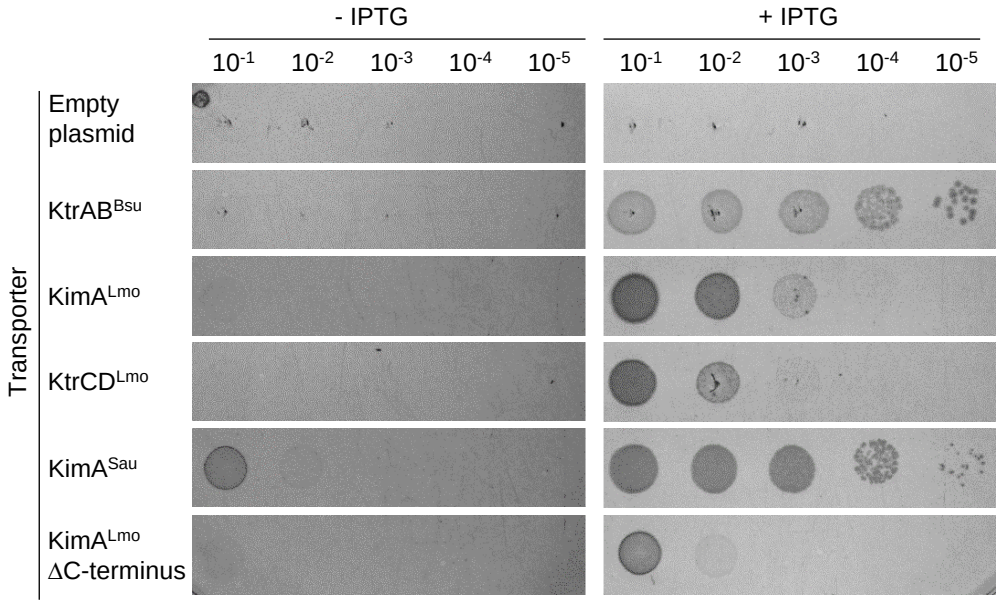

Fig. 3.2 Drop dilution assay to assess the activities of putative potassium transporters. *E. coli* LB650 strains harboring plasmids pWH844 (empty plasmid), pBP372 (*ktrAB^{Bsu}*, positive control), pBP384 (*kimA^{Lmo}*), pBP396 (*kimA^{Lmo}* ΔC-terminus), pBP385 (*Kim^{Sau}*) and pBP371 (*ktrCD^{Lmo}*) were grown to an OD_{600} of 0.3-0.5 in M9 minimal medium supplemented with 50 mM KCl. The cells were washed for 1 h in potassium-free M9 medium, the OD_{600} was adjusted to 0.1, serial ten-fold diluted and 5 µl of the diluted cell suspensions were plated on M9 plates containing 10 mM KCl. IPTG was added to a final concentration of 50 µM to induce the expression of the transporter genes. The plates were incubated for 24 h at 37°C.

Moreover, the *kimA*^{Lmo} variant lacking the C-terminal domain (*kimA*^{Lmo} ΔC) also restored growth, albeit less well than the strain producing the full-length protein. These results indicate that the N-terminal extracellular domain and the 11 TM helices of KimA^{Lmo} from *L. monocytogenes* are sufficient for mediating potassium import in *E. coli* (**Fig. 3.2**). Expression of *ktrAB*^{Bsu} from *B. subtilis* restores growth on low potassium concentrations agreeing with previous reports that KtrAB^{Bsu} is a high-affinity potassium transporter (Gundlach *et al.*, 2017; Holtman, *et al.*, 2003). Expression of KimA^{Sau} from *S. aureus E. coli* strain LB650 resulted in a much better growth than those strains expressing KimA^{Lmo} and KtrCD indicating that KimA^{Sau} is likely a high-affinity potassium transporter (**Fig. 3.2**). Thus, KimA^{Lmo} and KtrCD^{Lmo} from *L. monocytogenes* as well as KimA^{Sau} from *S. aureus* are indeed potassium transporters.

Apparent affinities of KimA and KtrCD for potassium - To determine the affinities of KimA^{Lmo}, the KimA^{Lmo} ΔC-terminus variant (ΔC-KimA^{Lmo}) and KtrCD from *L. monocytogenes* and KimA^{Sau} from *S. aureus*, we determined the growth rates of the *E. coli* strain LB650 synthesizing the potassium transporters in M9 minimal medium supplemented with different amounts of potassium. The strains carrying the empty plasmid and expressing the *B. subtilis ktrAB* genes served as negative and positive controls, respectively. The growth rates were plotted against the potassium concentrations and fitted to the Michaelis-Menten equation (Gundlach *et al.*, 2017). The V_{max} values and the apparent affinities are summarized in **Tab. 3.4**. As shown in **Fig. 3.3** and **3.4**, each *E. coli* strain required a different concentration of external potassium to reach half-maximal growth: The strains synthesizing the transporters KtrCD^{Lmo}, KimA^{Lmo}, ΔC-KimA^{Lmo}, KimA^{Sau} and KtrAB^{Bsu} required 6.31 ± 1.8 µM, 0.35 ± 0.1 µM, 2.99 ± 0.65 µM, 0.14 ± 0.02 µM and 0.03 ±0.01 µM, respectively.

Tab. 3.4 Michaelis-Menten constants of the potassium transporters

	Empty Vector	**KtrAB^{Bsu}**	**KimA^{Lmo}**	**KimA^{Lmo} ΔC-terminus**	**KtrCD^{Lmo}**	**KimA^{Sau}**
Apparent **K_M** [mM KCl]	**58.28** ± 14.60	**0.03** ± 0.01	**0.35** ± 0.10	**2.99** ± 0.65	**6.31** ± 1.80	**0.14** ± 0.02
V_{max} [µ (h^{-1})]	**0.82** ± 0.13	**0.73** ± 0.04	**0.52** ± 0.04	**0.40** ± 0.01	**0.59** ± 0.10	**0.62** ± 0.05

These results demonstrate that KtrCD^{Lmo} and KimA^{Lmo} from *L. monocytogenes* are transporters with low and moderately high affinities for potassium, respectively. Moreover, the C-terminal intracellular domain of KimA^{Lmo} is important for full activity of the transporter (**Fig. 3.1, B**; **Fig. 3.4**). In contrast to KtrCD^{Lmo} and KimA^{Lmo}, KimA^{Sau} from *S. aureus* is a high-affinity potassium transporter, which is in line with the observation that the *E. coli* strain LB650 synthesizing KimA^{Sau} and KtrAB^{Bsu} grew comparatively well with low amounts of potassium (**Fig. 3.2**).

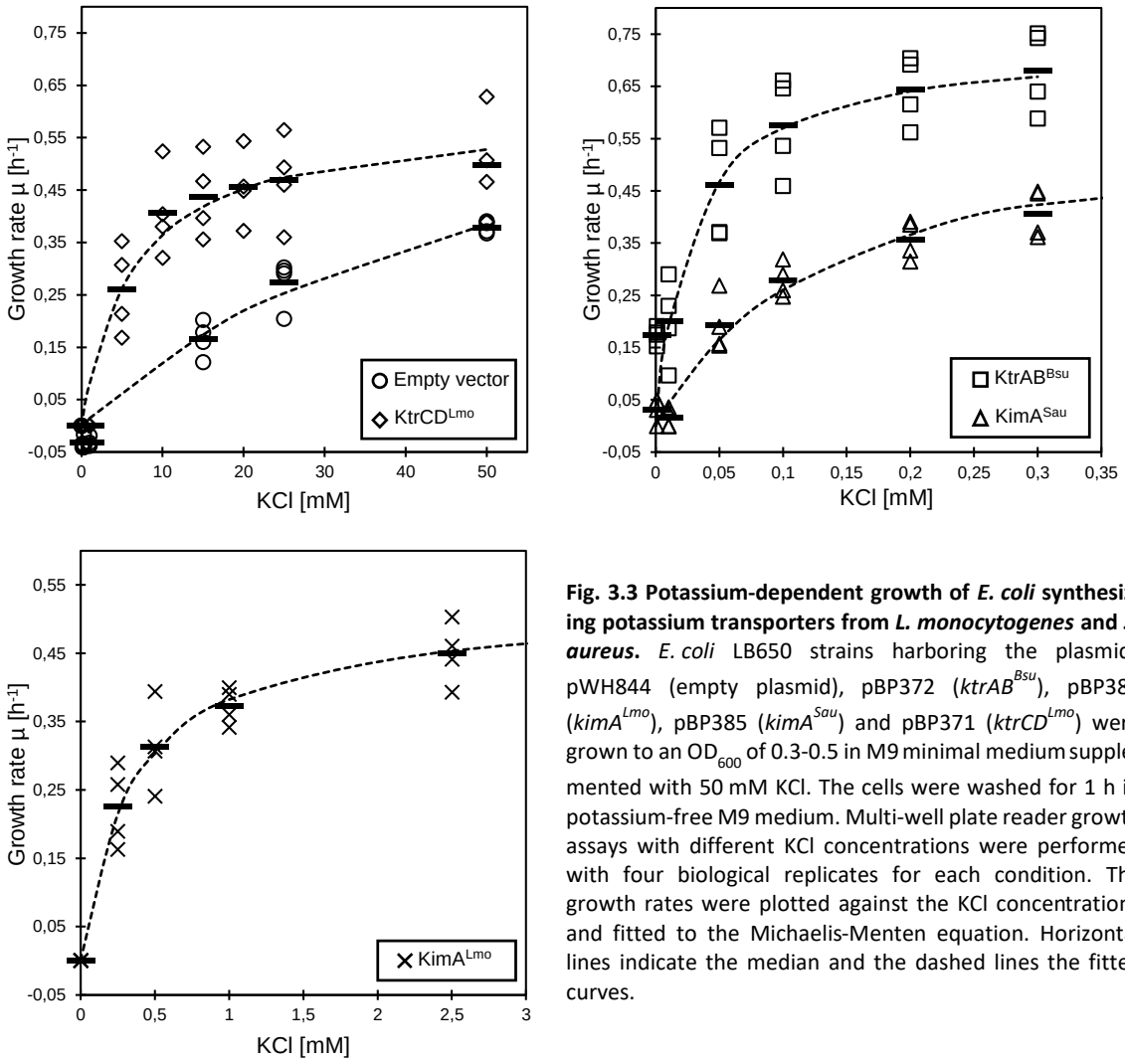

Fig. 3.3 Potassium-dependent growth of *E. coli* synthesizing potassium transporters from *L. monocytogenes* and *S. aureus*. *E. coli* LB650 strains harboring the plasmids pWH844 (empty plasmid), pBP372 (*ktrAB*^{Bsu}), pBP384 (*kimA*^{Lmo}), pBP385 (*kimA*^{Sau}) and pBP371 (*ktrCD*^{Lmo}) were grown to an OD_{600} of 0.3-0.5 in M9 minimal medium supplemented with 50 mM KCl. The cells were washed for 1 h in potassium-free M9 medium. Multi-well plate reader growth assays with different KCl concentrations were performed with four biological replicates for each condition. The growth rates were plotted against the KCl concentrations and fitted to the Michaelis-Menten equation. Horizontal lines indicate the median and the dashed lines the fitted curves.

Inhibition of KimA and KtrCD potassium transport activity by c-di-AMP - Several recent studies indicate that c-di-AMP is essential for viability of Gram-positive bacteria such as *B. subtilis*, *L. lactis, L. monocytogenes*, *S. agalactiae* and *S. aureus* because the nucleotide controls the influx of osmolytes like potassium, of which the accumulation leads to cell lysis due to water uptake (Devaux *et al.*, 2018; Gundlach *et al.*, 2017; Pham *et al.*, 2018; Woodward *et al.*, 2010; Zeden *et al.*, 2018). Thus, either synthesis of the potassium transporters their activity or both need to be tightly regulated. As shown in **Fig. 3.5**, the IPTG-dependent overexpression of the *ktrAB*^{Bsu} and *kimA*^{Lmo} genes encoding high-affinity potassium transporters KtrAB^{Bsu} and KimA^{Lmo}, respectively, in *E. coli* during growth in M9 minimal medium caused a strong increase of the cellular volume. Moreover, the growth of *E. coli* synthesizing the higher affinity KtrAB^{Bsu} transporter was in addition significantly reduced as illustrated by the decline of the optical density (**Fig. 3.5**; upper right corners). By contrast, in the absence of the inducer IPTG the growth and the volume of the cells containing the *ktrAB*^{Bsu} and *kimA*^{Lmo} genes were indistinguishable from that of the cells carrying the empty vector. Thus, once sufficient potassium has been taken up by the bacteria to cope with the osmolarity of the environment, the activities of osmolyte transporters have to be reduced to prevent further ion uptake and cell lysis. In case of KtrAB from *S. aureus* it has indeed been demonstrated that the activity of the transporter is inhibited by c-di-AMP (Corrigan *et al.*, 2013; Bai *et al.*, 2014). Like KimA^{Bsu} from *B. subtilis* the KimA^{Lmo} homolog from *L. monocytogenes* belongs to a novel class of high-affinity potassium transporters (see above; Gundlach *et al.*, 2017). However, whether

c-di-AMP directly binds to KimA^{Lmo} and KtrCD^{Lmo} to inhibit the transport activity of the proteins is unknown.

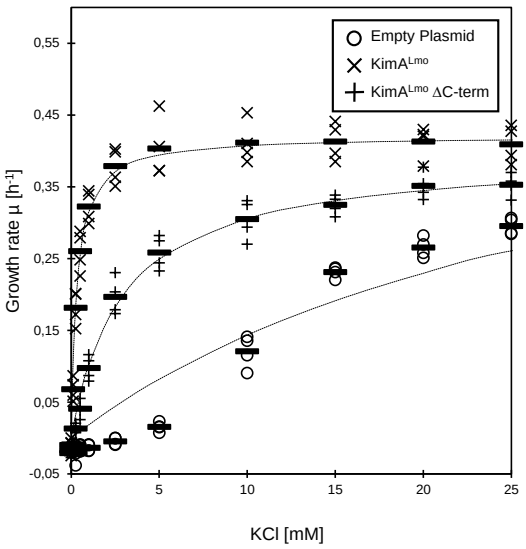

Fig. 3.4 Potassium-dependent growth of *E. coli* synthesizing the full-length and the C-terminally truncated KimA^{Lmo} protein. *E. coli* LB650 strains harboring the plasmids pWH844 (empty plasmid), pBP384 (*kimA^{Lmo}*) and pBP396 (*kimA^{Lmo}* ΔC-terminus) were grown to an OD_{600} of 0.3-0.5 in M9 minimal medium supplemented with 50 mM KCl. The cells were washed for 1 h in potassium-free M9 medium. Multi-well plate reader growth assays with different KCl concentrations were performed with four biological replicates for each condition. The growth rates were plotted against the KCl concentrations and fitted to the Michaelis-Menten equation. Horizontal lines indicate the median and the dashed lines the fitted curves.

To assess whether c-di-AMP affects the activity of KimA^{Lmo} and KtrCD^{Lmo}, we established a co-expression system using the *E. coli* strain LB2003, which carries unmarked mutations in the *kdp*, *kup* and *trk* genes and enable the use of multiple plasmids encoding chloramphenicol and ampicillin resistance genes (Stumpe & Bakker, 1997). Like the *E. coli* strain LB650, LB2003 is deficient in the Kdp, Kup and Trk potassium uptake systems, and is therefore only able to grow at low potassium concentrations when synthesizing a potassium transporter. Moreover, *E. coli* lacks c-di-AMP-producing and c-di-AMP-degrading enzymes, which is a prerequisite to assess the phenotypic effect of c-di-AMP on the activity of KimA^{Lmo} and KtrCD^{Lmo}. The plasmids pBP384 (*kimA^{Lmo}*), pBP396 (Δ*C-kimA^{Lmo}*) and pBP371 (*ktrCD^{Lmo}*) were used for the IPTG-dependent expression of ΔC-KimA^{Lmo}, KimA^{Lmo} and KtrCD^{Lmo}, respectively. The empty plasmid pWH844 served as a negative control. The *L. monocytogenes* DAC CdaA and the inactive CdaA* variant D171N (Rosenberg *et al.*, 2015) are encoded by the arabinose-inducible plasmids pBP370 and pBP373, respectively (Quintana *et al.*, 2019). The strains carrying pWH844, pBP384, pBP396 and pBP371 as well as either of the two DAC encoding plasmids were grown in M9 minimal medium supplemented with 30 mM, 0.35 mM, 3 mM and 7 mM KCl, respectively, conditions that allow half-maximal growth of the bacteria. As shown in **Fig. 3.6**, growth of the strains carrying the empty plasmid pWH844, and synthesizing the active and the catalytically inactive CdaA and CdaA* variants, respectively, was not reduced. Thus, neither the DAC proteins nor c-di-AMP affect growth of the *E. coli* strain. By contrast, growth of the bacteria synthesizing KimA^{Lmo} and KtrCD^{Lmo} was reduced when the active DAC CdaA was co-produced, indicating that c-di-AMP inhibits the transporter with a moderately high affinity for potassium and to a lesser extent also the low-affinity transporter (**Fig. 3.6**). In case of KtrCD^{Lmo}, a slight growth delay was also observed in the absence of an inducer for expression of wild type CdaA. Growth was not affected in the absence of a functional DAC and thus of c-di-AMP production. Moreover, c-di-AMP did not affect the activity of the C-terminally truncated ΔC-KimA^{Lmo} variant, indicating that the C-terminal intracellular domain of the transporter contributes to c-di-AMP-dependent regulation (see *Discussion*). Surprisingly, c-di-AMP did not inhibit the activity of KimA^{Sau} from *S. aureus* (data not shown). To conclude, the potassium transporters KimA^{Lmo} and KtrCD^{Lmo} from *L. monocytogenes* are both inhibited by c-di-AMP.

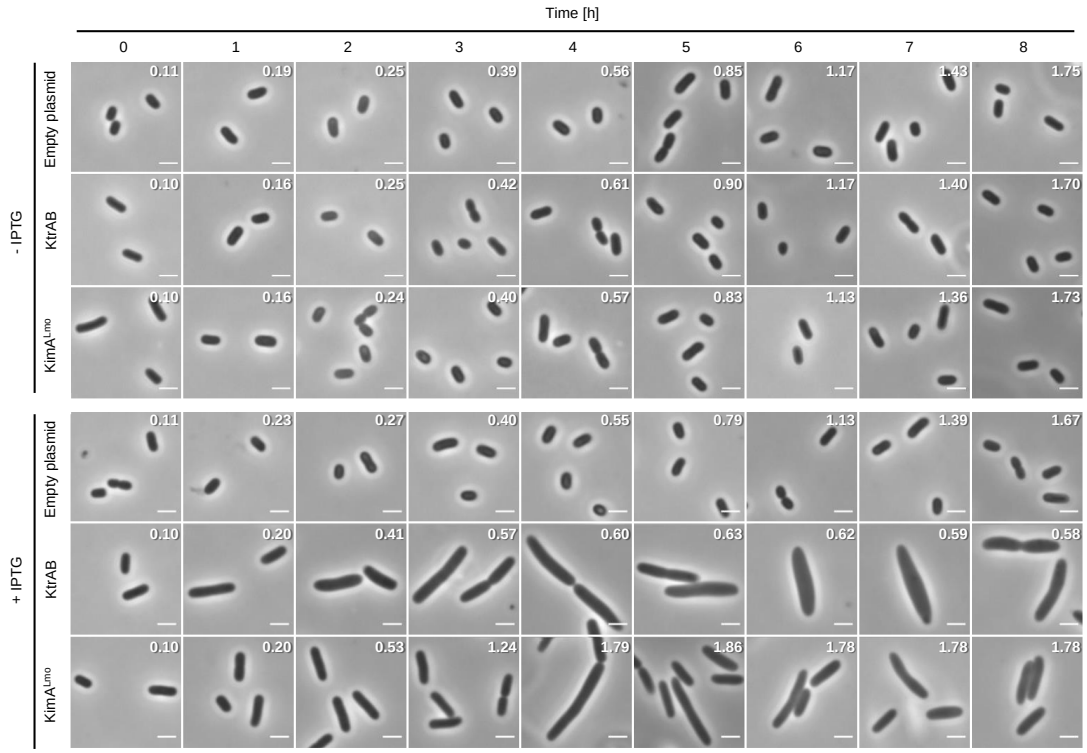

Fig. 3.5 Impact of unregulated potassium import on the cell volume of *E. coli*. Derivatives of the *E. coli* strain LB650 harboring plasmids pWH844 (empty plasmid), pBP372 (*ktrAB*^{Bsu}) and pBP384 (*kimA*^{Lmo}) were grown overnight in LB-K medium. The cells were washed and cultivated in M9 medium without and with 1 mM IPTG for the induction of the transporter genes. The OD_{600}, which is shown in the right upper corner of the microscopic pictures, was measured in hourly intervals. Scale bar, 2 µm.

c-di-AMP interaction with the KimA homologs and KtrCD^{Lmo} - To assess the interaction between c-di-AMP and the potassium transporters KimA^{Lmo}, ΔC-KimA^{Lmo}, KimA^{Sau}, and KtrCD^{Lmo} we performed a DRaCALA (see *Experimental procedures*). We also tested the interaction between c-di-AMP and the 156 and 158 amino acid long cytosolic C-terminal domains of KimA^{Lmo} and KimA^{Sau}, respectively. This domain could be involved in the c-di-AMP-dependent control of KimA potassium transport activity. The lysate of the *E. coli* strain DH5α containing the empty plasmids pWH844 or pGP172 served as negative controls. While the majority of the proteins showed no specific interaction with c-di-AMP in the DRaCALA assay, the potassium transporter KtrCD^{Lmo} gave a positive result (**Fig. 3.7**). To conclude, the potassium transport activity of KtrCD^{Lmo} from *L. monocytogenes* is inhibited by c-di-AMP *in vivo* and the nucleotide binds to the KtrC subunit of the KtrCD^{Lmo} transporter *in vitro*.

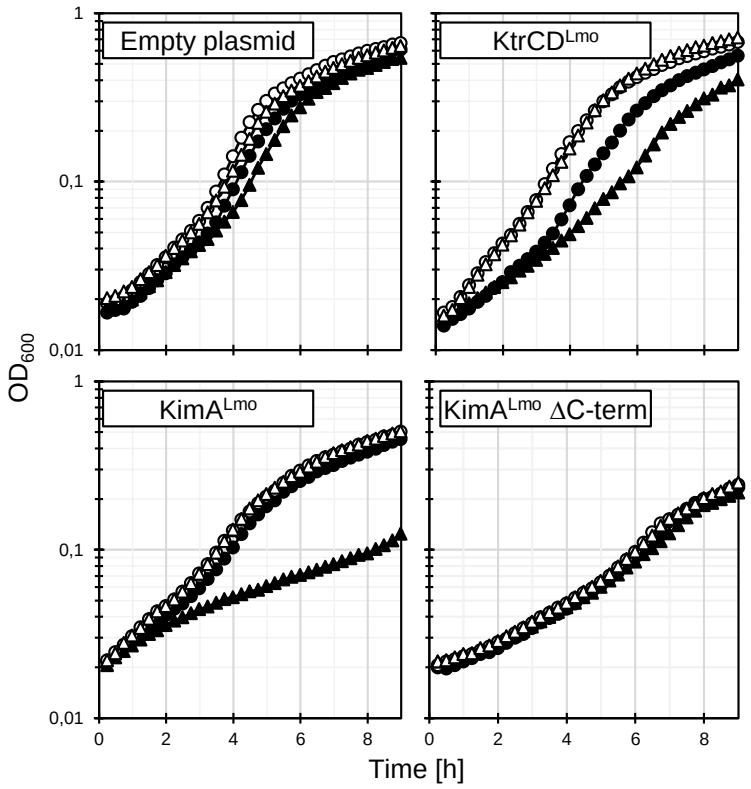

Fig. 3.6 Inhibition of potassium transporters by c-di-AMP. The *E. coli* strain LB2003 harboring the plasmids pWH844 (empty plasmid), pBP371 (*ktrCD*^{Lmo}), pBP384 (*kimA*^{Lmo}), pBP396 (*kimA*^{Lmo} ΔC-terminus) and either pBP370 (*cdaA*; filled symbols) or pBP373 (*cdaA* D171N; unfilled symbols) were grown to an OD_{600} of 0.3-0.5 in M9 medium and washed for one hour in potassium-free M9 medium. The growth assays were performed with (triangles) or without (circles) 0.005% (*w/v*) L-arabinose and at KCl concentrations that are equal to the K_M values of the transporters. Shown are the mean values of three biological replicates.

Discussion

In the present study, we have identified and characterized the potassium transporters KtrCD^{Lmo} and KimA^{Lmo} from *L. monocytogenes*. We have also demonstrated that *S. aureus* possesses a homolog of KimA (Sacol2443). The KimA homologs from *S. aureus* and *L. monocytogenes* belong to a novel class of high-affinity potassium transporters that are active at low external potassium concentrations (Gundlach *et al.*, 2017). By contrast, the KtrCD^{Lmo} transporter from *L. monocytogenes* has a much lower affinity for potassium than the homolog from *B. subtilis* (Holtmann *et al.*, 2003). As the external concentrations of potassium are rather low, it is tempting to speculate that *L. monocytogenes* possesses an additional high-affinity potassium transporter to be able to compete with other bacteria when the extracellular potassium is scarce. The phylogenetically related bacteria *B. subtilis* and *S. aureus* contain two high-affinity potassium transport systems that are active during growth at low potassium concentrations. *B. subtilis* employs the high-affinity potassium transporters KtrAB and KimA under potassium limiting growth conditions (Gundlach *et al.*, 2017; Holtmann *et al.*, 2003). *S. aureus* relies on the high-affinity transporter KdpFABC, whose synthesis and activity is regulated by the two-component system KdpDE (Gründling, 2013; Moscoso *et al.*, 2016; Price-Whelan *et al.*, 2013). Moreover, KimA^{Sau} could be important for growth of *S. aureus* when the extracellular potassium concentrations are low. In *L. monocytogenes*, additional potassium transport may be mediated by the KdpABCDE (Lmo2678-Lmo2682) system, as it is the case in *S. aureus*. The precise role of the KdpABCDE system and the KimA^{Sau} transporter from *L. monocytogenes* and *S. aureus*, respectively, in potassium homeostasis and their regulation in these bacteria remains to be investigated. Interestingly, also the *ktrCD* genes of *L. monocytogenes* might be subject to regulation on the level of gene expression. *ktrC* is located as last gene in an operon with two genes of unknown function and the genes *liaFSR*. The later three encode a three-component system involved in cell envelope stress response and a deletion of the *liaS* gene leads to higher expression of the operon, including *ktrC* (Fritsch *et al.*, 2011).

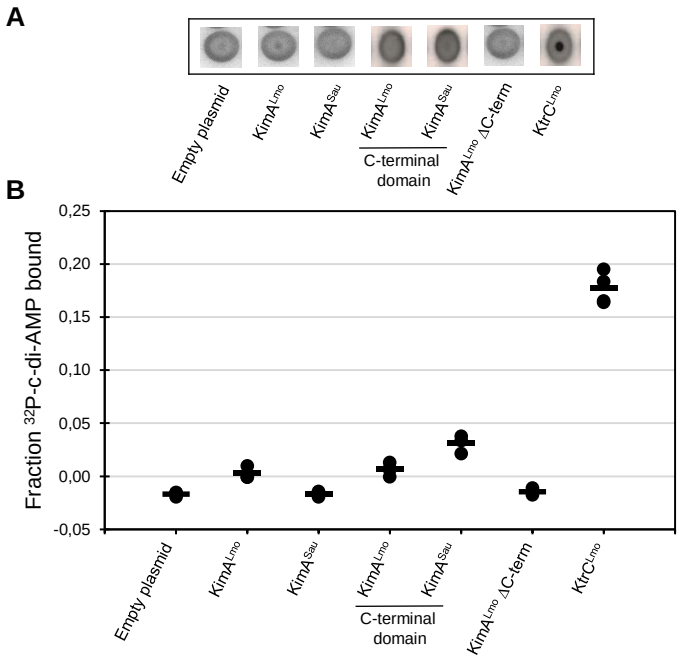

Fig. 3.7 Interaction between c-di-AMP and potassium transporters determined by DRaCALA. *A*, Autoradiographs showing the interaction between radiolabeled c-di-AMP (^{32}P-c-di-AMP) and the potassium transporters as well as the truncated variants that are present in whole cell lysates of the *E. coli* strain T7 Express I^q carrying the plasmids pGP172 (empty plasmid), or the derivatives pBP265 (*kimA*^{Lmo}), pBP266 (*kimA*^{Lmo} ΔC-terminus), pBP267 (*kimA*^{Sau}), or pWH844 (empty plasmid), or the derivatives pBP346 (*kimA*^{Lmo} C-terminal domain), pBP347 (*kimA*^{Sau} C-terminal domain) and pBP345 (*ktrC*^{Lmo}). Both empty vectors showed similar non-binding (data not shown). *B*, Fraction bound of ^{32}P-c-di-AMP is shown for lysates from *E. coli* induced overnight for the expression of the indicated gene. Data of three biological replicates and their mean values are depicted.

The *ktrD* gene is also the last gene of an operon, encoding two putative manganese transporters with a *yybP-ykoY* RNA motif in the promoter region of the operon, indicating potential regulation by this RNA motif. It will be interesting to elucidate the regulatory mechanisms of expression and activity of these transporters in *L. monocytogenes*.

As stated above, during growth under hyperosmotic conditions many bacteria take up potassium ions to prevent water efflux from the cytosol and to increase the cellular turgor (Kempf & Bremer, 1998). Once the cellular turgor has been adjusted to the environmental osmolarity, the transport of potassium ions across-the cell membrane has to be reduced to prevent osmotic swelling and cell lysis (Wood, 1999; Wood, 2011). A reduction of the ion uptake might be either achieved by proteolytic degradation or by controlling the activity of the transporters through binding of low-molecular weight ligands. It has indeed been shown that transport systems are rapidly degraded when the respective substrates are not available (Horak & Wolf, 1997). However, the cellular turgor is a physical variable that changes rapidly and needs to be tightly adjusted (Wood, 1999; Wood, 2011). Therefore, it is obvious that the regulation by inhibition is favorable over degradation, so the bacteria can quickly re-adjust if conditions change without having to depend on *de novo* synthesis of the transporter. Hence, the tight control of the cellular turgor requires the existence of low-molecular weight ligands, which specifically modulate the activity of potassium transporters and other osmolyte uptake systems. Indeed, in *S. aureus* it has been shown that the low-affinity potassium transporters KtrCB and KtrCD are inhibited by the second messenger c-di-AMP that binds to the RCK_C (regulator of conductance of K^+) domain of the KtrC gating component (Corrigan *et al.*, 2013). It also has recently been shown that *B. subtilis* KtrA and KtrC are functional redundant for potassium transporter regulation, if expressed in *E. coli* and that KtrC has a higher affinity for c-di-AMP, as KtrA (Rocha *et al.*, 2019). Moreover, c-di-AMP binds to the CabP protein and prevents potassium uptake by the CabP-TrkH protein complex in *S. pneumoniae* (Bai *et al.*, 2014). The cytoplasmatic regulatory subunit KtrC of the KtrCD potassium transporter is also bound by c-di-AMP in *Mycoplasma pneumoniae* (Blötz *et al.*, 2017). Differential regulation would require a kind of local signaling as it has been demonstrated for the second messenger c-di-GMP, which could be achieved by co-localization of synthesis and degradation machineries with the

targets of c-di-AMP signaling (Sarenko *et al.*, 2017). Here, we have demonstrated for the first time that the potassium transporters KtrCD^{Lmo} and KimA^{Lmo} from *L. monocytogenes* are inhibited by the second messenger c-di-AMP. This study also shows that the uncontrolled influx of potassium ions *via* the KtrAB^{Bsu} and KimA^{Lmo} results in osmotic swelling of *E. coli* (**Fig. 3.5**). In an accompanying paper it has been shown that c-di-AMP inhibits the potassium transport activity of the KimA homolog from *B. subtilis* (Gundlach *et al.*, 2019). Thus, c-di-AMP is required to reduce potassium uptake to toxic levels. Interestingly, c-di-AMP also controls the uptake of potassium at the level of transcription. For instance, c-di-AMP inhibits the sensor kinase KdpD of the KdpDE two-component system and thus reduces the expression of the *kdpFABC* operon encoding the high-affinity KdpFABC potassium transport system from *S. aureus* (Moscoso *et al.*, 2016; Price-Whelan *et al.*, 2013). Moreover, binding of c-di-AMP to the, in *L. monocytogenes* absent, *ydaO* riboswitch in the untranslated region of the *ktrAB* and *kimA* mRNAs prevents transcription beyond the riboswitch in *B. subtilis*, thereby reducing expression of the high-affinity potassium transporters KtrAB and KimA, respectively (Gundlach *et al.*, 2017; Nelson *et al.*, 2013). It should be noted that c-di-AMP also inhibits the uptake of other osmolytes such as glycine betaine and carnitine (Devaux *et al.*, 2018; Huynh *et al.*, 2016; Pham *et al.*, 2018; Schuster *et al.*, 2016; Whiteley *et al.*, 2017). Thus, c-di-AMP plays a central role in controlling the activities of potassium transporters and other osmolyte uptake systems, and the c-di-AMP-dependent regulation can occur at two different levels in a variety of bacteria. In the future, it will be interesting to investigate whether the synthesis of the *L. monocytogenes* potassium transporters KimA^{Lmo} and KtrCD^{Lmo}, which are both inhibited by c-di-AMP, is also regulated by the nucleotide. Moreover, it might be worth to study the role of the C-terminal cytosolic domain in the activity control of the KimA potassium transporter. Unfortunately, we could not find an interaction between c-di-AMP and the C-terminal domain of KimA^{Lmo} in *E. coli* cell lysates. However, this domain seems to be important for the c-di-AMP-mediated regulation of KimA^{Lmo} since the C-terminally truncated variant lacking 156 amino acids did not respond to the nucleotide *in vivo*.

Recently, it has been demonstrated that the control of potassium uptake is an essential function of c-di-AMP in *B. subtilis* (Gundlach *et al.*, 2017). A *B. subtilis* strain lacking all c-di-AMP-producing enzymes was only viable in medium containing low potassium concentrations. c-di-AMP is also essential in bacteria like *L. monocytogenes*, *S. agalactiae* and *S. aureus* to prevent the uptake of osmolytes to toxic levels (Devaux *et al.*, 2018; Pham *et al.*, 2018; Whiteley *et al.*, 2015). However, in these bacteria the control of glycine betaine and amino acid uptake seems to be the essential function of c-di-AMP. Thus, phylogenetically related bacteria have evolved species-specific mechanisms to regulate the cellular turgor, but they all use c-di-AMP in this essential process (Commichau *et al.*, 2018). It remains to be elucidated how c-di-AMP controls potassium homeostasis in *L. monocytogenes.* Moreover, it will be crucial to identify the osmo-signal sensing mechanism of the c-di-AMP system, which could be conserved among different bacteria (Commichau *et al.*, 2018; Pham *et al.*, 2018).

Acknowledgements

We thank Jasmin Gömann for the help with some experiments. We are grateful to Sabine Lentes for technical support. This work was supported by the grant CO 1139/2-1 from the Deutsche Forschungsgemeinschaft via the Prioritiy Program SPP1879, the Fonds der Chemischen Industrie and the Max-Buchner-Forschungsstiftung (MBFSt-Kennziffer 3381) to FMC.

4. Global effects of c-di-AMP on gene expression and protein biosynthesis in *Listeria monocytogenes*

Johannes Gibhardt, Samuel Hauf, Alexander Reder, Andrea Thürmer, Uwe Völker, Sven Halbedel and Fabian M. Commichau

Author contribution:
JG performed the experiments and data evaluation, SH and AT and SH performed the RNA-Seq, AR and UV performed the protein quantifications, JG and FMC wrote the manuscript.

Abstract

The nucleotide second messenger cyclic di-AMP (c-di-AMP) has been associated with various crucial cellular functions. c-di-AMP is essential in Firmicutes under most growth conditions and has been extensively investigated in the model bacterium *Bacillus subtilis* and in pathogenic bacteria, like *Listeria monocytogenes*, *Staphylococcus aureus* or *Streptococcus pneumoniae*. It is synthesized by diadenylate cyclases (DACs) and degraded by specific phosphodiesterases (PDEs) and has been shown to regulate activity of proteins, regulate translation by binding to RNA structures and to control gene expression by regulation of transcriptional regulators. Thus, c-di-AMP can act on all levels of protein synthesis. The second messenger has been associated with regulation of osmotic homeostasis by regulation of potassium and compatible solute import, cell wall biosynthesis, DNA repair mechanisms, regulation of central carbon and nitrogen metabolism and to modulate other nucleotide second messenger signaling pathways, like the stringent response. To elucidate the impact of c-di-AMP on the overall cellular function, we investigated changes in transcriptome and proteome of a *cdaA* deletion mutant, encoding the sole DAC in *L. monocytogenes* under defined growth conditions in *Listeria* synthetic medium (LSM). Changes in gene expression and protein biosynthesis revealed a total of 95 differently regulated genes and 21 proteins with different abundance. The deregulated influences important processes as the central carbon metabolism, nitrogen metabolism, cell wall and lipid biosynthesis, ion transport or expression of motility associated genes. The present report will help to identify novel targets of the c-di-AMP regulatory network and deepen the understanding about c-di-AMP signaling.

Introduction

Bacteria have to adapt to various stimuli and compete with other organisms to thrive in their environment. It is therefore important for cells to have a repertoire of sensing and signal modulation machineries to integrate these stimuli and respond properly. One key feature is the modulation of gene expression and protein biosynthesis to react to immediate changes in conditions or the long-term adaptation by acquisition of genome amplifications and evolution of mutations (Andersson & Hughes, 2009; López-Maury *et al.*, 2008). The fastest response, despite modulating gene expression or protein biosynthesis, is the modulation of protein activity by direct influence of stimuli or through ligand binding. One example for a direct influence is the regulation of mechanosensitive channels that directly react on changes in turgor upon a hypoosmotic shock, before other cellular processes catch up with the changes in external osmolarity (Hoffmann, *et al.*, 2008). An important tool that has evolved for the integration of environmental clues are second messenger molecules. Among them, nucleotide second messenger molecules play important role in adaptation to manifold environmental stimuli (Newton *et al.*, 2016). c-di-AMP is one of those nucleotide second messenger molecules (Commichau *et al.*, 2015; Corrigan *et al.*, 2013). It is synthesized and degraded by different set ups of DACs and PDEs, respectively, in different bacterial species (Commichau *et al.*, 2019). c-di-AMP has been connected to several important cellular functions, ranging from DNA damage repair, to cell wall metabolism, regulation of central carbon and nitrogen metabolism or lifestyle changes in different bacteria, like *B. subtilis*, *L. monocytogenes*, *S. aureus*, *Lactococcus lactis* or *Mycobacterium smegmatis* (Corrigan *et al.*, 2011; Kaplan Zeevi *et al.*, 2013; Luo & Helmann, 2012; Mehne *et al.*, 2013; Oppenheimer-Shaanan *et al.*, 2011; Whiteley *et al.*, 2013; Witte *et al.*, 2008; Witte *et al.*, 2013; Zhang & He, 2013; Zhu *et al.*, 2016). In the recent years however, it has been shown that the main function of c-di-AMP and the reason for its essentiality and toxicity, under different growth conditions (Gundlach *et al.*, 2015), is the regulation of osmohomeostasis (Devaux *et al.*, 2018; Gundlach *et al.*, 2017; Huynh *et al.*, 2016; Pham *et al.*, 2018; Schuster *et al.*, 2016; Whiteley *et al.*, 2015; Whiteley *et al.*, 2017; Zeden *et al.*, 2018). It was therefore also proposed that many phenotypes of mutants that affect c-di-AMP signaling, especially the cell wall-associated ones that are seen in an altered resistance to β-lactam antibiotics, might be at least in part indirect effects due to the role of c-di-AMP as major regulator of osmotic homeostasis in firmicutes (Commichau *et al.*, 2018). A link between c-di-AMP and cell wall metabolism however, seems to be established due to the regulation of CdaA activity, the sole DAC in many pathogenic firmicutes, by the phosphoglucosamine mutase GlmM that is involved in peptidoglycan precursor synthesis and able to inhibit CdaA activity (Tosi *et al.*, 2019; Zhu *et al.*, 2016). c-di-AMP has furthermore been shown to be involved in cross-regulation with other nucleotide second messenger signaling pathways, such as the stringent response (Corrigan *et al.*, 2015; Huynh *et al.*, 2015; Rao *et al.*, 2010; Whiteley *et al.*, 2015). Due to this cross-talk c-di-AMP probably also influences other, still unknown pathway, like regulation of the pleiotropic transcriptional regulator CodY and thereby processes like the import of oligopeptides *via* the Opp transporter that are important for *L. monocytogenes* as osmolytes (Geiger & Wolz, 2014; Whiteley *et al.*, 2017). To understand these indirect and direct effects of c-di-AMP is crucial for understanding the regulation of those important cellular processes. It has for example been shown that a *B. subtilis gdpP* deletion mutant, which accumulates higher intracellular concentrations of c-di-AMP, leads to an inhibition of biofilm formation and facilitates expression of motility associated genes (Gundlach *et al.*, 2016). Analysis of whole cell changes in gene expression and protein biosynthesis can therefore be a powerful tool to find novel direct and indirect processes that are regulated by a second messenger, such as c-di-AMP. We therefore investigated the impact of a *cdaA* deletion that encodes the only c-di-AMP synthesizing enzyme in *L. monocytogenes* under defined conditions. To the best

of our knowledge, this study is the first, to investigate the impact of lack of c-di-AMP on global changes in gene expression and protein biosynthesis. The transcriptomic and proteomic analyses revealed a broad impact of c-di-AMP on cellular functions and highlights possible new genes and whole operons that are directly or indirectly regulated by c-di-AMP, hence deepen our understanding of c-di-AMP signaling.

Experimental procedures

Bacterial strains and growth conditions – *L. monocytogenes* EGD-e and its derivatives were cultivated in BHI medium (Sigma-Aldrich) at 37°C and 220 rpm if not specified otherwise. *Escherichia coli* was grown in LB medium at 37°C and 220 rpm (strains **see Tab. 4.1**). For agar plates, medium was supplemented with 15 g/l Bacto Agar (Difco). Antibiotics and medium supplements were used with the following concentrations, if indicated: erythromycin (5 µg/ml), ampicillin (100 µg/ml), X-Gal (100 µg/ml; 5-bromo-4-chloro-3-indolyl-β-D-galactopyranoside; Sigma-Aldrich). As a minimal medium for *L. monocytogenes* the LSM medium (Whiteley *et al.*, 2017) was used with previously described changes (**see chapter 2**). For pouring minimal medium agar plates, 2 X concentrated medium was pre-warmed to 37°C and mixed with to 70°C pre-warmed 2 X Bacto agar, directly before pouring the plates.

Tab. 4.1 Strains

Name	Genotype	Description/Construction	Reference
E. coli			
XL1-Blue	*recA*1 *endA*1 *gyrA*96 *thi*$^{-}$1 *hsdR*17 *supE*44 *relA*1 *lac* [F′ *proAB lacI*^{q} *Z*ΔM15 Tn*10* (*Tet*^{R})]	Cloning	Stratagene
L. monocytogenes			
EGD-e	Wild type	Serotype 1/2a strain	Laboratory collection
BPL10	Δ*fliI*::P_{alf4}-RBS_{hly}-*mgfp* (A206K)	pBP351 →→ EGD-e	This work
BPL23	Δ*pgpH*	pBP355 →→ EGD-e	This work
BPL24	Δ*pdeA*	pBP356 →→ EGD-e	This work
BPL77	Δ*cdaA*	Chromosomal deletion of *cdaA*	Chapter 2
LMJR45	Δ*cdaR*	Chromosomal deletion of *cdaR*	Rismondo *et al.*, 2016

→→ transformation and gene deletion, :: = insertion/replacement

DNA manipulation – DNA amplification *via* PCR and transformation of *E. coli* was performed using standard procedures (Sambrook *et al.*, 1989). DNA fragments were purified using the PCR purification kit (Qiagen) and plasmid DNA was extracted using the NucleoSpin Plasmid Kit (Macherey and Nagel). Commercially available restriction enzymes, T4 DNA ligase and DNA polymerases were used as recommended by the manufacturers. DNA sequences were determined by the dideoxy chain termination method (Microsynth, Göttingen, Germany). Chromosomal DNA of *L. monocytogenes* was isolated using the NucleoSpin Microbial DNA Kit (Macherey and Nagel). Oligonucleotides were purchased from Sigma-Aldrich (Germany).

Plasmid construction – For the chromosomal replacement of the *fliI* gene by *mgfp* (A206K) and the chromosomal deletions of the *pgpH* and *pdeA* genes, plasmids pBP351, pBP355 and pBP356 were constructed, respectively (plasmids are listed in **Tab. 4.2**). The *mgfp* gene was amplified from plasmid pBP43 using oligonucleotides JH01 and JH02 (for the oligonucleotides see **Tab. 4.3**), with JH01

attaching the artificial *alf4* promoter and the ribosomal binding site of the *L. monocytogenes* gene *hly* to facilitate *mgfp* expression (Cascante-Estepa *et al.*, 2016; Stannek, 2015). The resulting PCR product was digested with *Eco*RI and ligated to pSH185 (pMAD-Δ*fliI*; Halbedel *et al.*, 2012), which was digested with the same enzymes and *via* sequencing a plasmid identified, in which the *gfp* gene lies in reverse orientation to the operon to minimize effects of the promoter of the operon on the *gfp* gene and of the *alf4* promoter on the following genes of the operon. For construction of pBP355 and pBP356, the up- and downstream regions of the genes *pgpH* and *pdeA* were amplified using oligonucleotide pairs JH17/JH18 and JH19/JH20 for *pgpH* and JH13/JH14 and JH15/JH16 for *pdeA*, respectively. The resulting PCR products were fused by SOE PCR using oligonucleotide pairs JH17/JH20 and JH13/JH16 for *pgpH* and *pdeA*, respectively (Horton *et al.*, 1990). The resulting up- and downstream fusion PCR products were subsequently digested with *Eco*RI and *Bam*HI and ligated to pMAD that was digested using the same enzymes (Arnaud *et al.*, 2004).

Tab. 4.2 Plasmids

Name	Insert/Features	Reference
pMAD	*bla ermC bgaB*	Arnaud *et al.*, 2004
pSH185	pMAD-Δ*fliI*	Halbedel *et al.*, 2012
pBP43	pUS19-*mgfp* (A206K)	Cascante-Estepa *et al.*, 2016
pBP351	pMAD-Δ*fliI*::P_{alf4}-RBS_{hly}-*mgfp* (A206K)	This work
pBP355	pMAD-Δ*pgpH*	This work
pBP356	pMAD-Δ*pdeA*	This work

bla = amp^R (100 µg/ml ampicillin), *ermC* = ery^R (5 µg/ml erythromycin), :: = insertion/replacement

L. monocytogenes strain construction – BPL10 was constructed by the chromosomal replacement of *fliI* by *mgfp* to have a non-motile and fluorescent strain. To have strains with defects in c-di-AMP degradation and investigate those effects, strains BPL23 and BPL24 were constructed, harboring chromosomal deletions of *pgpH* or *pdeA*, respectively. BPL10, BPL23 and BPL24 were constructed as follows. Preparing electrocompetent cells and the electroporation is described elsewhere (Monk *et al.*, 2008; **chapter 2**). The EGD-e wt was electroporated with plasmids pBP351, pBP355 or pBP356, respectively, and plated on BHI medium with erythromycin and X-Gal at 30°C for up to 72 h. Single, blue colonies were streaked on the same medium and incubated for up to 72 h at 42°C to force integration of the plasmids into the different gene loci. Several blue colonies were used to inoculate 5 ml of BHI medium without antibiotics at 30°C for 4 h, temperature was shifted to 42°C for 6 h, after which serial dilutions were plated on BHI agar plates with X-Gal and incubated at 42°C for up to 72 h. Erythromycin-sensitive, X-Gal negative bacteria were subjected to colony PCR as described elsewhere (Dussurget *et al.*, 2002). *fliI* replacement and *pgpH* or *pdeA* deletion was confirmed by Sanger sequencing.

Tab. 4.3 Oligonucleotides

Name	Restriction sites are underlined, complementary regions are in bold, sequences 5'→3'	Purpose and reference
JH01	AAAGAATTCTAATTCTTGTCAAGTGAAGGCGCGCTATGCTACAATACAGCTT-GGAAATCTA-GAAGGAGAGTGAAACCCATGAGTAAAGGAGAAGAACTTTTCACTGGAG	Fwd. P_{alf4}-RBS_{hly}-*mgfp* (A206K) (*Eco*RI)
JH02	TTTGAATTCTTATTTGTATAGTTCATCCATGCCATGTGTAATC	Rev. *mgfp* (A206K) (*Eco*RI)
JH13	AAAGAATTCGAATGCCTACACATCAAGGTATGGG	Fwd. *pdeA* upstream region (*Eco*RI)

Name	Restriction sites are underlined, complementary regions are in bold, sequences 5'→3'	Purpose and reference
JH14	**TACGCATCAATGTCGACCCCATTTTT**TTACATACCTTTTGCCTG	Rev. *pdeA* upstream region (*Sal*I)
JH15	**AAAAATGGGGTCGACATTGATGCGTA**TTGGAAGGGAGAAAC	Fwd. *pdeA* downstream region (*Sal*I)
JH16	TTTGGATCCGCGCCTCATAAACCGTTAATACATCG	Rev. *pdeA* downstream region (*Bam*HI)
JH17	AAAGAATTCCTGTACAGCATACGACTGCCGT	Fwd. *pgpH* upstream region (*Eco*RI)
JH18	**CTCCTATTTCAGTCGACTCTCTAATTTTG**TTTCCCTTCGTAAGCT	Rev. *pgpH* upstream region (*Sal*I)
JH19	**CAAAATTAGAGAGTCGACTGAAATAGGAG**GGCAAAAGATGACG	Fwd. *pgpH* downstream region (*Sal*I)
JH20	TTTGGATCCTCGCTGTGTTCACCATCTCTAGC	Rev. *pgpH* downstream region (*Bam*HI)

Fwd. = forward, Rev. = reverse

Motility assay – The *L. monocytogenes* wild type strain, the *fliI* mutant BPL10, the *pgpH* and *pdeA* mutants BPL23 and BPL24, respectively, and the *cdaA* mutant BPL77 (**see chapter 2**) were used to assess the impact of c-di-AMP on the motility. Strains were cultivated in 5 ml LSM overnight at 37°C and 220 rpm. The pre-cultures were used to inoculate 5 ml of LSM medium to an OD_{600} of 0.1 and the cells were incubated at 37°C and 220 rpm. Cells were harvested and resuspended in fresh LSM medium after reaching an OD_{600} of about 0.5 and 1 µl of OD_{600} 1.0 cell suspensions were used to stab inoculate LSM or BHI soft agar plates (0.3% (*w/v*) agar). Plates were incubated at 25°C or 37°C, as indicated and imaged every 24 h.

Growth of L. monocytogenes *wt and Δ*cdaA *mutant for transcriptomic and proteomic analysis* – To analyze the changes in the transcriptome and proteome of *L. monocytogenes*, if the sole c-di-AMP synthesizing enzyme CdaA is not present, the wild type strain EGD-e and the *cdaA* clean deletion mutant BPL77 (**see chapter 2**) were cultivated and processed as follows. Single colonies were propagated from LSM agar plates to 10 ml LSM overnight at 37°C and 220 rpm. Pre-cultures were used to inoculate 100 ml LSM medium to an OD_{600} of 0.05 and incubated at 37°C and 220 rpm. For the analysis of the proteome 40 OD_{600} units of cells were harvested by rapid cooling in liquid nitrogen to slow down cellular processes and subsequent centrifugation after reaching an OD_{600} of about 0.5 at 3300 g and 4°C for 10 min. Cell pellets were washed twice in ZAP (50 mM Tris pH 7.5 and 200 mM NaCl), with centrifugation steps in between. Resulting pellets were frozen in liquid nitrogen and stored at -80°C until further processing. Growth for the analysis of the transcriptome was performed similar. When the cultures reached OD_{600} of 0.5 ± 0.05, 25 ml were collected and quenched by adding of 25 ml ice cold killing buffer (20 mM Tris-HCl pH 7.5, 5 mM $MgCl_2$, 20 mM NaN_3). After 5 min incubation on ice, cells were harvested by centrifugation. mRNA extraction, library preparation and RNA sequencing where subsequently performed as described previously in detail (Hauf *et al.*, 2019).

mRNA isolation and RNA sequencing – Shortly, cell pellets were resuspended in 1 ml Lysis Buffer I (25% sucrose; 20 mM Tris-HCl pH 8, 0.25 mM EDTA) and 2 µl of lysozyme (100 mg ml–1) was added. After 5 min on ice, the samples were pelleted and resuspended in 300 µl Lysis Buffer II (3 mM EDTA, 200 mM NaCl). This solution was then mixed with 300 µl Lysis Buffer III (3 mM EDTA, 200 mM NaCl, 1% SDS) and the mixture was incubated at 95°C for 5 more minutes. Six hundred micro liter phenol/chloroform/isoamylalcohol (25:24:1) was added and vigorously mixed at room temperature for 5 min. Phases were separated by centrifugation, the aqueous upper phase was collected and the phenol/chloroform extraction was repeated. Afterward, the aqueous phase was mixed with 600 µl chloroform/isoamylalcohol (25:1), shaken vigorously for 5 min and phases were

separated by centrifugation. The chloroform extraction was repeated. Finally, RNA was precipitated by addition of 0.1 × volume 3 M sodium acetate (pH 5.2) and 1.5 volumes 96% ethanol and incubation at -20°C overnight and pelleted by centrifugation. The pellet was washed with 70% ethanol and resuspended in 100 µl DEPC treated water. Ten micro gram of total RNA were digested with DNAse using the RNase-Free DNase Set (Qiagen). RNA was then purified using RNA clean & concentrator columns (Zymo Research) for purification for RNA molecules longer than 200 nucleotides. RNA quality was assessed using Agilent Bioanalyzer RNA Nano chips. rRNA depletion was performed using the Ribo-Zero Bacteria Kit (Illumina). A total of approximately 2 µg purified RNA was treated with 10 µl Ribo-ZeroRemoval Solution and RNA concentrations were determined using a Qubit® fluorometer. After rRNA removal, the remaining RNA was pelleted by ethanol precipitation following the recommendations in the Ribo-Zero protocol (Hauf *et al.*, 2019).

RNA libraries were prepared using the TruSeq® Stranded mRNA Kit. The RNA libraries were sequenced in paired-end mode with 2 times 76 cycles on the Illumina MiSeq (MiSeq® Reagent Kit v3; 150 cycles). RNA transcripts were quantified by quasi-mapping of the reads to the *L. monocytogenes* EGD-e cDNA, provided by the Ensembl Genomes server (Kersey *et al.*, 2018), using the Salmon software (Patro *et al.*, 2017). Average expression from three biological replicates of the mutant divided by the average expression from three biological replicates of the wild type gave the differential expression ratio. Log_2- transformed transcript counts from three biological replicates were then used to calculate P values using Student's t-test. Significantly differentially expressed genes were defined as having a P-value less than 0.01 and an absolute differential expression factor of more than 2 as well as having an expression level of at least 16 TPM (Hauf *et al.*, 2019).

Protein isolation and proteome analysis – Cell pellets were resuspended in 200 µl UT (8 M urea/2 M thiourea) buffer and immediately released as individual drops directly into a pre-chilled 3 ml Teflon vessel filled with liquid nitrogen. A pre-cooled steel ball (8 mm diameter) was added to the vessel and the frozen cells were mechanically disrupted using the Micro-Dismembrator (Braun, Melsungen) at top speed (2600 rpm) for two minutes. The still frozen powder was instantly taken up in 1800 µl UT buffer and then sonified three times for 5 sec. at 50% intensity. Afterwards, the protein extract was centrifuged for 1 h at 4°C and 16000 g. The supernatant was transferred to a fresh tube and the protein concentration was determined with a Bradford assay kit (Pierce, Thermo Scientific, Bonn). Sample aliquots were stored at -80°C. Sample aliquots of 2 µg were diluted with 20 mM ammonium-bicarbonate (ABC) buffer until a final concentration of less than 1 M urea was reached. Following reduction by 2.5 mM DTT (30 min at 37°C) and alkylation by 10 mM Iodoacetamide (15 min at 37 in the dark), trypsin [20 ng/µl] was added and incubated at 37°C overnight. The reaction was stopped with a final concentration of 5% acetic acid and the peptide mixtures were desalted on C-18 reverse phase material (ZipTip μ-C18 Millipore Corporation, Billerica, MA). Peptides were eluted in 50 and 80% acetonitrile (ACN) each in 1% acetic acid. Pooled eluates were dried in a vacuum concentrator and resuspended in 20 µl of buffer A (2% ACN in 0.1% acetic acid) with a final concentration of 0.1 µg/µl protein (tryptic peptides) prior MS analysis.

Mass spectrometry measurements – The tryptic peptides were separated on an Accucore 150-C18 analytical column of 250 mm (25 cm x 75 µm, 2,6 µm C18 particles, 150 Å pore size, Thermo Fischer Scientific™, USA) using a Dionex Ultimate 3000 nano-LC system (Thermo Fischer Scientific™, Germany). The peptide elution was performed at a constant temperature of 40°C with a flow rate of 300 nL/min with a 60 minutes linear gradient (2% to 25%) of buffer (acetonitrile in 0.1% acetic acid). To design a species-specific spectral library MS/MS data were recorded on a Q Exactive™

HF-X mass spectrometer (Thermo Fischer Scientific™, Germany) in data-dependent mode (DDA). The DDA-MS measurement parameters are listed in **Tab. S4.2**. The final MS/MS analyses of samples were performed in data independent mode (DIA) on a Q Exactive™ HF-X mass spectrometer (Thermo Fischer Scientific™, Germany). The DIA-MS measurement parameters are listed in **Tab. S4.3**.

Analysis of mass spectrometry data – The ion library of *L. monocytogenes* EGD-e was generated using Spectronaut™ Pulsar 12 (v12.0.20491.9.26895) software (Biognosys AG, Switzerland). The ion library construction was done using the DDA-MS measurements and the settings summarized in **Tab. S4.4**. The DIA-MS analysis was also performed using Spectronaut™ Pulsar 12 with the parameters listed in **Tab. S4.5**. The DIA-MS data analysis was performed using R (Team, 2014) (version 3.52) and the tidyverse (Vienna, Austria, 2017, n.d.) and PECA (Suomi *et al.*, 2015) package. The raw MS2 total peak area of ions was median normalized on the global median. The median ion quantity was subsequently summed up for each peptide and sample to obtain the peptide intensity. The peptide intensities were used for the statistical ROPECA (reproducibility-optimized peptide change averaging) analysis workflow (Suomi & Elo, 2017). Proteins with a fold-change ≥ 2 and Q-value (FDR) < 0.05 were considered as significantly altered in their abundance.

Data analysis – The in gene expression or protein biosynthesis affected genes and proteins were later on analyzed using the Geneious software (Geneious Prime 2019.0.4 (https://www.geneious.com)) and the online resources ListiWiki (http://listiwiki.uni-goettingen.de) and SubtiWiki (http://subtiwiki.uni-goettingen.de), the Listeriomics website (https://listeriomics.pasteur.fr) and the annotation databases RAST and COG (Aziz *et al.*, 2008; Bécavin *et al.*, 2017; Tatusov *et al.*, 2000; Zhu *et al.*, 2018).

Results

Deletion of cdaA *leads to global alteration of gene expression and protein biosynthesis* – The *L. monocytogenes* wild type strain and a clean deletion mutant of the *cdaA* gene (**see chapter 2**), encoding the sole DAC of *L. monocytogenes*, were grown under defined conditions in LSM (growth curves are shown in **Fig. S4.1**) and changes in transcriptome and proteome analyzed (Whiteley *et al.*, 2017). 95 genes were differently expressed (at least a two-fold change and p<0,01), with 36 down- and 59 upregulated and 21 proteins showed a significant change in abundancy of at least 30% (p and p,fdr<0,01), with 11 showing a lower and 10 a higher abundance (in the Δ*cdaA* mutant compared to the wild type strain). Loci of the respective genes and the genes encoding the respective proteins were mapped on the *L. monocytogenes* EGD-e wt genome. As depicted in **Fig. 4.1**, differently expressed genes are more or less evenly distributed around the chromosome with some hotspots visible.

Among the most downregulated genes (**Tab. 4.4**) are genes encoding for proteins involved in cell division (Lmo2506-2507; FtsXE), a putative N-acetylmuramoyl-L-alanine amidase (Lmo1216) and the putative cell wall hydrolase Lmo2522, highlighting the impact of c-di-AMP on cell wall biogenesis and cell wall remodeling. Among others, genes involved in purine biosynthesis (*lmo1764-lmo1765*, *lmo1770-lmo1772*; *purD*, *purE*, *purS, purL*, *purC*), in arginine biosynthesis (*lmo2090-2091*; *argGH*) and *lmo0423*, encoding the in heat stress and cold adaptation involved sigma factor σ^S are upregulated. This demonstrates the impact c-di-AMP has on central cellular processes, like nucleotide and amino acid biosynthesis and regulation of stress responses.

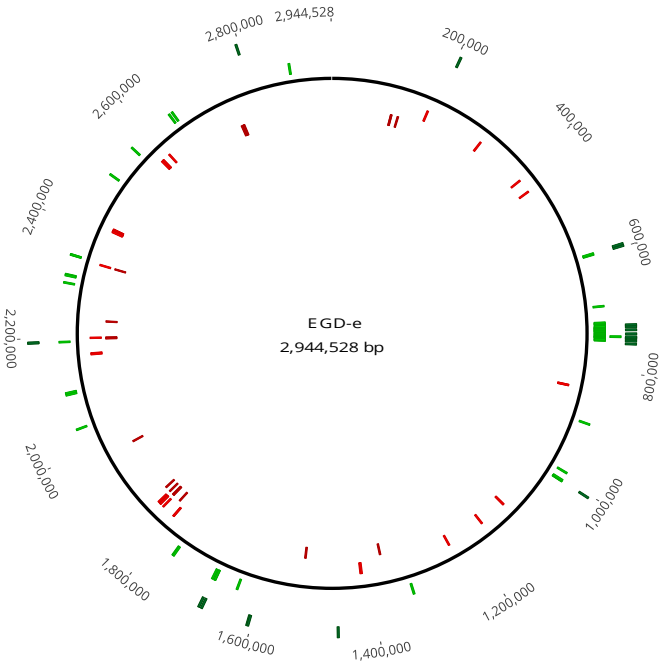

Fig. 4.1 Genome map of *L. monocytogenes* depicting differently expressed genes and proteins in a Δ*cdaA* mutant. The *L. monocytogenes* wt strain and the Δ*cdaA* mutant were grown in LSM at 37°C and harvested in the exponential growth phase. Differentially expressed genes and proteins were analyzed by RNA-Seq and Mass-spectrometry as described in the experimental procedures. Differentially expressed genes with a p<0.01 and at least a two-fold change in expression levels are depicted as light green and light red for up- and downregulated genes, respectively, in the Δ*cdaA* mutant. Proteins that show a different abundance with a p<0,01 and a p,fdr<0,01 and a signal to $\log_2$ ratio are mapped on their respective gene loci. Dark green and dark red depict proteins with a higher or lower abundance in the Δ*cdaA* mutant, respectively. The depiction shows that up- and downregulation of expression is distributed over the whole chromosome with some regions of higher occurrence, e.g. at 3 o'clock.
p, probability value; fdr, false discovery rate.

Tab. 4.4 The twenty most downregulated genes in *ΔcdaA*

Locus tag	Operon	Name	RAST info	Fold change
lmo2120	388	***cdaA***	Diadenylate cyclase CdaA	**-372.50**
lmo1216			N-acetylmuramoyl-L-alanine amidase, family 4	**-17.85**
lmo2522		yocH	Cell wall-binding protein	**-13.04**
lmo0186			Cell wall-binding protein	**-10.07**
lmo1764	310	**purD**	Phosphoribosylamine--glycine ligase	**-4.41**
lmo1771	310	purS	Phosphoribosylformylglycinamidine synthase, PurS subunit	**-3.86**
lmo2506	446	**ftsX**	Cell division protein FtsX	**-3.57**
lmo1770	310	**purL**	Phosphoribosylformylglycinamidine synthase, glutamine amidotransferase subunit	**-3.51**
lmo2507	446	**ftsE**	Cell division transporter, ATP-binding protein FtsE	**-3.50**
lmo2090	381	**argG**	Argininosuccinate synthase	**-3.42**
lmo1772	310	**purC**	Phosphoribosylaminoimidazole-succinocarboxamide synthase	**-3.37**
lmo2254		pbuO	Xanthine/uracil/thiamine/ascorbate permease family protein	**-3.22**
lmo2344	419	ytnI	glutaredoxin family protein	**-3.01**
lmo2505	446	**spl**	Peptidoglycan lytic protein P45	**-2.81**
lmo2349	419	tcyK	L-Cystine ABC transporter	**-2.76**
lmo2091	381	**argH**	Argininosuccinate lyase	**-2.71**
lmo2348	419	tcyL	L-Cystine ABC transporter	**-2.69**
lmo2345	419	ytmO	Bacterial luciferase family protein YtmO, in cluster with L-cystine ABC transporter	**-2.68**
lmo0423	74		RNA polymerase sigma-70 factor, ECF subfamily	**-2.64**
lmo1775	310	**purE**	Phosphoribosylaminoimidazole carboxylase catalytic subunit	**-2.64**

RAST = Rapid Annotation using Subsystem Technology (database), grey names = homologs of *B. subtilis* 169 (according to ListiWiki)

In the absence of c-di-AMP more genes are down- than upregulated and among the most upregulated genes, as shown in **Tab. 4.5** are mainly genes involved in motility (see below). *lmo2567*, encoding together with *lmo2568*, which was not deregulated, a putative ABC transporter under regulation of the LiaFSR three-component system (Fritsch *et al.*, 2011). This three-component system shows some interesting connections to the c-di-AMP metabolism (see discussion). Two other genes that are more highly expressed in the absence of *cdaA* are *lmo0559* and *lmo0560*, encoding a putative magnesium and cobalt transporter and the glutamate dehydrogenase, respectively, in *L. monocytogenes*. *lmo0560* is not among the twenty most upregulated genes and can be found with more detailed information and all differentially expressed genes and differently abundant proteins in **Tab. S4.1**. Interestingly, two sRNAs *rli31* and *rli32* are located directly in front of *lmo0559* and *lmo0560*, hinting at a regulatory function (**see chapter 6**).

Tab. 4.5 The twenty most upregulated genes in *ΔcdaA*

Locus tag	Operon	Name	RAST info	Fold change
lmo2567			FIG00774296: hypothetical protein	**10.84**
lmo0693	112		Flagellar motor switch protein FliN	**9.09**
lmo0691	112	**cheY**	Chemotaxis regulator	**8.94**
lmo0695	112		hypothetical protein	**8.66**
lmo0692	112	**cheA**	Signal transduction histidine kinase CheA	**8.43**
lmo0696	112	**flgD**	Flagellar basal-body rod modification protein FlgD	**8.11**
lmo0694	112		FIG00774728: hypothetical protein	**7.44**
lmo0697	112	**flgE**	Flagellar hook protein FlgE	**6.99**
lmo0699	112	**fliM**	Flagellar motor switch protein FliM	**6.69**
lmo0559			Magnesium and cobalt transport protein CorA	**6.60**
lmo0698	112		Flagellar motor switch protein FliN	**6.46**
lmo0974	155	**dltA**	D-alanine--poly(phosphoribitol) ligase subunit 1	**6.40**
lmo0973	155	**dltB**	D-alanyl transfer protein DltB	**5.78**
lmo0701	112		FIG00774560: hypothetical protein	**5.52**
lmo0702	112		FIG00774477: hypothetical protein	**5.38**
lmo0707	112	**fliD**	Flagellar hook-associated protein FliD	**5.34**
lmo0706	112	**flgL**	Flagellar hook-associated protein FlgL	**5.25**
lmo0647			FIG00774323: hypothetical protein	**5.21**
lmo0705	112	**flgK**	Flagellar hook-associated protein FlgK	**5.15**
lmo0700	112		Flagellar motor switch protein FliN	**5.03**

RAST = Rapid Annotation using Subsystem Technology (database)

c-di-AMP affects expression of multiple operons – Next, we identified all operons, in which expression of more than one gene was impacted. We identified that eight operons were down- and seven operons were upregulated. The genes *lmo1074* and *lmo1075* encoding homologs of the essential *B. subtilis* teichoic acid translocase TagG and TagH, *lmo1389-1390* and *lmo1738-lmo1739* encoding two ABC transporter of unknown function and putatively for amino acid transport, respectively were identified as downregulated operons. Moreover, nearly the whole operon 419, containing the genes *lmo2343*-lmo2350 was downregulated (**Fig. 4.2**). This operon encodes proteins that are homologs of the *B. subtilis ymtL* operon encoding an ABC transporter for cystine uptake and proteins involved in the conversion of S-methyl cysteine to cysteine and thereby involved in amino acid and sulfur metabolism (Burguière, *et al.*, 2005). Other downregulated operons (**see Tab. S4.1**)

encode proteins involved in arginine and purine biosynthesis, cell wall biosynthesis and modification of lipo- and wall teichoic acid.

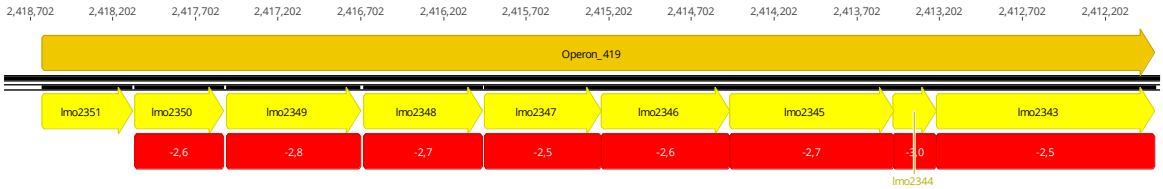

Fig. 4.2 Deletion of *cdaA* leads to the downregulation of genes of the amino acid metabolism. Depicted is operon 419 of *L. monocytogenes* EGD-e, consisting of 9 genes (*lmo2351-lmo2343*). All genes of the operon, except the first one show a 2.5 to 3.0-fold downregulation in the *cdaA* deletion mutant. The genes in the operon except the not downregulated *lmo2351* are homologs of the *B. subtilis* genes *snaA*, *tcyK*, *tcyL*, *tcyM*, *tcyN*, *cmoO*, *cmoI* and *cmoJ* with individual amino acid similarities of the encoded proteins between 65.1 and 77.6% (ListiWiki). The *B. subtilis* genes encode an ABC transporter for cystine uptake and genes for the conversion of S-methylcysteine to cysteine and are therefore involved in sulfur and amino acid metabolism. The first gene of the operon *lmo2351* encodes a protein of unknown function with an FMN reductase domain.

Among the upregulated operons was with operon 281, containing *lmo1636* and *lmo1637*, another ABC transporter encoding operon. Furthermore, operons involved in DNA double strand break repair (*lmo2221-lmo2222*) and biosynthesis of NAD (*lmo2023* and *lmo2025*) were upregulated, which again highlights a broad influence of c-di-AMP on different cellular processes. Most strikingly however was the upregulation of the operons 111, 112 and 295 as well as other individual genes that all are involved in motility and chemotaxis. As depicted in **Fig. 4.3**, the *flaA* gene, encoding the flagellin protein, as well as nearly the whole downstream operon of a size of 23.8 kb encoding many components of the flagellum was strongly upregulated.

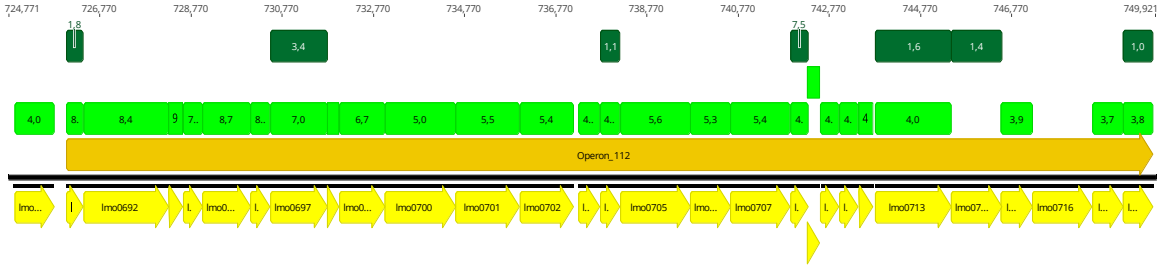

Fig. 4.3 Deletion of *cdaA* leads to the upregulation of motility associated genes. Depicted is the *flaA* gene and operon 112 of *L. monocytogenes* EGD-e. The operon consists of 28 genes (*lmo0691-lmo0718*). The flagellin encoding *flaA* and all genes of the operon except *fligG*, encoding the flagellar basal body protein and *fliI*, encoding a flagellar specific ATPase are 3.7 to 9.1-fold upregulated in the *cdaA* deletion mutant. Additionally, 7 encoded proteins show a higher abundancy (1-7.5 fold), including FliG.

c-di-AMP impacts synthesis of proteins involved in virulence, antibiotic resistance and motility – We also investigated changes in protein expression in the Δ*cdaA* strain to find possible regulatory effects on the level of translation, as it has been shown for *ydaO* mediated regulation of potassium transporter expression in *B. subtilis* (Gundlach *et al.*, 2017; Nelson *et al.*, 2013). As shown in **Tab. 4.6**, the at least 1.5-fold less abundant proteins were the DAC CdaA and its regulator CdaR, which most likely was less abundant due to effects of *cdaA* deletion on the polycistronic *cdaA-cdaR* mRNA (ribosomal binding site of *cdaR* is still present; **chapter 2**), homologs to the *B. subtilis* PbuO, LicB and YefA proteins and the proteins PanB and rpmI. Those proteins are putatively involved in transport processes, biosynthesis of coenzyme A, rRNA modification and translation.

Tab. 4.6 At least 1.5-fold downregulated proteins in *ΔcdaA*

Locus tag	Operon	Name	RAST info	Fold change
lmo2120	388	**CdaA**	Diadenylate cyclase CdaA	**-3.41**
lmo2119	388	**CdaR**	Regulator of CdaA activity	**-3.35**
lmo2254		PbuO	Xanthine/uracil/thiamine/ascorbate permease family protein	**-2.08**
lmo2683	482	LicB	PTS system, cellobiose-specific IIB component	**-1.93**
lmo1902	341	**PanB**	3-methyl-2-oxobutanoate hydroxymethyltransferase	**-1.83**
lmo1751	307	YefA	23S rRNA (Uracil-5-) -methyltransferase RumA	**-1.77**
lmo1784	312	**RpmI**	LSU ribosomal protein L35p	**-1.71**

RAST = Rapid Annotation using Subsystem Technology (database), grey names = homologs of *B. subtilis* 169 (according to ListiWiki)

The at least 1.5-fold more abundant proteins in the Δ*cdaA* mutant are listed in **Tab. 4.7** (all significantly (p and p,fdr<0.01) abundant protein are listed in **Tab. S4.1**). Among them was the PlcA protein, a phosphatidyl-inositol specific phospholipase that is an important virulence factor of *L. monocytogenes* for vacuolar escape. Interestingly, the *plcA* gene (*lmo0201*) is located in one operon the gene *lmo0200* encoding the master virulence regulator PrfA of *L. monocytogenes*. Expression of *prfA* and regulation of the ability of PrfA to modulate expression of the virulence genes is quite complex, involving different promoters for *prfA* expression, regulation by a temperature-dependent riboswitch, modulation of PrfA activity by e.g. glutathione and different affinities of PrfA to the binding regions of genes it regulates (de las Heras *et al.*, 2011; Lobel *et al.*, 2015; Reniere *et al.*, 2015). *plcA* however is part of the PrfA regulon and therefore also *prfA*, resulting in a positive feedback loop.

Tab. 4.7 At least 1.5-fold upregulated proteins in *ΔcdaA*

Locus tag	Operon	Name	RAST info	Fold change
lmo0708	112	**FliS**	Flagellar biosynthesis protein FliS	**7.45**
lmo0697	112	**FlgE**	Flagellar hook protein FlgE	**3.43**
lmo0689	111	**CheV**	Chemotaxis protein CheV	**2.17**
lmo0201	32	**PlcA**	Phosphatidylinositol-specific phospholipase C	**1.87**
lmo2115	387	BceB	Bacitracin export permease protein BceB	**1.87**
lmo0691	112	**CheY**	Chemotaxis regulator	**1.84**
lmo0713	112	**FliF**	Flagellar M-ring protein FliF	**1.63**
lmo2114	387	YxdL	Bacitracin export ATP-binding protein BceA	**1.53**

RAST = Rapid Annotation using Subsystem Technology (database), grey names = homologs of *B. subtilis* 169 (ListiWiki)

Among the other proteins with increased abundance were Lmo2114 and Lmo2115 that are homologs to the *B. subtilis* bacitracin ABC exporter (Clemens *et al.*, 2018), which therefore might also be involved in detoxification and resistance against cell wall acting antibiotics. Interestingly, the genes encoding the ABC transporter, *lmo2114* and *lmo2115* are in the vicinity of the *cdaA-cdaR* operon, with about 3 kb and the genes *lmo2116*, *lmo2115* and the essential *glmM* gene that encodes the phosphoglucosamine mutase GlmM an enzyme involved in cell wall biosynthesis and regulation of CdaA activity, between them. As in the transcriptomic analysis, also in the proteomic analysis motility was associated with c-di-AMP. Among the at least 1.5-fold more abundant proteins were the proteins FliS, FlgE, CheV, CheY and FliF (also **see Fig. 4.3**). We therefore investigated the motility of the *L. monocytogenes* wild type, the *cdaA* deletion mutant, a *fliI*::*mgfp* (A206K) mutant and deletion mutant of *cdaA*, *pgpH* and *pdeA*, with the last three encoding CdaR, the regulator of CdaA and the two PDEs PgpH and PdeA of *L. monocytogenes*, which degrade c-di-AMP. Strains were assessed on their ability to migrate on LSM or BHI soft agar plates (0.3% (*w/v*) agar)

at 25°C and 37°C. As shown in **Fig. 4.4**, the *fliI* mutant was as expected non-motile, the *cdaR* and *pdeA* mutants behaved similar to the wild type, whereas the *cdaA* and *pgpH* mutant showed a decreased migration radius. *L. monocytogenes* is usually non-motile at 37°C, but all strains, except the *fliI* and *cdaR* mutants showed some, if aberrant, migration with the *cdaA* mutant having the most uniform spread. Interestingly, on BHI no motility at 37°C was observed (data not shown), indicating a temperature-independent regulation of motility.

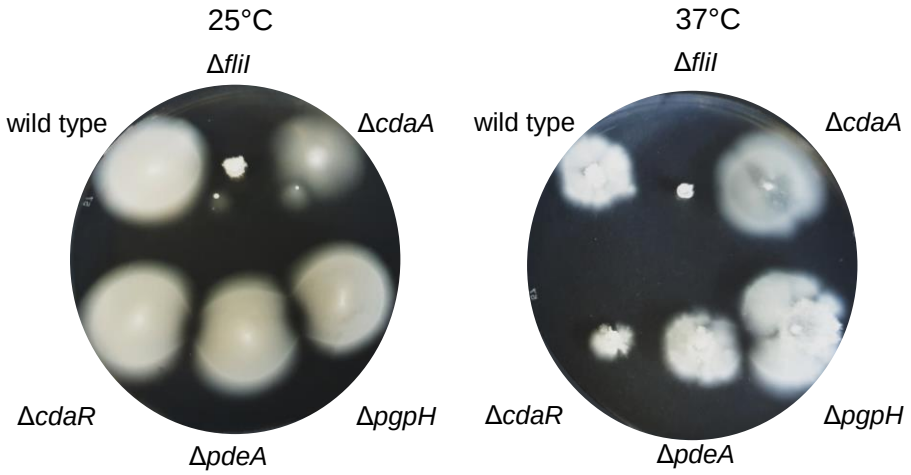

Fig. 4.4 c-di-AMP affects motility of *L. monocytogenes*. The wild type strain and mutants of *cdaA*, *cdaR*, *pdeA*, *pgpH* and a Δ*fliI*::*mgfp* mutant were investigated for their ability to spread on LSM agar plates. Bacteria were grown in LSM medium and 1 µl of cells with an OD_{600} of 1 were stab inoculated in LSM plates containing 0.3% (*w/v*) agar. Plates were incubated at 25°C and 37°C for 3 days.

Discussion

c-di-AMP influences processes ranging from DNA repair, over cell wall metabolism to the regulation of osmohomeostasis (Corrigan *et al.*, 2011; Gundlach *et al.*, 2017; Luo & Helmann, 2012; Oppenheimer-Shaanan *et al.*, 2011; Whiteley *et al.*, 2017; Witte *et al.*, 2008; Zeden *et al.*, 2018). We could show that changes in gene expression and protein biosynthesis reflect these phenotypes and present potential novel targets of c-di-AMP signaling on DNA and RNA level. **Fig. 4.5** summarizes the differently up- and downregulated genes in functional groups according to the COG database (Tatusov *et al.*, 2009). As shown, most upregulated genes are involved in motility processes or have an unknown function. Among these genes with an unknown function are *lmo2567* and *lmo2568*, encoding a putative ABC transporter. Interestingly, expression of these genes that might comprise a yet not annotated operon, is controlled by the three-component system LiaFSR (Fritsch *et al.*, 2011). The Lia system is known to respond to cell wall-acting peptide antibiotics, like bacitracin and modulate gene expression of *liaI* and *liaH* that encode proteins important for counteracting cell envelope stress by unknown mechanism. Interestingly the Lia system does not react to antibiotics in cell wall-less *B. subtilis* L-forms and it therefore might not sense antibiotics but their effect on the cell envelope and thereby might act as an indirect cell envelope protection system (Radeck *et al.*, 2017). Moreover, the Lia system is like c-di-AMP signaling conserved amongst firmicutes, which might indicate a functional relationship between those two signal transduction pathways that is further strengthened by the genomic localization of the *lmo1023* gene, encoding the c-di-AMP binding protein KtrC, that inhibits c-di-AMP dependent the potassium import of KtrD (**see chapter 3**).

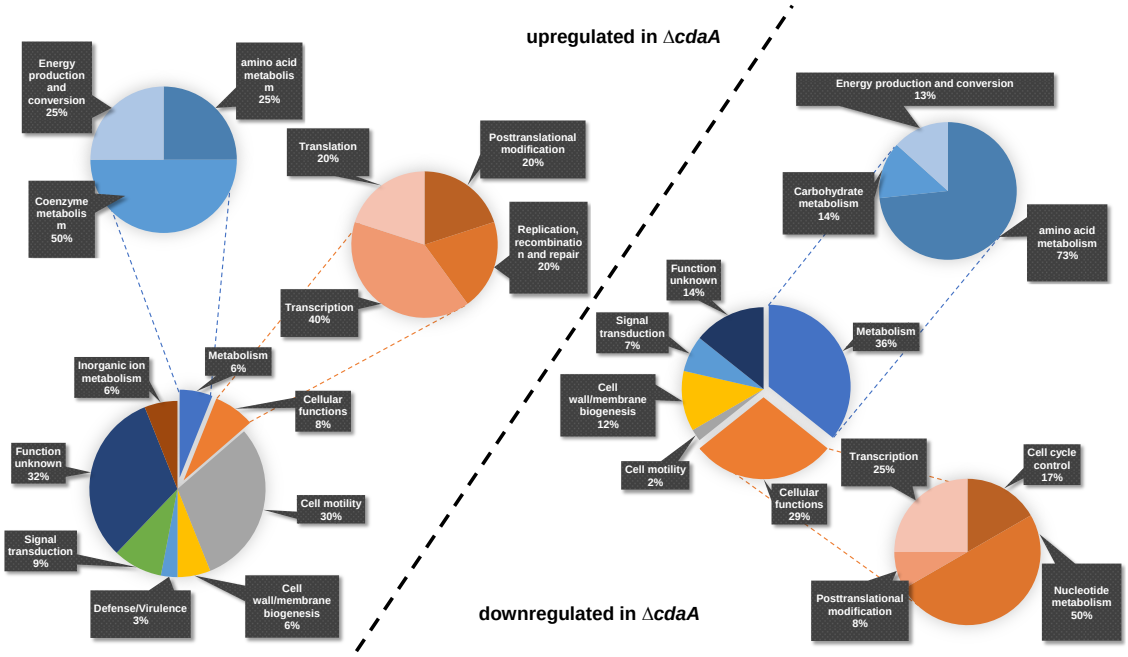

Fig. 4.5 Deletion of *cdaA* leads to the deregulation of genes involved in all cellular processes. Deletion of the *cdaA* gene leads to differential expression of 95 genes. 36 genes are down- and 59 are upregulated in the Δ*cdaA* mutant compared to the wild type. Down regulated genes encode proteins mainly involved in metabolism, of which the largest part is involved in amino acid metabolism, and proteins involved in cellular functions, such as nucleotide metabolism or transcription. Genes that code for proteins involved in cell wall and membrane biogenesis, signal transduction or with an unknown function make up the remaining third of downregulated genes. The genes that are upregulated in the Δ*cdaA* mutant are mainly involved in cell motility or have an unknown function. The remaining third are genes involved in cell wall or membrane biogenesis, signal transduction processes, cellular functions, metabolism, ion transport or virulence associated.

lmo1023 is the last gene in an operon consisting of *lmo1018-lmo1022* and *lmo1023*, with *lmo1020-1022* being *liaFSR*. Fritsch and colleagues could show that deletion of *liaS* leads to upregulation of the operon, including the *ktrC* gene, which might indicate regulation of *ktrC* expression in dependency of the LiaFSR three-component system and thereby connecting c-di-AMP regulated potassium import to sensing of cell envelope damage (Fritsch *et al.*, 2011). Interestingly, also the genes *lmo2114* and *lmo2115*, encoding an ABC transporter that are in direct vicinity of the *cdaA-cdaR* operon are involved in bacitracin resistance and are deregulated in the *cdaA* mutant. *lmo2115* is nearly 4-fold higher expressed in the *cdaA* mutant and both proteins, Lmo2114 and Lmo2115 have an over 1.5-fold higher abundancy, again highlighting interconnections between c-di-AMP and cell envelope stress responsive systems.

The most striking group of upregulated genes and overproduced proteins are motility associated. It is here interesting to note that in *B. subtilis* a *gdpP* PDE mutant has a similar phenotype than the *cdaA* mutant in *L. monocytogenes*, highlighting that c-di-AMP-dependent regulation of motility might be contrary in those two closely related bacteria (Gundlach *et al.*, 2016). Regulation of motility in *L. monocytogenes* strongly depends on the ambient temperature. Expression of the main flagellar component, flagellin, is repressed at physiological temperatures (37°C) and it involves multiple regulatory networks, including the orphan response regulator DegU that binds the promoter of the *motB* operon encoding among others the *gmaR* gene (see below) and is therefore essential for synthesis of flagellar components (Dons *et al.*, 1992; Gueriri *et al.*, 2008; Mauder *et al.*, 2008; Peel *et al.*, 1988). Interestingly, DegU is also important in the temperature-dependent expression of flagellar genes, including *flaA* expression, by antagonizing the transcriptional repressor MogR (Gueriri *et al.*, 2008; Gründling *et al.*, 2004). The ability of MogR to repress gene

expression is inhibited at 30°C and below by the moonlighting protein GmaR that acts as an anti-repressor and has furthermore enzymatic activity as a glycosyltransferase that is important for O-linked N-acetylglucosamine modification of flagellin (Shen *et al.*, 2006) Activity of GmaR, however, has no influence on its regulatory properties, which would make GmaR a trigger enzyme (Commichau & Stülke, 2008; Shen *et al.*, 2006). MogR has been shown to inhibit transcription of flagellar genes at 37°C, including the GmaR protein. The GmaR protein is a thermosensor protein that changes its conformation upon changes in temperature. At elevated temperatures it is more prone to proteolytic degradation, while on low temperatures it interacts with MogR, is more stable and prevents MogR repression of motility genes. At the same time, DegU acts as a transcriptional activator of GmaR expression in a temperature independent manner, meaning the temperature-dependent phenotype of a *degU* mutant is only due to the lack of MogR anti-repression by GmaR. If the temperature rises, GmaR-MogR interaction becomes weaker, GmaR is degraded and MogR represses GmaR and other flagellar genes again and the stimulating effect of DegU is not strong enough to overcome the inhibition of *gmaR* expression by MogR (Kamp & Higgins, 2008; Kamp & Higgins, 2011). Interestingly, the 5'-UTR of the *mogR* mRNA (which is expressional regulated by σ^B) is also an antisense RNA (*anti0677*) that hybridizes with the mRNA of *lmo0675-lmo0677*, encoding FliNPQ and thereby expression of *mogR* inhibits translation of the encoded genes (Toledo-Arana *et al.*, 2009). It has also been shown that the genes encoding the flagellar body components FlhB, FliM and FliY are required for expression of other flagellar components and deletion mutant of the respective genes also lead to repression of gene expression of other genes encoding flagellar components in a MogR and GmaR independent matter, suggesting further regulatory mechanisms of expression of flagellar components (Chen *et al.*, 2018). *L. monocytogenes* possesses also a c-di-GMP signaling network, which in contrast to *B. subtilis* has at least been shown to inhibit motility by regulating the synthesis of a cell aggregation-promoting exopolysaccharide (Chen *et al.*, 2014; Gao *et al.*, 2013; Köseoğlu *et al.*, 2015). It is unknown how c-di-AMP effects expression and biosynthesis of flagellar genes. Neither MogR, nor DegU, nor GmaR seem to be affected, but *fliM* and *fliY* are deregulated (together with nearly all genes in operon 112, which makes it unlikely that they are directly affected by c-di-AMP but more likely a consequence of deregulation of the whole operon. We therefore hypothesis that c-di-AMP might have a more direct role in regulation of motility gene expression or indirectly controls yet unknown regulatory mechanisms. The aberrant motility *L. monocytogenes* shows on LSM minimal medium soft agar plates at 37°C might be a hint that also nutrient conditions and thereby altered metabolism and gene expression might influence motility and allow motility at 37°C. It is, furthermore, interesting to note that the *pgpH* mutant showed an inconsistent phenotype with sometimes increased and sometimes decreased motility, whereas the *cdaA* mutant showed consistently increased motility at 37°C, but not at 25°C (**Fig. 4.4**). Possible reasons are the slower growth of the *cdaA* mutant compared to the wild type, which might be more pronounced at 25°C or that gene expression might be different, compared to 37°C. Moreover, it is unknown if the flagellar themselves show an altered activity. There are some indications that c-di-AMP affects the electron motive force, which would also affect ATP synthesis and flagellar activity (Manson *et al.*, 1977; Zeden *et al.*, 2018).

Genes that are downregulated in the *cdaA* mutant are mainly involved in carbon nitrogen metabolism, nucleotide metabolism and cell wall biogenesis. Most interesting is the lesser abundancy of the KdpD protein (Lmo2681) in the *cdaA* mutant. The *L. monocytogenes* KdpABC proteins are homologs to the *S. aureus* potassium importer. In *S. aureus*, the KdpDE two-component system regulates expression of this high affinity potassium transporter. The response regulator KdpE is not phosphorylated upon binding of c-di-AMP to the sensor kinase KdpD and therefore does not

facilitate *kdp(F)ABC* in *S. aureus*. Hence, c-di-AMP inhibits upregulation of the *kdp(F)ABC* genes (Corrigan *et al.*, 2013; Moscoso *et al.*, 2015). Interestingly, we did not see a significant effect on the expression of *kdpABC*, but it is nevertheless likely that c-di-AMP also acts as an inhibitor of *kdpABC* expression in *L. monocytogenes* and the higher abundancy of KdpD is an indicator that this is indeed the case. There might however be unknown regulatory mechanisms at play. Among the other downregulated processes were pathways involved in arginine, purine and cysteine metabolism that might hint at an imbalance in central metabolic pathways. The higher abundancy of the TCA cycle proteins CitZ, CitB and CitC that are the citrate synthase, aconitate hydratase and isocitrate dehydrogenase of *L. monocytogenes*, respectively, and the ability of c-di-AMP to inhibit the pyruvate carboxylase PycA indicates an involvement of c-di-AMP on regulation of central carbon metabolism, where the TCA cycle is an important intersection (Choi *et al.*, 2017; Sureka *et al.*, 2014; Whiteley *et al.*, 2017). Interestingly the citrate cycle of *L. monocytogenes* is incomplete, due to an absence of the *genes* encoding the α-ketoglutarate DH, succinyl-CoA synthetase and malate dehydrogenase. *L. monocytogenes* therefore utilizes a glutamate carboxylase to synthesize γ-amino butyric acid (GABA), which is converted together with α-ketoglutarate (the product of CitC) by a transaminase to glutamate and succinic semialdehyde (SSA). SSA is subsequently oxidized by a dehydrogenase to succinate which flows back into the TCA cycle (Feehily *et al.*, 2013). The pyruvate carboxylase is hereby the main source of oxaloacetate in *L. monocytogenes* (Schär *et al.*, 2010). Lack of PycA inhibition and overproduction of CitZBC would therefore lead to an increase flux and lead an increased accumulation of glutamate (Sureka *et al.*, 2014), which could as a consequence lead to an imbalance in amino acid and purine biosynthesis. Whiteley and colleagues could show that *citZ* mutations restored growth of a Δ*cdaA* mutant on complex medium, but interestingly mutations in *citB* and *citC* did not phenocopy this effect, which is why the authors hypothesized that accumulation of citrate is toxic for *L. monocytogenes* lacking c-di-AMP (Whiteley *et al.*, 2017). While it seems established that c-di-AMP regulates the flux of the TCA cycle, it is not yet fully understood which regulatory mechanisms, besides PycA inhibition, contribute to this phenotype. One possibility would be regulation of enzymes involved in the TCA cycle by a c-di-AMP responsive transcriptional modulator. Interestingly, the c-di-AMP binding protein CbpB is in the same operon with the protein CcpA, which is indeed a transcriptional regulator of the TCA cycle and it is therefore tempting to assume a relationship between c-di-AMP, CbpB, CcpC and the upregulation of CitZBC in the *L. monocytogenes* Δ*cdaA* mutant.

In summary, we show for the first time, the effect of a deletion of the sole DAC encoding gene *cdaA* in *L. monocytogenes*. c-di-AMP effects many cellular processes, ranging from cell wall metabolism, osmoregulation, nitrogen and central carbon metabolism and virulence determinants like motility on the level of gene expression and protein biosynthesis. This study provides interesting new perspectives and highlights potential new regulatory mechanisms of c-di-AMP signaling and will eventually lead to a deeper understanding of the regulatory network.

Acknowledgements

This work was supported by the grant CO 1139/2-1 from the Deutsche Forschungsgemeinschaft *via* the Priority Program SPP1879, the Fonds der Chemischen Industrie and the Max-Buchner-Forschungsstiftung (MBFSt-Kennziffer 3381) to FMC.

5. The inhibitory effect of DNA on the activity of the di-adenylate cyclase DisA of *Bacillus subtilis* is relieved by ions

Johannes Gibhardt, Anna-Lena Hagemann, Annette Garbe, Volkhard Kaever and Fabian M. Commichau

Author contribution:
JG performed the experiments. AH, AG and VK performed the c-di-AMP measurements. JG and FMC wrote the manuscript.

Abstract

Signal transduction by nucleotide second messenger molecules is an important tool for bacteria to sense and react to changing environmental conditions or stress conditions. Cyclic di-adenosine monophosphate (c-di-AMP) is unique among bacterial second messenger, as it is both toxic and essential for many bacteria that synthesize it. Synthesis and degradation are performed by di-adenylate cyclases (DACs) and specific phosphodiesterases (PDEs), respectively. The soil bacterium *Bacillus subtilis* possesses three DACs, the sporulation-specific CdaS, the membrane-bound CdaA and the DNA-integrity scanning protein DisA. The DisA cyclase has been shown to bind DNA and move along the chromosome, scanning it for DNA damage and being inhibited in DAC activity upon binding of branched nucleic acids, such as holiday junctions. c-di-AMP has furthermore been shown to regulate potassium and compatible solute homeostasis, which is the reason for its essentiality. We therefore aimed to investigate the role of DisA as a DAC in the context of osmoregulation. We demonstrate that DisA is inhibited by chromosomal DNA (cDNA) *in vitro* and that this inhibitory effect is counteracted by monovalent cations, such as potassium. We further show that a DisA G334E mutant that has been shown to be less-responsive to branched nucleic acids, is inhibited by cDNA similar to wild type DisA, but the inhibition is more easily counteracted by potassium ions. *In vivo*, a *B. subtilis* mutant that expresses DisA wild type or G334E mutant variant, as sole DAC, is able to adapt to osmotic stress. We further show that c-di-AMP concentrations decrease after salt stress with sodium chloride and not with potassium chloride, indicating a discrimination *in vivo*. We further show that DisA G334E is more active *in vivo* and beneficial over the wild type variant for adaptation to osmotic stress. In summary, we demonstrate regulation of DisA DAC activity in the context of osmoregulation.

Introduction

Adaptation to changing conditions and danger signals is one of the most important mechanisms in living organisms and facilitated by sophisticated cellular machineries that often involves signal integration by second messenger molecules. An important nucleotide second messenger in bacteria is c-di-AMP (Corrigan & Gründling, 2013). It has been shown to be involved in many cellular processes, like DNA damage repair, lifestyle changes, cell wall metabolism, regulation of central metabolic processes and regulation of potassium ion and compatible solute homeostasis (Corrigan *et al.*, 2011; Gundlach *et al.*, 2016 Gundlach *et al.*, 2017; Oppenheimer-Shaanan *et al.*, 2011; Sureka *et al.*, 2014; Witte *et al.*, 2008; Whiteley *et al.*, 2017). c-di-AMP is also a unique second messenger, because it is essential in firmicute bacteria, like *B. subtilis*, *Lactococcus lactis*, *Listeria monocytogenes*, or *Staphylococcus aureus* (Commichau *et al.*, 2015) and furthermore toxic for the bacteria if it accumulates (Gundlach *et al.*, 2015b). It is synthesized by a variety of different DAC domain containing proteins and PDEs (Commichau *et al.*, 2019). In *B. subtilis*, degradation c-di-AMP is degraded by the PDEs GdpP and PgpH (Gundlach *et al.*, 2015b; Huynh *et al.*, 2015; Mehne *et al.*, 2013; Rao *et al.*, 2010). For the synthesis, *B. subtilis* expresses the DACs CdaA and DisA, while the third DAC, CdaS, is sporulation-specific expressed (Mehne *et al.*, 2013; Mehne *et al.*, 2014). In other organisms, like the minimal organism *Mycoplasma pneumoniae* or the archaeon *Methanocaldococcus jannaschii*, novel types of DACs, CdaM and CdaZ, respectively, have recently been identified, suggesting a widespread conserved function of c-di-AMP in prokaryotes (Blötz *et al.*, 2018; Kellenberger *et al.*, 2015). CdaA interacts and is regulated by the proteins CdaR and the phosphoglucosamine mutase GlmM in *B. subtilis* and related bacteria, like *L. monocytogenes*, *S. aureus* or *L. lactis* and is the most abundant type of DAC that is present in many pathogenic firmicutes (Gundlach *et al.*, 2015b; Mehne *et al.*, 2013; Rismondo *et al.*, 2016; Tosi *et al.*, 2019; Zhu *et al.*, 2016). The DisA-type of cyclase is the second most abundant type of DAC and present in spore-forming firmicutes, like *B. subtilis* or *Clostridium difficile*, in Actinobacteria the hyperthermophilic bacterium *Thermotoga maritima* or the Archaeon *M. jannaschii* (Commichau *et al.*, 2019; Kellenberger *et al.*, 2015; Witte *et al.*, 2018). DisA forms homooctamers, with the monomers consisting of an N-terminal DAC domain that requires Mg^{2+} as a cofactor and a C-terminal helix-hairpin-helix (HhH) domain that typically bind the phosphate backbone of DNA (Witte *et al.*, 2008). Moreover, DisA strongly binds branched nucleotide substrates that resemble holiday junctions and is inhibited in DAC activity upon binding and a mutation of glycine 334 to glutamate (G334E), a putative DNA-binding residue of DisA, reduced its binding affinity to the branched nucleotide substrates and thereby their inhibitory effect, without an effect on DAC activity *in vitro* in the absence of DNA (Witte *et al.*, 2008). DisA has also been shown to move as foci along the DNA and in the cytoplasm as a GFP fusion protein and that it is required for the delay of spore formation and germination in response to DNA damage. (Bejerano-Sagie *et al.*, 2006; Campos *et al.*, 2014; Gándara & Alonso, 2015; Oppenheimer-Shaanan *et al.*, 2011). Moreover, DisA has been shown to inter act *in vitro* with the DNA segregation-associated protein RacA and the branch migration transferase RadA (Bejerano-Sagie *et al.*, 2006; Ben-Yehuda *et al.*, 2003; Zhang & He, 2013). Interaction with RadA furthermore inhibits DisA activity *in vitro* and is expressed in the same operon, but they only seem to co-localize transiently *in vivo* (Gándara *et al.*, 2017; Zhang & He, 2013). Intriguingly, c-di-AMP has been shown to be essential due to its regulation of potassium and osmolyte homeostasis in several bacteria, including *B. subtilis*, *L. lactis*, *L. monocytogenes*, *S. aureus* and *Streptococcus agalactiae* (Devaux *et al.*, 2018; Gundlach *et al.*, 2017; Pham *et al.*, 2018; Whiteley *et al.*, 2015; Whiteley *et al.*, 2017; Zeden *et al.*, 2018). It even has been proposed that many c-di-AMP associated phenotypes, especially those affecting cell wall-acting antibiotics may be indirectly caused by the impact of c-di-AMP on osmohomeostasis (Commichau *et al.*, 2018).

Interestingly, it has been shown for *B. subtilis* that none of the DAC encoding genes is essential by itself, rather the presence of c-di-AMP itself. It is sufficient if the CdaS cyclase is expressed with a promoter that is transcribed in vegetative cells (Mehne *et al.*, 2013). Even more so, a mutant with a deletion of all three DAC encoding genes does not show increased occurrence of suppressor mutations or DNA damage repair associated phenotypes, as long as it is grown under osmotically stable and favorable conditions in minimal medium containing a low potassium concentration (Gundlach *et al.*, 2017). We therefore challenged the current model of DisA reporting DNA damage by its DAC activity and investigated the role of DisA in an osmoregulatory context. Using *in vitro* assays, we show that DisA is inhibited by chromosomal DNA and that inhibition is counteracted by monovalent ions. Furthermore, a G334E mutant that is less inhibited by branched nucleotides *in vitro* (Witte *et al.*, 2008) is less inhibited by cDNA in the presence of potassium ions and inhibits increased activity *in vivo*, but not *in vitro*. Finally, we show that DisA as sole DAC is not only sufficient for survival of *B. subtilis* (Mehne *et al.*, 2013), but also sufficient for *B. subtilis* to adapt to salt stress. Moreover, the G334E mutant has a growth advantage under these conditions, which likely is due to an altered responsiveness in its DNA/ion interaction that affect its DAC activity.

Experimental Procedures

Bacterial strains and growth conditions – *B. subtilis* 168 and its derivatives were cultivated in LB medium (Sigma-Aldrich) at 37°C and 220 rpm if not specified otherwise. *Escherichia coli* was grown in LB medium at 37°C and 220 rpm (strains see **Tab. 5.1**). As solid medium for *B. subtilis* SP medium was used (8 g/l nutrient broth, 0.25 g/l $MgSO_4 \cdot 7H_20$, 1 g/l KCl, 0.5 mM $CaCl_2$, 10 µM MnCl2, 4.4 mg/l iron ferric ammonium citrate). For agar plates, medium was supplemented with 15 g/l Bacto Agar (Difco). Antibiotics and medium supplements were used with the following concentrations, if indicated. For *B. subtilis* erythromycin (2 µg/ml), lincomycin (25 µg/ml), kanamycin (5 µg/ml), chloramphenicol (5 µg/ml) were used and for *E. coli* ampicillin or carbenicillin (100 µg/ml), chloramphenicol (30 µg/ml), IPTG (1 mM or 50 µM; Isopropyl β-D-1-thiogalactopyranoside; Sigma-Aldrich) and L-arabinose (0.005% (*w/v*)) were used.

DNA manipulation – DNA amplification *via* PCR and transformation of *E. coli* was performed using standard procedures (Sambrook *et al.*, 1989). DNA fragments were purified using the PCR purification kit (Qiagen) and plasmid DNA was extracted using the NucleoSpin Plasmid Kit (Macherey and Nagel). Commercially available restriction enzymes, T4 DNA ligase and DNA polymerases were used as recommended by the manufacturers. DNA sequences were determined by the dideoxy chain termination method (Microsynth, Göttingen, Germany). Chromosomal DNA of *B. subtilis*, *L. monocytogenes* or *E. coli* were isolated using the NucleoSpin Microbial DNA Kit (Macherey and Nagel). Oligonucleotides were purchased from Sigma-Aldrich (Germany).

Tab. 5.1 Strains

Name	Genotype	Description/Construction	Reference
E. coli			
BL21(DE3)	F⁻ *ompT gal dcm lon hsdS*$_B$($r_B^- m_B^-$) λ(DE3 [*lacI lacUV*5-*T7p07 ind*1 *sam*7 *nin*5]) [*malB*$^+$]$_{K\text{-}12}$(λ^S)	Protein expression	Stratagene
Rosetta (DE3)	F$^-$ *ompT hsdS*$_B$(r_B^- m_B^-) *gal dcm* (DE3) pRARE (*cat*)	Protein expression	Novagen

Name	Genotype	Description/Construction	Reference
XL1-Blue	*recA*1 *endA*1 *gyrA*96 *thi*$^{-}$1 *hsdR*17 *supE*44 *relA*1 *lac* [F′ *proAB lacI*^{q} *Z*ΔM15 Tn*10* (*Tet*^{r})]	Cloning	Stratagene
B. subtilis			
168	*trpC2*	Wild type	Laboratory collection
GP2032	*trpC2 ΔcdaS::ermC ΔcdaA::cat*	Deletion of *cdaS* and *cdaA*	Gundlach *et al.*, 2015
BP170	*trpC2 disA* (wt) *aphA3*	*disA-aphA3* (wt) $_{LFH}$→ 168	This work
BP171	*trpC2 disA* (G334E) *aphA3*	*disA-aphA3* (G334E) $_{LFH}$→ 168	This work
BP172	*trpC2* Δ*cdaS*::*ermC* Δ*cdaA*::*cat disA* (wt) *aphA3*	BP170 $_{cDNA}$→ GP2032	This work
BP173	*trpC2* Δ*cdaS*::*ermC* Δ*cdaA*::*cat disA* (G334E) *aphA3*	BP171 $_{cDNA}$→ GP2032	This work
L. monocytogenes			
EGD-e	Wild type	Serotype 1/2a strain	Laboratory collection

$_{LFH}$→ transformation with a long-flanking homology PCR, $_{cDNA}$→ transformation with chromosomal DNA, *cat* = cm^{R} (5 µg/ml / 30 µg/ml chloramphenicol (*B. subtilis* / *E. coli*)), *ermC* = ery^{R} (2 µg/ml erythromycin & 25 µg/ml lincomycin), *aphA3* = kan^{R} (5 µg/ml kanamycin)

Plasmid construction – For the expression and purification of N-terminal His$_6$-tagged DisA (G334E), plasmid pBP392 was constructed as follows (plasmids are listed in **Tab. 5.2**). The *disA* gene was amplified from *B. subtilis* cDNA using the oligonucleotide pair FX111/FX112 with the addition of the 5'-phosphorylated oligonucleotide JH106 (oligonucleotides are listed in **Tab. 5.3**). It introduces the G334E mutation, which reduces inhibition of DisA by branched nucleotides, *via* the combined chain reaction. The resulting PCR product was digested using *Nde*I and *Xba*I and ligated to pET19b that was cut with the same enzymes. (Bi & Stambrook, 1997; Witte *et al.*, 2008). Plasmids pBP394 and pBP395 allow L-arabinose inducible expression of DisA and DisA (G334E) in *E. coli*, respectively. The *disA* wt gene was amplified from *B. subtilis* cDNA and the G334E mutant allele from the plasmid pBP392 using oligonucleotides JH 109 and JH110. The resulting PCR product was digested with *Kpn*I and *Xba*I and ligated to pBAD33 that was cut with the same enzymes.

Tab. 5.2 Plasmids

Name	Insert/Features	Reference
pBAD33	P_{BAD} *cat araC*	Guzman *et al.*, 1995
pET19b	P_{T7} N-His$_6$-MCS *bla*	Novagen
pDG670	MCS *aphA3* MCS *bla*	Guérout-Fleury *et al.*, 1995
pGP172	P_{T7} N-*Strep*-tag II *bla*	Merzbacher *et al.*, 2004
pGP2563	pET19b-*disA*	Mehne *et al.*, 2013
pGP2593	pGP172-*cdaS* (*B. cereus*)	Mehne, 2014
pBP392	pET19b-*disA* (G334E)	This work
pBP394	pBAD33-*disA*	This work
pBP395	pBAD33-*disA* (G334E)	This work

bla = amp^{R} (100 µg/ml ampicillin or carbenicillin), *ermC* = ery^{R} (5 µg/ml erythromycin), *cat* = cm^{R} (30 µg/ml chloramphenicol (*E. coli*)), MCS = multiple cloning site

Transformation of B. subtilis – To induce natural competence of *B. subtilis*, cells were overnight in 4 ml LB medium at 28°C and the precultures used to inoculate 10 ml MNGE medium (), supplemented with 0.1 % (*w/v*) CAA and incubated at 37°C and 220 rpm from OD$_{600}$ 0.1 to 1.3. Cells were diluted 1:1 with pre-warmed MNGE medium, lacking CAA to induce nutrient starvation. Growth was continued for another hour. 400 µl of the cells were mixed with DNA and incubated for 30 minutes at 37°C. Afterwards 100 µl of expression mix (2.5 % (*w/v*) yeast extract, 2.5 % (*w/v*)

CAA and 250 µg/ml tryptophan) was added and the cells incubated for another hour at 37°C and 220rpm. Eventually, cells were plated on selective SP agar plates.

B. subtilis *strain construction* – To investigate the influence of the G334E mutant of DisA in *B. subtilis*, strains BP170 to BP173 were constructed. About 1 kb of *disA* or the *disA* G334E mutant gene, including its stop codon, were amplified from the *B. subtilis* wt cDNA or pBP392, respectively. The *aphA3* gene, encoding the kanamycin resistance, was amplified from pDG670, without promoter or terminator using oligonucleotides JH116 and JH117 (Guérout-Fleury *et al.*, 1995). About 1 kb downstream of the *disA* gene was amplified using oligonucleotides JH118 and JH119. The three PCR fragments were fused by long-flanking homology PCR as described elsewhere (Wach, 1996). *B. subtilis* 168 was subsequently transformed with the LFH PCR products to construct BP170 and BP171, containing the wt or G334E mutant allele introduced into the natural *disA* locus with a downstream *apha3* gene integrated into the operon and expression driven by the promoter of the operon. Therefore, selection was performed using 5 instead of 10 µg/ml kanamycin and it was only used as selection marker on plates and in the pre-cultures to prevent an effect of selective pressure of *aphA3* expression on *disA* expression. Correct sequences were confirmed by sanger sequencing. Strains BP172 and BP173 were constructed by transformation of the *cdaA* and *cdaS* mutant GP2032, with the cDNA of strains BP172 and BP173, respectively. The correct sequence of the *disA* locus and absence of *cdaA* and *cdaS* was verified by sequencing and PCRs, respectively. BP172 and BP173 express DisA wt or the G334E mutant as sole DACs, respectively.

Tab. 5.3 Oligonucleotides

Name	Restriction sites are underlined, complementary regions or mutations are in bold, sequences 5'→3'	Purpose and reference
FX111	AAACATATGGAAAAAGAGAAAAAAGGGGCGAAACACG	Fwd. *disA* (*Nde*I), Mehne *et al.*, 2013
FX112	TTTGGATCCTCACAGTTGTCTGTCTAAATAATGCTTCTCTTG	Rev. *disA* (*Bam*HI), Mehne *et al.*, 2013
JH53	AAAGAATTCA*AGGGAGA*TATGAACATTGGGAAGAATTAAAAATAAG	Fwd. *B. subtilis ktrAB* (*Eco*RI), Gundlach *et al.*, 2017
JH54	TTTGGATCCTCACCCTGTAAACACTTCGCCATCA	Rev. *B. subtilis ktrAB* (*Bam*HI), Gundlach *et al.*, 2017
JH106	P-GGCGAGTGCAGAAGAATTAGATGAAGTAGAGG**A**AATCGGTGAAGTACGAGCCC	5'-phosphorylated GGA→GAA (DisA G334E)
JH109	AAAGGTACCTT*AGGAGG*ATAATAGATGGAAAAAGAGAAAAAAGGG	Fwd. RBS_{disA}-*disA* (*Kpn*I)
JH110	TTTTCTAGATCACAGTTGTCTGTCTAAATAATGCTTCTCTTGC	Rev. *disA* (*Xba*I)
JH114	CTGTCATCTATATTGCAGTTTGTTGCTCCG	Fwd. *disA* (intragenic, LFH)
JH115	**CCTTCCTCTGAAGATGTGTCACAGTTG**TCTGTCTAAATAATGCTTCTCTTGC	Rev. *disA* (LFH)
JH116	**CAACTGTGACACATCTTCAGAGGAAGG**AAATAATAA**ATG**GCTAAAATGAGAA-TATCAC	Fwd. RBS_{aphA3}-*apha3* (w/o promoter)
JH117	**TAACCGAAACGCGAAGATGTGCTAAAACAA**TTCATCCAGTAAAATATAA-TATTTTATTTTCTCCCAATC	Rev. *apha3* (w/o terminator)
JH118	**TTGTTTTAGCACATCTTCGCGTTTCGGTTA**AAACCTTATGAATACGGG-TATATTAATGTTG	Fwd. *disA* downstream region, LFH)
JH119	CAGGAAGCACAACAGGCTTAACCGCATTGG	Rev. *disA* downstream region, LFH)

Fwd. = forward, Rev. = reverse, w/o = without, *apha3* =kan^R (5 µg/ml kanamycin)

Protein production, purification and dialysis – To assess DAC activity, *E. coli* BL21 was transformed with plasmids pGP2563 (pET19b-*disA*) and pGP2593 (pGP172-$cdaS^{Bce}$). For expression of DisA G334E (PBP392) *E. coli* Rosetta (DE3) was used, since expression in BL21 was suboptimal. Bacteria

were cultivated overnight in 20 ml BHI medium (Sigma-Aldrich) at 28°C and 220 rpm and precultures used to inoculate 1 l BHI medium containing the appropriate antibiotics, 0.5% (*w/v*) glycerol and 50 µl Antifoam Y-30 (Sigma-Aldrich) in 2 l baffled flasks to an OD_{600} of 0.1. Bacteria were incubated at 37°C and 220 rpm until an OD_{600} of 0.8-1.2 and protein expression induced with 1 mM IPTG. Growth was resumed for another 3 hours and bacteria harvested by centrifugation. Bacterial cells were disrupted in 15 ml of the buffers ZAP (50 mM Tris-HCl pH7.5, 200 mM NaCl) or buffer W (100 mM Tris-HCl pH 8, 150 mM NaCl, 1 mM EDTA) with the addition of 15 µl DNaseI (1U/µl Sigma-Aldrich) and 1 cOmplete protease inhibitor tablet (Sigma-Aldrich) using a French press system with 18000 psi. Cell disruption and purification of the His- and *Strep*-tagged proteins was performed using Ni^{2+}-NTA and Streptavidin columns (IBA, Göttingen) with imidazole or desthiobiotin (Sigma-Aldrich), as previously described (Mehne *et al.*, 2014; Rosenberg *et al.*, 2015). Protein purification was assessed using coomassie-stained SDS-PAGE (Sambrook *et al.*, 1989) and pooled fractions of enriched protein of interest were dialyzed overnight in the 1000-fold volume at 4°C in 10 mM Tris-HCl pH 7.5, 5% (*w/v*) glycerol and 1 mM 1,4-dithiothreitol (DTT, Sigma-Aldrich), to have the DACs in a salt-free environment.

In vitro *DAC assays* – 100 nM of freshly dialyzed DACs were incubated in 10 mM Tris pH 7.5 with 0.1 % (*w/v*) bovine serum albumin, 100 µM ATP, 10 mM $MgCl_2$ in a total volume of 200 µl at 37°C for the indicated time frame. Reactions were stopped by freezing the reaction tubes in liquid nitrogen and subsequent heated for 10 min at 95°C, followed by the extraction of c-di-AMP (see next part). For assays where DNA, ions or both were added, the reactions were stopped after 30 min. If indicated, chromosomal DNA of *B. subtilis* 168, *E. coli* XL-1blue or *L. monocytogenes* EGD-e or PCR product of *B. subtilis ktrAB* (JH53/JH54) was added in the indicated concentration. The additives NaCl, KCl, sucrose or potassium phosphate were added as indicated. The potassium phosphate solution was prepared by titration of 1 M KH_2PO_4 to 1 M K_2HPO_4 (approximately 4 to 1 ratio) to pH 7.5 at 37°C and dilution to 0.55 M that equals a molarity of 1 M potassium in the solution.

Determination of the c-di-AMP concentration – The stopped reactions were centrifuged for 10 min at 20000 g and 4°C after the heating step and 175 µl of the supernatant was added to 800 µl extraction mix (acetonitril:methanol (1:1)) and incubated overnight at -20°C. Afterwards the mixtures were centrifuged again and the supernatants were transferred to new tubes and evaporated using SpeedVac at 60°C for about 2 h. Extract pellets were resuspended in 200 µl H_2O and ^{13}C,^{15}N-c-di-AMP as internal standard added and the samples analyzed by LC-MS/MS, as described elsewhere (Rismondo *et al.*, 2016).

Salt shock and determination of the intracellular c-di-AMP concentration - *B. subtilis* strains BP172 and BP173 were grown in 10 ml LB medium with the appropriate antibiotics overnight at 28°C and 220 rpm. Main cultures (100 ml LB) were inoculated to an OD_{600} of 0.05 and incubated at 37°C and 220 rpm. When cells reached the exponential growth phase (OD_{600} 0.5 ± 0.1), samples were taken (t_0) and the salt shock induced as follows. 25 ml culture were added to 25 ml pre-warmed LB medium without osmolytes or with NaCl or KCl to reach a final concentration of 1.5 M salt. Growth was continued and additional samples taken 30 min (t_1) and 3 h (t_2) after the salt stress. Determination of the intracellular c-di-AMP concentration in DAC expressing *E. coli* was performed similar. *E. coli* XL1-blue harboring plasmids pBAD33 or the derivatives pBP394 or pBP395 for the expression of DisA or DisA G334E, respectively, were grown overnight in 5 ml LB with 0.02% (*w/v*) D-glucose at 28°C and 220rpm. Precultures were used to inoculate 50 ml LB medium with to an OD_{600} of 0.05 and bacteria grown until the early exponential phase (OD_{600} 0.2 ± 0.05) and expression of DACs was induced by addition of 0.005% (*w/v*) L-arabinose. After an additional 1.5 hours samples

were taken to determine the protein and c-di-AMP concentrations. Sampling, cell disruption, c-di-AMP extract, measuring of the c-di-AMP concentration and normalization to the protein concentration were exactly performed as previously described (**chapter 2**; Rismondo *et al.*, 2016). To assess the growth behavior after osmotic stress, bacteria were incubated as described above, or using the Synergy Mx multiwell platereader, equipped with the Gen5 software (02.09.2001, Bio-Tek Instruments) Cultures were handled the similar, but the exponential growing overday cultures were adjusted to an OD_{600} of 0.1 in LB and 200 µl added to the wells of a 96-well plate (Microtest Plate 96-Well,F, Sarstedt). Bacteria were incubated for 1.25 hours at 37°C with medium shaking and the OD_{600} measured in 15 min intervals. Subsequently, either 200 µl of the cultures were transferred to empty wells or 100 µl added to LB medium, or to 100 µl LB medium containing 3 M NaCl, KCl or sucrose, to obtain a final osmolyte concentration of 1.5 M, respectively. Eventually, growth was resumed using the same settings.

Results

DisA is inhibited by chromosomal DNA – The DAC cyclase DisA, with an N-terminal His_6-tag, was purified from *E. coli* and dialyzed overnight in salt-free buffer. DisA was incubated with its cofactor Mg_{2+} and its substrate ATP, as described in the experimental procedures and c-di-AMP extracted after different time points. As shown in **Fig. 5.1, A**, the enzyme shows a similar activity in the first 120 min and we therefore performed all subsequent DAC assays for 30 min.

Next, we assessed the ability of chromosomal DNA to inhibit DAC activity of DisA. Therefore, we incubated DisA with different amounts of *B. subtilis* cDNA and also tested the impact of cDNAs from other bacteria, like *E. coli* or *L. monocytogenes*. Furthermore, we analyzed if cDNA has an effect on DAC activity of the sporulation-specific DAC CdaS from *B. subtilis*, which was purified via *Strep*-tag purification. As expected, DAC activity of CdaS was not influenced by cDNA, while DisA was strongly inhibited in a concentration dependent matter and inhibition was independent of the cDNA donor organism (**Fig. 5.1, B**).

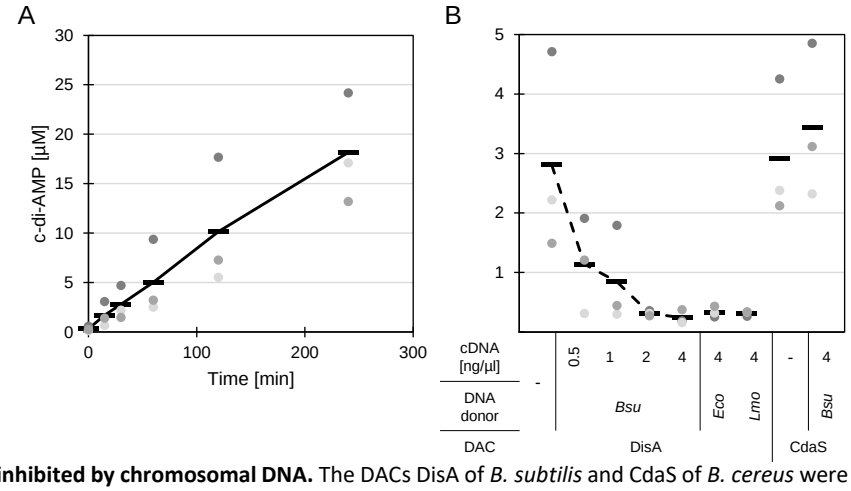

Fig. 5.1 DisA is inhibited by chromosomal DNA. The DACs DisA of *B. subtilis* and CdaS of *B. cereus* were purified *via* His- and *Strep*-tag purification, respectively. Proteins were dialyzed overnight in 10 mM Tris-HCl pH 7.5, 5% (*w/v*) glycerol and 1mM DTT at 4°C. 100 nM of DAC was incubated in 10 mM Tris-HCl pH 7.5 with 100 µM ATP, 10 mM $MgCl_2$ and 0.1 % (*w/v*) BSA at 37°C. (A) DisA activity over time. Reactions were stopped after the indicated time points and c-di-AMP extracted. (B) Impact of cDNA on DAC activity. DisA or CdaS were incubated without or with the indicated concentrations of cDNA. The reactions were stopped after 30 min of incubation and c-di-AMP was extracted. Data of three biological replicates are shown as the mean of two technical replicates per measurement point. Horizontal lines depict the mean of the three biological replicates. cDNA = chromosomal DNA, *Bsu* = *B. subtilis*, *Eco* = *E. coli*, *Lmo* = *L. monocytogenes*.

Addition of ions counteract the inhibitory effect of cDNA – Next, we wanted to analyze if osmolytes have an effect on the inhibitory effect of cDNA. We therefore incubated DisA with or without 1 ng/µl *B. subtilis* cDNA, as indicated, and added 0, 1, 10, 50 or 100 mM of the osmolytes KCl, NaCl or sucrose to the mixture and analyzed c-di-AMP synthesize after 30 min of incubation. As depicted in **Fig. 5.2**, addition of osmolytes does not influence DAC activity of DisA in the absence of DNA. Furthermore, in the presence of cDNA, the non-ionic osmolyte sucrose has no effect on DisA activity, but the ionic osmolytes KCl and NaCl counteract the inhibitory effect of cDNA at concentrations greater than 10 mM. We also tested if double stranded DNA (dsDNA) has an impact on DisA activity in our assay conditions and incubated DisA with either 0.25 or 1 ng/µl of a ~2 kb PCR product of the *B. subtilis ktrAB* operon, with or without 50 mM of KCl and compared the effects to the effect of cDNA. While we could observe an effect of dsDNA on DisA activity and higher activity if potassium ions were present, but the effect was not as pronounced, as with cDNA and we therefore continued the experiments using cDNA (**Fig. S5.1**).

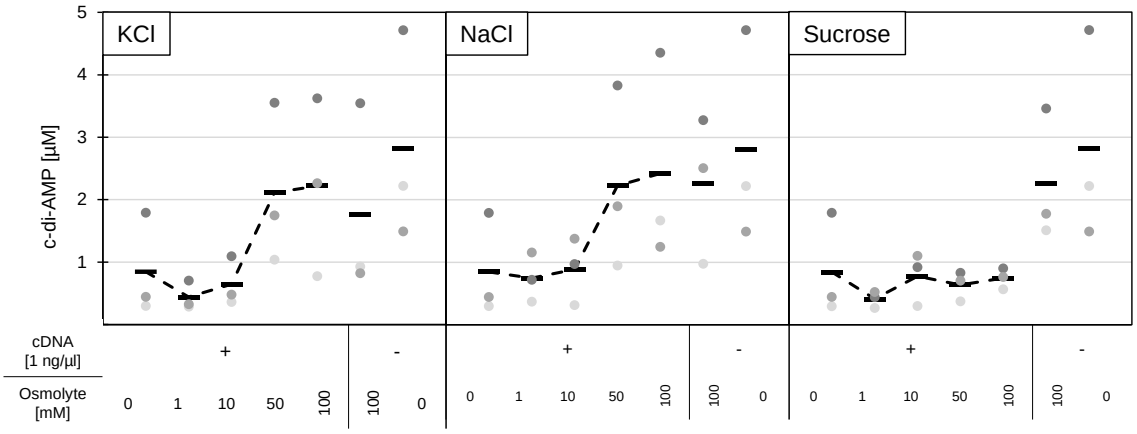

Fig. 5.2 DNA-dependent inhibition of DisA is counteracted by monovalent ions. The DACs DisA of *B. subtilis* was purified *via* His-tag purification and subsequently dialyzed overnight in 10 mM Tris-HCl pH 7.5, 5% (*w/v*) glycerol and 1mM DTT at 4°C. 100 nM of DisA was incubated in 10 mM Tris-HCl pH 7.5 with 100 µM ATP, 10 mM $MgCl_2$ and 0.1 % (*w/v*) BSA at 37°C for 30 min when the reactions were stopped and c-di-AMP extracted. Samples were incubated with or without 1 ng/µl of *B. subtilis* cDNA and with or without the indicated concentration of the two ionic osmolytes NaCl or KCl or the non-ionic osmolyte sucrose. Data of three biological replicates are shown as the mean of two technical replicates per measurement point. Horizontal lines depict the mean of the three biological replicates. cDNA = chromosomal DNA.

DisA G334E mutant shows similar activity and inhibition by cDNA in vitro – To assess whether similar effects can be observed for DisA with an altered DNA-binding, we purified and dialyzed DisA with an amino acid exchange of glycine 334 to glutamate (G334E), which has been shown to have a decreased binding capability to branched nucleotides and to be less inhibited by them (Witte *et al.*, 2008). We first analyzed c-di-AMP formation over time and compared it to the wild type DisA. As described by Witte and colleagues, DisA G334E has the same activity as the wild type enzyme *in vitro* (Witte *et al.*, 2008; **Fig. 5.3, A**). Next, we assessed the effect of cDNA of DisA G334E activity and observed a similar inhibitory effect of cDNA on the mutant as we saw for the wild type enzyme (**Fig. 5.3, B**). Therefore, we compared the effects of addition of potassium ions on the activity of the mutant enzyme.

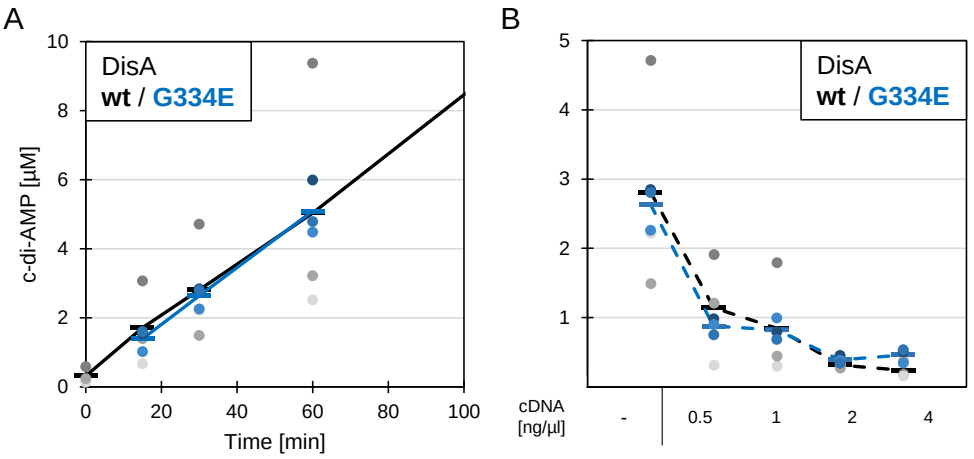

Fig. 5.3 DisA G334E is also inhibited by chromosomal DNA *in vitro*. The G334E mutant of *B. subtilis* DisA was purified *via* His-tag purification and subsequently dialyzed overnight in 10 mM Tris-HCl pH 7.5, 5% (*w/v*) glycerol and 1mM DTT at 4°C. 100 nM of DisA G334E was incubated in 10 mM Tris-HCl pH 7.5 with 100 µM ATP, 10 mM $MgCl_2$ and 0.1 % (*w/v*) BSA at 37°C. (A) DisA G334E activity over time. Reactions were stopped after the indicated time points and c-di-AMP extracted. Data of the mutant in red is overlaid on the measurements previously obtained for wt DisA in black, as a comparison. (B) Impact of cDNA on DAC activity of DisA G334E. The DAC was incubated without or with the indicated concentrations of *B. subtilis* cDNA. The reactions were stopped after 30 min of incubation and c-di-AMP was extracted. Data of three biological replicates are shown as the mean of two technical replicates per measurement point. Horizontal lines depict the mean of the three biological replicates. cDNA = chromosomal DNA.

As shown in Fig. 5.4, addition of potassium does not increase activity of DisA G334E in the absence of cDNA, only in the presence of it. Moreover, the inhibition of DAC activity seems to be slightly better counteracted by potassium ions at lower concentrations, compared to the wild type, with similar activities at higher concentrations. Eventually, we also assessed the DAC activities of DisA wild type and G334E mutant *in vivo*, to see whether the mutation might have an effect under more natural conditions. Indeed, we observed higher activity of DisA G334E, compared to the wild type enzyme (about 1.5-fold), if expressed in *E. coli*, which does not possess c-di-AMP (Fig. S5.2). This suggests that the mutant has a higher activity *in vivo*, but not *in vitro*.

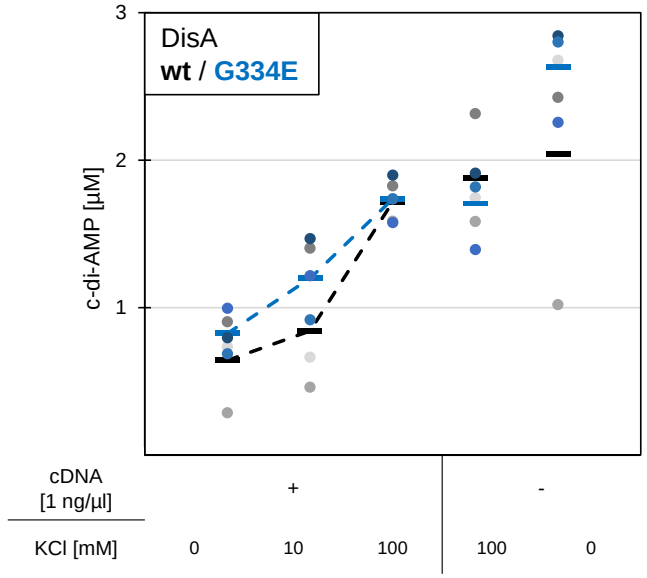

Fig. 5.4 DNA-dependent inhibition of DisA G334E is released at lower potassium concentrations than wild type DisA. The *B. subtilis* DisA wild type and G334E mutant were purified *via* His-tag purification and subsequently dialyzed overnight in 10 mM Tris-HCl pH 7.5, 5% (*w/v*) glycerol and 1mM DTT at 4°C. 100 nM of DAC was incubated in 10 mM Tris-HCl pH 7.5 with 100 µM ATP, 10 mM $MgCl_2$ and 0.1 % (*w/v*) BSA at 37°C for 30 min when the reactions were stopped and c-di-AMP extracted. Samples were incubated with or without 1 ng/µl of *B. subtilis* cDNA and with or without the indicated concentration of KCl. Data of three biological replicates are shown as the mean of two technical replicates per measurement point. Horizontal lines depict the mean of the three biological replicates. cDNA = chromosomal DNA.

DisA G334E mutation affects B. subtilis *ability to adapt after salt stress* – To investigated the effect of DisA and the G334E mutation on c-di-AMP concentrations and the capability of *B. subtilis* to adapt after a hyperosmotic stress *in vivo,* we constructed strains harboring DisA or the G334E

mutant as sole DACs (BP172 and BP173, respectively). We grew the strains, referred to as DisA (wt) and DisA (G334E), in LB medium until exponential growth and shocked them by the addition of LB containing NaCl or KCl to a final concentration of 1.5 M and compared the intracellular c-di-AMP concentration before the salt shock (t_0), to 30 min (t_1) after it and 3 hours (t_2) after it. We also compared the effects of salt shocked to non-salt shocked conditions (-osmolytes). As shown in **Fig. 5.5**, without osmolytes c-di-AMP levels do not change much from t_0 to t_1, but rise from t_1 to t_2, indicating higher c-di-AMP concentrations in later growth phases, which is consistent with previous reports (Corrigan *et al.*, 2015).

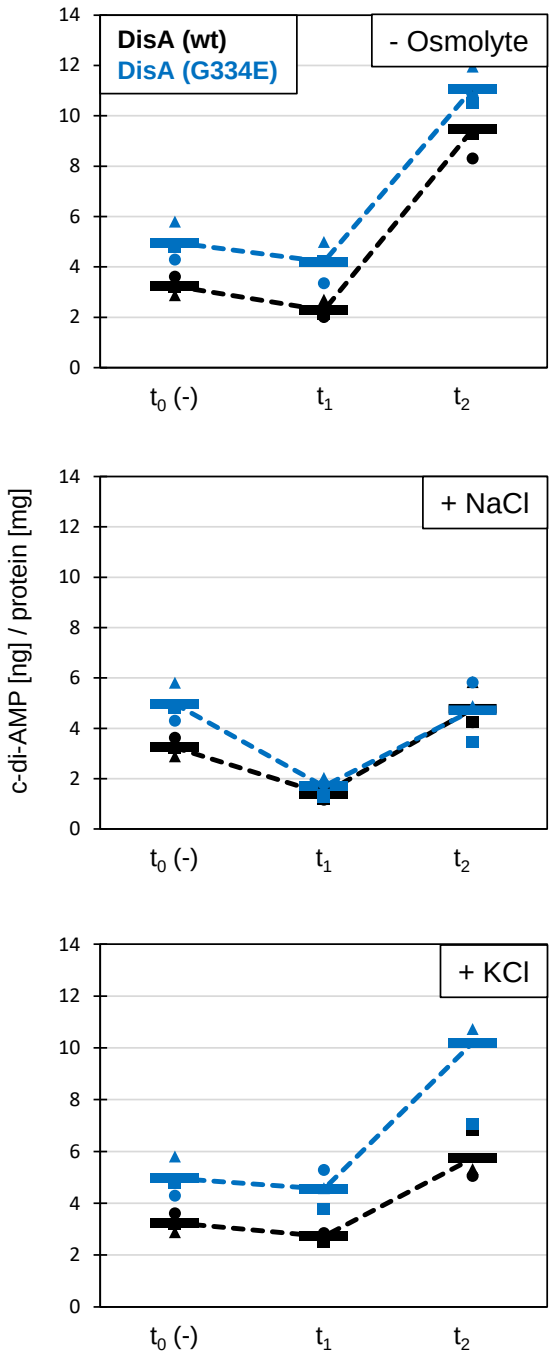

Fig. 5.5 DisA DNA-binding affects c-di-AMP concentration after osmotic stress *in vivo*. *B. subtilis* containing either the wild type DisA or the G334E mutant as sole DAC was grown in LB medium at 37°C until exponential growth. Samples for determination of the intracellular c-di-AMP concentration were taken (t_0) and the cultures split to flasks with prewarmed LB medium with or without the indicated osmolytes and growth was resumed. The final concentrations of NaCl or KCl were 1.5 M. Samples for c-di-AMP concentration measurements were again taken after 30 min (t_1) and 3 hours (t_2). Data of three biological replicates are shown as the mean of two technical replicates per measurement point. Horizontal lines depict the mean of the three biological replicates.

Interestingly, in the G334E mutant, a higher c-di-AMP concentration is observed, with is in agreement with the higher observed concentration, if expressed in *E. coli* (**Fig. S5.2**). In NaCl-shocked cells, c-di-AMP concentrations rapidly decrease (t_0 to t_1) and normalize afterwards (t_1 to t_2), with

no difference between the DisA wild type and DisA G334E expressing strain (Fig. 5.5). Interestingly, osmotic shock with KCl did not affect the initial c-di-AMP concentration (t_0 to t_1), but was followed with an increase of intracellular c-di-AMP levels (t_1 to t_2), with the mutant reaching about 2-fold higher c-di-AMP concentrations three hours after the salt shock (Fig. 5.5). This suggests that the cells are able to distinguish between the sources of the osmotic stress and adapt accordingly. Since we did not see a difference in the effects of NaCl and KCl *in vitro*, this effect is likely contributed to the PDEs, or the different – transport specific – abilities of the salts to accumulate intracellular, or a combination of both. It also demonstrates that DisA as sole cyclase is able to regenerate the c-di-AMP pool after osmotic stress and that the DNA-binding mutation of G334E can influence this ability. To assess whether the inhibitory effect of cDNA on DisA activity can be influenced by other potassium containing compounds, we took another look at the activity of DisA *in vitro*. We compared effects of KCl and potassium hydrogen phosphate (see experimental procedures) on the inhibitory effect on cDNA and surprisingly not only detected that inhibition by DNA was completely abolished in the presence of already 10 mM potassium hydrogen phosphate (in terms of the potassium ions), but also activity of DisA seemed to be stimulated. In the presence of potassium hydrogen phosphate alone, the measured c-di-AMP concentration after 30 min was about 10-fold higher, as in the untreated samples or the potassium chloride treated samples, indicating an effect of phosphate on DisA activity (Fig. S5.3).

Finally, we also tested whether a *B. subtilis* mutant containing DisA as sole DAC is able to recover after an osmotic stress and if the G334E mutant affects this ability. Similar to the c-di-AMP experiments, the strains BP172 (DisA (wt)) and BP173 (DisA (G334E)) were incubated in LB and shocked with the addition of 1.5 M of the osmolytes NaCl, KCl or sucrose and the growth was observed. As shown in Fig. 5.6, growth was inhibited after the osmotic shock for about two to three hours in all samples. In the case of sucrose, wt and G334E mutant displayed similar abilities to recover, with the mutant showing a slightly faster adaptation. Interestingly, in the case of the ionic osmolytes NaCl and KCl, the mutant was able to adapt much faster, especially if the cells were shocked with KCl, compared to the wild type. The wild type was also able to adapt, as all cultures had a similar OD_{600} after 20 hours (see Fig. S5.4). This indicates that DisA as sole cyclase is sufficient for *B. subtilis* to survive a hyperosmotic stress and that DNA-binding of DisA that seems to effect intracellular c-di-AMP concentrations is involved in the ability of DisA to fulfill this task.

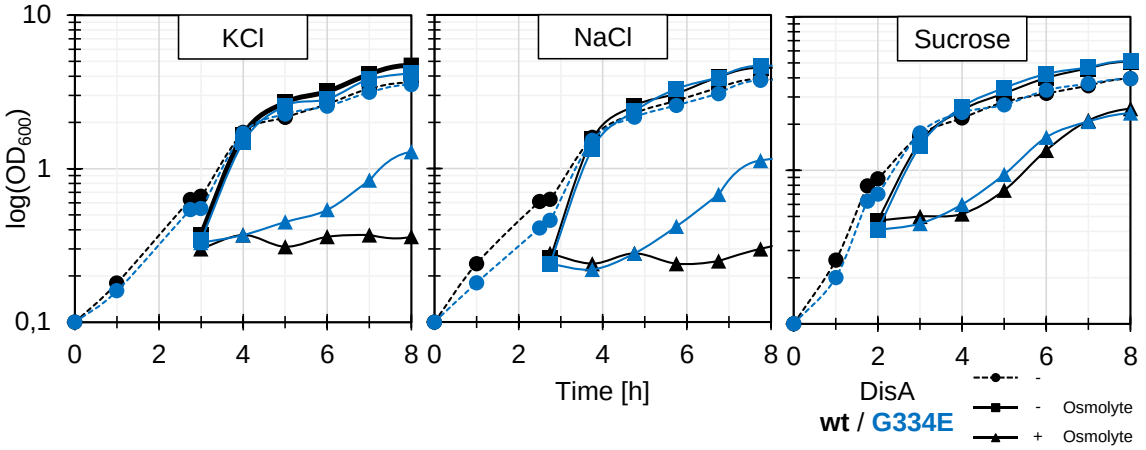

Fig. 5.6 The DisA G334E mutation affects resistance of *B. subtilis* to salt stress. *B. subtilis* containing either DisA (wt) or DisA (G334E) as sole DAC was grown in LB medium at 37°C. Cultures were splitted in the exponential growth phase and either further incubated without change (-) or with after the addition of 1.5 M of the indicated osmolytes (+ osmolytes) or an equivalent volume of LB without osmolytes (- osmolytes). Depicted are exemplary growth curves with hourly measurement of the OD_{600}.

Discussion

c-di-AMP has been shown to be essential due to its regulation of homeostasis of potassium and other osmolytes in a variety of bacteria (Devaux *et al.*, 2018; Gundlach *et al.*, 2017; Pham *et al.*, 2018; Whiteley *et al.*, 2015; Whiteley *et al.*, 2017; Zeden *et al.*, 2018). This discovery, the absence of DisA in many firmicutes and the apparent lack of DNA damage repair defects, which would be noticeable by increased accumulation of gene unspecific mutations and strain instability, lead us to challenge the current models of DisA regulation. The ability of DisA of being inhibited in DAC activity upon binding has been described simultaneously with the discovery of c-di-AMP and DisA as first DAC (Witte *et al.*, 2008). Interestingly, Witte and colleagues did not see an effect of double or single stranded DNA on DisA activity, while in other studies also an effect of ssDNA has been observed (Gándara *et al.*, 2017). Since we aimed to investigate the inhibitory effect of DNA on DisA activity in an osmoregulatory context, we chose to use chromosomal DNA as a DisA inhibitor, because it should in principle contain every possible conformation, from a bacterial population, including strand breaks and nicks from the purification and, furthermore, allows sequence independent observations. As shown in **Fig. 5.1**, DisA is indeed strongly inhibited by cDNA, in a concentration dependent matter and the effect is DisA-specific, as CdaS another DAC did not show an altered activity in the presence of cDNA. We wondered if dsDNA is also able to inhibit DisA activity in our monovalent cation-free assay setup and indeed, we saw an effect, although cDNA has a stronger inhibitory effect (**Fig. S5.1**). Interestingly, if we compare our experimental setup with previously published setups, it is likely that no inhibitory effects of dsDNA were observed in those studies due to NaCl concentrations of 50 mM or above (Gándara *et al.*, 2017; Witte *et al.*, 2008). Interestingly, the study where 50 mM NaCl was in the reaction mixture observed an influence of ssDNA on DisA activity, which was not observed in the study using 100 mM, highlighting that assay ion concentrations can greatly influence behavior of DNA-binding proteins (Gándara *et al.*, 2017; Witte *et al.*, 2008). Indeed, it has also been reported that increase in extracellular potassium and the resulting increase of macromolecular crowding impacts the DNA-binding ability of the RNA polymerase (Cagliero & Jin, 2013). Intriguingly, it has also been reported that a DisA mutant that interferes with dimerization of DisA molecules and therefore should not form octamers but tetramers *via* tetramerization of the HhH domains, showed salt sensitive dissociation of the tetramers with already 10 mM NaCl (Müller *et al.*, 2015b). This further indicates that interaction of cations with DisA might impact its conformational arrangement and thereby may affect its DNA-binding properties.

Next, we assessed the influence of osmolytes on DisA activity in the presence of cDNA and did only observe increased DAC activity in the presence of sufficient amounts of the ionic osmolytes NaCl and KCl, but not the non-ionic osmolyte sucrose *in vitro* (**Fig. 5.2**). Interestingly the ions Mg^{2+}, Ca^{2+}, Na^{+} and K^{+} are the main cationic ions associated with the negatively charged phosphate backbone of the DNA helix, the proposed binding site of DisA (Pasi *et al.*, 2015; Witte *et al.*, 2008). Since the DNA purification most likely does not result in salt-free DNA and the assay contains 10 mM of Mg^{2+} ions, the effect of additional monovalent ions may be specific, but this has to be investigated in further studies. Remarkably, DisA activity was strongly increased in the presence of potassium hydrogen phosphate, which may indicate competition of the DNA phosphate backbone with free phosphate for the DisA DNA-binding domain or secondary, unknown effects (**Fig. S5.3**).

When assessing the *in vitro* role of the G334E mutation of DisA, which has been shown to reduce binding to branched nucleic acids and their inhibitory effect, we only observed a slight improve in potassium dependent release of DNA inhibition, but no change in DNA inhibition itself (**Fig. 5.3** &

Fig. 5.4; Witte *et al.*, 2008). Interestingly, the mutant showed the same activity as DisA wild type *in vitro*, but a higher activity *in vivo* if expressed in *E. coli* (**Fig. S5.2**). This indicates that activities of wild type and G334E mutant are not altered, but that the mutant is less-stronger inhibited as the wild type enzyme *in vivo*. Looking at the DisA octameric structure (Witte *et al.*, 2008), it is obvious that DNA-binding domains of the two tetramers are facing opposite directions. We hypothesize that DisA interacts with dsDNA strands of the folded and condensed chromosome *in vivo* and that this is also the reason why strong effects of dsDNA have not been observed so far, since the used PCR products may be too short to allow the necessary folding for double-sided DisA interaction.

In vivo we demonstrated that DisA as sole DAC is able to take part in modulation of the intracellular c-di-AMP pool and adaptation to osmotic stress. Furthermore, the G334E mutant probably leads to a faster adaptation after an osmotic stress by contributing to a faster replenishment of the c-di-AMP pool, because it is less strongly inhibited by DNA (**Fig. 5.5** & **Fig. 5.6**). We therefore propose a model, in which DisA-DNA interaction is regulated by the osmotic conditions in dependency of cell size and ion concentration.

After a hyperosmotic shock, water will flow out of the cell, leading to shrinkage of the cellular volume, which results in a transiently higher concentration of DNA (Wood, 1999; Wood, 2011; Wood *et al.*, 2001). DisA that has to compete with other DNA-binding proteins and affected by intracellular ion concentrations might now show a tighter binding to DNA or is more compressed between two DNA strands, resulting in inhibition of DAC activity. c-di-AMP is probably further degraded by the PDEs, allowing import of osmolytes that fist lead to an increase in internal potassium, followed by rehydration and finally import or *de novo* synthesis of compatible solutes. The first two might influence DisA binding to DNA, increasing c-di-AMP synthesis again to inhibit osmolyte importer again and prevent an accumulation that would be toxic for the cell (Gundlach *et al.*, 2015; Gundlach *et al.*, 2017). This might also explain the difference we saw in intracellular c-di-AMP levels, in dependency whether the osmolyte was NaCl or KCl. For NaCl, the above-mentioned model could be true, but for KCl, c-di-AMP synthesis should not be lowered to much, since it would lead to a too fast and too high accumulation of intracellular potassium. The cells must therefore have evolved mechanisms to distinguish the source of the osmotic stress. While the CdaA cyclase may play a role as a general turgor sensor, DisA may act as a sensor for macromolecular crowding and intracellular ion concentration (**see chapter 2**). If the cells are exposed to a sudden upshift with potassium, the intracellular concentration would probably also rise immediately to a certain level due to active potassium import systems that are an important determinant for the intracellular turgor and thereby cell expansion (Whatmore & Reed, 1990; Wood, 1999). This would result in a higher initial intracellular concentration of monovalent cations, opposed to NaCl and DisA would therefore presumably be less inhibited. The different effect of sucrose *in vivo* is probably due to *B. subtilis* ability to metabolize it and thereby quicker reduce its concentrations and the resulting osmotic pressure (Gay *et al.*, 1983). For a hypoosmotic shock, c-di-AMP levels should be stable or rise to prevent further increase in intracellular osmolytes, with the simultaneously release of osmolytes to decrease the osmotic gradient. Here, DisA should stay active or even increase in activity, due to osmotic swelling and a subsequent decrease in DNA concentration (Wood, 1999) and it will be interesting to elucidate DisA function under those conditions.

On the basis of our findings, we think that it is compelling to postulate that the main regulator of DisA activity is not the DNA damage repair function, which our findings do not exclude, but that it is more likely a side function of DisA or that the related phenotypes are of secondary nature due to increased osmotic stress, as it has been proposed for other phenotypes (Commichau *et al.*,

2018). There are three main reasons for that. First, many bacteria produce c-di-AMP and its important role in osmoadaptation has been shown by different studies and many of the studied bacteria that are closely related to *B. subtilis* do not have a DisA homolog (Commichau *et al.*, 2019; Devaux *et al.*, 2018; Gundlach *et al.*, 2017; Pham *et al.*, 2018; Whiteley *et al.*, 2015; Whiteley *et al.*, 2017; Zeden *et al.*, 2018). This makes it unlikely that DNA damage repair is a main function of DisA. Secondly, *B. subtilis* is viable without any obvious effects, like increased accumulation of mutations if only one DAC is present, independent of which or if any DAC is present at all, providing that the cells are grown under osmotically stable conditions, with a low potassium concentration (Gundlach *et al.*, 2015; Gundlach *et al.*, 2017; Mehne *et al.*, 2013). Finally, it has been shown that this is also true for other bacteria. *L. monocytogenes* CdaA can be replaced by *B. subtilis* DisA, without any severe consequences, demonstrating that the role of DACs as synthesizer of c-di-AMP, as an osmolyte responsive second messenger, is interchangeable even between species, indicating a conserved role and source of regulation between DAC enzymes (Whiteley *et al.*, 2017).

In the present study, we demonstrated inhibition of the enzyme DisA by cDNA on its DAC activity and the anti-inhibitory effect of ionic osmolytes on this effect *in vitro*. We furthermore could show that a G334E mutant is as inhibited by cDNA, but inhibition is easier relieved by potassium ions. Finally, we showed that *B. subtilis* with DisA as sole cyclase is able to adapt after an osmotic stress and that DisA is sufficient to modulate c-di-AMP concentrations accordingly. The G334E mutant thereby shows increased DAC activity *in vivo* and positively effects *B. subtilis* ability to adapt after a hyperosmotic shock by faster replenishing the intracellular c-di-AMP pool. We therefore show a DNA damage-independent role of regulation of DisA activity in the broader context of c-di-AMP as major regulator of osmohomeostasis in *B. subtilis*.

Acknowledgements

This work was supported by the grant CO 1139/2-1 from the Deutsche Forschungsgemeinschaft *via* the Priority Program SPP1879, the Fonds der Chemischen Industrie and the Max-Buchner-Forschungsstiftung (MBFSt-Kennziffer 3381) to FMC.

6. The sRNA *rli31* affects lysozyme resistance, motility and gene expression in *Listeria monocytogenes*

Johannes Gibhardt, Julian Schwanbeck, Samuel Hauf, Alexander Reder, Andrea Thürmer, Uwe Völker, Sven Halbedel and Fabian M. Commichau

Author contribution:
JG and JS performed the experiments, JG analyzed the data, SH and AT and SH performed the RNA-Seq, AR and UV performed the protein quantifications, JG and FMC wrote the manuscript.

Abstract

Pathogenic bacteria have to overcome the host immune system and natural defensive barriers to successfully thrive inside the host. One important part of the innate immune system is the peptidoglycan (PG) hydrolyzing enzyme lysozyme. It hydrolyzes 1,4-β-linkages between N-acetylmuramic acid (NAM) and N-acetyl-D-glucosamine (NAG), leading to a weakening of the cell wall and subsequently lysis of the bacteria due to the high intracellular turgor pressure. Bacteria protect themselves against lysozyme by modifying their PG. *Listeria monocytogenes* produces the enzymes OatA, PgdA and PbpX that confer lysozyme resistance. The second messenger cyclic diadenosine monophosphate (c-di-AMP) has been linked to cell wall biogenesis and previous studies have linked the diadenylate cyclase (DAC) CdaA and its regulatory protein CdaR to increased resistance towards lysozyme. We evolved *L. monocytogenes* to become lysozyme resistant and identified suppressor mutations in the promoter region of the small RNA *rli31*. Interestingly, expression of PbpX and PgdA has been shown to be influenced by the small RNA *rli31*. We demonstrate that *L. monocytogenes* rapidly adapts towards lysozyme through acquisition of *rli31* promoter mutations and show by RNA sequencing that the sRNA affects gene expression of genes involved in cell wall modifications, ion transport and motility and discuss possible cross-talk between *rli31* and c-di-AMP signaling in *L. monocytogenes*.

Introduction

Pathogenic bacteria have to overcome several natural barriers to successfully infect their host, including physical barriers, like the epidermis or the acidic environment of the stomach, competition with organisms of the host's microbiota and evading detection by the immune system. The first response to a bacterial infection is facilitated by the humoral and cell-mediated response of the innate immune system, followed by responses of the adaptive immune system (Spiering, 2015). The glycoside hydrolase lysozyme is one of the first defenses bacteria encounter upon contact to the host. The enzyme class itself, however, is also important for bacteria to actively remodel the structure and composition of their cell wall. It hydrolyses the 1,4-β-linkage between the main PG glycan sugars NAM and NAG and has also pore forming properties. Through the weakening of the protective cell wall and the high turgor pressure, the bacteria will eventually lyse (Callewaert *et al.*, 2010; Vollmer *et al.*, 2008). Lysis and fragmentation of the PG furthermore leads to the release of components, like lipoteichoic acids that are subsequently detected by components of the innate immune system, leading to an inflammatory response (Ragland *et al.*, 2017). Lysozyme is found ubiquitous in nature and can be found in higher animals, as well as, in invertebrates, highlighting its early evolutionary origin (Callewaert *et al.*, 2010). In mammals, lysozyme is found in high concentrations on the skin, in the blood, liver, urine, milk, tear fluid, on mucosal surfaces and it can reach high concentrations of about 1 mg/ml (Callewaert *et al.*, 2010; Ragland *et al.*, 2017). Bacteria have therefore evolved mechanisms to counteract lysozyme. Counteracting a bactericidal compound is in general achieved by several different mechanism: degradation of the compound, secretion if it acts intracellular, biofilm formation as a diffusion barrier or modulating the target of the compound either through regulatory processes or genetically by acquisition of mutations or horizontal gene transfer, as it is often the case for the development of antibiotic resistances (Munita & Arias, 2016). Interestingly, recent studies have shown that bacteria may have adapt to lysozyme in a way that it can be beneficial for surviving antibiotic treatment. It has been shown that bacteria can adapt to a cell wall-less life style, called L-forms, under osmotically stabilizing conditions, as they are for example present in a host cell. Treatment of lysozyme promote transition to the L-form lifestyle and renders the bacteria thereby immune against cell wall acting antibiotics, like β-lactam antibiotics, which could be a clinically relevant new mode of persistence against antibiotic treatment (Burke, 2018; Kawai *et al.*, 2018). In case of lysozyme, the modification of its target, the PG is the prevalent mechanism, but there are also bacteria, like *Pseudomonas aeruginosa* and *Escherichia coli* that synthesize lysozyme inhibitors (Clarke *et al.*, 2010; Monchois *et al.*, 2001; Ragland *et al.*, 2017). Bacteria synthesize for example the enzymes PgdA, OatA and PbpX that N-deacetylate NAG, O-acetylate NAM or carboxylase the PG, respectively, and therefore decrease the binding affinity of lysozyme to it, rendering the cells immune (Burke *et al.*, 2014; Ragland *et al.*, 2017). Synthesis of these enzymes has to be regulated in order for the bacteria to adapt to their environment. In case of *L. monocytogenes*, the transcriptional activator PrfA is the major regulator of virulence determinants. Environmental signals, such as the temperature, and molecules like glutathione influence PrfA amount and activity, resulting in a fine-tuned expression of virulence related genes (de las Heras, *et al.*, 2011; Lobel *et al.*, 2015; Reniere *et al.*, 2015; Scortti *et al.*, 2007). In a similar manner *L. monocytogenes* has to detect the presence of lysozyme and other cell wall-acting compounds and adapt its gene expression accordingly. For *L. monocytogenes* the regulation of gene expression or translation *via* cis-acting RNA elements, like the temperature-depended *prfA* riboswitch that controls expression of PrfA or *via* trans-acting RNA elements, like small RNAs (sRNAs), play an important role. They can modulate translation by binding to mRNA, protein activity by RNA-protein interaction (Mellin & Cossart, 2012; Sesto *et al.*, 2014 Thorsing *et al.*, 2018). One of these sRNAs is *rli31*. It has been identified in

a transposon mutagenesis study by Burke and colleagues to regulate expression of the PG modulating enzymes PgdA and PbpX (Burke *et al.*, 2014). The mode of action of *rli31* however remained elusive, as no direct interaction of it has been identified, so far. Interestingly, *rli31* interacts with the protein SpoVG and also with the mRNA encoding it, but the consequence of this interaction is unknown. SpoVG has been proposed to be an RNA-binding posttranscriptional regulator (Burke *et al.*, 2016). Another impact factor on the bacterial cell wall is the nucleotide second messenger c-di-AMP. It is synthesized by DACs and degraded by specific phosphodiesterases (PDEs) and it has been shown to be essential in firmicutes (Commichau *et al.*, 2015). c-di-AMP has been implicated in regulation of various cellular processes, ranging from DNA damage repair, over the regulation of lifestyle changes and the modification of the cell wall, to the regulation of osmotic homeostasis, by regulation of ion and compatible solute transport processes (Corrigan *et al.*, 2011; Gundlach *et al.*, 2016; Gundlach *et al.*, 2017; Oppenheimer-Shaanan *et al.*, 2011; Pham *et al.*, 2018; Whiteley *et al.*, 2015; Whiteley *et al.*, 2017; Witte *et al.*, 2008; Witte *et al.*, 2013; Zeden *et al.*, 2018). It has been suggested that many cell wall related phenotypes of c-di-AMP, such as the decreased resistance of DAC mutants to cell wall-acting antibiotics, may just be indirect effects due to c-di-AMPs role as major regulator of osmohomeostasis (Commichau *et al.*, 2018). It is however established that there is some cross-talk between c-di-AMP signaling and cell wall biogenesis. The gene encoding the only DAC in many pathogenic firmicutes *cdaA* is co-transcribed with the gene *cdaR*, encoding a regulator of CdaA activity and this operon is genetically conserved with the *glmM* gene, encoding the phosphoglucosamine mutase GlmM (Gundlach *et al.*, 2015; Mehne *et al.*, 2013; Rismondo *et al.*, 2016). Interestingly GlmM is both, an essential enzyme that converts glucosamine-6-phosphate to glucosamine-1-phosphate, one of the earliest precursor molecules for NAM and NAG biosynthesis and a repressor of CdaA activity (Tosi *et al.*, 2019; Zhu *et al.*, 2016; **see chapter 2**). As shown in **chapter 4**, a *cdaA* mutant shows altered gene expression and protein biosynthesis of pathways involved in cell wall metabolism, which further suggest a direct connection between c-di-AMP signaling and cell wall metabolism. Furthermore, we previously identified that a *cdaR* deletion mutant is increased resistant towards lysozyme and another study identified, among others, mutations in the *cdaA* gene upon evolving *Streptococcus suis* towards lysozyme resistance (Rismondo *et al.*, 2016; Wichgers Schreur *et al.*, 2012). We therefore set out to evolve lysozyme resistant *L. monocytogenes*, to elucidate the connection between the osmoregulatory function of c-di-AMP signaling and its interconnections to the cell wall metabolism. Strikingly, we found, as previously studies reported, a connection between the sRNA *rli31* and lysozyme resistance and could further elucidate the role of the sRNA on regulation of gene expression and highlight possible interconnections to the c-di-AMP signaling network.

Experimental Procedures

Bacterial strains and growth conditions – *L. monocytogenes* 10403S, EGD-e and EGD-e mutants were cultivated in BHI medium (Sigma-Aldrich) at 37°C and 220 rpm if not specified otherwise. *E. coli* was grown in LB medium at 37°C and 220 rpm (strains see **Tab. 6.1**). For agar plates, medium was supplemented with 15 g/l Bacto Agar (Difco). Antibiotics and medium supplements were used with the following concentrations, if indicated: erythromycin (5 µg/ml), X-Gal (100 µg/ml; 5-bromo-4-chloro-3-indolyl-β-D-galactopyranoside; Sigma-Aldrich). Lysozyme from chicken egg white (15000 units/mg; Serva) and penicillin G (Serva) were used in the indicated concentrations.

DNA manipulation – DNA amplification *via* PCR and transformation of *E. coli* was performed using standard procedures (Sambrook *et al.*, 1989). DNA fragments were purified using the PCR

purification kit (Qiagen) and plasmid DNA was extracted using the NucleoSpin Plasmid Kit (Macherey and Nagel). Commercially available restriction enzymes, T4 DNA ligase and DNA polymerases were used as recommended by the manufacturers. DNA sequences were determined by the dideoxy chain termination method (Microsynth, Göttingen, Germany). Chromosomal DNA of *L. monocytogenes* was isolated using the NucleoSpin Microbial DNA Kit (Macherey and Nagel). Oligonucleotides were purchased from Sigma-Aldrich (Germany).

Tab. 6.1 Strains, Plasmids and Oligonucleotides

Strains			
Name	**Genotype**	**Description/Construction**	**Reference**
E. coli			
XL1-Blue	*recA*1 *endA*1 *gyrA*96 *thi*$^{-}$1 *hsdR*17 *supE*44 *relA*1 *lac* [F′ *proAB lacI*^{q} *Z*ΔM15 Tn*10* (*Tet*^{r})]	Cloning	Stratagene
L. monocytogenes			
10403S	Wild type	Serotype 1/2a strain	Laboratory collection
EGD-e	Wild type	Serotype 1/2a strain	Laboratory collection
BPL10	Δ*fliI*::P_{alf4}-RBS_{hly}-*mgfp* (A206K)	Chromosomal deletion of *fliI* and reverse oriented replacement by *mgfp*	Chapter 4
BPL23	EGD-e Δ*pgpH*	Chromosomal deletion of *pgpH*	Chapter 4
BPL24	EGD-e Δ*pdeA*	Chromosomal deletion of *pdeA*	Chapter 4
LMJR45	EGD-e Δ*cdaR*	Chromosomal deletion of *cdaR*	Rismondo *et al.*, 2016
BPL25	EGD-e P_{rli31} ($G_{597,748}$A) $C_{1,224,119}$T (*lmo1199*, silent)	Suppressor 2-I (2 mg/ml lysozyme)	This work
BPL26	EGD-e P_{rli31} ($T_{597,758}$TT) $G_{2,348,663}$A (*lmo2622*, H232Y)	Suppressor 2-II (2 mg/ml lysozyme)	This work
BPL27	EGD-e P_{rli31} ($T_{597,758}$TT)	Suppressor 4-I (4 mg/ml lysozyme)	This work
BPL28	EGD-e P_{rli31} ($G_{597,759}$A)	Suppressor 4-II (4 mg/ml lysozyme)	This work
BPL34	EGD-e Δ*rli31*	pBP340 →→ EGD-e	This work
Plasmids			
Name	**Insert/Features**		**Reference**
pMAD	*bla ermC bgaB*		Arnaud *et al.*, 2004
pBP340	pMAD-Δ*rli31*		This work
Oligonucleotides			
Name	**Restriction sites are underlined, complementary regions are in bold, sequences 5'→3'**		**Purpose**
JSL08	**AAACTCGAGCACATTTTTCGCGTGCTGGAAAGC**ATAATTATGTAGAAATAGAGATGCTCTGAA		Fwd. *rli31* downstream region (*Xho*I)
JSL09	TTTGGATCCCGTATTCAAAGTGAGCACGTTCATTTCTATCAATC		Rev. *rli31* downstream region (*Bam*HI)
JSL10	TTTGAATTCCGATAGATACCTTGGCTCTCGGCTTTG		Fwd. *rli31* upstream region (*Eco*RI)
JSL11	**GCTTTCCAGCACGCGAAAAATGTGCTCGAGTTT**TCTCTATGGGATAAGTATATCTTACATTACTTTTATG		Rev. *rli31* upstream region (*Xho*I)

→mutation event, →→ transformation and gene deletion, *bla* = amp^{R} (100 µg/ml ampicillin), *ermC* = ery^{R} (5 µg/ml erythromycin), Fwd. = forward, Rev. = reverse

Plasmid construction – For the chromosomal deletion of the *rli31* gene, pBP340 was constructed. The up- and downstream regions of the 144nt large sRNA *rli31* (lmos23; genome position 597,806-597,949), while sparring out the *rli31* ORF and leaving promoter and downstream regions intact (deletion from 597,822-597,941), were amplified using oligonucleotide pairs JSL10/JSL11 and JSL08/JSL09, respectively. The resulting PCR products were fused by SOE PCR using oligonucleotides JSL10 and JSL09, digested with *Eco*RI and *Bam*HI and ligated to pMAD (Arnaud *et al.*, 2004; Horton *et al.*, 1990), which was digested using the same enzymes (plasmids and oligonucleotides are listed in **Tab. 6.1**).

L. monocytogenes *strain construction* – For the chromosomal deletion of the *rli31* gene, strain BPL34 was constructed as follows. Electrocompetent cells were prepared as described by Monk and colleagues and electroporation performed as previously described (Monk *et al.*, 2008; **chapter 2**). The EGD-e wt was electroporated with plasmid pBP340 (pMAD-Δ*rli31*) and plated on BHI medium with erythromycin and X-Gal at 30°C for up to 72 h. Single, blue colonies were streaked on the same medium and incubated for up to 72 h at 42°C to force integration into the *rli31* locus. Several blue colonies were used to inoculate 5 ml of BHI without antibiotics at 30°C for 4 h, temperature was shifted to 42°C for 6 h, after which serial dilutions were plated on BHI medium with X-Gal and incubated at 37°C for up to 72 h. Erythromycin-sensitive, X-Gal negative bacteria were subjected to colony PCR as described elsewhere (Dussurget *et al.*, 2002). *rli31* deletion was confirmed by Sanger sequencing and the strain designated BPL34.

Evolution experiment, isolation of lysozyme resistant suppressor mutants and WGS – L. monocytogenes EGD-e was grown in BHI medium from different single colonies overnight at 37°C and 220 rpm. Pre-cultures were used to inoculate 20 ml BHI medium to an OD_{600} of 0.05 with or without 2 or 4 mg/ml of lysozyme. Bacteria were incubated for 18 hours at 37°C and 220 rpm, the OD_{600} measured and the cells re-inoculated into fresh medium with the same lysozyme concentration. This was repeated for 4 passages until improved growth in the presence of lysozyme was visible and cultures with lysozyme reached similar OD_{600} after 18 hours as the wild type without lysozyme. Emerging suppressor mutants were re-streaked twice on BHI agar plates and two independent colonies of each concentration and the EGD-e wild type strain were subjected to WGS. WG illumina sequencing was performed by the G2L Göttingen, the resulting reads analyzed using the Geneious software (Geneious Prime 2019.0.4 (https://www.geneious.com)) and potential mutations re-sequenced by Sanger Sequencing (Microsynth, Göttingen). The resulting suppressor mutants were designated BPL25, BPL26, BPL27 and BPL28, which are clone I and II, respectively of the evolution with 2 mg/ml lysozyme (BPL25 & BPL26) and with 4 mg/ml (BPL27 & BPL28). BPL27 was further investigated and is here also referred to as P_{rli31}* (concept based on Barrick & Lenski, 2013).

Motility assay – The *L. monocytogenes* wild type strain, the *fliI* mutant BPL10 (**see chapter 4**), *rli31* mutant BPL34 and the P_{rli31}* mutant BPL27 were used to assess the impact of *rli31* on the motility. Strains were cultivated in 5 ml BHI overnight at 37°C and 220 rpm. The pre-cultures were used to inoculate 5 ml of BHI medium to an OD_{600} of 0.05 and the cells were incubated at 37°C and 220 rpm. Cells were harvested and resuspended in fresh BHI medium after reaching an OD_{600} of about 0.5 and 1 µl of OD_{600} 1.0 cell suspensions were used to stab inoculate BHI soft agar plates (0.3% (*w/v*) agar). Plates were incubated at 25°C or 37°C, as indicated and imaged every 24 h.

Lysozyme autolysis assay – To assay if the isolated suppressor mutants were indeed more lysozyme resistant and the possible effect of c-di-AMP on lysozyme resistance, the *L. monocytogenes* wild type strains EGD-e and 10403S, as well as the EGD-e based mutants of *pgpH*, *pdeA, cdaR* (BPL23, BPL24, LMJR45) and the evolved lysozyme resistant suppressor mutants (BPL25-BPL28)

were analyzed for their ability to withstand lysozyme. Bacteria were inoculated from overnight cultures in 10 ml BHI medium to an OD_{600} of 0.05 and grown until they reached an OD_{600} of 0.8 ±0.1. Cells were harvested by centrifugation (3300 g, 4°C, 10 min). The cells were washed in 50 mM Tris-HCl, pH8 and finally adjusted in the same buffer to an OD_{600} of 1.2. 10 µg/ml of lysozyme, 25 µg/ml penicillin G or nothing was added and decline of OD_{600} observed using 100µl samples in 96-well plates (Microtest Plate 96-Well,F, Sarstedt) at 37°C and 237 cpm (4 mm) using an Epoch2 multiwell plate reader, equipped with the Gen5 software (02.09.2001; BioTek Instruments). The OD_{600} was normalized to the OD_{600} at time point 0 (% of initial OD_{600}) and mean values of four biological replicates were used to assess the different strains (modified from Rismondo *et al.*, 2016).

Growth of L. monocytogenes Δrli31 *and* P_{rli31}** mutants for transcriptomic and proteomic analysis* – To analyze the changes in the transcriptome and proteome of *L. monocytogenes* between the deletion and promoter mutant of *rli31*, strains BPL34 and BPL27 were cultivated and processed as follows. Single colonies were propagated from BHI agar plates to 10 ml BHI medium overnight at 37°C and 220 rpm. Pre-cultures were used to inoculate 100 ml BHI medium to an OD_{600} of 0.05 and incubated at 37°C and 220 rpm. For the analysis of the proteome 40 OD_{600} units of cells were harvested by rapid cooling in liquid nitrogen to slow down cellular processes and subsequent centrifugation after reaching an OD_{600} of about 0.5 at 3300 g and 4°C for 10 min. Cell pellets were washed twice in ZAP (50 mM Tris pH 7.5 and 200 mM NaCl), with centrifugation steps in between. Resulting pellets were frozen in liquid nitrogen and stored at -80°C until further processing. Growth for the analysis of the transcriptome was performed similar. When the cultures reached OD_{600} of 0.5 ± 0.05, 25 ml were collected and quenched by adding of 25 ml ice cold killing buffer (20 mM Tris-HCl pH 7.5, 5 mM $MgCl_2$, 20 mM NaN_3). After 5 min incubation on ice, cells were harvested by centrifugation. mRNA extraction, library preparation and RNA sequencing where subsequently performed as described previously in detail (Hauf *et al.*, 2019).

mRNA isolation and RNA sequencing – Further processing was performed as previously described (**see chapter 4**).

Protein isolation and proteome analysis – Further processing was performed as previously described (**see chapter 4**).

Data analysis – The in gene expression or protein biosynthesis affected genes and proteins were later on analyzed using the Geneious software (Geneious Prime 2019.0.4 (https://www.geneious.com)) and the online resources ListiWiki (http://listiwiki.uni-goettingen.de) and SubtiWiki (http://subtiwiki.uni-goettingen.de), the Listeriomics website (https://listeriomics.pasteur.fr) and the annotation databases RAST and COG (Aziz *et al.*, 2008; Bécavin *et al.*, 2017; Tatusov *et al.*, 2000; Zhu *et al.*, 2018).

Results

L. monocytogenes *rapidly adapts to lysozyme* – To elucidate the ability of *L. monocytogenes* to adapt to lysozyme, the EGD-e wild type strain was evolved in the presence of this muralytic enzyme. The bacteria were cultivated in BHI without or with 2 or 4 mg/ml lysozyme and passaged every 18 hours. As depicted in **Fig. 6.1**, the OD_{600} after 18 hours of growth increased in the cultures treated with lysozyme already in the second passage and reached wild type levels in passage three and four. This evolution experiment demonstrates on the one hand that even in the first two

passage *L. monocytogenes* is able to withstand quite high lysozyme concentrations and moreover that the bacteria can rapidly adapt to lysozyme stress and after grow like the wild type even with lysozyme concentrations four times higher as have been reported in human liquids (Ragland *et al.*, 2017). From the last passage putative suppressor mutants were isolated and subjected to WGS.

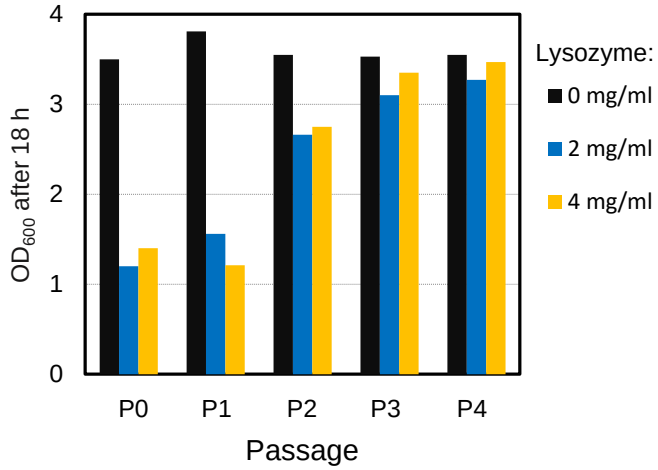

Fig. 6.1 *L. monocytogenes* rapidly adapts to lysozyme. The *L. monocytogenes* EGD-e wild type strain was inoculated in BHI medium and grown at 37°C. Pre-cultures were used to inoculate BHI fresh medium to an OD_{600} of 0.05 without or with the indicated concentration of lysozyme. Every 18 h the OD_{600} was measured and fresh medium inoculated to an OD_{600} of 0.05. Passage four was subsequently used to isolate lysozyme resistant suppressor mutants

L. monocytogenes *EGD-e adapts to lysozyme by acquisition of mutations in the promoter of the sRNA* rli31 – WGS of the suppressor mutants revealed that all four isolates acquired mutations upstream of the gene *lmos23* that encodes the sRNA *rli31* (**Fig. 6.2, A**). Further analysis revealed that the mutations affect a region that shows all characteristics of a prokaryotic promoter region. As depicted in **Fig. 6.2, B**, suppressor mutants 2-I and 2-II, which were evolved in the presence of 2 mg/ml lysozyme have acquired mutations in the spacing region between the -35 and -10 regions (guanine to adenine exchange and a thymine insertion, respectively). Suppressor mutants 4-I has acquired the same mutation as mutant 2-II and suppressor mutant 4-II has a mutation in the -10 region, leading to a guanine to adenine exchange. Interestingly, the mutation of isolate 4-II seems to be a natural occurring variant in *L. monocytogenes*, as it is the wild type allele of the 10403S wt strain. The guanine to adenine mutation in the spacing region probably leads to a lower melting temperature and the thymine insertion mutations to an improved spacing between the -35 and -10 region. The mutation in the -10 region results in an optimal TATAAT sequence. We therefore assumed that all mutations increased the expression of the adjacent sRNA *rli31*. The expression of the promoter and *rli31* probably also influence the expression of the downstream located gene *lmo0559*, encoding a putative magnesium or cobalt transporter. Predictions of transcriptional start sites and terminators suggest that *lmo0559* does not have its own promoter region and that, although transcriptional terminators are predicted between *rli31* and *lmo0559*, they are in part co-transcribed (Listeriomics website, Bécavin *et al.*, 2017; Dar *et al.*, 2016; Wurtzel *et al.*, 2012). It has to be noted that suppressor mutants 2-I and 2-II had second site mutations. Mutant 2-I harbored a silent mutation in the gene *lmo1199*, encoding CbiH a precorrin-3B C17-methyltransferase involved in cobalamin biosynthesis and mutant 2-II had a mutation in the gene *lmo2622*, leading to a histidine to tyrosine exchange of amino acids 232 in the encoded RplN, a ribosomal protein (LSU ribosomal protein L14p/L23e). Since all four isolates evolved similar mutations in the promoter of *rli31*, we assumed that the mutations in isolates 2-I and 2-II were second site mutations and not primary reason for the improved growth in the presence of lysozyme. The mutation could however be due to increased expression of *rli31* and therefore be potential targets of the sRNA.

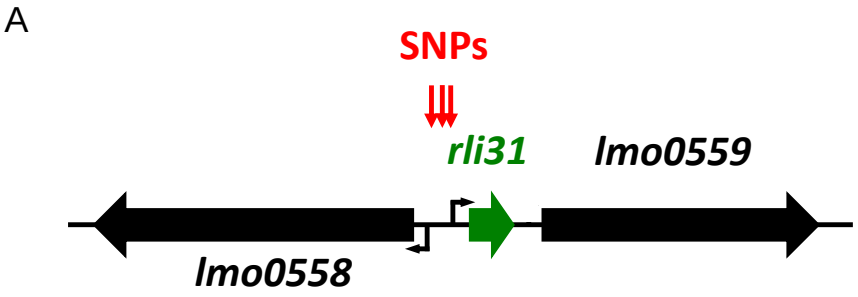

B

	-35	-10	Spacing
EGD-e wt	TTT TTGATT TTTATGAAATATTTT	TGTAAT	15 nt
Suppressor 2-I	TTT TTGATT TTTATAAAATATTTT	TGTAAT	15 nt
Suppressor 2-II	TTT TTGATT TTTATGAAATATTTTTTGTAAT		16 nt
Suppressor 4-I	TTT TTGATT TTTATGAAATATTTTTTGTAAT		16 nt
Suppressor 4-II	TTT TTGATT TTTATGAAATATTTT	TATAAT	15 nt
10403S wt	TTT TTGATT TTTATGAAATATTTT	TATAAT	15 nt

Fig. 6.2 Genome position of the identified SNPs upstream of the sRNA *rli31* and comparison of the promoter mutations. WGS revealed SNPS in the same region in all four lysozyme resistant isolates of *L. monocytogenes* EGD-e. (A) Illustration of the *rli31* operon. The SNPs are located between the two genes of unknown function *lmo0558* and *lmo559*. The sRNA *rli31* is localized between these two genes. (B) Comparison of the identified mutations. The SNPs were identified as mutations of the *rli31* promoter. Suppressor 2-I harbors a guanine to adenine exchange in the spacing region between the -35 and -10 region, suppressor 2-II and 4-I harbor an additional thymine in the spacing region and suppressor 4-II a has evolved a guanine to adenine change in the -10 region. The later mutation is also present as a natural variation in the *L. monocytogenes* wild type strain 10403s. Suppressor 2/4 = isolated from BHI with 2 or 4 mg/ml lysozyme, respectively, WGS = whole genome sequencing, SNP = single nucleotide polymorphism, nt = nucleotide

Evaluation of the lysozyme resistance of the suppressor mutants – To assess the if the isolated suppressor mutants are indeed increased resistant against lysozyme, we performed autolysis assays. The wild type strain, the evolved mutants and the 10403S wt strain, with the naturally -10 promoter variant found in suppressor 4-II, where assayed together with mutants affecting the c-di-AMP metabolism to investigate a possible link between c-di-AMP signaling, lysozyme resistance and *rli31*. We evaluated the previously as increased lysozyme resistant identified *cdaR* deletion mutant and deletion mutants of the *pdeA* and *pgpH* genes, encoding the two c-di-AMP specific PDEs in *L. monocytogenes*. It was hypothesized previously that the increased intracellular concentration of c-di-AMP in the *cdaR* mutant is responsible for the increased lysozyme resistance and we assumed the PDEs should behave similar if the resistance is due to c-di-AMP and not caused by the CdaR protein itself (Rismondo *et al.*, 2016). Bacteria were grown in BHI to the late exponential phase and cells of an OD_{600} of 1.2 were resuspended in 50 mM Tris-HCl, pH 8. Subsequently lysozyme (10 µg/ml), penicillin G (25 µg/ml) or nothing was added and decline of OD_{600} at 37°C was recorded. Without addition of lysozyme or penicillin G, the OD_{600} remained quite stable over the measured time period and only no extreme lysis was visible, demonstrating that the different strains do not show lysozyme or penicillin G independent autolysis (**Fig. S6.1**). With the addition of penicillin G, the OD_{600} decreased to about 80% of the initial OD_{600} and state stable at this range over the measured time, without difference between the strains, demonstrating that resistance against β-lactam antibiotics is not influenced by *rli31* or the c-di-AMP mutants under the tested conditions (**Fig. S6.1**).

As shown in **Fig. 6.3**, the OD_{600} of the EGD-e wild type strain rapidly decreased in the presence of lysozyme, indicating lysis. In contrast to that, 10403S wild type strain lysed with a much slower rate, indicating a higher resistance towards lysozyme. The *cdaR* mutant showed as previously reported an increased resistance towards lysozyme (Rismondo *et al.*, 2016). The *pdeA* mutant showed an intermediate phenotype between wt and *cdaR*, while the *pgpH* mutant showed the same rate of lysis as the wt.

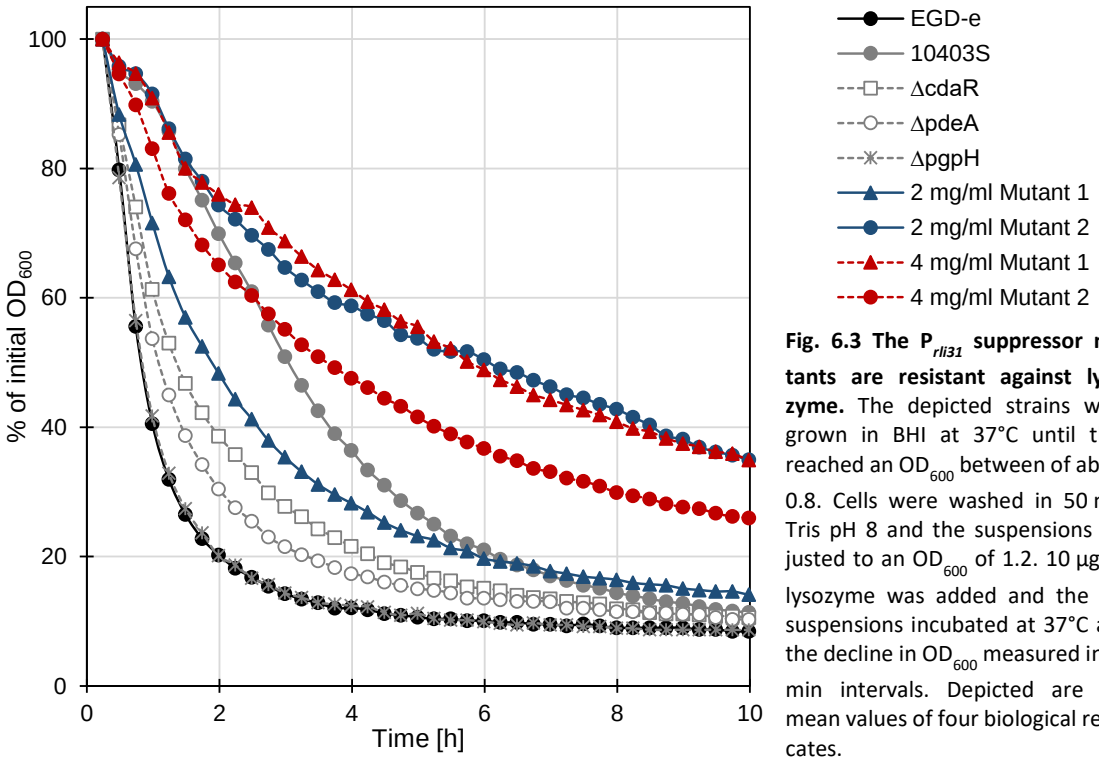

Fig. 6.3 The P_{rli31} suppressor mutants are resistant against lysozyme. The depicted strains were grown in BHI at 37°C until they reached an OD_{600} between of about 0.8. Cells were washed in 50 mM Tris pH 8 and the suspensions adjusted to an OD_{600} of 1.2. 10 µg/ml lysozyme was added and the cell suspensions incubated at 37°C and the decline in OD_{600} measured in 15 min intervals. Depicted are the mean values of four biological replicates.

Comparing the ability of the evolved suppressor strains to withstand lysozyme, mutant 2-I (G→A in the spacing region) showed the lowest increase of lysozyme resistance, between the *cdaR* mutant and the 10403S wt. Mutant 4-2, which has the same -10 region sequence as the 10403S strain, showed a great increase in resistance compared to the EGD-e strain and also an increased resistance compared to the 10403S strain, suggesting that downstream effects, like targets of the sRNA may have evolved apart in these two strains. Finally, mutant 2-II and 4-I, having the improved spacing between the -35 and -10 promoter regions, showed the highest increase in resistance, suggesting highest expression of *rli31* in those two isolates. To conclude all four isolates indeed showed increased resistance towards lysozyme. Next, we wanted to identify the regulatory network of the sRNA. We therefore constructed a Δ*rli31* mutant (BPL34) and compared gene expression and protein biosynthesis using RNA sequencing and whole proteome mass spectrometry, respectively. We also investigated strain BPL27 (suppressor mutant 4-I), showing the highest lysozyme resistance and no second site mutations and the wild type EGD-e strain as a reference. The mutant 4-I will be referred to as P_{rli31}* from here on.

rli31 *affects expression of peptidoglycan remodeling and motility genes in* L. monocytogenes – The analysis of changes in gene transcription between the Δ*rli31* mutant and the wild type showed no significant change in the gene expression except for a 40-fold decrease in *lmo0559* expression, the downstream gene of *ri31*. This suggests that deletion of *rli31* effects expression of the gene. It remains to be elucidated if this effect is a regulatory one or an unwanted side effect. In the P_{rli31}* mutant, no significant changes were detected that showed a at least 2-fold change in expression

compared to the wild type. The less than 2-fold expression changes are nevertheless shown in **Tab. S6.1**. We therefore compared expression levels between the *rli31* deletion mutant and P_{rli31}*, that were significant and showed a greater than 2-fold change. Unfortunately, only the genes *lmo0559* and *lmo1336*, encoding a 5-formyltetrahydrofolate cyclo-ligase, matched those criteria. We therefore lowered the significance cut-off to p<0.05 and the cut-off for fold-change to 1.5 to detect possible weak influence of *rli31* that may explain the how *rli31* leads to lysozyme resistance. The results are shown in **Tab. 6.2** and further information, including the p-values and even less sure deregulated genes can be found in **Tab. S6.1**.

Tab. 6.2 Genes differently regulated in *Δrli31* compared to P_{ril31}*

Locus tag	Operon	Name	RAST info	Fold change
lmo0559[1]			Magnesium and cobalt transport protein CorA	**-70.92**
lmo2805	508		hypothetical protein	**-2.12**
lmo0540		**pbpX**	penicillin-binding protein, putative	**-1.84**
lmo2150			FIG00774336: hypothetical protein	**-1.71**
lmo0620			FIG00774170: hypothetical protein	**-1.60**
lmo1494	246	mtn	5'-methylthioadenosine nucleosidase / S-adenosylhomocysteine nucleosidase	**1.49**
lmo0689	111	cheV	Chemotaxis protein CheV	**1.51**
lmo0688	111	**gmaR**	glycosyl transferase, group 2 family protein	**1.52**
lmo2077	378	ydiC	Inactive homolog of metal-dependent proteases, putative molecular chaperone	**1.54**
lmo1047	168	**moaA**	Molybdenum cofactor biosynthesis protein MoaA	**1.54**
lmo1912	343	**dgcB**	GGDEF domain protein, DGC	**1.55**
lmo2758		**guaB**	Inosine-5'-monophosphate dehydrogenase	**1.58**
lmo1903			bacteriocin transport accessory protein	**1.59**
lmo2667	477		PTS system, galactitol-specific IIA component	**1.60**
lmo0715	112	**fliH**	Flagellar assembly protein FliH	**1.60**
lmo1911	343	**dgcA**	GGDEF domain protein, DGC	**1.62**
lmo0934	144	yhbA	Epoxyqueuosine (oQ) reductase QueG	**1.62**
lmo0710	112	**flgB**	Flagellar basal-body rod protein FlgB	**1.67**
lmo1913	343	ydaJ	Lmo1913 protein	**1.69**
lmo2575	462	czcD	Cobalt-zinc-cadmium resistance protein CzcD	**1.72**
lmo1045	168		Molybdenum cofactor biosynthesis protein MoaD	**1.74**
lmo0585			extracellular protein	**1.76**
lmo2586	465	yrhE	Formate dehydrogenase related protein	**1.77**
lmo0718	112		FIG00774152: hypothetical protein	**1.79**
lmo0716	112	**fliI**	Flagellum-specific ATP synthase FliI	**1.81**
lmo0901		gmuC	PTS system, cellobiose-specific IIC component	**1.84**
lmo1034	166	glpK	Unknown pentose kinase TM0952	**1.89**
lmo1336		yqgN	5-formyltetrahydrofolate cyclo-ligase	**2.37**
lmo0755	119	ypmR	FIG006988: Lipase/Acylhydrolase with GDSL-like motif	**2.44**
lmo0324			FIG00774236: hypothetical protein	**2.75**
lmo0699	112	**fliM**	Flagellar motor switch protein FliM	**2.77**
lmo0349	58		FIG00774379: hypothetical protein	**3.60**
lmo0685	111	motA	Flagellar motor rotation protein MotA	**4.44**

RAST= Rapid Annotation using Subsystem Technology (database), grey names=homologs of *B. subtilis* 169 (ListiWiki), gene names in underlined = significant (p<0,01) but below 2-fold regulated in wt/P_{rli31}*, [1] = significant and 40.34-fold downregulated in Δ*rli31*/wt

Only four genes, besides *lmo0559* showed a slight downregulation in the Δ*rli31* strain compared to the P_{rli31}* suppressor mutant. Three hypothetical proteins of unknown function and *lmo0540* encoding the peptidoglycan carboxylase PbpX, that has been shown to be *rli31* regulated by an unknown mechanism (Burke *et al.*, 2014). The upregulated genes were fascinatingly mainly associated with motility, like *fliM*, *fliI*, *motA*, *flgB*, *fliH*, *cheV* and interestingly the gene encoding the MogR anti-repressor GmaR (*lmo0688*) that is necessary for expression of flagellar genes at temperatures below the physiological 37°C (Gueriri *et al.*, 2008; Gründling *et al.*, 2004). Besides the motility genes, the genes *lmo0755* (encoding a putative phospholipase) and *lmo2575* (encoding a putative cation exporter) could be of interest in the lysozyme phenotype by their putative actions on the cell envelope and ion transport (and therefore osmoregulatory effects). Interestingly with *lmo1911* and *lmo1912* two genes are upregulated that encode the c-di-GMP diguanylate cyclases DgcA and DgcB, which might indicate an involvement of c-di-GMP signaling (Chen *et al.*, 2014). Finally, the genes *lmo1336* that encodes a protein involved in tetrahydrofolate metabolism, in which cobalamin plays a role were upregulated, as well. In suppressor mutant 2-I a silent mutation in *lmo1199* was found, encoding CbiH that is involved in cobalamin biosynthesis and as seen in **Tab. S6.1** the *lmo1148* gene, encoding the cobalamin synthase might be differently expressed, in dependency of *rli31*, suggesting a possible regulatory context between them. We also analyzed possible changes of *rli31* on the protein expression, but unfortunately no statistically significant differences could be measured. We nevertheless included the results in the supplementary **Tab. S6.1** and annotated for the genes *lmo0540*, encoding PbpX and *lmo0559*, which lies downstream of *ri31* that in all P*rli31** samples peptides were found but no peptides were found in the *rli31* mutant, suggesting strong downregulation in this strain. Interestingly, as seen in **Tab. S6.1**, we also detect, even though not significant a nearly 2-fold change in *lmo0415* expression, which encodes the second known target of *rli31* (Burke *et al.*, 2014).

rli31 *affects motility in* L. monocytogenes *EGD-e* – To assess whether the potential changes in gene expression also lead to phenotypes, we assessed the influence of *rli31* on the motility of *L. monocytogenes*. As expected, no motility was observed at 37°C due to the temperature-dependent repression of motility and also the *fliI* mutant showed no motility at 25°C (Gueriri *et al.*, 2008; Gründling *et al.*, 2004; Halbedel *et al.*, 2012; **see Fig. 6.4**). The *rli31* deletion mutant showed a similar migration as the wild type and only the P_{rli31}* mutant showed a slight decrease in motility.

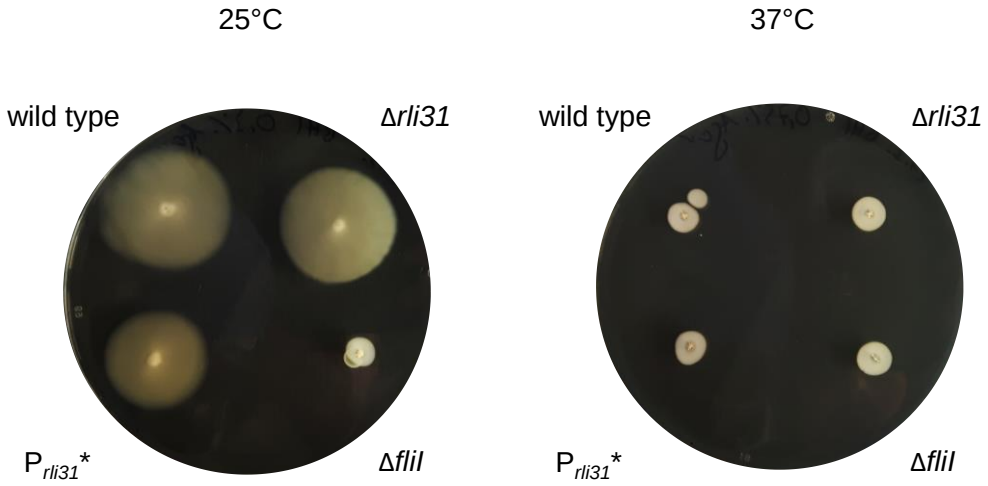

Fig. 6.4 *rli31* affects motility of *L. monocytogenes*. The wild type strain, the mutants Δ*rli31*, the suppressor mutant 4-I (P_{rli31}*) and a *fliI*::*mgfp* mutant were investigated for their ability to spread on BHI agar plates. Bacteria were grown in BHI medium and 1 µl of cells with an OD_{600} of 1 were stab inoculated in BHI plates containing 0.3% (*w/v*) agar. Plates were incubated at 25°C and 37°C for 3 days.

Discussion

In the present study, we demonstrated that *L. monocytogenes* EGD-e rapidly adapts lysozyme resistance by acquisition of mutations in the promoter of the sRNA *rli31* (**Fig. 6.1** & **Fig. 6.2**). Interestingly, in a study by Burke and colleagues they found *rli31* as a regulator of lysozyme resistance the other way around. They screened for the 10403S wild type using a transposon library for lysozyme sensitive mutants and identified *rli31*, *pgdA*, *pbpX*, *degU*, *walI*, *dltB*, *dltD*, the *vir* operon, *prsA2*, *lmo2473* and *lmo2768* as insertion loci that lead to lysozyme sensitivity (Burke *et al.*, 2014). Of these only *rli31*, *pgdA*, *pbpX* and *degU* showed lysozyme sensitivity, but no sensitivity against, cationic antimicrobial peptides or cell wall-acting antibiotics, suggesting that those four are involved in a lysozyme specific phenotype. Of those we only see an effect of *rli31* on expression of *pgdA* and *pbpX*, confirming the findings of Burke and colleagues that *rli31* affects their expression, even though no direct interaction of *rli31* was observed (Burke *et al.*, 2014; **Tab. S6.1**). So far, only the known binding targets of *rli31* are the protein and mRNA of SpoVG *in vitro*, which they could show to be a global RNA-binding posttranscriptional regulator (Burke *et al.*,2016). Interestingly, deletion of *spoVG* rescued the lysozyme sensitivity and also the *in vivo* virulence attenuation of the *rli31*mutant and a *spoVG* mutant was non-motile. Remarkably, RNase J1 mutants arose, which could restore swarming motility. These observations lead to the interesting hypothesis that *rli31* is indeed involved in regulation of motility. (i) A *degU* mutant affects lysozyme resistance and DegU is important for regulation of motility gene expression (Burke *et al.*, 2014; Dons *et al.*, 1992; Gueriri *et al.*, 2008; Mauder *et al.*, 2008; Peel *et al.*, 1988). (ii) *rli31* binds the *spoVG* mRNA and the SpoVG protein *in vitro* and a deletion of *spoVG* leads to motility defects that require suppressor mutations in an RNA degrading enzyme (RNase J1) to regain swarming motility (Burke *et al.*, 2016). (iii) Motility genes are differently expressed in a *rli31* mutant, compared to an evolved P_{rli31}* lysozyme resistant suppressor (**Tab. S6.1**). (iv) the P_{rli31}* mutant shows decreased swarming motility (**Fig. 6.4**). It is unknown how *rli31* might influence motility gene expression, but the transcriptomic data suggests a few possibilities. On the one hand, expression of c-di-GMP synthesizing enzymes seems to be altered. In *E. coli*, c-di-GMP is a major regulator of motility, while in *B. subtilis* no effect of c-di-GMP has been shown, but motility is instead regulated by the interaction of the proteins SlrR and SinI with SinR and motility genes are upregulated in a high c-di-AMP *gdpP* PDE mutant (Gundlach *et al.*, 2016; Mukherjee & Kearns; Vlamakis *et al.*, 2013). The role of c-di-GMP in *L. monocytogenes* is not well studied, but increased levels lead to higher synthesis of an exopolysaccharide that inhibits motility, suggesting that the situations in *B. subtilis* and *L. monocytogenes* are different (Chen *et al.*, 2014; Gao *et al.*, 2013; Köseoğlu *et al.*, 2015). Increased levels of c-di-GMP may also influence gene expression of motility genes or of genes required for lysozyme resistance, but this has yet to be elucidated. The role of c-di-AMP in motility of *B. subtilis* and *L. monocytogenes* is another interesting aspect. While high c-di-AMP concentrations seem to increase expression of motility genes in *B. subtilis*, low c-di-AMP levels seem to lead to the same phenotype in *L. monocytogenes*, suggesting fundamental differences in regulation of motility gene expression (Gundlach *et al.*, 2016; **chapter 4**). In *B. subtilis* motility is mainly regulated by interaction of SinI or SlrR with SinR that integrates environmental signals and regulate expression of biofilm and motility genes in a mutual exclusive order. *B. subtilis* has furthermore the DegSU two component system (Mukherjee & Kearns; Vlamakis *et al.*, 2013). In contrast to this, *L. monocytogenes* motility is mainly regulated by the ambient temperature. At physiological temperatures, motility is repressed by MogR, whose mRNA is at the same time an antisense RNA to *fliINQ* mRNA. If the temperature sinks to 30°C and below, the thermosensor protein GmaR, which as a moonlighting enzyme, also modifies the flagellin, becomes stable and less prone to degradation, due to conformational changes and binds MogR. Binding prevents GmaR degradation and allows

transcription of the motility genes by DegU. DegU is an orphan response regulator, without sensory histidine kinase, in *L. monocytogenes* and regulation of it is still not fully known. An increase in temperature eventually leads to dissociation of the MogR-GmaR complex, degradation of GmaR and inhibition of motility gene expression, because with MogR present, the effect of DegU is not strong enough (Dons *et al.*, 1992; Gueriri *et al.*, 2008; Kamp & Higgins, 2008; Kamp & Higgins, 2011; Mauder *et al.*, 2008; Peel *et al.*, 1988; Shen *et al.*, 2006). Interestingly, expression of *gmaR* is 1.5-fold up-regulated in the Δ*rli31* mutant compared to P_{rli31}* (**Tab. S6.1**). This indicated *gmaR* repression in a *rli31*-dependent manner, which would lead to a decrease in motility gene expression in *L. monocytogenes* with an increased expression of *rli31* and therefore lysozyme resistance (**Fig. 6.4**). It has to be noted that these data were gathered at 37°C when *gmaR* expression is usually repressed. It will be interesting to see the effect of *rli31* at lower temperatures and to see if *gmaR* expression is even more elevated. In the context of the pathogenic lifestyle of *L. monocytogenes*, the downregulation of motility genes upon contact with lysozyme and probable overexpression of *rli31* as a consequence would make sense, since flagellin is a potent trigger of the innate immune system (Ragland *et al.*, 2017). As described in **chapter 4**, c-di-AMP affects motility gene expression, as well. The common grounds of lysozyme resistance of *cdaR*, *pdeA* and P_{rli31} mutants and altered motility in a c-di-AMP and *rli31* dependent matter, led us to reinvestigate the differences in gene expression that have been described previously (**chapter 4**). Surprisingly, we found overexpression of *lmo0559* and *lmo0560*, the two genes directly downstream of *rli31* (**see Fig. 6.5**)

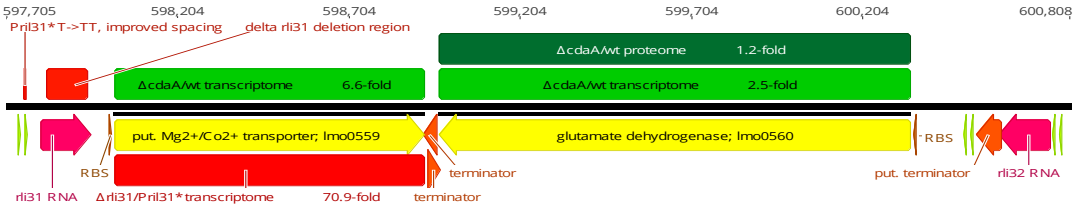

Fig. 6.5 c-di-AMP signaling and *rli31*. Depicted is the locus of the sRNA *rli31*. It lies upstream of the *lmo0559* gene encoding a putative magnesium or cobalt transporter. Downstream of *lmo0559* lies the reverse orientated *lmo0560* gene encoding the glutamate dehydrogenase of *L. monocytogenes*, followed by the sRNA *rli32*. The sites of mutation in P_{rli31}* and the deletion region in Δ*rli31* are depicted, as well as transcriptional changes in gene expression of Δ*rli31 vs.* the P_{rli31}* (*lmo0559*,70.9-fold downregulated). Furthermore, changes in gene expression of Δ*cdaA vs.* the wild type (see **chapter 4**; light green, *lmo0559* 6.6- and *lmo0560* 2.5-fold upregulated) and protein abundancy (dark green 1.2-fold higher abundancy of Lmo0560) are shown. -10/-35 = promoter regions, RBS = ribosomal binding site, *vs.* = *versus*.

While expression of *lmo0560*, encoding the glutamate dehydrogenase of *L. monocytogenes*, may be independent of *rli31*, it may be influenced by *rli32* that lies in front of the gene (although both have their own promoters and terminators). Most interesting is that *lmo0559* is upregulated in a *cdaA* deletion mutant. As described in the results part, expression of *lmo0559* probably depends on *rli31* expression, due to the lack of an own transcriptional start site. Nucleotides smaller than 200 nt were not included in the performed RNA sequencing, meaning the 144 nt sRNA could not be detected. Assuming that *rli31* is upregulated in a *cdaA* mutant, it should negatively affect *gmaR* expression and thereby inhibit motility, suggesting that either an unknown factor is at play or that c-di-AMP and *rli31* lead to similar phenotypes utilizing different pathways. A tempting hypothesis is that c-di-AMP can modulate *rli31* binding to its targets in addition of regulating its expression, there is however no experimental evidence supporting this hypothesis, at the moment. Nevertheless, an interesting connection and possible cross-regulation of sRNA regulation and c-di-AMP signaling that is worth further analysis in the future. We therefore propose the following model for

a possible regulation of motility and cell wall remodeling genes by *rli31*, which is depicted in **Fig. 6.6**.

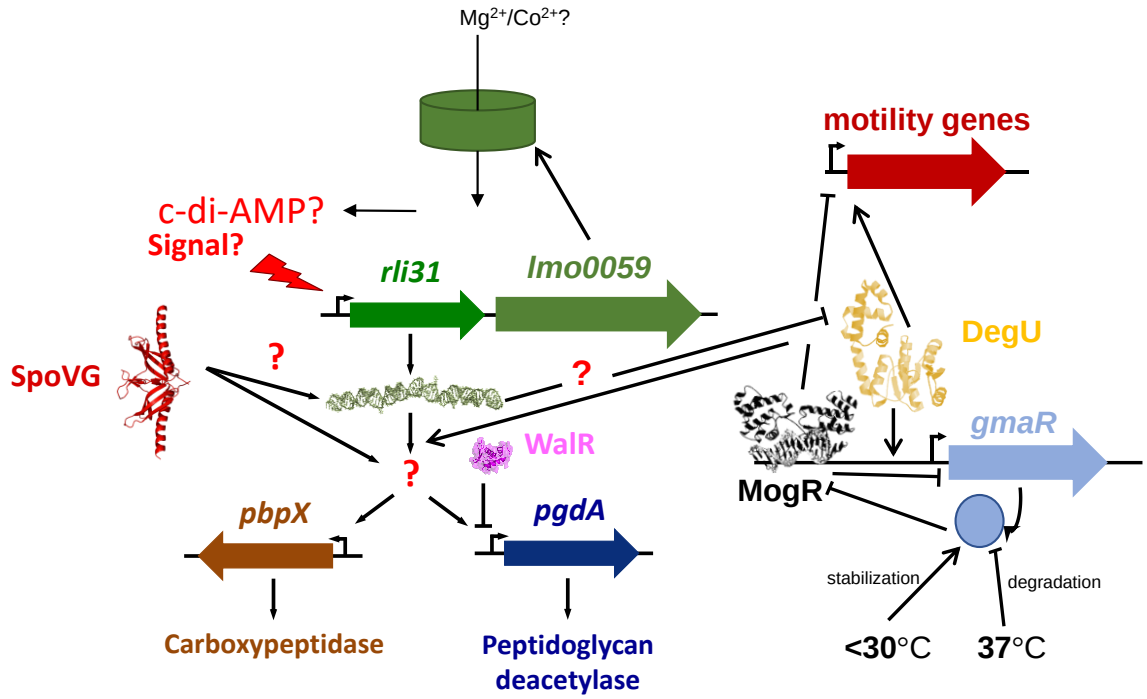

Fig. 6.6 Model depicting the role of *rli31* in peptidoglycan remodeling. The sRNA *rli31* has been shown to affect the expression of the carboxypeptidase PbpX and the peptidoglycan deacetylase PgdA that is also regulated by the WalR response regulator. The RNA chaperon SpoVG has further been identified as interacting with the sRNA with unknown outcome. So far, neither the signal, nor the direct target are known. Our findings have shown that *rli31* is furthermore involved in regulation of motility genes and also the expression of the downstream of *rli31* located gene, *lmo0059*, encoding a putative magnesium or cobalt ion transporter may be influenced by *rli31* expression. Interestingly, *rli31*, leads to higher expression of *gmaR* that encoded the anti-repressor of MogR that might lead to altered expression of motility genes. DegU, which is also involved in *gmaR* expression and in lysozyme resistance may be the most promising target for *rli31*. It is also possible that c-di-AMP or a c-di-AMP-derived signal affects expression of *rli31*, as the downstream gene *lmo0559*, which shares the TSS with *rli31* is overexpressed in a *cdaA* mutant.

c-di-AMP or a c-di-AMP-derived signal that indicates cell wall or osmotic stress leads to upregulation of *rli31-lmo0559* expression. Putative increased import of magnesium or cobalt ions could influence either DAC activity, as divalent ions are cofactors for c-di-AMP synthesis, with cobalt for *L. monocytogenes* DAC *in vitro* (Rosenberg *et al.*, 2015). Or act as osmolytes and thereby alter DAC activity (**see chapter 2**). Increased expression leads to modulation of DegU in a way that it no longer stimulates *gmaR* and motility gene expression, but switches to expression of PG remodeling enzymes. Interestingly, Burke *et al.*, found no impact of *rli31* on expression or translation of *degU* and *vice versa*, they did however not investigate RNA-protein interaction, because *rli31* deletion or overexpression did not have a motility phenotype in the used 10403s wt strain (Burke *et al.*, 2014). Fascinatingly, in the EGD-e wt strain only the P_{rli31}* had a slight influence on motility (**Fig. 6.4**), suggesting a difference between 10403S and EGD-e in regulation of motility and indeed it has been shown that MogR of 10403S does not complement the more stringent temperature phenotype of EGD-e MogR, highlighting possible differences in regulation of motility gene expression in the more pathogenic 10403S and the more attenuated EGD-e strain (Glaser *et al.*, 2001; Gründling *et al.*, 2004). Another explanation is that over expression of *rli31* only lacks a phenotype in 10403S, because it already has a stronger promoter (**Fig. 6.1, B**) and further overexpression of *rli31* may not increase its effect on motility, but only on lysozyme resistance, if the first one is only a side effect by increased recruitment of DegU to the genes *pgdA* and *pbpX* (direct regulation by

DegU has not been investigated yet and is therefore hypothetical). *rli31* may, therefore, act as a modulator of the orphan response regulator DegU, controlling its targets and this in cross-talk with the c-di-AMP signaling network as a possible signal input for cell envelope stress.

Acknowledgements

This work was supported by the grant CO 1139/2-1 from the Deutsche Forschungsgemeinschaft *via* the Priority Program SPP1879, the Fonds der Chemischen Industrie and the Max-Buchner-Forschungsstiftung (MBFSt-Kennziffer 3381) to FMC.

7. Discussion

Regulation of diadenylate cyclase activity

In this study the synthesis of the nucleotide second messenger cyclic di-AMP (c-di-AMP), its function on regulating potassium homeostasis in *Listeria monocytogenes* and its global effect on gene expression are investigated.

c-di-AMP is synthesized by enzymes containing a diadenylate cyclase (DAC) domain and in the recent years it has become increasingly implicated in regulation of osmotic homeostasis in several bacteria (Devaux *et al.*, 2018; Gundlach *et al.*, 2017; Pham *et al.*, 2018; Whiteley *et al.*, 2015; Whiteley *et al.*, 2017; Zeden *et al.*, 2018). In the time before discovering that both, essentiality and major function of c-di-AMP are related to osmotic homeostasis, the regulation of cell wall homeostasis was the most prominent hypothesis for the main function of c-di-AMP signaling (Commichau *et al.*, 2015; Corrigan *et al.*, 2011; Dengler *et al.*, 2013; Luo & Helmann, 2012; Rismondo *et al.*, 2016; Witte *et al.*, 2013). Regulation of cell wall homeostasis may not be the main function or reason of its essentiality and many cell wall-related phenotypes might be secondary effects, as a result of an altered osmoregulation (Commichau *et al.*, 2018). Nevertheless, osmotic homeostasis and cell wall remodeling need to be adjusted to each other accordingly; cross-talk between them is therefore likely. The most interesting aspect about it, is the regulation of CdaA by the phosphoglucosamine mutase GlmM.

GlmM has been found to interact with the DAC CdaA in *Bacillus subtilis*, *Lactococcus lactis*, *Staphylococcus aureus* and we could confirm the interaction for *L. monocytogenes* (Gundlach *et al.*, 2015b; Tosi *et al.*, 2019; Zhu *et al.*, 2016; **chapter 2**). In all these organisms GlmM and CdaA show a physical interaction. To investigate the effect of GlmM on CdaA *in vivo* without impact of CdaR or the PDEs, CdaA and GlmM were co-expressed with the c-di-AMP regulated KimA potassium transporter. A potassium transporter deficient strain was grown with specific potassium concentrations and expressed the KimA transporter from *L. monocytogenes* was expressed (**see chapter 3**). Growth of *Escherichia coli* in this screening system is dependent on the uptake of potassium, which can be inhibited by c-di-AMP if a DAC is expressed. We could demonstrate that co-expression of GlmM and CdaA impact c-di-AMP synthesis if expressed in *E. coli*. GlmM is able to inhibit CdaA, as seen by the improved growth rate (**Fig. 2.7**), which has been also shown for *L. lactis* and *S. aureus*. In *L. lactis*, GlmM can inhibit CdaA and a suppressor mutation in the c-di-AMP elevated *gdpP* mutant that restored osmotic resistance were identified to be loss- and gain-of function mutations in *cdaA* and *gdpP*, respectively. In one case an amino acid exchange in the essential GlmM enzyme (I154F) appeared. This mutation had two effects, a decrease in cellular c-di-AMP concentration and at the same time a reduction in the PG precursor UDP-N-acetylglucosamine (UDP-NAG). UDP-NAG levels were higher in the *gdpP* mutant, demonstrating that UDP-NAG concentrations seem to be impact by the c-di-AMP concentration. The authors furthermore could show that the I154F GlmM mutant lead to a stronger inhibition of CdaA, directly linking enzymatic activity for cell wall precursor synthesis and osmoregulation by c-di-AMP synthesis (Zhu *et al.*, 2016). Interestingly, the 154F mutation is a natural variant in the GlmM homologs of *B. subtilis*, *L. monocytogenes* and *S. aureus*, indicating a naturally stronger GlmM-dependent inhibition of CdaA activity in these bacteria. The second study in *S. aureus* demonstrated three very interesting details about CdaA regulation: (i) Tosi and colleagues could show that CdaA and GlmM both form dimers, interact with each other and that multi-homodimers of CdaA need to interact for enzymatic function. (ii) They furthermore demonstrated that GlmM interaction with CdaA disturbs this

multimerization and thereby inhibits c-di-AMP synthesis. (iii) the effect of GlmM seems to be stronger than the effect of CdaR on CdaA activity in *S. aureus*, compared to *L. monocytogenes* (**chapter 2**; Tosi *et al.*, 2019). There are however a few questions that remained unanswered and should be addressed in future studies. Co-localization of GlmM and CdaA *in vivo*, effect on GlmM activity on CdaA activity and investigation of GlmM from other organisms that do not possess c-di-AMP have the same effects. In *L. monocytogenes* CdaR seems to be able to decrease c-di-AMP concentrations to a level where KimA activity is no longer impaired, while GlmM only achieves an intermediate effect, although the strongest effect is seen when CdaR and GlmM are present (**Fig. 2.7**). The most likely reason for this difference may be an evolutionary adaption of c-di-AMP regulation that differs in coccoid bacteria, such as *S. aureus*, *Streptococcus pneumoniae* or *L. lactis* from rod-shaped bacteria, such as *B. subtilis* or *L. monocytogenes*. In both bacteria, CdaR consists of an amino-terminal transmembrane (TM) domain and four YbbR domains of unknown function. In contrast to that, the coccoid bacteria have CdaR variants with only three or two YbbR domains or mutated pseudogenes, like in *L. lactis* (Rismondo *et al.*, 2016; Zhu *et al.*, 2016). This hints at a divergent evolution between rod-shaped and coccoid bacteria for the regulation of CdaA activity. Intriguingly the role of CdaR itself in regulating CdaA activity might be the key to explain this difference. While GlmM seems to play a role in regulation of DAC activity of CdaA, there are still open questions about this regulatory process. In *B. subtilis*, both GlmM and CdaA are expressed equally and constitutively, which indicates that another factor, like enzymatic activity of GlmM has to influence the inhibition of CdaA by GlmM. It is also unclear, if enzymatic activity or other factors influence co-localization and interaction of GlmM with CdaA *in vivo* and needs to be investigated in future studies.

Regulation of CdaA by CdaR

CdaR has been shown to effect CdaA activity in *B. subtilis*, *L. monocytogenes* and to lesser extend also in *S. aureus* (Mehne *et al.*, 2013; Rismondo *et al.*, 2016; Tosi *et al.*, 2019). CdaR, called YbbR in *S. aureus*, has also been linked to an increased acid susceptibility in this bacterium. In the study by Bowman and colleagues, a *cdaR* mutant did not show significantly increased c-di-AMP concentrations under the used conditions, but an increased acid sensitivity and accumulated suppressor mutations that circumvented this phenotype (Bowman *et al.*, 2016). Mutations occurred, among others, in genes encoding for a putative proline/betaine transporter or the gene encoding for the DAC CdaA (DacA in *S. aureus*). Interestingly, growth assays showed, that the *cdaR* mutant phenocopied the growth defect of a low c-di-AMP *cdaA* (G206S) mutant under acidic conditions, indicating that under acidic stress a *cdaR* mutant might show lower c-di-AMP concentrations than the wild type. Surprisingly, although c-di-AMP concentrations did increase with acidic stress, they increased even further in the *cdaR* mutant and even more so in the suppressor mutants. This increase, however, was observed also at neutral pH, although more prominent for the suppressor strains than the *cdaR* mutant alone (Bowman *et al.*, 2016). In *L. monocytogenes* on the other hand, a *cdaR* mutant showed about 40% elevated c-di-AMP concentration under growth in complex medium and a 10% decrease if CdaR was overexpressed, indicating inhibition of CdaR under the used conditions. Surprisingly, a *cdaR* mutant did not show an altered resistance towards cell wall-acting antibiotics but an increase resistance towards lysozyme (Rismondo *et al.*, 2016). Fascinatingly, in a study by Wichgers Schreur and colleagues, lysozyme resistant mutants were found to have a mutation in the CdaA homolog of *Streptococcus suis* (Wichgers Schreur *et al.*, 2012). We pursued this interesting link between c-di-AMP metabolism and cell wall biosynthesis by evolving *L. monocytogenes* to become more lysozyme resistance (**chapter 6**). Interestingly, all suppressor mutants

evolved mutations in the promoter region of a small RNA (*rli31*) that is known to effect PG remodeling by regulating abundance of the PG deacetylase PgdA and the putative carboxypeptidase PbpX by a still to be elucidated mechanism (Burke *et al.*, 2014; Burke & Portnoy, 2016). The cell wall-related phenotypes of c-di-AMP metabolic mutants might, however, be at least in part indirect effects, due to an altered osmoregulation (Commichau *et al.*, 2018). We could show that CdaR on the one hand is indeed a membrane localized protein and that the YbbR domains are located outside of the cell (**Fig. 2.2** & **Fig. 2.3**). This eliminates the hypothesis that the YbbR domains may interact with the DAC domain directly, as some unusual DAC-YbbR domain hybrid enzymes, like CdaZ of the methanogenic archaeon *Methanocaldococcus jannaschii* might indicate and is in good accordance with a BACTH study, showing self-interaction of the DAC domain of CdaA and the YbbR domains of CdaR, but only interaction of CdaA and CdaR in their full-length, TM domain containing, variants (Commichau *et al.*, 2019; Kellenberger *et al.*, 2015; Rismondo *et al.*, 2016). We could, furthermore, directly link CdaR to metabolic activity and normal growth of *L. monocytogenes* under osmotic stress conditions, demonstrating its putative role as a sensor for changes in osmolarity for regulating CdaA activity (**Fig. 2.1**). After identifying the role of CdaR on osmoregulation, we set out to elucidate how the protein might act as an osmolarity sensor. There have been three main hypotheses: (i) CdaR might sense cell wall alterations and convey the signal input on CdaA. (ii) CdaR might act as a proper localizer for CdaA, facilitating self-interaction and/or interaction with other proteins. (iii) CdaR might act as a signal amplifier for cell envelope stress and influence proper interaction and localization of CdaA with itself and/or other proteins.

The basis of these models is derived from known mechanisms of cell-wall interacting signal transduction protein, like PrkA, combined with our current knowledge of CdaR and osmotic regulation in general. To further elucidate: (i) CdaR might sense the constitution of the cell wall. Similar functions are known from PrkA-like proteins (PrkC in *B. subtilis*). PrkA is a TM protein with an intracellular kinase domain and three C-terminal and extracellular PASTA domains (for Penicillin binding proteins and serine/threonine kinase associated; Manuse *et al.*, 2016). Those domains have been shown to bind peptidoglycan (PG) and possible detect specific changes in PG composition and in turn alter activity of the intracellular kinase domain. Increased phosphorylation of its targets WalR, CpgA, YvcK and GpsB leads to increased expression of the *walR* regulon and alters activity of YvcK, CpgA and GpsB, respectively, eventually leading to an altered cell wall architecture and metabolism. One has to note though that the function of and the signals that are perceived by PASTA domain containing kinases in various organisms are not fully understood and might have evolved differently in different bacteria (Manuse *et al.*, 2016). This might be also true for CdaR. The above-mentioned differences in YbbR domain repeats between different bacteria might suggest as much. In addition, structural analysis has shown that YbbR domains share a common fold, while having a rather un-conserved amino acid similarity (Barb *et al.*, 2010). This might hint at a general role of them as PG interacting, or self-interacting proteins with distinct differences from species to species and would be an interesting subject for further studies. This led to the hypothesis that CdaR might act as a membrane anchor or localizer for CdaA (ii). In this model, the YbbR domains would determine the location of CdaA, *via* protein-protein interaction with the TM domains. The YbbR domains could determine the localization of the complex, e.g. at the septum to facilitate interactions with other proteins, leading to clustering of functional complexes. Interaction of CdaA, but especially CdaR in a two-hybrid assay (**Fig. 2.6**) would be in favor of this model. There is however the question how alteration of the osmolarity would impact CdaA activity in a CdaR-dependent matter. CdaR could either regulate CdaA self-interaction, if the strain in the cell wall is large enough to alter the putative interaction between the YbbR domains and the cell wall (with CdaR acting as an anchor for CdaA and PDEs, stabilizing complex formation and thereby altering activity)

or CdaA and the PDEs might have osmosensing abilities that are at least in part independent of CdaA. This model could be indeed the case, considering that *L. lactis* has no functional *cdaR* gene and that the phenotypes of a *cdaR* mutant in *L. monocytogenes* on osmotic adaption (**Fig. 2.1**) are not as strong as it has been shown for PDE mutants (Huynh *et al.*, 2016; Zhu *et al.*, 2016; **chapter 2**). A possible mechanism for CdaA and the PDEs to at least partially sense osmotic stress on their own is given by the recent proposed model of osmosensing by the PhoQ/PhoP two-component system in *E. coli* (Yuan *et al.*, 2017). It has been shown that the two-component system responds to an osmotic upshift *via* the PhoQ kinase. Kinase mutants lacking the periplasmic sensor domain, which is important for PhoQ to detect other environmental clues, were still responsive to changes in osmolarity. The authors could show, that osmotic activation is dependent on the length of the TM helices and lateral pressure through the membrane. In their proposed model, the lateral pressure leads to conformational changes in the TM domain that in the end alter catalytic activity of the cytosolic kinase domain (Yuan *et al.*, 2017). A similar model could be possible for CdaA, PdeA or PgpH that are all membrane-bound proteins with cytosolic enzymatic domains, with a huge contribution to osmoregulation in Firmicutes. Another possible clue are of course alterations in ion concentrations. Interestingly, *in vitro* a truncated variant of *L. monocytogenes* or *S. aureus* CdaA is most active with cobalt or manganese (cobalt predominantly for *L. monocytogenes* and manganese for *S. aureus* as a cofactor (Rosenberg *et al.*, 2015; Tosi *et al.*, 2019). DACs of the DisA family usually show highest activity with magnesium as a cofactor and CdaA from *S. aureus* also shows some activity with magnesium, rising the questions if the natural cofactor of full-length CdaA variants *in vivo* might be magnesium after all (Tosi *et al.*, 2019; Witte *et al.*, 2008). If cobalt and/or manganese are the natural cofactors for cyclases of the CdaA type, their availability and competition with the intracellular much higher concentrated magnesium ions could contribute to regulation of DAC activity, depending on their different affinities, concentrations and alterations due to osmotic stress (Foster *et al.*, 2014; Groisman *et al.*, 2013). The third model is a combination of the first two. (iii) CdaR might have two different functions. On the one hand CdaR might determine localization and/interaction of CdaA with itself and putatively other components of the c-di-AMP metabolism and on the other hand modulate self-sensing properties by acting as an enlarged interaction surface with the cell wall two magnify signal input. In this model CdaA and PDEs would not be fully dependent on CdaR, but presence of CdaR would facilitate the magnitude of DAC activity and finetune it (**see Fig. 2.8**).

The role of the YbbR domains of the diadenylate cyclase regulator CdaR

To investigate how CdaR might sense changes in osmolarity and convey these signals to CdaA, to modulate its activity, we took a closer look at the function of the YbbR domains and the membrane localization of CdaR *in vivo*. As seen in **Fig. 2.5**, a *cdaR* mutant is still able to adjust its intracellular c-di-AMP concentration, but shows in general a decrease of c-di-AMP compared to the wild type and the range of adaptation seems to be decreased. A mutant expressing CdaR without its TM domain behaves like the *cdaR* deletion mutant. Taken together with the topology assays that showed that the TM domain is both, necessary and sufficient for correct membrane localization of the adjacent C-terminus (**Fig. 2.3**), it can be stated that extracellular localization of the YbbR domains is necessary for proper CdaR-dependent regulation of CdaA activity. This is especially of interest considering the effect of a mutant expressing CdaR without any YbbR domains, meaning only the TM domain. In this mutant we could only measure about a fifth of the c-di-AMP amount compared to the wild type strain. We concluded from this phenotype that expression of the TM domain without the YbbR domains disturbs CdaA dimerization. Considering the before mentioned

three hypotheses that CdaR might (i) sense cell wall alterations, (ii) act as a localizer and anchor for CdaA or (iii) act as a scaffolding protein with cell envelope signal amplifying function, to stabilize CdaA self-interaction, model two or three are in good agreement with the observed phenotypes. If CdaR would sense alterations in cell wall composition, the effect of CdaR should be slight conformational rearrangements of CdaR and in consequence of CdaA and thereby specific changes in activity upon YbbR domain interaction with an altered cell wall. A mutant without the sensory YbbR domains should therefore behave like the wild type, except when a signal is perceived. In contrast to that, expression of YbbR-less CdaR impacts CdaA activity per se. In the other two models, where CdaR is important for proper interaction and/or localization of CdaA, the YbbR domains would be a determinant for self-interaction. It has been shown that the YbbR domains are able to self-interact in the cytosol, if the TM domains are truncated and, furthermore, that CdaA self-interacts, although weaker in the full-length variant compared to mutants lacking TM domains. Moreover, CdaA and CdaR only interact with each other as full-length proteins, presumably *via* their TM domains (Rismondo *et al.*, 2016). Hence, it can be hypothesized that CdaA and CdaR self-interactions might be influenced by their membrane localization in a negative way. Considering this, expression of CdaR TM domain that interacts with the TM domains of CdaA could destabilize CdaA self-interaction, if not stabilized by YbbR domain interaction. The phenotype of the YbbR-less CdaR expressing *L. monocytogenes* strain is in support of this hypothesis (**Fig. 2.5**). Interestingly, a complementation strain shows the opposite phenotype of the *cdaR* deletion mutant. Higher c-di-AMP concentrations and a greater change upon osmotic change can be detected, which is in agreement with the proposed model (**see Fig. 2.8**).

When we compared our experimental findings to what is known about the impact of CdaR on the cellular c-di-AMP concentration in *L. monocytogenes*, we noticed two interesting differences. On the one hand, effects of *cdaR* deletion and complementation lead to decreased and increased c-di-AMP level, respectively, which is diametrically opposed to what is known from previous experiments and on the other hand c-di-AMP concentrations were in general lower than previously observed (Rismondo *et al.*, 2016). The experimental procedures of these two experiments were distinct by two factors that may be the root for the differences. In Rismondo *et al.*, the bacteria were cultivated in BHI, a very nutrient rich complex medium and c-di-AMP concentrations were measured at an OD_{600} of 1, the late exponential growth phase (the c-di-AMP concentration in the wild type, which was set to 100% was 99.4 ± 13.4 ng c-di-AMP per mg of protein; Gibhardt, 2015; Rismondo *et al.*, 2016). In contrast to this set up, we determined c-di-AMP concentrations in LSM, a defined medium and at an OD_{600} at the early- and mid-exponential phase. It is not known, how c-di-AMP concentration may change upon osmotic stress in dependency of the growth phase, but it is known from c-di-AMP and also other second messenger molecules, c-di-GMP that plays a role in *E. coli* lifestyle changes from exponential to the stationary growth phase that the growth phase is a determinant for nucleotide second messenger concentrations (Hengge *et al.*, 2015). Similar as for c-di-AMP, the main determinants for the intracellular c-di-GMP concentration are synthesis and degradation by specialized cyclases and PDEs. Interestingly, expression of the PDE PdeH is inhibited and expression of the diguanylate cyclase DgcE increased during the entry into the stationary phase of *E. coli* and together with other factors the increase in c-di-GMP inhibits motility and facilitates adhesion and matrix production of *E. coli* in the stationary phase (Hengge *et al.*, 2015; Pesavento *et al.*, 2008). For c-di-AMP, there are studies that demonstrate a cross-talk with the (p)ppGpp regulated stringent response, leading to altered concentrations of c-di-AMP, while the (p)ppGpp concentration depends on the growth phase and nutrient availability (Corrigan *et al.*, 2015). Corrigan and colleagues could show for *S. aureus* that c-di-AMP levels are indeed rising in late growth phases and that gene expression patterns of cells with a high c-di-AMP

concentration overlap in parts with those of cells undergoing the stringent response. They furthermore could show that high c-di-AMP levels activate the RelA enzyme, leading to an increase in (p)ppGpp by an indirect and unknown mechanism (Corrigan *et al.*, 2015). Interestingly, other studies have also demonstrated inhibition of c-di-AMP PDEs by (p)ppGpp, indicating a tight cross-regulation of those two nucleotide second messenger pathways that might play a role in osmoregulation and will be discussed further below (Corrigan *et al.*, 2015; Huynh *et al.*, 2015; Rao *et al.*, 2010; Whiteley *et al.*, 2015). To conclude, c-di-AMP levels in *L. monocytogenes* in the early exponential phase might, like in *S. aureus*, may be lower compared to later growth phases. Fascinatingly, cellular turgor is, through the accumulation of intracellular osmolytes, which is favored by lower c-di-AMP concentrations, a determinant for cell division in Gram-positive bacteria. In the exponential phase osmolyte import in general has to be controlled tighter, to prevent an excessive increase in turgor that might be detrimental and therefore favors higher c-di-AMP levels (Rojas *et al.*, 2018). The second big difference in the experimental set ups was the medium composition. In a complex medium like BHI, in which a multitude of ionic and peptide osmolytes are present. In contrast to that, the *Listeria* synthetic medium (LSM) features defined amounts of amino acids, trace elements, vitamins and low amounts of potassium (4.8 mM) and, therefore, compared to a complex medium like BHI or LB a limited, defined amount of low complexity osmotic active substances (Whiteley *et al.*, 2017). The key difference might be the presence of oligopeptides in complex media that act as osmolytes in *L. monocytogenes* and are at least indirectly regulated by the impact of c-di-AMP on the stringent response and thereby expression of oligopeptide permeases (Whiteley *et al.*, 2015; Whiteley *et al.*, 2017). In a minimal medium, lower amounts of c-di-AMP are needed to balance the import of the less abundant osmolytes, like it has been demonstrated for potassium uptake and c-di-AMP levels in *B. subtilis* (Gundlach *et al.*, 2017).

The different media compositions and or growth phase might also have an impact on the role of CdaR as a regulator. We therefore hypothesized that CdaR can act on CdaA as an inhibitor and activator, meaning it can in general modulate the activity of CdaA, in dependency of different stimuli. Nevertheless, additional experiments in *E. coli* provided an alternative hypothesis. Using the before mentioned *E. coli*- and KimA transporter-based c-di-AMP reporter system, we investigated impact of CdaR and CdaR variants on CdaA activity. Interestingly, in *E. coli*, CdaR seems to inhibit CdaA activity if it is membrane localized and at least one YbbR domain is present. In contrast to the findings in *L. monocytogenes*, the mutant lacking all YbbR domains did not show a growth phenotype corresponding to low c-di-AMP, but rather showed an intermediate phenotype, similar to GlmM, meaning it is still able to act in part as an inhibitor on CdaA. This difference of phenotype in *L. monocytogenes* and *E. coli* can be a consequence of the differences between the Gram-positive and Gram-negative cell envelope, since the CdaA-CdaR complex would presumably be located in the inner membrane of *E. coli* and the YbbR domains therefore present in the periplasm. Furthermore, different compositions in the lipid bilayer, composition of PG or interactions with other proteins could influence CdaA activity and the impact of regulator molecules on its activity (Silhavy *et al.*, 2010). Another difference and is the lack of other proteins of the c-di-AMP signaling pathway in *E. coli*. Usually this is an advantage for studying DAC activity and the influence of single regulators on cyclases, but in this case we were wondering if other components of the signaling pathway might have an influence on CdaA activity or the role of CdaR. To elucidate this, we employed a bacterial two hybrid protein-protein interaction assay and indeed found protein-protein interactions between synthesis and degradation machineries (**Fig. 2.6**). It is therefore possible that CdaA and CdaR might be influences by PdeA and PgpH and *vice versa* and this potential cross-talk and the resulting local signaling should be the topic of further studies.

Regulation of other diadenylate cyclases

In contrast to *L. monocytogenes*, *B. subtilis* has two other types of cyclases - DisA and CdaS. CdaS is sporulation specific expressed and only implicated in spore formation and germination with a putative role of its autoregulatory N-terminal helices in regulating its activity (Mehne *et al.*, 2013; Mehne *et al.*, 2014; Zheng *et al.*, 2015).

In light of the recent implications of c-di-AMP being a major regulator of osmotic homeostasis in bacteria, we challenged the so far known model of DisA regulation and investigated the hypothesis that DisA activity might me controlled by changes in osmolarity. Interestingly there are several examples of osmotic stress altering the DNA-binding of proteins. It has been shown that interaction of the RNA polymerase with the DNA is released after condensation of the DNA due to macromolecular crowding during the initial phase of a hyperosmotic shock (Cagliero *et al.*, 2013; Wood, 1999). Another example is the interaction between the transcriptional repressor of the glycine betaine importer encoding *busAA*-*busAB* operon by BusR. BusR interaction with the RNA polymerase-DNA complex is inhibited by increased ionic strength, e.g. increased potassium ion concentration after the first response to a hyperosmotic stress, allowing expression of the glycine betaine transporter for import of compatible solutes as a secondary response (Romeo *et al.*, 2007). Intriguingly, BusR has also been identified as a c-di-AMP binding protein in *S. agalactiae* (Devaux *et al.*, 2018), highlighting an additional layer of regulation.

The second vegetative DAC of *B. subtilis*, DisA, is present in vegetative cells and regulated by its interaction with DNA (Witte *et al.*, 2008). It is the second most abundant DAC and present in many spore-forming Firmicutes and as sole DAC in many Actinobacteria, but interestingly, c-di-AMP is not essential in Actinobacteria, like *Mycobacterium tuberculosis*, containing DisA as a sole cyclase (Yang *et al.*, 2014; Commichau *et al.*, 2015). DisA has been implicated to scan the DNA for damages, like double strand breaks, stall and being inhibited upon contact with such structures (Bejerano-Sagie *et al.*, 2006; Oppenheimer-Shaanan *et al.*, 2011; Witte *et al.*, 2008). Furthermore, its interaction with other proteins involved in DNA repair mechanisms have supported this hypothesis (Gándara *et al.*, 2017; Zhang & He, 2013). There have, however, been observations that contradict the hypothesis of DisA being a major factor in regulation of DNA damage repair. A *B. subtilis* mutant can grow normally if only one c-di-AMP producing enzyme is present without showing instability due to accumulation of mutations, indicating that the nucleotide itself is the determinant for normal cellular growth and not the producing enzyme (Mehne *et al.*, 2013; Gundlach *et al.*, 2017). Closely related bacteria, like *L. monocytogenes* or *S. aureus* harbor only one cyclase of the CdaA-type (Corrigan *et al.*, 2011; Commichau *et al.*, 2015; Rismondo *et al.*, 2016; Rosenberg *et al.*, 2015). Moreover, as afore mentioned, in Actinobacteria that often harbor DisA as the sole DAC, the corresponding gene is not essential (Commichau *et al.*, 2015; Yang *et al.*, 2014). Taken together, this does not exclude a function of DisA in DNA repair, but it suggests that it is not its main regulatory function.

As described in **chapter 5**, interaction of DisA with chromosomal DNA inhibited its activity in a DNA concentration-dependent matter (**Fig. 5.1**). Additionally, an increase in the concentration of ionic osmolytes, such as potassium or sodium, but not the nonionic saccharide sucrose, released the inhibitory effect of DNA on DisA activity (**Fig. 5.2**). We could further demonstrate that a DisA variant with a mutation that decreased DNA-binding (G334E; Witte *et al.*, 2008) is more active than the wild type variant *in vivo*, but not *in vitro* (**Fig. S5.2** & **Fig. 5.3**, respectively). Interestingly, *in vivo* c-di-AMP measurements showed that upon osmotic stress with NaCl the c-di-AMP concentration first decreases and then increases (**Fig. 5.5**). This allows the cell to accumulate osmolytes

as a counter measure and afterwards prevents excessive accumulation. Comparing the G334E mutant with the wild type DisA, there is no difference between time point one (shortly after the hyperosmotic shock) and time point two (when the cells began to resume growth after a stagnation). We presume that the G334E mutant might replenish the c-di-AMP pool faster than the wild type, which seems indeed to be the case if the cells are stressed with KCl (**Fig. 5.5**). Interestingly, c-di-AMP levels seem to stay stable after the osmotic stress and then rise, with the mutants reaching higher concentrations compared to the strain harboring wild type DisA. In the case of potassium as a stressor it makes sense for the cells to not lower the c-di-AMP concentration to prevent excessive accumulation of potassium *via* c-di-AMP regulated potassium transport systems (Gundlach *et al.*, 2017). *B. subtilis* must therefore have developed mechanisms to distinguish if the osmotic stress is caused by ions or other solutes and in case of ions also between the ions. DisA could be a candidate to discriminate between different ions. It has been shown that the affinity of DNA to the most prevalent ions in the cytoplasm is highest for calcium ions, followed by magnesium, potassium and sodium, with the latter two having similar affinities (Korolev *et al.*, 1999). Interestingly the study also described that under physiological concentrations of the different cations they show similar degrees of DNA-binding. This means that potassium ions can outcompete the stronger binding calcium ions due to the higher concentration of potassium ions, opening the opportunity that changes in intracellular ion concentration due to osmotic stress could transiently change the balance of DNA-ion interaction. This might be the reason why we see a difference on DisA-DNA inhibition and ion addition *in vitro*, compared to the *in vivo* measurements. *In vitro* NaCl and KCl addition both release DisA inhibition by DNA, while *in vivo* the influx of the ions would be a major determinant, meaning the rate of influx of the ions in the cytoplasm. Since potassium and not sodium uptake, as an osmolyte, is known to be the first response of bacteria to a hyperosmotic shock, the influx of potassium should *in vivo* have a stronger impact on DNA-binding proteins and is in line with our observations (**Fig. 5.5**). Interestingly, *in vitro* studies of DisA G334E activity showed that it is as strongly inhibited by chromosomal DNA as the wt DisA variant, but release of inhibition is slightly altered, meaning a lower potassium concentration seems to be sufficient to let DisA dissociate from the DNA (Fig.5.4). A reason for this could be that the G334E mutation affects binding to certain DNA structures more than the general binding to DNA and other factors like macromolecular crowding, competition with other DNA-binding proteins might affect the impact of the mutation *in vivo*.

Considering that DisA is not the sole cyclase in *B. subtilis* a system of CdaA sensing turgor changes and DisA sensing changes in macromolecular crowding and DNA-ion effects may have evolved. The CdaA system might be sufficient for bacteria to adapt to osmotic stress, sensing fundamental physical changes that occur independent of the osmotic stressor and the DisA system may have evolved as a fine tuning or special adaptation. Actinobacteria with DisA as a sole DAC might therefore have other, c-di-AMP-independent osmoregulatory systems that detect turgor changes as in Proteobacteria, like *E. coli* (Sleator & Hill, 2002; Wood, 1999).

c-di-AMP-regulated osmotic homeostasis in *Listeria monocytogenes*

Regulation of osmotic homeostasis has been shown to be the major determinant of c-di-AMP essentiality in Firmicutes (Gundlach *et al.*, 2017; Whiteley *et al.*, 2015; Whiteley *et al.*, 2017; Zeden *et al.*, 2018). Uptake of potassium is the first response of bacteria to a hyperosmotic shock, but the set up and characteristics of potassium transport is not well studied in *L. monocytogenes*. As described in **chapter 3**, homologs of the *B. subtilis* low affinity KtrCD transporter and the high

affinity KimA transporter, as well as a homolog to the *S. aureus* two component system KdpDE and the transcriptional controlled KdpABC high affinity transporter were identified. Our main interest in studying the potassium transport processes was the investigation of c-di-AMP-dependent regulation, as it has been shown for *B. subtilis* KtrAB and the development of a c-di-AMP reporter system, suitable for *in vivo* antibiotic screening (Corrigan *et al.*, 2013; Kim *et al.*, 2015). We identified that the homologs of KtrCD and KimA of *L. monocytogenes* are indeed low and high affinity potassium transporters, respectively, with their affinities comparable to previous findings (Gundlach *et al.*, 2017; Holtmann *et al.*, 2003). We also identified KtrC as a novel c-di-AMP binding protein in *L. monocytogenes* and that both KimA and the KtrCD transporter are inhibited by c-di-AMP *in vivo* (**Fig. 3.7** and **Fig. 3.6**, respectively). Interestingly, we also observed a strong phenotype if the potassium transporters were overexpressed in *E. coli*. Overexpression resulted in osmotic swelling of bacteria, highlighting the importance of regulated osmolyte influx (**Fig. 3.5**). This phenotype is in excellent agreement with previous observations that lack of c-di-AMP leads to osmotic swelling and consequently to lysis of the bacteria, while high c-di-AMP levels lead to an aberrant curli morphology that can be explained by a decrease in intracellular osmolytes and subsequent water-loss (Gundlach *et al.*, 2017; Mehne *et al.*, 2014). These osmoregulation related phenotypes highlight the importance of a well-balanced uptake and regulation of osmolytes, where c-di-AMP plays a major role in Firmicutes. As summarized in **Fig. 7.1** and in comparison, to **Fig. 1.3**, the knowledge about osmoregulatory systems and the role of c-di-AMP in *L. monocytogenes* and other bacteria have greatly increased.

c-di-AMP has been identified to regulate various osmolyte transport systems in Firmicutes. It regulates potassium uptake in *B. subtilis*, *S. aureus*, *S. pneumoniae*, *L. lactis* and *L. monocytogenes* (Bai *et al.*, 2014; Corrigan *et al.*, 2015; Gundlach *et al.*, 2017; Pham *et al.*, 2018; Quintana *et al.*, 2019; **chapter 3**). Besides the regulation of potassium homeostasis, c-di-AMP has also been implicated in the regulation of glycine betaine, oligopeptide and carnitine uptake in several different bacteria that as compatible solutes all play an important role in osmotic adaptation (Commichau *et al.*, 2018; Devaux *et al.*, 2018; Huynh *et al.*, 2016; Pham *et al.*, 2018; Schuster *et al.*, 2016; Whiteley *et al.*, 2015; Whiteley *et al.*, 2017).

It can therefore be state that c-di-AMP is the major regulator for osmoregulation in Firmicutes. As a second messenger and “essential poison” c-di-AMP levels need to be tightly adjusted (Gundlach *et al.*, 2015b). Due to its regulation of osmotic homeostasis its synthesis and degradation must react to changes in osmolarity. We could show that both DACs CdaA from *L. monocytogenes* and DisA from *B. subtilis* indeed are regulated by changes in osmolarity (**chapters 2 and 5**, respectively). CdaA might thereby be, in dependency of CdaR, a turgor-reactive DAC, while DisA senses macromolecular crowding and the intracellular ion composition. While CdaA seems to connect osmotic adaptation to cell wall biosynthesis *via* GlmM, DisA might connect osmotic stress to cell cycle arrest and facilitating stress responses like DNA repair mechanisms *via* RadA.

While many aspects still need to be elucidated, the present studies shed new insight in the regulation of c-di-AMP synthesis and might also provide new insight into regulation of degradation and a phenomenon termed local signaling for the second messenger c-di-GMP (Sarenko *et al.*, 2017). Like for c-di-GMP, it can be imagined for c-di-AMP that a certain intracellular concentration is present in dependency of the environmental conditions, with local pools of higher or lower concentrations. Such a local signaling can be achieved by specific co-localization of synthesizing and or degrading enzymes with receptor molecules (DNA, RNA or proteins). It would allow a fine tuning and fast response of membrane transport if diffusion distances for the second messenger would be reduced in this way.

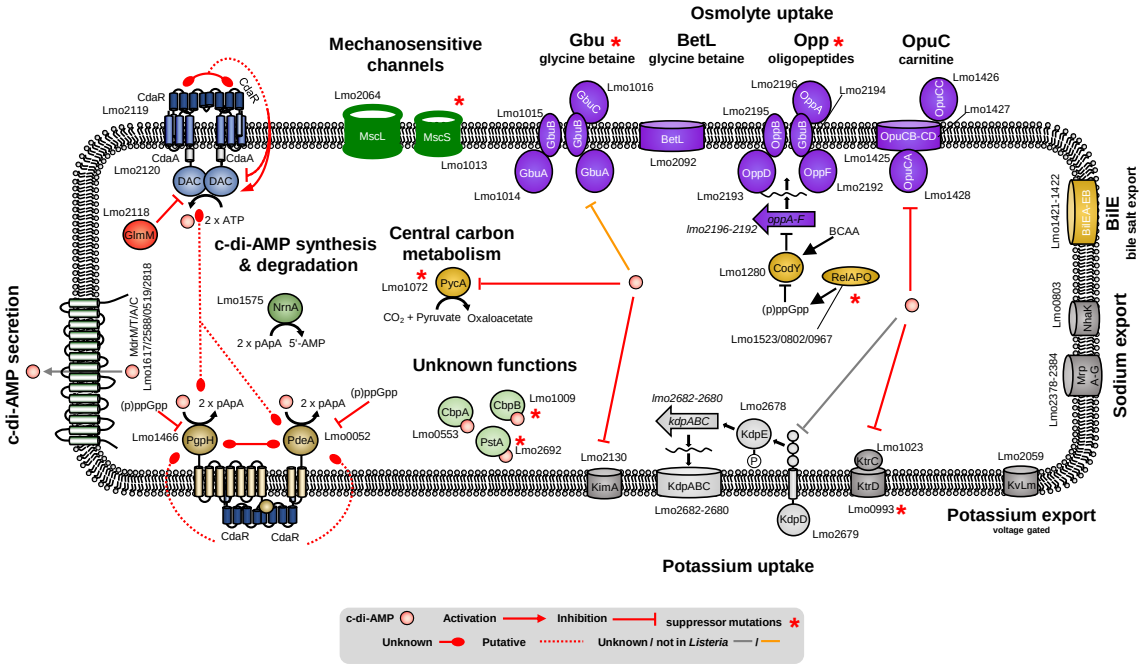

Fig. 7.1 The current knowledge about c-di-AMP signaling and osmoregulation in *L. monocytogenes*. c-di-AMP is synthesized by the sole DAC of *L. monocytogenes*, CdaA. CdaA is controlled by the two regulatory proteins CdaR and GlmM. Our current knowledge is depicted as self-interaction of the YbbR domains modulating CdaA activity in dependency of the strain in the cell envelope. The effects of GlmM on CdaA activity seem to be less pronounced than the effects of CdaR in *L. monocytogenes* compared to *S. aureus* and *vice versa*. *L. monocytogenes* possesses multi drug resistance efflux transporter that can secrete c-di-AMP and might, like the phosphodiesterases (PDEs) PdeA and PgpH contribute to rapid decrease of intracellular c-di-AMP. Protein-protein interaction experiments, furthermore hint to an interaction between PDEs, CdaA and CdaR. *L. monocytogenes* also possesses homologs of a nano-Rnase (NrnA) and two mechanosensitive channels (MscL and MscS) that might contribute to c-di-AMP degradation and osmoregulation, respectively. c-di-AMP also inhibits the pyruvate carboxylase PycA and binds to the proteins of unknown function CbpA, CbpB and PstA. *L. monocytogenes* furthermore possesses osmolyte uptake system for glycine betaine (Gbu and BetL), oligopeptides (Opp), carnitine (OpuC) and a bile salt specific exporter (BilE). While OpuC has been shown to be directly inhibited by c-di-AMP, Opp and Gbu are indirectly implicated by occurrence of suppressor mutations in *L. monocytogenes*. For Gbu, regulation by c-di-AMP in other bacteria was observed. The Opp system is also indirectly linked to c-di-AMP homeostasis due to the cross-talk between the stringent response and c-di-AMP and the occurrence of c-di-AMP-dependent suppressor mutations in the RelA enzyme. *L. monocytogenes* also possesses several homologs of ion transport systems, among them the voltage gated KvLm potassium exporter and potassium import systems. Of those, the KdpD protein is known to bind c-di-AMP in *S. aureus* and regulate expression of the KdpABC high affinity transporter. KtrAB, is regulated by c-di-AMP on the protein level in *S. aureus*, as we demonstrate also for KtrCD of *L. monocytogenes*. Last but not least, we could identify KimA as a potassium uptake system in *L. monocytogenes* and show for that also this class of potassium transporter is inhibited by c-di-AMP (based on Commichau *et al.*, 2018).

Moreover, this would allow interesting fine-tuning mechanisms where the activity of the receptor molecule would directly impact the activity of DAC or PDE and it would lead to even more complex regulatory networks. Our protein-protein interaction study (chapter 2) does indeed hint at the possibility of protein-protein interaction between components of the synthesis, degradation machineries and targets of c-di-AMP signaling and it will be interesting to study the occurrence and possible regulatory consequences of these interactions and the impact of c-di-AMP on novel targets in future studies.

c-di-AMP affects global gene expression and protein biosynthesis

One important aspect of future studies on c-di-AMP signaling will be the identification and elucidation of the regulation of novel c-di-AMP regulated processes. As described in chapter 4, we investigated the effect on *L. monocytogenes* if its sole DAC encoding gene *cdaA* is deleted under

defined growth conditions. We identified a total of 95 genes and 21 proteins that are at least 2- or 1-5-fold differently regulated, respectively, compared to the wild type strain. Among these were many genes involved in cellular processes like replication or transcription, carbon and nitrogen metabolism, signal transduction processes, cell wall and membrane biogenesis, motility and genes of unknown function. As one can immediately deduct from this list, c-di-AMP impacts a lot of different cellular processes. The big remaining question here is if these processes are directly regulated by c-di-AMP or indirect consequences due to the altered osmotic equilibrium this strain probably has.

As described above, c-di-AMP signaling shows cross-talk with other cellular processes, like the stringent response, cell wall biosynthesis or DNA-related mechanism. It is therefore likely that the changes in gene expression and protein biosynthesis are at least in part indirect effects. Interestingly, among the differently expressed genes also 15 operons with at least two impacted genes were differently expressed, hinting at transcriptional regulation of these operons either directly or indirectly by c-di-AMP. Among those are for example genes involved in cystine/cysteine metabolism, cell division and cell wall biosynthesis, purine biosynthesis and two operons involved in synthesis of flagellar subunits. Interestingly motility in *L. monocytogenes* is regulated by a mainly ambient temperature-dependent system.

The motility assay we performed did show an impact of c-di-AMP on swim behavior in *L. monocytogenes* with an increase in the *cdaA* deletion mutants at 37°C (**Fig. 4.4**). This phenotype was not observed as pronounced at 25°C. It is however unclear, if the difference in swim distance is due to the slower growth or decreased motility and how motility genes are expressed in the *cdaA* mutant at 25°C. Interestingly, a *B. subtilis gdpP* mutant showed in a transcriptomic study an inhibition of biofilm genes and reduced biofilm formation (Gundlach *et al.*, 2016). In *B. subtilis* motile and sessile lifestyle are mutual exclusive and regulated by the DNA-binding protein SinR and its interaction with the antagonists SinI and SlrR (Vlamakis *et al.*, 2013). Indeed, in the high c-di-AMP containing *B. subtilis* Δ*gdpP* strain, motility genes, like the gene encoding the flagellin encoding *hag* were upregulated. Therefore, c-di-AMP may regulate motility differently, between these two closely related bacteria. In other bacteria, like *E. coli*, differentiation between motile and sessile lifestyle is regulated by the "older brother" of c-di-AMP, c-di-GMP that is also present in *B. subtilis*, but does not control biofilm formation in it (Gao *et al.*, 2013; Hengge, 2009). In *L. monocytogenes* one important determinant for virulence is also an important determinant for motility. The expression of the flagellin encoding gene, which is called *flaA* in *L. monocytogenes*, is repressed at temperatures that signal a host environment (37°C) and expressed at lower temperatures that signal the presence outside a host organism (Dons *et al.*, 1992; Peel *et al.*, 1988). In this process the orphan response regulator DegU plays an important role (orphan because the gene of the corresponding sensor kinase DegS is absent in the *L. monocytogenes* genome). DegU inhibits its own expression and it binds the promoter that governs expression of *gmaR*, encoding the anti-repressor to MogR, the repressor of motility genes (including *gmaR*). The temperature sensitive GmaR protein, as well as the temperature-sensitive GmaR-MogR interaction, eventually regulates motility gene expression (Kamp & Higgins, 2009; Kamp & Higgins, 2011; Shen *et al.*, 2006; for more details see **chapter 4** and **chapter 6**). The operon of *gmaR* also contains the *motB* genes, encoding proteins of the flagellum, which is an additional reason why DegU is essential for motility in *L. monocytogenes* (Gueriri *et al.*, 2008; Mauder *et al.*, 2008). Interestingly the global regulator CodY that is also implicated in stringent response-dependent regulation of *opp* expression, has also been shown to regulate, among others, motility genes (Gibhardt, 2015; Lobel & Herskovits, 2016; Whiteley *et al.*, 2015). It has also been shown that c-di-GMP effects motility in *L. monocytogenes*. Deletion of all three c-di-GMP PDEs, which leads to higher c-di-GMP levels, lead to increased

synthesize of an exopolysaccharide that inhibits motility probably by increasing cell aggregation (Chen *et al.*, 2014; Köseoğlu *et al.*, 2015). This, moreover, highlights that the effects of c-di-AMP on regulation of motility gene expression could be different in *B. subtilis* and *L. monocytogenes*.

It is unclear, however, if c-di-AMP directly regulates motility expression or if it is *via* cross-talk with the stringent response or c-di-GMP signaling that both can influence CodY activity by decreasing GTP pool (Elbakush *et al.*, 2018; Geiger & Wolz, 2014) or if there is a connection between c-di-AMP and the small RNA *rli31* that was identified in a suppressor mutant screen on the search for mutants that mimic the effect of CdaR on lysozyme resistance. We could observe an influence of *rli31* on motility that may be affected by c-di-AMP signaling (**chapter 6**). Interestingly, while swarming of the CdaR mutant seems to be like the wild type at 25°C, it was, in contrast to all other investigated strains, strongly inhibited at 37°C on LSM plates. Contrarily to previous studies that show strict temperature-dependent motility regulation, the motility assay on LSM plates at 37°C displayed a temperature-independent regulation of motility, especially the *cdaA* deletion strain showed an increased motility (**chapter 4**). The temperature independent regulation of motility might therefore be influenced by c-di-AMP.

This is just one example of the many research possibilities of finding new c-di-AMP-regulated processes. With the data in hand, we can find new targets of c-di-AMP regulated transcription factors, such as BusR in *L. lactis or S. agalactiae* or new RNA structures like the *ydaO* (*kimA*) riboswitch that governs potassium transporter expression in *B. subtilis* (Devaux *et al.*, 2018; Nelson *et al.*, 2013; Pham *et al.*, 2018).

Overall, the omics data gathered will help us to expand our understanding of the c-di-AMP signaling network in *L. monocytogenes* and help uncover yet unknown regulatory pathways.

Outlook

We could show that the two most abundant cyclases CdaA and DisA are both regulated by osmoregulatory mechanisms, namely cellular turgor (CdaA with CdaR) and molecular crowding and DNA-ion interaction (DisA). We furthermore could show potential cluster building of synthesis and degradation machinery in *L. monocytogenes* that will be interesting subjects for further studies. As summarized in Fig. 7.2, *L. monocytogenes* possesses a great repertoire of osmolyte uptake and efflux systems.

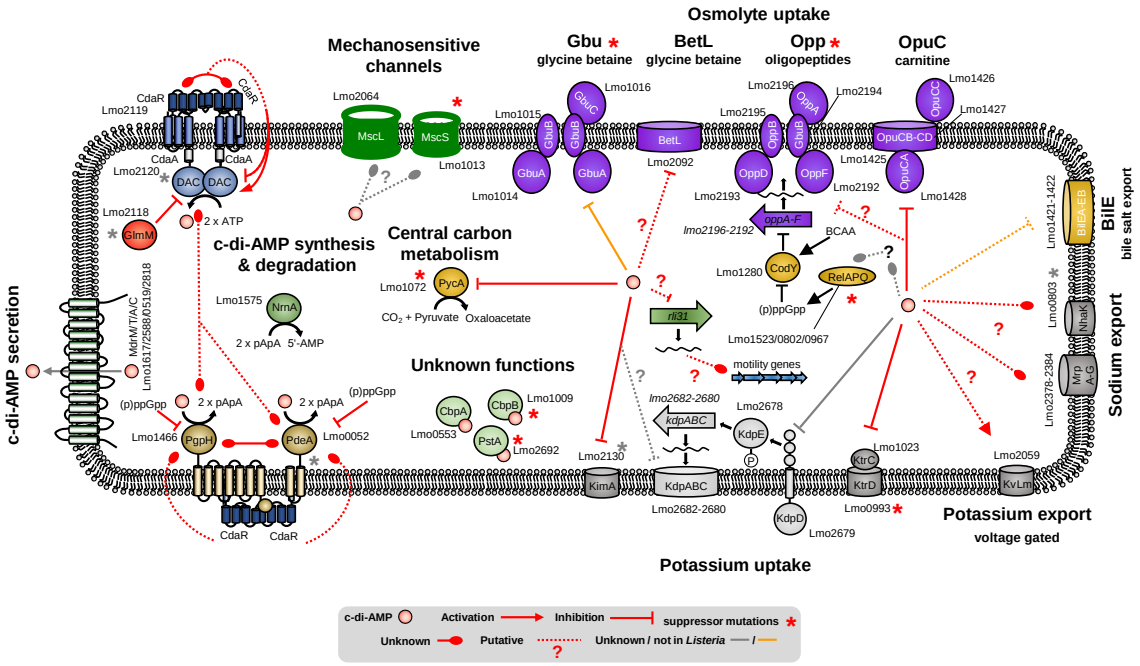

Fig. 7.2 An outlook on c-di-AMP signaling and osmoregulation in *L. monocytogenes*. In addition to what is discussed and shown in Fig. 7.1, c-di-AMP might affect other osmoregulatory systems in *L. monocytogenes* that have been connected to c-di-AMP metabolism and or osmoregulation in other organisms or that would make sense to be regulated by c-di-AMP as the major regulator of osmotic homeostasis in Firmicutes. *L. monocytogenes* possesses two mechanosensitive channels that may be a fitting target for the osmoregulator c-di-AMP. It could, furthermore, regulate glycine betaine transport by Gbu, despite the currently contradicting studies in *L. monocytogenes* and might also regulate uptake via the BetL system. Furthermore, regulation of the Opp oligopeptide importers is tightly linked to c-di-AMP via the cross-talk with the stringent response and frequent occurrence of suppressor mutations and suggests therefore the possibility of a more direct influence of c-di-AMP on Opp activity. It would, moreover, be interesting to study if c-di-AMP has an effect on BilE activity, despite studies showing no binding so far and to see if it impacts potassium and sodium efflux systems that would physiologically make sense to be c-di-AMP regulated. In future studies it would, furthermore, be interesting to analyze the cross-talk between the stringent response and c-di-AMP pathways. Moreover, it will be interesting to see if KdpD in *L. monocytogenes* also regulate *kdpABC* expression in dependency of c-di-AMP and if c-di-AMP, as it is the case for other potassium uptake systems, controls KdpABC activity directly. Lastly, the elucidation of the function of yet unknown proteins like CbpA, CbpB and PstA and the regulation of degradation, synthesis and the potential cross-talk between those two interesting determinants of the intracellular c-di-AMP concentration can be important aspects of future studies of this fascination nucleotide second messenger (modified from Commichau *et al.*, 2018).

It will be interesting in the future to elucidate if other osmoregulatory system in *L. monocytogenes* or related bacteria are also regulated by c-di-AMP. Regulation could hereby occur on all levels from transcription, over translation, to control of protein activity. Possible targets for such a regulation are yet not studied osmolyte systems, mechanosensitive channels, osmolyte export systems and proteins of other signaling pathways that are non to interfere with c-di-AMP signaling. Analysis of c-di-AMP dependent expression could be analyzed by promoter-reporter gene fusion

experiments. For the analysis of c-di-AMP protein interactions, DRaCALAs can be performed (**see chapter 3**). Another important subject will be the study of the Kdp potassium transporter in *L. monocytogenes*. In *S. aureus* it is known that its expression is regulated by the KdpDE two-component system, which is also present in *L. monocytogenes*. Furthermore, given that the Kdp system is also a high-affinity potassium importer, it would make sense to have a two-level regulation, meaning also regulation of the transporter activity, by c-di-AMP, as it is known for KtrAB in *B. subtilis*. The Kdp system could be investigated, similar to the characterization of KtrCD and KimA potassium transporters (**see chapter 3**). It will be also interesting to study the role of the c-di-AMP binding proteins of yet unknown function (CbpA, CbpB and PstA) and their regulation by c-di-AMP. Moreover, identifying novel pathways or processes that might be regulated by c-di-AMP will enhance the knowledge about nucleotide signaling and possible open novel research possibilities. The data about differentially expressed genes and c-di-AMP influenced protein abundancy will be a great starting point to elucidate possible new regulatory pathways. As demonstrated in **chapter 4** and discussed above, regulation of motility gene expression might already be a new c-di-AMP regulated pathway in *L. monocytogenes*, with possible implications of the sRNA *rli31* (**chapter 6**).

The most interesting will be the studies of synthesis and degradation of c-di-AMP and the regulation by osmotic changes and possible cross-talk. The next important experiments should be the analysis of the influence of CdaR on CdaA self-interaction and determination if CdaA-CdaR interaction is transient and subject to regulation or consecutive. Possible experiments to analyze this, are the expression of CdaA-split Gfp fusion proteins or CdaA/CdaR fluorophore fusion proteins to analyze CdaA self-interaction or CdaA-CdaR co-localization, respectively. Evaluation of c-di-AMP synthesis in mutants with an increased or decreased cell wall structure, by differential expression of cell wall-metabolic enzymes or the study of c-di-AMP synthesis in cell wall-less bacteria (L-forms) could further help to determine the exact mode of action CdaR has on CdaA activity. For analysis of CdaA regulation by GlmM, *in vitro* and *in vivo* studies should be conducted to compare effects of GlmM from *L. monocytogenes* and GlmM of non-c-di-AMP synthesizing bacteria, such as *E. coli* on the c-di-AMP concentration.

As discussed above, we could increase the knowledge of DAC regulation and propose novel hypothesis for regulation of DAC activity and a potential interaction between synthesis and degradation machineries. It will be very interesting to study those regulatory mechanisms further in the future. This might ultimately also lead to the discovery of novel antibiotics that target c-di-AMP signaling and thereby osmoregulation. Especially in combination with cell wall-weakening antibiotics of the β-lactam class, this could lead to novel and putatively effective combination treatments to fight the ever-increasing occurrence of multi-resistant pathogenic bacteria.

8. Supplementary Data

Chapter 2

Tab. S2.1 Plasmids

Name	Insert/Features	Reference
pBAD33	P_{BAD}-mcs *araC cat*	Guzman *et al.*, 1995
pGP172	P_{T7}-mcs *bla*	Merzbacher *et al.*, 2004
pIMK3	P_{help}-*lacO*-mcs *lacI neo*	Monk *et al.*, 2008
pMAD	*bla ermC bgaB*	Arnaud *et al.*, 2004
pKTop	P_{lac}-mcs-*phoA*$_{66\text{-}1416}$-*lacZ*$_{12\text{-}180}$ *aphA*3	Karimova *et al.*, 2009
pUT18	P_{lac}-mcs-*cya*T18 *bla*	Karimova *et al.*, 1998
pUT18C	P_{lac}-*cya*T18-mcs *bla*	Karimova *et al.*, 1998
pUT18C-zip	P_{lac}-*cya*T18-yeast GCN4 leucine zipper *bla*	Karimova *et al.*, 1998
p25-N	P_{lac}-mcs-*cya*T25 *aphA*3	Claessen *et al.*, 2008
pKT25	P_{lac}-*cya*T25-mcs *aphA*3	Karimova *et al.*, 1998
pKT25-zip	P_{lac}-*cya*T25-yeast GCN4 leucine zipper *aphA*3	Karimova *et al.*, 1998
pBP131	pGP172-*prfA* (*lmo0200*)	This work
pBP223	pGP172-*cdaR* (Δaa 1-28)	This work
pBP224	pUT18-*cdaR* (*lmo2119*)	Rismondo *et al.*, 2016
pBP225	pUT18C-*cdaR*	Rismondo *et al.*, 2016
pBP226	p25-N-*cdaR*	Rismondo *et al.*, 2016
pBP227	pKT25-*cdaR*	Rismondo *et al.*, 2016
pBP232	pUT18-*cdaA* (*lmo2120*)	Rismondo *et al.*, 2016
pBP233	pUT18C-*cdaA*	Rismondo *et al.*, 2016
pBP234	p25-N-*cdaA*	Rismondo *et al.*, 2016
pBP235	pKT25-*cdaA*	Rismondo *et al.*, 2016
pBP250	pKTop-*cdaR*	This work
pBP251	pKTop-*cdaR* (aa 1-33; ΔYbbR domains)	This work
pBP252	pKTop-*cdaR* (aa 34-452; ΔTM domain)	This work
pBP253	pKTop-*prkA* (*lmo1820*)	This work
pBP254	pKTop-*prfA*	This work
pBP255	pIMK3-*cdaR* (aa 32-452; ΔTM domain)	This work
pBP256	pIMK3-*cdaR* (aa 1-320; ΔYbbR domain 4)	This work
pBP257	pIMK3-*cdaR* (aa 1-230; ΔYbbR domain 3-4)	This work
pBP258	pIMK3-*cdaR* (aa 1-130; ΔYbbR domain 2-4)	This work
pBP259	pIMK3-*cdaR* (aa 1-33; ΔYbbR domain 1-4)	This work
pBP260	pBAD33-*cdaA-cdaR* (aa 34-452; ΔTM domain)	This work
pBP261	pBAD33-*cdaA-cdaR* (aa 1-320; ΔYbbR domain 4)	This work
pBP262	pBAD33-*cdaA-cdaR* (aa 1-230; ΔYbbR domain 3-4)	This work
pBP263	pBAD33-*cdaA-cdaR* (aa 1-130; ΔYbbR domain 2-4)	This work
pBP264	pBAD33-*cdaA-cdaR* (aa 1-33; ΔYbbR domain 1-4)	This work
pBP269	pUT18-*pdeA* (*lmo0052*)	This work
pBP270	pUT18C-*pdeA*	This work
pBP271	p25-N-*pdeA*	This work
pBP272	pKT25-*pdeA*	This work
pBP273	pUT18-*pgpH* (*lmo1466*)	This work

Name	Insert/Features	Reference
pBP274	pUT18C-*pgpH*	This work
pBP275	p25-N-*pgpH*	This work
pBP276	pKT25-*pgpH*	This work
pBP277	pUT18-*kimA* (*lmo2130*)	This work
pBP278	pUT18C-*kimA*	This work
pBP279	p25-N-*kimA*	This work
pBP280	pKT25-*kimA*	This work
pBP352	pMAD-Δ*cdaA* (*cdaA* up- and downstream region)	This work
pBP359	pUT18-*glmM* (*lmo2118*)	This work
pBP360	pUT18C-*glmM*	This work
pBP361	p25-N-*glmM*	This work
pBP362	pKT25-*glmM*	This work
pBP370	pBAD33-*cdaA*	Quintana *et al.*, 2019
pBP373	pBAD33-*cdaA* D171N	Quintana *et al.*, 2019
pBP384	pWH844-*kimA*	Chapter 3
pBP387	pBAD33-*cdaA*-*cdaR*	This work
pBP388	pBP387-*glmM*	This work
pBP389	pBP370-*glmM*	This work
pGP976	pUT18-*rnY*^{Bsu}	Commichau *et al.*, 2009
pGP977	pUT18C-*rnY*^{Bsu}	Commichau *et al.*, 2009
pGP978	p25-N-*rnY*^{Bsu}	Commichau *et al.*, 2009
pGP979	pKT25-*rnY*^{Bsu}	Commichau *et al.*, 2009

cat = cm^R (30 µg/ml chloramphenicol), *bla* = amp^R (100 µg/ml ampicillin), *neo*/*aphA*3 = kan^R (50 µg/ml kanamycin); mcs = multiple cloning site; *ermC* = ery^R (5 µg/ml erythromycin); ^{Bsu} = from *B. subtilis*

Tab. S2.2 Oligonucleotides

Name	Restriction sites are underlined, complementary regions are in bold, sequences 5'→3'	Purpose and reference
FC205	TTTAGATCTTTAATTTAATTTTCCCCAAGTAGCAGGACATGC	Rev. *prfA* (*Bgl*II)
FC206	AAAGAGCTCGATGAACGCTCAAGCAGAAGAATTCAAA	Fwd. *prfA* (*Sac*I)
FC336	AAATCTAGAGATGGGTAAATATTTCGGTACGGATGGAGTTAG	Fwd. *glmM* (*Xba*I)
FC337	TTTGGTACCCGATCGTTAAGTGCCATTTCTGAACGAACAACCG	Rev. *glmM* (*Kpn*I)
JH05	AAAGAATTCAGAATTGCGTTCCACGGATACATTAAAAC	Fwd. *cdaA* upstream region (*Eco*RI)
JH06	**CCTCCTTTCGTCGACGTGCCTCTT**GAAAACCATTTATAATCAC	Rev. *cdaA* upstream region (*Sac*I)
JH07	**AAGAGGCACGTCGACGAAAGGAGG**CAAAAGCGAATGATG	Fwd. *cdaA* downstream region (*Sac*I)
JH08	TTTGGATCCCACTTTCCGGCGTGCCTTCTTG	Rev. *cdaA* downstream region (*Bam*HI)
JH21	AAACCATGGATCGAATTTTAAATAATAAATGGTCGATTC	Fwd. *cdaR* (*Nco*I), Rismondo *et al.*, 2016
JH22	TTTGTCGACTTATGTGCTTTTGGAAGGTACTTCAATGG	Rev. *cdaR* (*Sal*I), Rismondo *et al.*, 2016
JH51	AAATCTAGACACGGAGGTGAAGTGATGGATTTTTCCAATATGTCGATATTGCAT	Fwd. *cdaA* (*Xba*I), Quintana *et al.*, 2019
JH103	TTTCTGCAGTTATGTGCTTTTGGAAGGTACTTCAATGGATG	Rev. *cdaR* (*Pst*I)
JH104	AAACTGCAGAGAAGGAGAGTAATGAAATGGGTAAATATTTCG	Fwd. *glmM* (*Pst*I)

Name	Restriction sites are underlined, complementary regions are in bold, sequences 5'→3'	Purpose and reference
JH105	TTTAAGCTTTTAATCGTTAAGTGCCATTTCTGAACGAACAAC	Rev. *glmM* (*Hind*III)
JH121	AAAGGATCCCATGGATCGAATTTTAAATAATAAATGGTCGATTCGAAT	Fwd. *cdaR* (*Bam*HI)
JH122	TTTGGTACCGCTGTGCTTTTGGAAGGTACTTCAATGGATGC	Rev. *cdaR* (*Kpn*I)
JH123	AAAGGATCCCATGACGACTTTTTCTACGACGTCTTCTAGTGATTC	Fwd. *cdaR* (Δaa 1-33; *Bam*HI)
JH124	TTTGGTACCGCGGCGTTATTATTATTTGCATTAACTGATGTAAAAAGG	Rev. *cdaR* (Δaa 34-452; *Kpn*I)
JH126	AAAGGATCCCATGATGATTGGTAAGCGATTAAGCGATCG	Fwd. *prkA* (*Bam*HI)
JH127	TTTGGTACCGCATTTGGATAAGGGACTGTACCTTCATCG	Rev. *prkA* (*Kpn*I)
JH128	AAATCTAGACATGAACGCTCAAGCAGAAGAATTCAAAAAATATTTAG	Fwd. *prfA* (*Xba*I)
JH129	TTTGGTACCGCATTTAATTTTCCCCAAGTAGCAGGACATGC	Rev. *prfA* (*Kpn*I)
JH130	AAACCATGGCCACGACTTTTTCTACGACGTCTTCTAG	Fwd. *cdaR* (Δaa 1-31; *Nco*I)
JH131	TTTGTCGACTTAGGCGTTATTATTATTTGCATTAACTGATGTAAAAAGG	Rev. *cdaR* (Δaa 34-452; *Sal*I)
JH132	TTTGTCGACTTAGTTATTTGCTTCAGACTTTTTTACGGTCTTAATC	Rev. *cdaR* (Δaa 321-452; *Sal*I)
JH133	TTTGTCGACTTACTTGCCGACTTTTTCAACTGGCACG	Rev. *cdaR* (Δaa 231-452; *Sal*I)
JH134	TTTGTCGACTTATTCTTGTACATTTACGTTGACTGTTGCTGGATTC	Rev. *cdaR* (Δaa 131-452; *Sal*I)
JH135	**CGTAGAAAAAGTCGTCATCATTCGCTTTTG**CCTCCTTTCCATTTAG	Rev. *cdaA*
JH136	**CAAAAGCGAATGATGACGACTTTTTCTACG**ACGTCTTCTAGTGATTC	Fwd. *cdaR* (Δaa 1-33)
JH137	TTTCTGCAGTTAGGCGTTATTATTATTTGCATTAACTGATGTAAAAAGG	Rev. *cdaR* (Δaa 34-452; *Pst*I)
JH138	TTTCTGCAGTTAGTTATTTGCTTCAGACTTTTTTACGGTCTTAATC	Rev. *cdaR* (Δaa 321-452; *Pst*I)
JH139	TTTCTGCAGTTACTTGCCGACTTTTTCAACTGGCACG	Rev. *cdaR* (Δaa 231-452; *Pst*I)
JH140	TTTCTGCAGTTATTCTTGTACATTTACGTTGACTGTTGCTGGATTC	Rev. *cdaR* (Δaa 131-452; *Pst*I)
JH160	AAATCTAGAGATGTCAGGCTATTTTCAAAAACGAATGCTTAAATATCC	Fwd. *pdeA* (*Xba*I)
JH161	TTTGGTACCCGTGTTTCTCCCTTCCAATACGCATCAATGG	Rev. *pdeA* (*Kpn*I)
JH162	AAATCTAGAGGTGAAACTAGCCAAGAAATGGAGAGATTGG	Fwd. *pgpH* (*Xba*I)
JH163	TTTGGTACCCGATCTTTGTCATCAGGATATTGAATTCGTTGATGATATATTC	Rev. *pgpH* (*Kpn*I)
JH164	AAATCTAGAGATGGCTTCGCCGCTAAAAAGACTATTAATCG	Fwd. *kimA* (*Xba*I)
JH165	TTTGGTACCCGTTCTTTTAAATGATAAGGATATGTGGAAACTACTACATCC	Rev. *kimA* (*Kpn*I)
JR28	TTTGGATCCTTATGTGCTTTTGGAAGGTAC	Rev. *cdaR* (*Bam*HI)
JR56	AAAGAGCTCGAATAATAATAACGCCACGACTTTTTCTACG	Fwd. *cdaR* (Δaa 1-28; *Sac*I)

Fwd. = forward, Rev. = reverse, aa=amino acids,

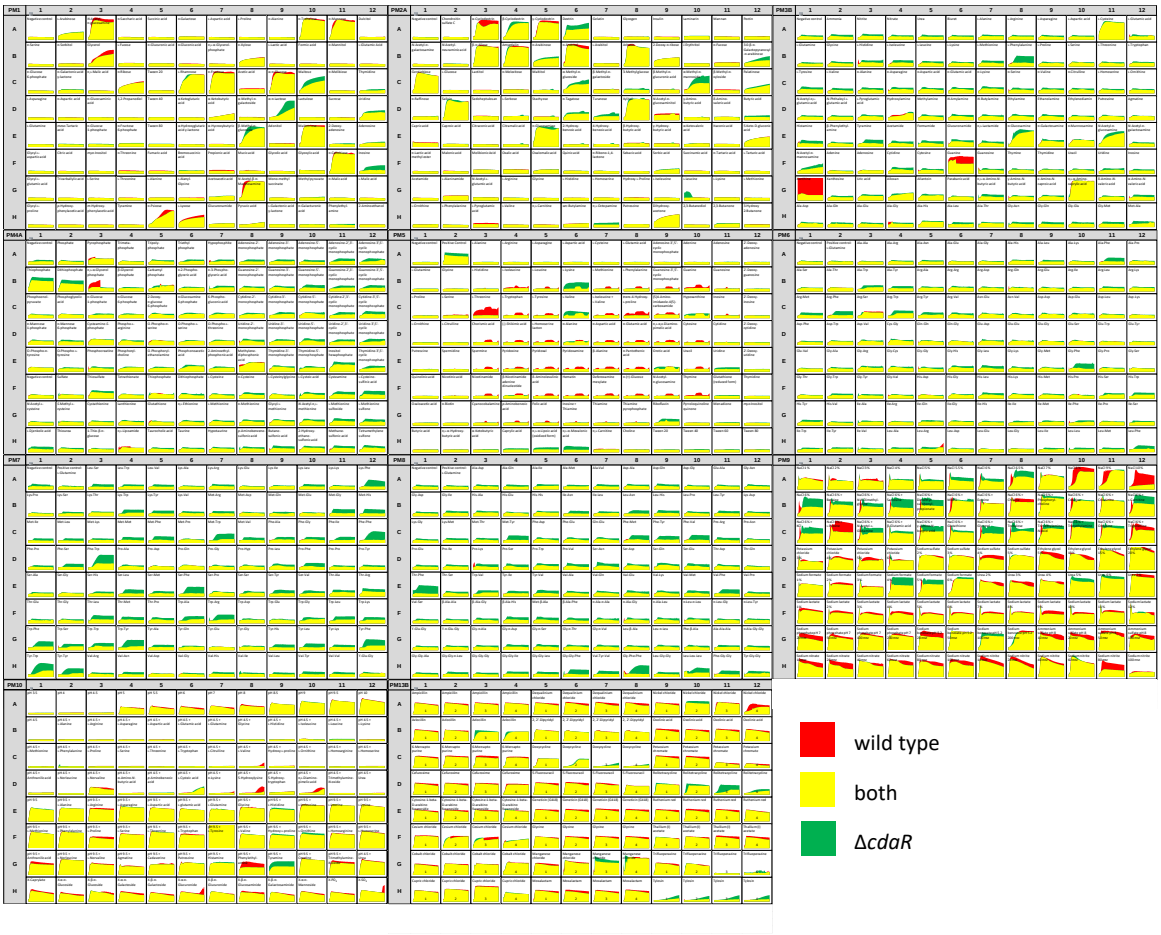

Fig. S2.1 Biolog Phenotype Microarray (PM). Images of plate PM1-10 and PM13B. Metabolic activity of the wild type is shown in red and of the Δ*cdaR* mutant in green. Overlapping regions between them are shown in yellow.

Chapter 4

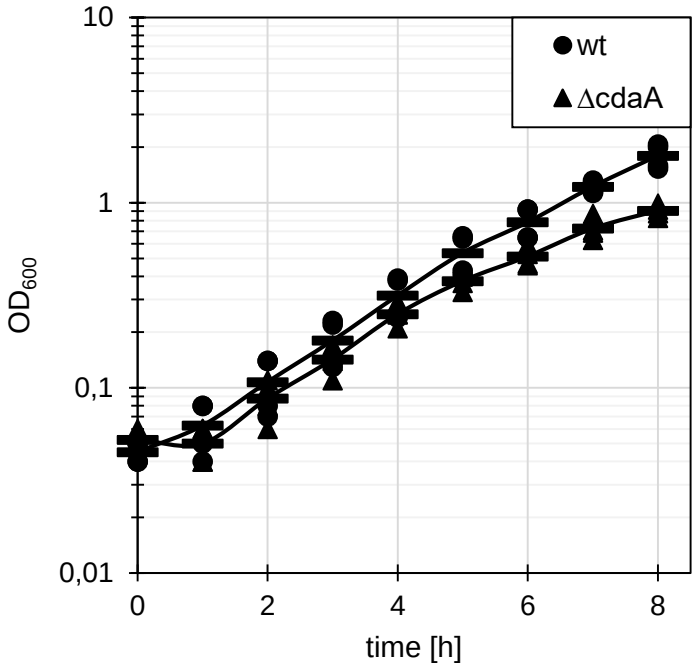

Fig. S4.1 The *cdaA* deletion strain grows similar to the wild type in LSM. The *L. monocytogenes* wt and the Δ*cdaA* mutant (BPL77) were cultivated overnight in 5 ml LSM at 37°C and 220 rpm from single colonies. Preculture were used to inoculate 10 ml LSM to an OD_{600} of 0.05 and cultures incubated at 37°C and 220 rpm. The OD_{600} was measured hourly. Shown are measurements of four biological replicates and the mean OD_{600} values as horizontal lines.

Tab. S4.1 Complete list of differentially expressed genes or synthesized proteins in *ΔcdaA vs.* the wt

Locus tag	Operon	Name	RAST info	Function (COG)	Transcriptome Δ*cdaA*/wt		Proteome Δ*cdaA*/wt		
					Fold change	p	Fold change	p	p,fdr
lmo0118	20	**lmaA**	hypothetical protein	*Function unknown*			**-1.32**	0.0E+00	6.0E-04
lmo0119	20		FIG00774706: hypothetical protein	*Not in COGs*			**-1.46**	1.0E-04	1.6E-03
lmo0136	22	appB	Oligopeptide transport system permease protein OppB	*Amino acid transport and metabolism; Inorganic ion transport and metabolism;*			**-1.29**	2.0E-04	3.0E-03
lmo0186			Cell wall-binding protein	*Function unknown*	**-10.07**	0.0E+00			
lmo0201	32	**plcA**	Phosphatidylinositol-specific phospholipase C	*Defense/virulence mechanisms*			**1.87**	0.0E+00	0.0E+00
lmo0286		ykrV	Glutamine-dependent 2-keto-4-methylthiobutyrate transaminase	*Amino acid transport and metabolism*	**-2.37**	4.9E-03			
lmo0394		**P60**	peptidoglycan lytic protein P45	*Cell wall/membrane biogenesis*	**-2.56**	4.7E-03			
lmo0423	74		RNA polymerase sigma-70 factor, ECF subfamily	*Transcription*	**-2.64**	3.4E-03			
lmo0557	90		Phosphoglycerate mutase family 1	*Carbohydrate transport and metabolism*			**1.22**	0.0E+00	0.0E+00
lmo0559			Magnesium and cobalt transport protein CorA	*Inorganic ion transport and metabolism*	**6.6**	2.5E-03			
lmo0560		rocG	NADP-specific glutamate dehydrogenase	*Amino acid transport and metabolism*	**2.46**	3.0E-04	**1.18**	0.0E+00	0.0E+00
lmo0647			FIG00774323: hypothetical protein	*Not in COGs*	**5.21**	5.0E-04			
lmo0683	111	cheR	Chemotaxis protein methyltransferase CheR	*Cell motility; Signal transduction mechanisms;*	**2.68**	5.4E-03			
lmo0684	111		FIG00774517: hypothetical protein	*Not in COGs*	**2.08**	4.1E-03			
lmo0687	111		FIG00774408: hypothetical protein	*Not in COGs*	**2.17**	6.5E-03			
lmo0689	111	cheV	Chemotaxis protein CheV	*Cell motility; Signal transduction mechanisms;*			**2.17**	0.0E+00	0.0E+00
lmo0690		**flaA**	Flagellin protein FlaA	*Cell motility*	**3.96**	0.0E+00			
lmo0691	112	**cheY**	Chemotaxis regulator	*Signal transduction mechanisms*	**8.94**	6.0E-04	**1.84**	0.0E+00	0.0E+00
lmo0692	112	**cheA**	Signal transduction histidine kinase CheA	*Cell motility; Signal transduction mechanisms;*	**8.43**	3.0E-04			
lmo0693	112		Flagellar motor switch protein FliN	*Cell motility; Intracellular trafficking and secretion;*	**9.09**	2.0E-04			
lmo0694	112		FIG00774728: hypothetical protein	*Not in COGs*	**7.44**	2.2E-03			
lmo0695	112		hypothetical protein	*Cell motility*	**8.66**	3.0E-04			
lmo0696	112	**flgD**	Flagellar basal-body rod modification protein FlgD	*Cell motility*	**8.11**	1.0E-04			
lmo0697	112	**flgE**	Flagellar hook protein FlgE	*Cell motility*	**6.99**	3.0E-04	**3.43**	7.0E-04	8.2E-03
lmo0698	112		Flagellar motor switch protein FliN	*Cell motility; Intracellular trafficking and secretion;*	**6.46**	0.0E+00			
lmo0699	112	**fliM**	Flagellar motor switch protein FliM	*Cell motility*	**6.69**	4.0E-04			
lmo0700	112		Flagellar motor switch protein FliN	*Cell motility; Intracellular trafficking and secretion; Signal transduction mechanisms;*	**5.03**	2.0E-03			
lmo0701	112		FIG00774560: hypothetical protein	*Not in COGs*	**5.52**	4.0E-03			
lmo0702	112		FIG00774477: hypothetical protein	*Function unknown*	**5.38**	5.7E-03			
lmo0703	112		UDP-N-acetylenolpyruvoylglucosamine reductase (EC 1.1.1.158)	*Not in COGs*	**4.8**	4.0E-04			
lmo0704	112		FIG00774686: hypothetical protein	*Not in COGs*	**4.75**	1.5E-03	**1.05**	2.0E-04	3.6E-03
lmo0705	112	**flgK**	Flagellar hook-associated protein FlgK	*Cell motility*	**5.15**	1.0E-04			
lmo0706	112	**flgL**	Flagellar hook-associated protein FlgL	*Cell motility*	**5.25**	0.0E+00			
lmo0707	112	**fliD**	Flagellar hook-associated protein FliD	*Cell motility*	**5.34**	0.0E+00			
lmo0708	112	fliS	Flagellar biosynthesis protein FliS	*Cell motility; Posttranslational modification, protein turnover, chaperones; Intracellular trafficking and secretion;*	**4.46**	1.0E-04	**7.45**	1.0E-04	1.0E-03
lmo0709	112		FIG00774899: hypothetical protein	*Not in COGs*	**4.83**	3.0E-04			
lmo0710	112	**flgB**	Flagellar basal-body rod protein FlgB	*Cell motility*	**4.71**	2.0E-04			
lmo0711	112	**flgC**	Flagellar basal-body rod protein FlgC	*Cell motility*	**4.25**	8.0E-04			
lmo0712	112	**fliE**	Flagellar hook-basal body complex protein FliE	*Cell motility; Intracellular trafficking and secretion;*	**4.41**	9.0E-04			

Locus tag	Operon	Name	RAST info	Function (COG)	Transcriptome Δ*cdaA*/wt		Proteome Δ*cdaA*/wt		
					Fold change	p	Fold change	p	p,fdr
lmo0713	112	**fliF**	Flagellar M-ring protein FliF	*Cell motility; Intracellular trafficking and secretion;*	**4**	1.0E-02	**1.63**	1.0E-04	1.0E-03
lmo0714	112	**fliG**	Flagellar motor switch protein FliG	*Cell motility*			**1.37**	6.0E-04	6.9E-03
lmo0715	112	**fliH**	Flagellar assembly protein FliH	*Not in COGs*	**3.94**	9.7E-03			
lmo0717	112	yjbJ	Soluble lytic murein transglycosylase precursor	*Cell wall/membrane biogenesis*	**3.68**	4.7E-03			
lmo0718	112		FIG00774152: hypothetical protein	*Not in COGs*	**3.75**	1.0E-03	**1.01**	1.0E-04	1.9E-03
lmo0723	114		methyl-accepting chemotaxis protein	*Cell motility; Signal transduction mechanisms;*			**1.18**	0.0E+00	0.0E+00
lmo0809	127		Spermidine Putrescine ABC transporter permease component potC	*Amino acid transport and metabolism*	**-2.43**	5.6E-03			
lmo0810	127		ABC transporter, periplasmic spermidine putrescine-binding protein PotD	*Amino acid transport and metabolism*	**-2.61**	1.3E-03			
lmo0858		exuR	DNA-binding transcriptional regulator	*Transcription*	**2.28**	2.8E-03			
lmo0954	149		FIG00774399: hypothetical protein	*Not in COGs*	**2.43**	5.8E-03			
lmo0971	155	**dltD**	Poly(glycerophosphate chain) D-alanine transfer protein DltD	*Cell wall/membrane biogenesis*	**3.9**	6.1E-03			
lmo0973	155	**dltB**	D-alanyl transfer protein DltB	*Cell wall/membrane biogenesis*	**5.78**	3.3E-03			
lmo0974	155	**dltA**	D-alanine--poly(phosphoribitol) ligase subunit 1	*Cell wall/membrane biogenesis*	**6.4**	5.4E-03	**1.04**	0.0E+00	0.0E+00
lmo1074	174	tagG	Teichoic acid translocation permease protein TagG	*Carbohydrate transport and metabolism; Cell wall/membrane biogenesis;*	**-2.25**	5.0E-04			
lmo1075	174	tagH	Teichoic acid export ATP-binding protein TagH	*Carbohydrate transport and metabolism; Cell wall/membrane biogenesis;*	**-2.15**	1.1E-03			
lmo1126	182		acetyltransferase, GNAT family	*Transcription; General function prediction only;*	**-2.23**	1.6E-03			
lmo1216			N-acetylmuramoyl-L-alanine amidase, family 4	*Cell motility; Intracellular trafficking and secretion;*	**-17.85**	7.0E-04			
lmo1301	206		acetyltransferase, GNAT family	*Translation*	**2.01**	7.0E-04			
lmo1348	213	**gcvT**	Aminomethyltransferase	*Amino acid transport and metabolism*			**-1.06**	0.0E+00	0.0E+00
lmo1389	224	yufO	Unspecified monosaccharide ABC transport system	*General function prediction only*	**-2.28**	1.9E-03			
lmo1390	224	yufP	Unspecified monosaccharide ABC transport system	*General function prediction only*	**-2.06**	5.1E-03			
lmo1433	235	pdhD	Glutathione reductase	*Energy production and conversion*			**1.11**	0.0E+00	3.0E-04
lmo1498	247	yrrM	FIG011945: O-methyltransferase family protein	*General function prediction only*			**-1.18**	1.0E-04	1.0E-03
lmo1566	265	**citC**	Isocitrate dehydrogenase [NADP]	*Energy production and conversion*			**1.2**	0.0E+00	0.0E+00
lmo1567	265	**citZ**	Citrate synthase	*Energy production and conversion*			**1.12**	0.0E+00	0.0E+00
lmo1597			FIG00774834: hypothetical protein	*Not in COGs*	**2.41**	5.3E-03			
lmo1636	281	yhcH	ABC transporter	*Defense/virulence mechanisms*	**2.39**	6.3E-03			
lmo1637	281		ABC transporter, permease protein	*General function prediction only*	**2.55**	1.6E-03	**1.04**	0.0E+00	0.0E+00
lmo1641		**citB**	Aconitate hydratase	*Energy production and conversion*	**4.69**	6.0E-04	**1.21**	0.0E+00	0.0E+00
lmo1699	295		methyl-accepting chemotaxis protein	*Cell motility; Signal transduction mechanisms;*	**3.18**	1.3E-03			
lmo1700	295		FIG00774912: hypothetical protein	*Not in COGs*	**4.53**	1.9E-03			
lmo1738	305	artP	Amino acid ABC transporter	*Amino acid transport and metabolism; Signal transduction mechanisms;*	**-2.38**	9.0E-04			
lmo1739	305	artR	amino acid ABC transporter	*Amino acid transport and metabolism*	**-2.32**	4.8E-03			
lmo1751	307	yefA	23S rRNA (Uracil-5-) -methyltransferase RumA	*Translation*			**-1.77**	1.0E-04	2.0E-03
lmo1764	310	**purD**	Phosphoribosylamine--glycine ligase	*Nucleotide transport and metabolism*	**-4.41**	5.5E-03			
lmo1765	310	**purH**	IMP cyclohydrolase/Phosphoribosylaminoimidazolecarboxamide formyltransferase	*Nucleotide transport and metabolism*			**-1.05**	0.0E+00	0.0E+00
lmo1766	310	**purN**	Phosphoribosylglycinamide formyltransferase	*Nucleotide transport and metabolism*			**-1.18**	7.0E-04	8.1E-03
lmo1770	310	**purL**	Phosphoribosylformylglycinamidine synthase, glutamine amidotransferase subunit	*Nucleotide transport and metabolism*	**-3.51**	3.1E-03			
lmo1771	310	purS	Phosphoribosylformylglycinamidine synthase, PurS subunit	*Nucleotide transport and metabolism*	**-3.86**	9.0E-04			

Locus tag	Operon	Name	RAST info	Function (COG)	Transcriptome Δ*cdaA*/wt		Proteome Δ*cdaA*/wt		
					Fold change	p	Fold change	p	p,fdr
lmo1772	310	**purC**	Phosphoribosylaminoimidaz-ole-succinocarboxamide synthase	*Nucleotide transport and metabolism*	**-3.37**	1.4E-03			
lmo1773	310	**purB**	Adenylosuccinate lyase	*Nucleotide transport and metabolism*	**-2.42**	2.8E-03			
lmo1775	310	**purE**	Phosphoribosylaminoimidazole carboxylase catalytic subunit	*Nucleotide transport and metabolism*	**-2.64**	2.0E-03	**-1.24**	0.0E+00	0.0E+00
lmo1784	312	**rpmI**	LSU ribosomal protein L35p	*Translation*			**-1.71**	7.0E-04	8.1E-03
lmo1902	341	**panB**	3-methyl-2-oxobutanoate hydroxymethyltransferase	*Coenzyme transport and metabolism*			**-1.83**	0.0E+00	0.0E+00
lmo1967	356	**telA**	Tellurite resistance protein	*Inorganic ion transport and metabolism*	**2.37**	9.2E-03			
lmo2023	365	**nadB**	L-aspartate oxidase	*Coenzyme transport and metabolism*	**2.75**	7.4E-03			
lmo2025	365	**nadA**	Quinolinate synthetase	*Coenzyme transport and metabolism*	**3.11**	5.0E-03			
lmo2090	381	**argG**	Argininosuccinate synthase	*Amino acid transport and metabolism*	**-3.42**	2.0E-03			
lmo2091	381	**argH**	Argininosuccinate lyase	*Amino acid transport and metabolism*	**-2.71**	6.7E-03			
lmo2114	387	yxdL	Bacitracin export ATP-binding protein BceA	*Defense/virulence mechanisms*			**1.53**	0.0E+00	0.0E+00
lmo2115	387	bceB	Bacitracin export permease protein BceB	*Defense/virulence mechanisms*	**3.89**	2.0E-04	**1.87**	0.0E+00	0.0E+00
lmo2119	388	***cdaR***	Regulator of CdaA activity	*Function unknown*			**-3.35**	0.0E+00	0.0E+00
lmo2120	388	***cdaA***	Diadenylate cyclase CdaA	*Function unknown*	**-372.5**	4.0E-04	**-3.41**	0.0E+00	0.0E+00
lmo2149			hypothetical protein	*General function prediction only*			**-1.49**	0.0E+00	1.0E-04
lmo2207		yetJ	FIG01231219: hypothetical protein	*General function prediction only*	**2.59**	1.9E-03			
lmo2221	405		DNA double-strand break repair Rad50 ATPase	*Function unknown*	**2.22**	3.0E-03			
lmo2222	405	yhaO	DNA double-strand break repair protein Mre11	*Replication, recombination and repair*	**2.2**	2.1E-03			
lmo2254		pbuO	Xanthine/uracil/thiamine/ascorbate permease family protein	*General function prediction only*	**-3.22**	3.7E-03	**-2.08**	0.0E+00	1.0E-04
lmo2257				*Not in COGs*	**3.72**	2.7E-03			
lmo2258			ribulose-phosphate 3-epimerase family protein	*Not in COGs*	**2.26**	1.3E-03			
lmo2343	419	ytnJ	Coenzyme F420-dependent N5,N10-methylene tetrahydromethanopterin reductase	*Energy production and conversion*	**-2.49**	1.6E-03			
lmo2344	419	ytnI	glutaredoxin family protein	*Posttranslational modification, protein turnover, chaperones*	**-3.01**	1.3E-03			
lmo2345	419	ytmO	Bacterial luciferase family protein YtmO, in cluster with L-cystine ABC transporter	*Energy production and conversion*	**-2.68**	7.0E-04			
lmo2346	419	tcyN	L-Cystine ABC transporter, ATP-binding protein TcyN	*Amino acid transport and metabolism*	**-2.6**	4.3E-03			
lmo2347	419	tcyM	L-Cystine ABC transporter	*Amino acid transport and metabolism*	**-2.54**	2.7E-03			
lmo2348	419	tcyL	L-Cystine ABC transporter	*Amino acid transport and metabolism*	**-2.69**	3.1E-03			
349	419	tcyK	L-Cystine ABC transporter	*Amino acid transport and metabolism; Signal transduction mechanisms;*	**-2.76**	3.1E-03			
lmo2350	419	ytmI	acetyltransferase, GNAT family	*Transcription; General function prediction only;*	**-2.63**	5.1E-03			
lmo2433			putative esterase	*General function prediction only*	**3.07**	2.0E-04			
lmo2486	441		FIG00774998: hypothetical protein	*Transcription; Signal transduction mechanisms; Function unknown;*	**4.35**	3.2E-03			
lmo2504			peptidoglycan lytic protein P45	*Cell wall/membrane biogenesis; Function unknown;*	**-2.14**	8.0E-04			
lmo2505	446	**spl**	peptidoglycan lytic protein P45	*Cell wall/membrane biogenesis; Function unknown;*	**-2.81**	0.0016			
lmo2506	446	**ftsX**	Cell division protein FtsX	*Cell cycle control, mitosis and meiosis*	**-3.57**	2.0E-03			
lmo2507	446	**ftsE**	Cell division transporter, ATP-binding protein FtsE	*Cell cycle control, mitosis and meiosis*	**-3.5**	2.0E-03			
lmo2522		yocH	Cell wall-binding protein	*Cell wall/membrane biogenesis; Function unknown;*	**-13.04**	0.0E+00			
lmo2567			FIG00774296: hypothetical protein	*Not in COGs*	**10.84**	3.1E-03			
lmo2575	462	czcD	Cobalt-zinc-cadmium resistance protein CzcD	*Inorganic ion transport and metabolism*	**2.34**	1.3E-03			
lmo2681	481	**kdpB**	Potassium-transporting ATPase B chain	*Inorganic ion transport and metabolism*			**-1.31**	0.0E+00	0.0E+00

Locus tag	Operon	Name	RAST info	Function (COG)	Transcriptome Δ*cdaA*/wt		Proteome Δ*cdaA*/wt		
					Fold change	p	Fold change	p	p,fdr
lmo2683	482	licB	PTS system, cellobiose-specific IIB component	*Carbohydrate transport and metabolism*			**-1.93**	0.0E+00	4.0E-04
lmo2684	482	licC	PTS system, cellobiose-specific IIC component	*Carbohydrate transport and metabolism*			**-1.14**	0.0E+00	5.0E-04
lmo2720		ytcI	Acyl-coenzyme A synthetases/AMP-(fatty) acid ligases	*Lipid transport and metabolism*			**1.47**	0.0E+00	0.0E+00
lmo2785		**kat**	Catalase	*Inorganic ion transport and metabolism*	**2.07**	1.0E-03			

RAST= Rapid Annotation using Subsystem Technology (database), COG=Clusters of Orthologous Groups (database), grey names=homologs of *B. subtilis* 169 (ListiWiki)

Tab. S4.2 Data-dependent acquisition mass spectrometry (DDA-MS) settings

Reversed phase liquid chromatography (RPLC)	
instrument	Ultimate 3000 RSLC (Thermo Scientific)
trap column	75 µm inner diameter, packed with 3 µm C18 particles (Acclaim™ PepMap™100, Thermo Scientific)
analytical column	Accucore™ 150-C18, (Thermo Fisher Scientific™) 25 cm x 75 µm, 2,6 µm C18 particles, 150 Å pore size
buffer system	0.1% (v/v) acetic acid, 2% (v/v) ACN (buffer A) 100%(v/v) ACN in 0.1% (v/v) acetic acid (buffer B)
flow rate	300 nl/min
gradient	linear gradient of buffer B from 2% (v/v) up to 25% (v/v)
gradient duration	60 min
column oven temperature	40°C
Mass spectrometry (MS)	
instrument	Q Exactive™ HF-X mass spectrometer (Thermo Scientific™)
Ion source	Triversa NanoMate® (Advion)
operation mode	data-dependent
Full MS	
MS scan resolution	60,000
AGC target	3e6
maximum ion injection time for the MS scan	45 ms
Scan range	300 to 1650 m/z
Spectra data type	profile
dd-MS2	
Resolution	15,000
MS/MS AGC target	1e5
maximum ion injection time for the MS/MS scans	22 ms
Spectra data type	profile
selection for MS/MS	12 most abundant isotope patterns with charge ≥2+ and <7+ from the survey scan
isolation window	1.3 *m/z*
Fixed first mass	100 m/z
dissociation mode	higher energy collisional dissociation (HCD)

normalized collision energy	27 %
dynamic exclusion	30 s
Charge exclusion	Unassigned, 1,>6

Tab. S4.3 Data-independent acquisition mass spectrometry (DIA-MS) settings

Reversed phase liquid chromatography (RPLC)			
instrument	Ultimate 3000 RSLC (Thermo Scientific)		
trap column	75 µm inner diameter, packed with 3 µm C18 particles (Acclaim™ Pep-Map™100, Thermo Scientific™)		
analytical column	Accucore™ 150-C18, (Thermo Fisher Scientific™) 25 cm x 75 µm, 2,6 µm C18 particles, 150 Å pore size		
buffer system	0.1% (v/v) acetic acid, 2% (v/v) ACN (buffer A) 100%(v/v) ACN in 0.1% (v/v) acetic acid (buffer B)		
flow rate	300 nl/min		
gradient	linear gradient of buffer B from 2% (v/v) up to 25% (v/v)		
gradient duration	60 min		
column oven temperature	40°C		
Mass spectrometry (MS)			
instrument	Q Exactive™ HF-X mass spectrometer (Thermo Scientific™)		
electrospray	Nanospray Flex Ion Source		
operation mode	data-independent		
Full MS			
MS scan resolution	120,000		
AGC target	3e6		
maximum ion injection time for the MS scan	60 ms		
Scan range	350 to 1200 m/z		
Spectra data type	profile		
DIA settings			
Resolution	30,000		
MS/MS AGC target	3e6		
maximum ion injection time for the MS/MS scans	auto		
Spectra data type	profile		
selection for MS/MS	1		
isolation windows	**window number**	**Center of window [m/z]**	**window width [m/z]**
	1	359.5	
	2	377.6	
	3	395.7	
	4	413.8	
	5	431.9	
	6	450.0	
	7	468.1	
	8	486.1	

	9	504.2	
	10	522.3	
	11	540.4	
	12	558.5	
	13	576.6	
	14	594.6	
	15	612.7	
	16	630.8	
	17	648.9	
	18	667.0	
	19	685.1	
	20	703.2	
	21	721.2	
	22	739.3	
	23	757.4	
	24	775.4	
	25	793.6	19.1 for all mass windows
	26	811.7	
	27	829.8	
	28	847.8	
	29	865.9	
	30	884.0	
	31	902.1	
	32	920.2	
	33	938.3	
	34	956.4	
	35	974.4	
	36	992.5	
	37	1010.6	
	38	1028.7	
	39	1046.8	
	40	1064.9	
	41	1082.9	
	42	1101.0	
	43	1119.1	
	44	1137.2	
	45	1155.3	
	46	1173.4	
	47	1192.5	
Fixed first mass	-		
dissociation mode	higher energy collisional dissociation (HCD)		
normalized collision energy	27 %		

Tab. S4.4 Spectronaut Pulsar setting for library generation

Ion library generation settings in Spectronaut using Pulsar search engine	
Fasta database	*L. monocytogenes* EGD-e
Fasta file number of protein entries	2873
Cleavage rule	Trypsin/P
Missed cleavages	2

Ion library generation settings in Spectronaut using Pulsar search engine	
Variable modifications	Methionine-oxidation
Static modifications	-
Min. peptide length	7 aa
Max. peptide length	52 aa
FDR_{PSM}	0.01
$FDR_{Peptide}$	0.01
$FDR_{Protein}$	0.01
m/z range	300 – 1800 m/z
Number of fragment ions	6 to 10
Min. ion length	3 aa
Scan range	300 to 1650 m/z
Calibration search (MS1 & MS2)	dynamic
Main search (MS1 & MS2)	dynamic
iRT calibration min. R^2	0.8

Tab. S4.5 Spectronaut Pulsar DIA-MS analysis settings

DIA-MS analysis settings	
Fasta database	*Listeria monocytogenes* EGD-e
Fasta file number of protein entries	2873
Cleavage rule	Trypsin/P
Missed cleavages	2
Variable modifications	Methionine-oxidation
Data Extraction MS1 tol.	dynamic
Data Extraction MS2 tol.	dynamic
XIC extraction window	dynamic
Calibration mode	Automatic with iRT precision
Protein Identification Q-value cutoff	0.01
Precursor Identification Q-value cut-off	0.001
Use interference correction?	TRUE
Min. precursor-ions to keep	2
Min. fragment-ions to keep	3
Quantity MS-level	MS2
Data filtering	Q-value percentile
Data filtering fraction	0.5
Workflow profiling strategy	iRT profiling
Workflow profiling row selection	Min. Q-value Row selection (cutoff = 0.001)
Workflow profiling target selection	Profile only non-identified Precursor (identification criterion: Q-value < 0.0001)
Workflow profiling carry-over exact Peak Boundaries	TRUE
Protein Inference Workflow	automatic

Chapter 5

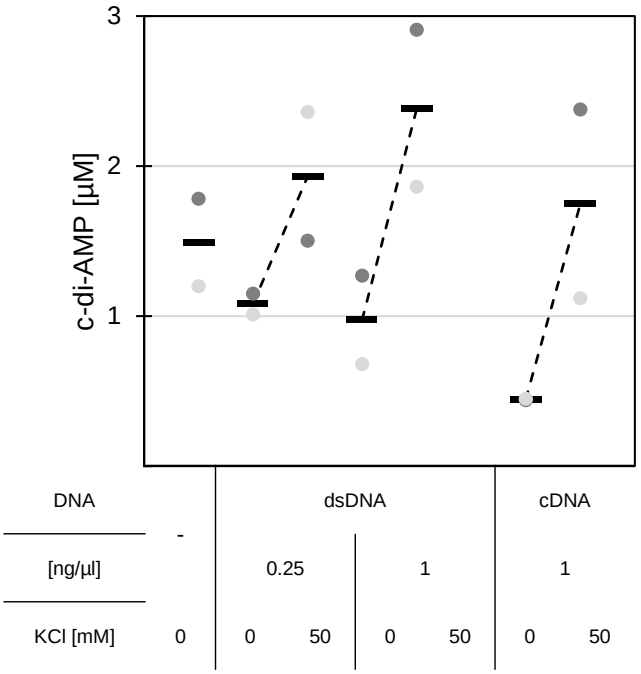

Fig. S5.1 cDNA has a greater inhibitory effect on DisA activity compared to dsDNA. The DACs DisA of *B. subtilis* was purified *via* His-tag purification and subsequently dialyzed overnight in 10 mM Tris-HCl pH 7.5, 5% (*w/v*) glycerol and 1mM DTT at 4°C. 100 nM of DisA was incubated in 10 mM Tris-HCl pH 7.5 with 100 µM ATP, 10 mM $MgCl_2$ and 0.1 % (*w/v*) BSA at 37°C for 30 min when the reactions were stopped and c-di-AMP extracted. Samples were incubated with or without the indicated concentration of *B. subtilis* cDNA or a 2 kb PCR product and with or without the indicated concentration of KCl. Data of two technical replicates are shown. Horizontal lines depict the mean of the two technical replicates. cDNA = chromosomal DNA, dsDNA = double-stranded DNA.

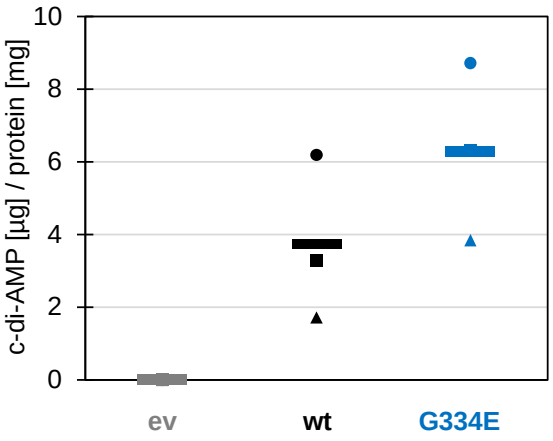

Fig. S5.2 DisA G334E is more active *in vivo*. *E. coli* XL1-blue transformed with the empty vector pBAD33 (ev), pBP394 (DisA wt) or pBP395 DisA (G334E) was grown in LB medium at 37°C until cells grew exponentially. 0.005% (*w/v*) L-arabinose was added to induce DAC expression and cultures incubated for another one and a half hours. Samples were taken and c-di-AMP concentrations determined. Data of three biological replicates are shown as the mean of two technical replicates per measurement point. Horizontal lines depict the mean of the three biological replicates.

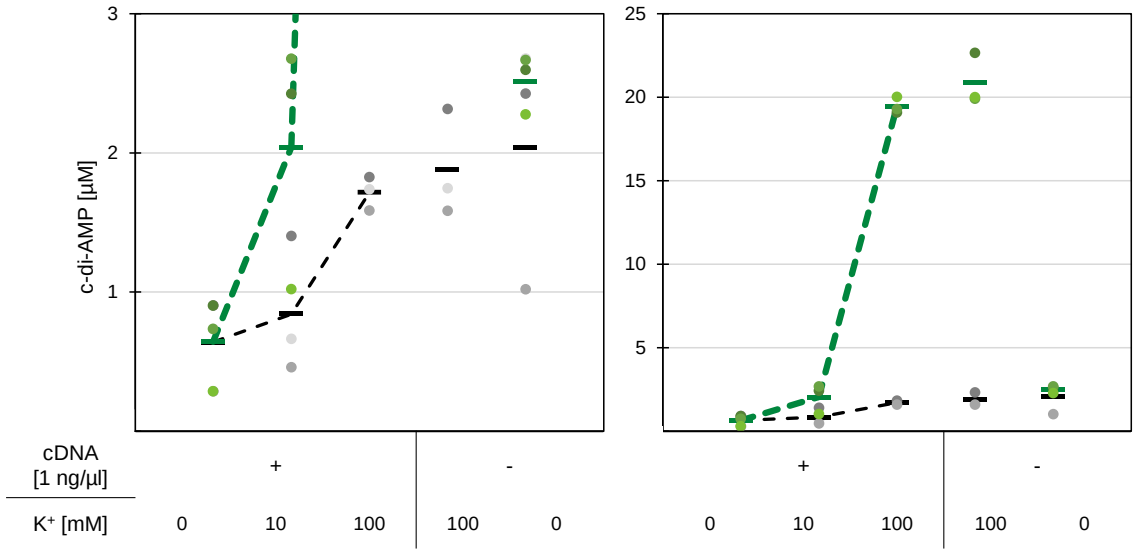

Fig. S5.3 DisA activity is influenced by other potassium ion-containing solutes. The DisA enzyme was purified *via* His-tag purification and subsequently dialyzed overnight in 10 mM Tris-HCl pH 7.5, 5% (*w/v*) glycerol and 1mM DTT at 4°C. 100 nM of DisA was incubated in 10 mM Tris-HCl pH 7.5 with 100 µM ATP, 10 mM $MgCl_2$ and 0.1 % (*w/v*) BSA at 37°C for 30 min when the reactions were stopped and c-di-AMP extracted. Samples were incubated with or without 1 ng/µl of *B. subtilis* cDNA and with or without the indicated concentration of KCl (black) or a mixture of potassium dihydrogen phosphate and dipotassium hydrogen phosphate. The potassium hydrogen phosphate salts where herby titrated to achieve a solution of pH 7.5, the potassium concentration calculated and the depicted amount equimolar to the potassium chloride concentration added. Both figures depict the same data with a different range of the depicted c-di-AMP concentration for better discrimination. Data of three biological replicates are shown as the mean of two technical replicates per measurement point. Horizontal lines depict the mean of the three biological replicates. cDNA = chromosomal DNA.

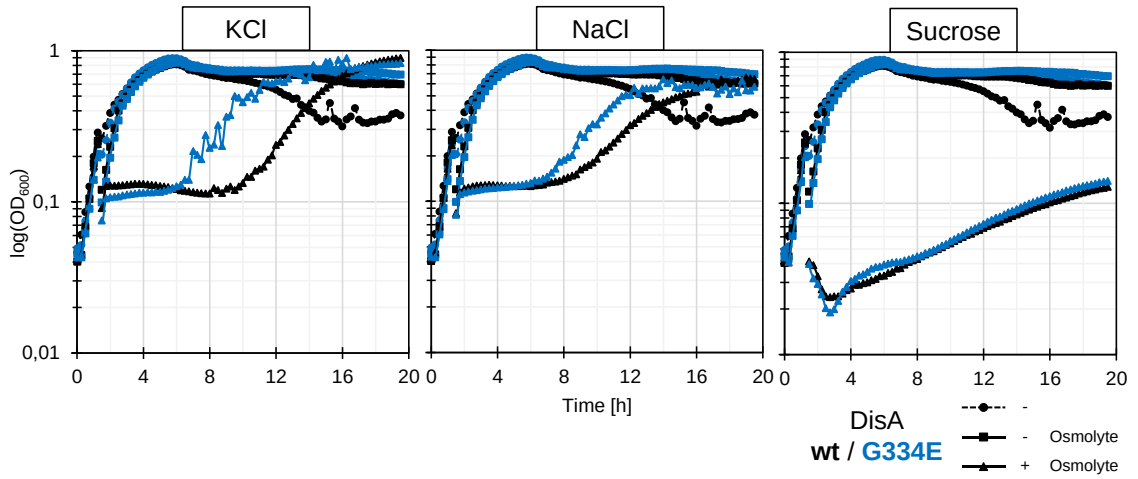

Fig. S5.4 The DisA G334E mutation affects resistance of *B. subtilis* to salt stress. B. subtilis containing either DisA (wt) or DisA (G334E) as sole DAC was grown in 200 µl LB medium at 37°C with medium shaking using a Synergy Mx multiwell plate reader. Cultures were grown for 1.25 hours and 100 µl of cells were added to 100 µl of pre-warmed LB containing the indicated osmolytes to a final concentration of 1.5 M, LB without osmolytes or 200 µl of cells were transferred without any additions and growth was resumed. Depicted are mean values of three biological replicates with two technical replicates, each. The OD_{600} was measured in 15 min intervals.

Chapter 6

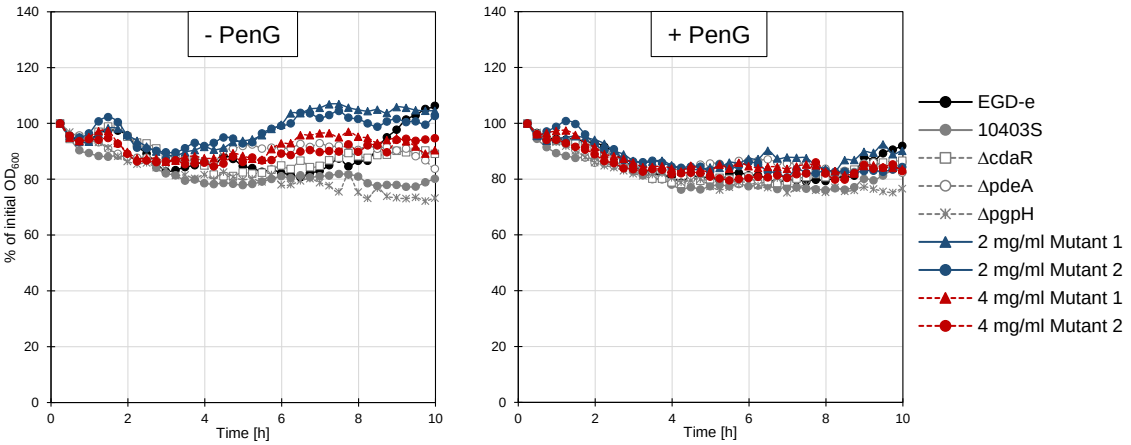

Fig. S6.1 The P_{rli31} suppressor mutants are do not show an altered autolysis with or without penicillin G. The depicted strains were grown in BHI at 37°C until they reached an OD_{600} between of about 0.8. Cells were washed in 50 mM Tris pH 8 and the suspensions adjusted to an OD_{600} of 1.2. Nothing (-PenG) or 25 µg/ml penicillin G were added and the cell suspensions incubated at 37°C and the decline in OD_{600} measured in 15 min intervals. Depicted are the mean values of four biological replicates.

Tab. S6.1 Complete list of differentially expressed genes or synthesized proteins in *Δrli31 vs.* P_{rli31}*

Locus tag	Operon	Name	RAST info	Function (COG)	Transcriptome Δ*rli31*/P_{rli31}*		Proteome Δ*rli31*/P_{rli31}*
					Fold change	p	Fold change NS[1]
lmo0130		yhgE	5'-nucleotidase	Nucleotide transport and metabolism			**1.7**
lmo0131		**pdeB**	FIG00774523: hypothetical protein, c-di-GMP PDE	Signal transduction mechanisms			**1.87**
lmo0257			RNA-2',3'-PO4:RNA-5'-OH ligase	Function unknown			**-1.49**
lmo0286		ykrV	Glutamine-dependent 2-keto-4-methylthiobutyrate transaminase	Amino acid transport and metabolism	**1.58**	7.2E-02	
lmo0324			FIG00774236: hypothetical protein	Not in COGs	**2.75**	4.4E-02	
lmo0342	58	tkt	Transketolase	Carbohydrate transport and metabolism	**1.7**	5.6E-02	
lmo0349	58		FIG00774379: hypothetical protein	Not in COGs	**3.6**	2.3E-02	
lmo0370	63		Alkylphosphonate utilization operon protein PhnA	Inorganic ion transport and metabolism			**-1.9**
lmo0415		**pgdA**	Peptidoglycan N-acetylglucosamine deacetylase	Cell wall/membrane biogenesis	**-1.96**	8.3E-02	**-4.14**
lmo0422	74	**lstR**	Transcriptional regulator, PadR family	Transcription			**-1.82**
lmo0427	75	fruA	PTS system, fructose-specific IIB component	Carbohydrate transport and metabolism			**1.66**
lmo0440			FIG00774042: hypothetical protein	Not in COGs			**-1.63**
lmo0444		yhgE	FIG00776024: hypothetical protein	Function unknown			**1.49**
lmo0485		yfhC	Putative nitroreductase family protein SACOL0874	Energy production and conversion			**1.88**
lmo0540		**pbpX**	penicillin-binding protein, putative	Defense/virulence mechanisms	**-1.84**	9.1E-03	**ND in Δ[2]**
lmo0559[3]			Magnesium and cobalt transport protein CorA	Inorganic ion transport and metabolism	**-70.92**	3.0E-04	**ND in Δ[2]**
lmo0585			extracellular protein	Not in COGs	**1.76**	4.9E-02	
lmo0590	95		Dihydroxyacetone kinase family protein	General function prediction only; Function unknown;			**1.94**

Locus tag	Operon	Name	RAST info	Function (COG)	Transcriptome Δ*rli31*/P_{rli31}*		Proteome Δ*rli31*/P_{rli31}*
					Fold change	p	Fold change NS[1]
lmo0591	95		FIG00775146: hypothetical protein	Function unknown			**1.49**
lmo0620			FIG00774170: hypothetical protein	General function prediction only	**-1.6**	4.0E-02	**-1.91**
lmo0669	109	yhxD	oxidoreductase, short-chain dehydrogenase/reductase family	Lipid transport and metabolism; Secondary metabolites biosynthesis, transport and catabolism; General function prediction only;			**2.13**
lmo0682	111	**flgG**	Flagellar basal-body rod protein FlgG	Cell motility	**3.5**	5.5E-02	
lmo0685	111	motA	Flagellar motor rotation protein MotA	Cell motility	**4.44**	3.0E-02	
lmo0688	111	**gmaR**	glycosyl transferase, group 2 family protein	Cell wall/membrane biogenesis; General function prediction only;	**1.52**	4.9E-02	**6.05**
lmo0689	111	cheV	Chemotaxis protein CheV	Cell motility; Signal transduction mechanisms;	**1.51**	3.9E-02	**1.85**
lmo0698	112		Flagellar motor switch protein FliN	Cell motility; Intracellular trafficking and secretion;	**4.05**	7.9E-02	
lmo0699	112	**fliM**	Flagellar motor switch protein FliM	Cell motility	**2.77**	1.5E-02	
lmo0706	112	**flgL**	Flagellar hook-associated protein FlgL	Cell motility	**1.64**	6.4E-02	
lmo0710	112	**flgB**	Flagellar basal-body rod protein FlgB	Cell motility	**1.67**	1.9E-02	
lmo0711	112	**flgC**	Flagellar basal-body rod protein FlgC	Cell motility	**2.33**	6.7E-02	
lmo0715	112	**fliH**	Flagellar assembly protein FliH	Not in COGs	**1.6**	3.9E-02	
lmo0716	112	**fliI**	Flagellum-specific ATP synthase FliI	Cell motility; Intracellular trafficking and secretion;	**1.81**	1.8E-02	
lmo0717	112	yjbJ	Soluble lytic murein transglycosylase precursor	Cell wall/membrane biogenesis	**1.71**	7.3E-02	
lmo0718	112		FIG00774152: hypothetical protein	Not in COGs	**1.79**	1.9E-02	
lmo0755	119	ypmR	FIG006988: Lipase/Acylhydrolase with GDSL-like motif	Amino acid transport and metabolism	**2.44**	1.4E-02	
lmo0772	122		Transcriptional regulator, GntR family	Transcription			**-2.21**
lmo0775			FIG00774607: hypothetical protein	Not in COGs			**1.58**
lmo0784	124	levD	PTS system, mannose-specific IIB component / PTS system, mannose-specific IIA component	Carbohydrate transport and metabolism			**1.62**
lmo0811			Carbonic anhydrase precursor	Inorganic ion transport and metabolism			**1.63**
lmo0834	129		FIG00774832: hypothetical protein	Not in COGs	**1.9**	5.4E-02	
lmo0880			Putative peptidoglycan bound protein (LPXTG motif)	Cell wall/membrane biogenesis			**2.32**
lmo0891	136	**rsbT**	Anti-sigma B factor RsbT	Signal transduction mechanisms			**1.55**
lmo0895	136	**sigB**	RNA polymerase sigma factor SigB	Transcription			**1.57**
lmo0901		gmuC	PTS system, cellobiose-specific IIC component	Carbohydrate transport and metabolism	**1.84**	2.8E-02	
lmo0934	144	yhbA	Epoxyqueuosine (oQ) reductase QueG	Energy production and conversion	**1.62**	2.7E-02	
lmo0935	144	cspR	tRNA (cytosine34-2'-O-)-methyltransferase	Translation	**1.58**	5.9E-02	
lmo1034	166	glpK	Unknown pentose kinase TM0952	Energy production and conversion	**1.89**	4.3E-02	
lmo1045	168		Molybdenum cofactor biosynthesis protein MoaD	Coenzyme transport and metabolism	**1.74**	3.4E-02	
lmo1047	168	**moaA**	Molybdenum cofactor biosynthesis protein MoaA	Coenzyme transport and metabolism	**1.54**	4.5E-02	
lmo1095			PTS system, cellobiose-specific IIB component	Carbohydrate transport and metabolism			**1.55**
lmo1131		cydC	Transport ATP-binding protein CydC	Energy production and conversion; Posttranslational modification, protein turnover, chaperones;			**3**
lmo1132		ygaD	Transport ATP-binding protein CydD	Defense/virulence mechanisms			**2.02**

Locus tag	Operon	Name	RAST info	Function (COG)	Transcriptome Δ*rli31*/P_{rli31}*		Proteome Δ*rli31*/P_{rli31}*
					Fold change	p	Fold change NS[1]
lmo1148			Cobalamin synthase	Coenzyme transport and metabolism	**-2.26**	7.4E-02	
lmo1157			Propanediol dehydratase reactivation factor small subunit	Not in COGs	**-2.56**	6.2E-02	
lmo1241			putative exported protein	Function unknown			**1.72**
lmo1265			FIG00774764: hypothetical protein	Not in COGs	**1.73**	5.9E-02	
lmo1316	209	**cdsA**	Phosphatidate cytidylyltransferase	Lipid transport and metabolism			**2.02**
lmo1336		yqgN	5-formyltetrahydrofolate cycloligase	Coenzyme transport and metabolism	**2.37**	6.1E-03	**2.26**
lmo1354	215	yqhT	Aminopeptidase YpdF (MP-, MA-, MS-, AP-, NP- specific)	Amino acid transport and metabolism			**1.51**
lmo1418	231		Alkaline phosphodiesterase I / Nucleotide pyrophosphatase	General function prediction only			**1.63**
lmo1494	246	mtn	5'-methylthioadenosine nucleosidase / S-adenosylhomocysteine nucleosidase	Nucleotide transport and metabolism	**1.49**	3.6E-02	
lmo1600		**aroA**	Chorismate mutase I / 2-keto-3-deoxy-D-arabino-heptulosonate-7-phosphate synthase I beta	Amino acid transport and metabolism			**1.49**
lmo1701	296		FIG00774597: hypothetical protein	Not in COGs			**-1.54**
lmo1713		mreBH	Cell-shape determining protein MreBH	Cell cycle control, mitosis and meiosis			**1.72**
lmo1726	301	yulF	oxidoreductase, Gfo/Idh/MocA family	General function prediction only			**1.56**
lmo1743	306		FIG00774678: hypothetical protein	Not in COGs			**1.54**
lmo1850	327	ypoP	Transcriptional regulator, MarR family	Transcription			**-1.53**
lmo1867	331		Pyruvate,phosphate dikinase	Carbohydrate transport and metabolism			**1.73**
lmo1903			bacteriocin transport accessory protein	Posttranslational modification, protein turnover, chaperones; Energy production and conversion;	**1.59**	3.1E-03	
lmo1911	343	**dgcA**	GGDEF domain protein, DGC	Signal transduction mechanisms	**1.62**	2.0E-04	
lmo1912	343	**dgcB**	GGDEF domain protein, DGC	Signal transduction mechanisms	**1.55**	1.2E-02	
lmo1913	343	ydaJ	Lmo1913 protein	Not in COGs	**1.69**	5.5E-03	
lmo2055	372	ylbF	ComK regulator	Function unknown			**1.52**
lmo2067		yxeI	Choloylglycine hydrolase	Defense/virulence mechanisms			**1.61**
lmo2077	378	ydiC	Inactive homolog of metal-dependent proteases, putative molecular chaperone	Posttranslational modification, protein turnover, chaperones	**1.54**	2.7E-02	
lmo2150			FIG00774336: hypothetical protein	Not in COGs	**-1.71**	4.4E-02	
lmo2152	392		thioredoxin, putative	Posttranslational modification, protein turnover, chaperones; Energy production and conversion;			**1.72**
lmo2157		**sepA**	alkyl sulfatase	Secondary metabolites biosynthesis, transport and catabolism			**1.65**
lmo2183	396		Heme transporter IsdDEF, permease component IsdF	Inorganic ion transport and metabolism			**1.9**
lmo2184	396	ygaD	Heme transporter IsdDEF, lipoprotein IsdE	Inorganic ion transport and metabolism			**1.53**
lmo2186	396		NPQTN cell wall anchored protein IsdC	Cell wall/membrane biogenesis			**1.61**
lmo2199	398	ohrA	Organic hydroperoxide resistance protein	Posttranslational modification, protein turnover, chaperones			**1.5**
lmo2230			arsenate reductase	Signal transduction mechanisms			**1.5**
lmo2345	419	ytmO	Bacterial luciferase family protein YtmO, in cluster with L-cystine ABC transporter	Energy production and conversion			**2.82**
lmo2349	419	tycK	L-Cystine ABC transporter, periplasmic cystine-binding protein TcyK	Amino acid transport and metabolism; Signal transduction mechanisms;			**3.4**
lmo2407			FIG00774515: hypothetical protein	Not in COGs	**-1.72**	7.4E-02	**-2.72**

Locus tag	Operon	Name	RAST info	Function (COG)	Transcriptome Δ*rli31*/P_{rli31}*		Proteome Δ*rli31*/P_{rli31}*
					Fold change	p	Fold change NS[1]
lmo2463	436		FIG00774322: hypothetical protein	General function prediction only			**1.5**
lmo2522		yocH	Cell wall-binding protein	Cell wall/membrane biogenesis; Function unknown;			**-1.56**
lmo2575	462	czcD	Cobalt-zinc-cadmium resistance protein CzcD	Inorganic ion transport and metabolism	**1.72**	4.1E-02	
lmo2586	465	yrhE	Formate dehydrogenase related protein	General function prediction only	**1.77**	4.5E-02	
lmo2652		manR	PTS system, IIA component	Transcription; Carbohydrate transport and metabolism; Signal transduction mechanisms;			**1.75**
lmo2658	476	yhxD	Histone acetyltransferase HPA2 and related acetyltransferases	Transcription; General function prediction only;			**-1.65**
lmo2663	477	yjmD	Galactitol-1-phosphate 5-dehydrogenase	Amino acid transport and metabolism; General function prediction only;	**1.64**	6.0E-02	
<u>lmo2667</u>	477		PTS system, galactitol-specific IIA component	Carbohydrate transport and metabolism; Signal transduction mechanisms;	**1.6**	3.1E-02	**1.57**
lmo2691			Membrane-bound lytic murein transglycosylase D precursor	Cell wall/membrane biogenesis; Cell motility; Intracellular trafficking and secretion;			**1.6**
lmo2697	485		Phosphoenolpyruvate-dihydroxyacetone phosphotransferase	Function unknown			**1.57**
lmo2758		**guaB**	Inosine-5'-monophosphate dehydrogenase	Nucleotide transport and metabolism; General function prediction only;	**1.58**	3.6E-02	
lmo2805	508		hypothetical protein	Not in COGs	**-2.12**	3.6E-02	

[1] = changes in protein abundance are **non**-significant changes, [2] = detected in all P_{rli31}* samples but no peptide was found in Δ*rli31*, [3] = significant and 40.34 fold downregulated in Δ*rli31*/wt, RAST= Rapid Annotation using Subsystem Technology (database), COG=Clusters of Orthologous Groups (database), grey names=homologs of *B. subtilis* 169 (ListiWiki), gene names <u>underlined</u> = significant (p<0,01) but below 2-fold regulated in <u>wt/P_{rli31}*</u>

9. References

Andersson, D. I., Hughes. D. (2009) Gene amplification and adaptive evolution in bacteria. *Annu. Rev. Genet.* **43**, 167-195.

Archer, K. A., Durack, J., Portnoy, D. A. (2014) STING-dependent type I IFN production inhibits cell-mediated immunity to *Listeria monocytogenes*. *PLoS Pathog.* **10**, e1003861.

Arnaud, M., Chastanet, A., Débarbouillé, M. (2004) New vector for efficient allelic replacement in naturally non-transformable, low-GC-content, Gram-positive bacteria. *Appl. Environ. Microbiol.* **70**, 6887-6891.

Aziz, R. K., Bartels, D., Best, A. A., DeJongh, M., Disz, T., Edwards, R. A., Formsma, K., Gerdes, S., Glass, E. M., Kubal, M., *et al.* (2008) The RAST Server: Rapid Annotations using Subsystems Technology. *BMC Genomics.* **9**, 75.

Bai, Y., Yang, J., Zarrella, T. M., Zhang, Y., Metzger, D. W., Bai, G. (2014) Cyclic di-AMP impairs potassium uptake mediated by a cyclic di-AMP binding protein in *Streptococcus pneumoniae*. *J. Bacteriol.* **196**, 614-623.

Bai, Y., Yang, J., Zhou, X., Ding, X., Eisele, L. E., Bai, G. (2012) *Mycobacterium tuberculosis* Rv3586 (DacA) is a diadenylate cyclase that converts ATP or ADP into c-di-AMP. *PLoS one.* **7**, e35206.

Barb, A. W., Cort, J. R., Seetharaman, J., Lew, S., Lee, H. W., Acton, T., Xiao, R., Kennedy, M. A., Tong, L., Montelione, G. T., *et al.* (2010) Structures of domains I and IV from YbbR are representative of a widely distributed protein family. *Protein Sci.* **20**, 396-405.

Barreteau, H., Kovac, A., Boniface, A., Sova, M., Gobec, S., Blanot, D. (2008) Cytoplasmic steps of peptidoglycan biosynthesis. *FEMS Microbiol. Rev.* **32**, 168-207.

Barrick, J. E., Lenski, R. E. (2013) Genome dynamics during experimental evolution. *Nat. Rev. Genet.* **14**, 827-839.

Bécavin, C., Koutero, M., Tchitchek, N., Cerutti, F., Lechat, P., Maillet, N., Hoede, C., Chiapello, H., Gaspin, C., Cossart, P. (2017) Listeriomics: an interactive web platform for systems biology of *Listeria. mSystems.* **2**, e00186-16.

Bejerano-Sagie, M., Oppenheimer-Shaanan, Y., Berlatzky, I., Rouvinski, A., Meyerovich, M., Ben-Yehuda, S. (2006) A checkpoint protein that scans the chromosome for damage at the start of sporulation in *Bacillus subtilis*. *Cell.* **125**, 679-690.

Ben-Yehuda, S., Rudner, D. Z., Losick, R. (2003) RacA, a bacterial protein that anchors chromosomes to the cell poles. *Science.* **299**, 532-536.

Bi, W., Stambrook, P. J. (1997) CCR: a rapid and simple approach for mutation detection. *Nucleic Acids Res.* **25**, 2949-2951.

Blötz, C., Treffon, K., Kaever, V., Schwede, F., Hammer, E., Stülke, J. (2017) Identification of the components involved in cyclic di-AMP signaling in *Mycoplasma pneumoniae*. *Front. Microbiol.* **8**, 1328.

Bochner, B. R., Gadzinski, P., Panomitros, E. (2001) Phenotype MicroArrays for high-throughput phenotypic testing and assay of gene function. *Genome Res.* **11**, 1246-1255.

Boura, M., Keating, C., Royet, K., Paudyal, R., O'Donoghue, B., O'Byrne, C. P., Karatzas, K. (2016) Loss of SigB in *Listeria monocytogenes* strains EGD-e and 10403S confers hyperresistance to hydrogen peroxide in stationary phase under aerobic conditions. *Appl. Environ. Microbiol.* **82**, 4584-4591.

Bowman, L., Zeden, M. S., Schuster, C. F., Kaever, V., Gründling, A. (2016) New insights into the cyclic diadenosine monophosphate (c-di-AMP) degradation pathway and the requirement of the cyclic dinucleotide for acid stress resistance in *Staphylococcus aureus*. *J. Biol. Chem.* **291**, 26970-26986.

Burguière, P., Fert, J., Guillouard, I., Auger, S., Danchin, A., Martin-Verstraete, I. (2005) Regulation of the *Bacillus subtilis* ytmI operon, involved in sulfur metabolism. *J. Bacteriol.* **187**, 6019-6030.

Burke, T. P. (2018) The unexpected effects of the combination of antibiotics and immunity. *Cell.* **172**, 891-893.

Burke, T. P., Loukitcheva, A., Zemansky, J., Wheeler, R., Boneca, I. G., Portnoy, D. A. (2014) *Listeria monocytogenes* is resistant to lysozyme through the regulation, not the acquisition, of cell wall-modifying enzymes. *J. Bacteriol.* **196**, 3756-3767.

Burke, T. P., Portnoy, D. A. (2016) SpoVG is a conserved RNA-binding protein that regulates *Listeria monocytogenes* lysozyme resistance, virulence, and swarming motility. *mBio.* **7**, e00240.

Cagliero, C., Jin, D. J. (2013) Dissociation and re-association of RNA polymerase with DNA during osmotic stress response in *Escherichia coli*. *Nucleic Acids Res.* **41**, 315-326.

Callewaert, L., Michiels, C. W. (2010) Lysozymes in the animal kingdom. *J. Biosci.* **35**, 127-160.

Campeotto, I., Zhang, Y., Mladenov, M. G., Freemont, P. S., Gründling, A. (2015) Complex structure and biochemical characterization of the *Staphylococcus aureus* cyclic diadenylate monophosphate (c-di-AMP)-binding protein PstA, the founding member of a new signal transduction protein family. *J. Biol. Chem.* **290**, 2888-2901.

Campos, S. S., Ibarra-Rodriguez, J. R., Barajas-Ornelas, R. C., Ramírez-Guadiana, F. H., Obregón-Herrera, A., Setlow, P., Pedraza-Reyes, M. (2014) Interaction of apurinic/apyrimidinic endonucleases Nfo and ExoA with the DNA integrity scanning protein DisA in the processing of oxidative DNA damage during *Bacillus subtilis* spore outgrowth. *J. Bacteriol.* **196**, 568-578.

Cascante-Estepa, N., Gunka, K., Stülke, J. (2016) Localization of components of the RNA-degrading machine in *Bacillus subtilis*. *Front. Microbiol.* **7**, 1492.

Chen, L. H., Köseoğlu, V. K., Güvener, Z. T., Myers-Morales, T., Reed, J. M., D'Orazio, S. E., Miller, K. W., Gomelsky, M. (2014) Cyclic di-GMP-dependent signaling pathways in the pathogenic Firmicute *Listeria monocytogenes*. *PLoS Pathog.* **10**, e1004301.

Cheng, C., Wang, H., Ma, T., Han, X., Yang, Y., Sun, J., Chen, Z., Yu, H., Hang, Y., Liu, F., *et al.* (2018) Flagellar basal body structural proteins FlhB, FliM, and FliY are required for flagellar-associated protein expression in *Listeria monocytogenes*. *Front. Microbiol.* **9**, 208.

Chico-Calero, I., Suárez, M., González-Zorn, B., Scortti, M., Slaghuis, J., Goebel, W., Vázquez-Boland, J. A., European *Listeria* Genome Consortium. (2002) Hpt, a bacterial homolog of the microsomal glucose-6-phosphate translocase, mediates rapid intracellular proliferation in *Listeria*. *Proc. Natl. Acad. Sci. U.S.A.* **99**, 431–436.

Chin, K. H., Liang, J. M., Yang, J. G., Shih, M. S., Tu, Z. L., Wang, Y. C., Sun, X. H., Hu, N. J., Liang, Z. X., Dow, J. M., *et al.* (2015) Structural insights into the distinct binding mode of cyclic di-AMP with SaCpaA-RCK. *Biochemistry.* **54**, 4936-4951.

Choi, P. H., Sureka, K., Woodward, J. J., Tong, L. (2015) Molecular basis for the recognition of cyclic-di-AMP by PstA, a PII-like signal transduction protein. *Microbiologyopen*. **4**, 361-374.

Choi, P. H., Vu, T. M. N., Pham, H. T., Woodward, J. J., Turner, M. S., Tong, L. (2017) Structural and functional studies of pyruvate carboxylase regulation by cyclic di-AMP in lactic acid bacteria. *Proc. Natl. Acad. Sci. USA.* **114,** E7226-E7235.

Claessen, D., Emmins, R., Hamoen, L. W., Daniel, R. A., Errington, J., Edwards, D. H. (2008) Control of the cell elongation-division cycle by shuttling of PBP1 protein in *Bacillus subtilis*. *Mol. Microbiol.* **68**, 1029-1046.

Clarke, C. A., Scheurwater, E. M., Clarke, A. J. (2010) The vertebrate lysozyme inhibitor Ivy functions to inhibit the activity of lytic transglycosylase. *J. Biol. Chem.* **285**, 14843-14847.

Clemens, R., Zaschke-Kriesche, J., Khosa, S., Smits, S. (2018) Insight into two ABC transporter families involved in lantibiotic resistance. *Front. Mol. Biosci.* **4**, 91.

Commichau, F. M., Dickmanns, A., Gundlach, J., Ficner, R., Stülke, J. (2015) A jack of all trades: the multiple roles of the unique essential second messenger cyclic di-AMP. *Mol. Microbiol.* **97**, 189-204.

Commichau, F. M., Gibhardt, J., Halbedel, S., Gundlach, J., Stülke, J. (2018) A delicate connection: c-di-AMP affects cell Integrity by controlling osmolyte transport. *Trends Microbiol.* **26**, 175-185.

Commichau, F. M., Heidemann, J. L., Ficner, R., Stülke, J. (2019) Making and breaking of an essential poison: the cyclases and phosphodiesterases that produce and degrade the essential second messenger cyclic di-AMP in bacteria. *J. Bacteriol.* **201**, e00462-18.

Commichau, F. M., Rothe, F. M., Herzberg, C., Wagner, E., Hellwig, D., Lehnik-Habrink, M., Hammer, E., Völker, U., Stülke, J. (2009) Novel activities of glycolytic enzymes in *Bacillus subtilis*: interactions with essential proteins involved in mRNA processing. *Mol. Cell Proteom.* **8**, 1350-1360.

Commichau, F. M., Stülke, J. (2008) Trigger enzymes: bifunctional proteins active in metabolism and in controlling gene expression. *Mol. Microbiol.* **67**, 692-702.

Corrigan, R. M., Abbott, J. C., Burhenne, H., Kaever, V., Gründling, A. (2011) c-di-AMP is a new second messenger in *Staphylococcus aureus* with a role in controlling cell size and envelope stress. *PLoS Pathog.* **7**, e1002217.

Corrigan, R. M., Bowman, L., Willis, A. R., Kaever, V., Gründling, A. (2015) Cross-talk between two nucleotide-signaling pathways in *Staphylococcus aureus*. *J. Biol. Chem.* **290**, 5826-5839.

Corrigan, R. M., Campeotto, I., Jeganathan, T., Roelofs, K. G., Lee, V. T., Gründling, A. (2013) Systematic identification of conserved bacterial c-di-AMP receptor proteins. *Proc. Natl. Acad. Sci. U.S.A.* **110**, 9084-9089.

Corrigan, R. M., Gründling, A. (2013) Cyclic di-AMP: another second messenger enters the fray. *Nat. Rev. Microbiol.* **11**, 513-524.

Dar, D., Shamir, M., Mellin, J. R., Koutero, M., Stern-Ginossar, N., Cossart, P., Sorek, R. (2016) Term-seq reveals abundant ribo-regulation of antibiotics resistance in bacteria. *Science.* **352**, aad9822.

de las Heras, A., Cain, R. J., Bielecka, M. K., Vázquez-Boland, J. A. (2011) Regulation of *Listeria* virulence: PrfA master and commander. *Curr. Opin. Microbiol.* **14**, 118–127.

Dengler, V., McCallum, N., Kiefer, P., Christen, P., Patrignani, A., Vorholt, J. A., Berger-Bächi, B., Senn, M. M. (2013) Mutation in the c-di-AMP cyclase *dacA* affects fitness and resistance of methicillin resistant *Staphylococcus aureus*. *PLoS one.* **8**, e73512.

Devaux, L., Sleiman, D., Mazzuoli, M.-V., Gominet, M., Lanotte, P., Trieu-Cuot, P., Kaminski, P.-A., Firon, A. (2018) Cyclic di-AMP regulation of osmotic homeostasis is essential in Group B *Streptococcus*. *PLoS Genet.* **14**, e1007342.

Dons, L., Rasmussen, O. F., Olsen, J.E. (1992) Cloning and characterization of a gene encoding flagellin of *Listeria monocytogenes*. *Mol. Microbiol.* **6**, 2919-2929.

Dussurget, O., Cabanes, D., Dehoux, P., Lecuit, M., Buchrieser, C., Glaser, P., Cossart, P. (2002) *Listeria monocytogenes* bile salt hydrolase is a PrfA-regulated virulence factor involved in the intestinal and hepatic phases of listeriosis. *Mol. Microbiol.* **45**, 1095-1106.

Elbakush, A. M., Miller, K. W., Gomelsky, M. (2018) CodY-mediated c-di-GMP-dependent inhibition of mammalian cell invasion in *Listeria monocytogenes*. *J. Bacteriol.* **200**, e00457-17.

Even, S., Burguière, P., Auger, S., Soutourina, O., Danchin, A., Martin-Verstraete, I. (2006) Global control of cysteine metabolism by CymR in *Bacillus subtilis. J. Bacteriol.* **188**, 2184-2197.

Farber, J. M., Peterkin, P. I. (1991) *Listeria monocytogenes*, a food-borne pathogen. *Microbiol. Rev.* **55**, 476-511.

Fedorov, R., Meshcheryakov, V., Gongadze, G., Fomenkova, N., Nevskaya, N., Selmer, M., Laurberg, M., Kristensen, O., Al-Karadaghi, S., Liljas, A., *et al.* (2001) Structure of ribosomal protein TL5 complexed with RNA provides new insights into the CTC family of stress proteins. *Acta Crystallogr. D.* **57***, 968–976.*

Feehily, C., O'Byrne, C. P., Karatzas, K. A. (2013) Functional γ-aminobutyrate shunt in *Listeria monocytogenes*: role in acid tolerance and succinate biosynthesis. *Appl. Environ. Microbiol.* **79**, 74-80.

Foster, A. W., Osman, D., Robinson, N. J. (2014) Metal preferences and metallation. *J.Biol. Chem.* **289**, 28095-29103.

Freitag, N. E., Port, G. C., Miner, M. D. (2009) *Listeria monocytogenes* - from saprophyte to intracellular pathogen. *Nat. Rev. Microbiol.* **7**, 623-628.

Fritsch, F., Mauder, N., Williams, T., Weiser, J., Oberle, M., Beier, D. (2011) The cell envelope stress response mediated by the $LiaFSR_{Lm}$ three-component system of *Listeria monocytogenes* is controlled via the phosphatase activity of the bifunctional histidine kinase $LiaS_{Lm}$. *Microbiology.* **157**, 373-386.

Gándara, C., Alonso, J. C. (2015) DisA and c-di-AMP act at the intersection between DNA-damage response and stress homeostasis in exponentially growing *Bacillus subtilis* cells. *DNA Repair (Amst.).* **27**, 1-8.

Gándara, C., de Lucena, D. K. C., Torres, R., Serrano, E., Altenburger, S., Graumann, P. L., Alonso, J. C. (2017) Activity and in vivo dynamics of *Bacillus subtilis* DisA are affected by RadA/Sms and by holliday junction-processing proteins. *DNA Repair (Amst.).* **55**, 17-30.

Gao, A., Serganov, A. (2014) Structural insights into recognition of c-di-AMP by the *ydaO* riboswitch. *Nat. Chem. Biol.* **10**, 787-792.

Gao, X., Mukherjee, S., Matthews, P. M., Hammad, L. A., Kearns, D. B., Dann, C. E. (2013) Functional characterization of core components of the *Bacillus subtilis* cyclic-di-GMP signaling pathway. *J. Bacteriol.* **195**, 4782-4792.

Gardan, R., Cossart, P., Labadie, J., European *Listeria* Genome Consortium. (2003) Identification of *Listeria monocytogenes* genes involved in salt and alkaline-pH tolerance. *Appl. Environ. Microbiol.* **69**, 3137-3143.

Gay, P., Le Coq, D., Steinmetz, M., Ferrari, E., Hoch, J. A. (1983) Cloning structural gene *sacB*, which codes for exoenzyme levansucrase of *Bacillus subtilis*: expression of the gene in *Escherichia coli. J. Bacteriol.* **153**, 1424-1431.

Geiger, T., Wolz, C. (2014) Intersection of the stringent response and the CodY regulon in low GC Gram-positive bacteria. *Int. J. Med. Microbiol.* **304**, 150-155.

Gertz, S., Engelmann, S., Schmid, R., Ohlsen, K., Hacker, J., Hecker, M. (1999) Regulation of σ^B-dependent transcription of *sigB* and *asp23* in two different *Staphylococcus aureus* strains. *Mol. Gen. Genet.* **261**, 558-566.

Gibhardt, J. (2015) Cyclic di-AMP metabolism and osmoregulation in *Listeria monocytogenes*. Master's thesis. *Georg-August-Universität Göttingen.*

Glaser, P., Frangeul, L., Buchrieser, C., Rusniok, C., Amend, A., Baquero, F., Berche, P., Bloecker, H., Brandt, P., Chakraborty, T. *et al.* (2001) Comparative genomics of *Listeria* species. *Science.* **294**, 849-852.

Gomelsky M. (2011) cAMP, c-di-GMP, c-di-AMP and now cGMP: bacteria use them all!. *Mol. Microbiol.* **79**, 562-565.

Gray, M. L., Killinger, A. H. (1966) *Listeria monocytogenes* and listeric infections. *Bacteriol. Rev.* **30**, 309–382.

Gray, W. T., Govers, S. K., Xiang, Y., Parry, B. R., Campos, M., Kim, S., Jacobs-Wagner, C. (2018) Nucleoid size scaling and intracellular organization of translation across-bacteria. *bioRxiv.* 479840.

Groisman, E. A., Hollands, K., Kriner, M. A., Lee, E. J., Park, S. Y., Pontes, M. H. (2013) Bacterial Mg^{2+} homeostasis, transport, and virulence. *Annu. Rev. Genet.* **47**, 625-646.

Gründling, A. (2013) Potassium uptake systems in *Staphylococcus aureus*: new stories about ancient systems. *mBio*. **4**, e00784-13.

Gründling, A., Burrack, L. S., Bouwer, H. G., Higgins, D. E. (2004) *Listeria monocytogenes* regulates flagellar motility gene expression through MogR, a transcriptional repressor required for virulence. *Proc. Natl. Acad. Sci. U.S.A.* **101**, 12318-12323.

Gueriri, I., Cyncynatus, C., Dubrac, S., Arana, A. T., Dussurget, O., Msadek, T. (2008) The DegU orphan response regulator of *Listeria monocytogenes* autorepresses its own synthesis and is required for bacterial motility, virulence and biofilm formation. *Microbiology.* **154**, 2251-2264.

Guérout-Fleury, A. M., Shazand, K., Frandsen, N., Stragier, P. (1995) Antibiotic-resistance cassettes for *Bacillus subtilis*. *Gene*. **167**, 335-336.

Gundlach, J., Dickmanns, A., Schröder-Tittmann, K., Neumann, P., Kaesler, J., Kampf, J., Herzberg, C., Hammer, E., Schwede, F., Kaever, V., *et al.* (2015) Identification, characterization, and structure analysis of the cyclic di-AMP-binding PII-like signal transduction protein DarA. *J. Biol. Chem.* **290**, 3069-3080.

Gundlach, J., *et al.* (2019) unpublished.

Gundlach, J., Herzberg, C., Kaever, V., Gunka, K., Hoffmann, T., Weiß, M., Gibhardt, J., Thürmer, A., Hertel, D., Daniel, R., *et al.* (2017) Control of potassium homeostasis is an essential function of the second messenger cyclic di-AMP in *Bacillus subtilis*. *Sci. Signal.* **10**, eaal3011.

Gundlach, J., Mehne, F. M., Herzberg, C., Kampf, J., Valerius, O., Kaever, V., Stülke, J. (2015) An essential poison: synthesis and degradation of cyclic di-AMP in *Bacillus subtilis*. *J. Bacteriol.* **197**, 3265-3274.

Gundlach, J., Rath, H., Herzberg, C., Mäder, U., Stülke, J. (2016) Second messenger signaling in *Bacillus subtilis*: accumulation of cyclic di-AMP inhibits biofilm formation. *Front. Microbiol.* **7**, 804.

Guzman, L. M., Belin, D., Carson, M. J., Beckwith, J. (1995) Tight regulation, modulation, and high-level expression by vectors containing the arabinose P_{BAD} promoter. *J. Bacteriol.* **177**, 4121-4130.

Halbedel, S., Hahn, B., Daniel, R. A., Flieger, A. (2012) DivIVA affects secretion of virulence-related autolysins in *Listeria monocytogenes*. *Mol. Microbiol.* **83**, 821-839.

Hauf, S., Herrmann, J., Miethke, M., Gibhardt, J., Commichau, F. M., Müller, R., Fuchs, S., Halbedel, S. (2019) Aurantimycin resistance genes contribute to survival of *Listeria monocytogenes* during life in the environment. *Mol. Microbiol.* doi: 10.1111/mmi.14205.

Hengge, R. (2009) Principles of c-di-GMP signaling in bacteria. *Nat. Rev. Micribiol.* **7**, 263-273.

Hengge, R., Gründling, A., Jenal, U., Ryan, R., Yildiz, F. (2015) Bacterial signal transduction by cyclic di-GMP and other nucleotide second messengers. *J. Bacteriol.* **198**, 15-26.

Hoffmann, T., Boiangiu, C., Moses, S., Bremer, E. (2008) Responses of *Bacillus subtilis* to hypotonic challenges: physiological contributions of mechanosensitive channels to cellular survival. *Appl. Environ. Microbiol.* **74**, 2454-2460.

Holtmann, G., Bakker, E. P., Uozumi, N., Bremer, E. (2003) KtrAB and KtrCD: two K^+ uptake systems in *Bacillus subtilis* and their role in adaptation to hypertonicity. *J. Bacteriol.* **185**, 1289-1298.

Horak, J., Wolf, D. H. (1997) Catabolite inactivation of the galactose transporter in the yeast *Saccharomyces cerevisiae*: ubiquitination, endocytosis, and degradation in the vacuole. *J. Bacteriol.* **179**, 1541-1549.

Horton, R. M., Cai, Z. L., Ho, S. N., Pease, L. R. (1990) Gene splicing by overlap extension: tailor-made genes using the polymerase chain reaction. *Biotechniques*. **8**, 528-535.

Huynh, T. N., Choi, P. H., Sureka, K., Ledvina, H. E., Campillo, J., Tong, L., Woodward, J. J. (2016) Cyclic di-AMP targets the cystathionine beta-synthase domain of the osmolyte transporter OpuC. *Mol. Microbiol.* **102**, 233-243.

Huynh, T. N., Luo, S., Pensinger, D., Sauer, J. D., Tong, L., Woodward, J. J. (2015) An HD-domain phosphodiesterase mediates cooperative hydrolysis of c-di-AMP to affect bacterial growth and virulence. *Proc. Natl. Acad. Sci. U.S.A.* **112**, E747-E756.

Huynh, T. N., Woodward, J. J. (2016) Too much of a good thing: regulated depletion of c-di-AMP in the bacterial cytoplasm. *Curr. Opin. Microbiol.* **30**, 22-29.

Kalia, D., Merey, G., Nakayama, S., Zheng, Y., Zhou, J., Luo, Y., Guo, M., Roembke, B. T., Sintim, H. O. (2013) Nucleotide, c-di-GMP, c-di-AMP, cGMP, cAMP, (p)ppGpp signaling in bacteria and implications in pathogenesis. *Chem. Soc. Rev.* **42**, 305–341.

Kamp, H. D., Higgins, D. E. (2009) Transcriptional and post-transcriptional regulation of the GmaR antirepressor governs temperature-dependent control of flagellar motility in *Listeria monocytogenes*. *Mol. Microbiol.* **74**, 421-425.

Kamp, H. D., Higgins, D. E. (2011) A protein thermometer controls temperature-dependent transcription of flagellar motility genes in *Listeria monocytogenes. PLoS Pathog.* **7**, e1002153.

Kaplan Zeevi, M., Shafir, N. S., Shaham, S., Friedman, S., Sigal, N., Nir Paz, R., Boneca, I. G., Herskovits, A. A. (2013) *Listeria monocytogenes* multidrug resistance transporters and cyclic di-AMP, which contribute to type I interferon induction, play a role in cell wall stress. *J. Bacteriol.* **195**, 5250-5261.

Karimova, G., Pidoux, J., Ullmann, A., Ladant, D. (1998) A bacterial two-hybrid system based on a reconstituted signal transduction pathway. *Proc. Natl. Acad. Sci. U.S.A.* **95**, 5752-5756.

Karimova, G., Robichon, C., Ladant, D. (2009) Characterization of YmgF, a 72-residue inner membrane protein that associates with the *Escherichia coli* cell division machinery. *J. Bacteriol.* **191**, 333-346.

Kawai, Y., Mickiewicz, K., Errington, J. (2018) Lysozyme counteracts β-lactam antibiotics by promoting the emergence of L-form bacteria. *Cell.* **172**, 1038-1049.e10.

Kearse, M., Moah, R., Wilson, A., Stones-Havas, S., Cheung, M., Sturrock, S. Buxton, S., Cooper, A., Markowitz, S., Duran, C., *et al.* (2012) Geneious basic: an integrated and extendable desktop software platform for the organization and analysis of sequence data. *Bioinformatics* **28**, 1647-1649.

Kellenberger, C. A., Chen, C., Whiteley, A. T., Portnoy, D. A., Hammond, M. C. (2015) RNA-based fluorescent biosensors for live cell imaging of second messenger cyclic di-AMP. *J. Am. Chem. Soc.* **137**, 6432-6435.

Kempf, B., Bremer, E. (1998) Stress responses of *Bacillus subtilis* to high osmolarity environments: uptake and synthesis of osmoprotectants. *J. Biosci.* **23**, 447-455.

Kersey, P. J., Allen, J. E., Allot, A., Barba, M., Boddu, S., Bolt, B. J., Carvalho-Silva, D., Christensen, M., Davis, P., Grabmueller, C., *et al.* (2017) Ensembl Genomes 2018: an integrated omics infrastructure for non-vertebrate species. *Nucleic Acids Res.* **46**, D802-D808.

Kim, H., Youn, S. J., Kim, S. O., Ko, J., Lee, J. O., Choi, B. S. (2015) Structural studies of potassium transport protein KtrA regulator of conductance of K^+ (RCK) C domain in complex with cyclic diadenosine monophosphate (c-di-AMP). *J. Biol. Chem.* **290**, 16393-16402.

Ko, R., Smith, L. T., Smith, G. M. (1994) Glycine betaine confers enhanced osmotolerance and cryotolerance on *Listeria monocytogenes*. *J. Bacteriol.* **176**, 426-431.

Korolev, N., Lyubartsev, A. P., Rupprecht, A., Nordenskiöld, L. (1999) Competitive binding of Mg^{2+}, Ca^{2+}, Na^+, and K^+ ions to DNA in oriented DNA fibers: experimental and Monte Carlo simulation results. *Biophys. J.* **77**, 2736-2749.

Köseoğlu, V. K., Heiss, C., Azadi, P., Topchiy, E., Güvener, Z. T., Lehmann, T. E., Miller, K. W., Gomelsky, M. (2015) *Listeria monocytogenes* exopolysaccharide: origin, structure, biosynthetic machinery and c-di-GMP-dependent regulation. *Mol. Microbiol.* **96**, 728-743.

Nollet, J. (1748) *Recherches sur les causes du bouillonnement des liquides.* In: *Mémoires de Mathématique et de Physique, tirés des registres de l'Académie Royale des Sciences de l'année 1748.* 57–104.

Laxminarayan, R., Duse, A., Wattal, C., Zaidi, A. K. M., Wertheim, H. F. L., Sumpradit, N., Vlieghe, E., Hara, G. L., Gould, I. M., Goossens, H., *et al.* (2013) Antibiotic resistance-the need for global solutions. *Lancet. Infect. Dis.* **13**, 1057–1098.

Lima, A., Durán, R., Schujman, G. E., Marchissio, M. J., Portela, M. M., Obal, G., Pritsch, O., de Mendoza, D., Cerveñansky, C. (2011) Serine/threonine protein kinase PrkA of the human pathogen *Listeria monocytogenes*: biochemical characterization and identification of interacting partners through proteomic approaches. *J. Proteom.* **74**, 1720–1734.

Lobel, L., Herskovits, A. A. (2016) Systems level analyses reveal multiple regulatory activities of CodY controlling metabolism, motility and virulence in *Listeria monocytogenes*. *PLoS Genet.* **12**, e1005870.

Lobel, L., Sigal, N., Borovok, I., Belitsky, B. R., Sonenshein, A. L., Herskovits, A. A. (2015) The metabolic regulator CodY links *Listeria monocytogenes* metabolism to virulence by directly activating the virulence regulatory gene *prfA*. *Mol. Microbiol.* **95**, 624–644.

López-Maury, L., Marguerat, S., Bähler, J. (2008) Tuning gene expression to changing environments: from rapid responses to evolutionary adaptation. *Nat. Rev. Genet.* **9**, 583-593.

Low, J. C., Donachie, W. (1997) A review of *Listeria monocytogenes* and listeriosis. *Vet. J.* **153**, 9–29.

Lu, M., Steitz, T. A. (2000) Structure of *Escherichia coli* ribosomal protein L25 complexed with a 5S rRNA fragment at 1.8-Å resolution. *Proc. Natl. Acad. Sci. U.S.A.* **97**, 2023-2038.

Luo, Y., Helmann, J. D. (2012) Analysis of the role of *Bacillus subtilis* σ^M in β-lactam resistance reveals an essential role for c-di-AMP in peptidoglycan homeostasis. *Mol. Microbiol.* **83**, 623-639.

Manikandan, K., Sabareesh, V., Singh, N., Saigal, K., Mechold, U., Sinha, K. M. (2014) Two-step synthesis and hydrolysis of cyclic di-AMP in *Mycobacterium tuberculosis*. *PLoS one.* **9**, e86096.

Manson, M. D., Tedesco, P., Berg, H. C., Harold, F. M., van der Drift, C. (1977) A protonmotive force drives bacterial flagella. *Proc. Natl. Acad. Sci. U.S.A.* **74**, 3060-3064.

Manuse, S., Fleurie, A., Zucchini, L., Lesterlin, C., Grangeasse, C. (2016) Role of eukaryotic-like serine/threonine kinases in bacterial cell division and morphogenesis. *FEMS Microbiol. Rev.* **40**, 41-56.

Martínez-Antonio, A., Medina-Rivera, A., Collado-Vides, J. (2009) Structural and functional map of a bacterial nucleoid. *Genome Biol.* **10**, 247.

Mauder, N., Williams, T., Fritsch, F., Kuhn, M., Beier, D. (2008) Response regulator DegU of *Listeria monocytogenes* controls temperature-responsive flagellar gene expression in its unphosphorylated state. *J. Bacteriol.* **190**, 4777-4781.

McFarland, A. P., Burke, T. P., Carletti, A. A., Glover, R. C., Tabakh, H., Welch, M. D., Woodward, J. J. (2018) RECON-dependent inflammation in hepatocytes enhances *Listeria monocytogenes* cell-to-cell spread. *mBio.* **9**, e00526-18.

McFarland, A. P., Luo, S., Ahmed-Qadri, F., Zuck, M., Thayer, E. F., Goo, Y. A., Hybiske, K., Tong, L., Woodward, J. J. (2017) Sensing of bacterial cyclic dinucleotides by the oxidoreductase RECON promotes NF-κB activation and shapes a proinflammatory antibacterial state. *Immunity.* **46**, 433-445.

Mehne, F. M. P. (2014) Bildung und Homöostase von c-di-AMP in *Bacillus subtilis*. Dissertation. *Georg-August-Universität Göttingen*. http://hdl.handle.net/11858/00-1735-0000-0022-5F16-8, accessed 03.02.2019.

Mehne, F. M. P., Gunka, K., Eilers, H., Herzberg, C., Kaever, V., Stülke, J. (2013) Cyclic di-AMP homeostasis in *Bacillus subtilis*: both lack and high level accumulation of the nucleotide are detrimental for cell growth. *J. Biol. Chem.* **288**, 2004-2017.

Mehne, F. M., Schröder-Tittmann, K., Eijlander, R. T., Herzberg, C., Hewitt, L., Kaever, V., Lewis, R. J., Kuipers, O. P., Tittmann, K., Stülke, J. (2014) Control of the diadenylate cyclase CdaS in *Bacillus subtilis*: an autoinhibitory domain limits cyclic di-AMP production. *J. Biol. Chem.* **289**, 21098-21107.

Mellin, J. R., Cossart, P. (2012) The non-coding RNA world of the bacterial pathogen *Listeria monocytogenes. RNA Biol.* **9**, 372-378.

Mengaud, J., Dramsi, S., Gouin, E., Vazquez-Boland, J. A., Milon, G., Cossart, P. (1991) Pleiotropic control of *Listeria monocytogenes* virulence factors by a gene that is autoregulated. *Mol. Microbiol.* **5**, 2273–2283.

Mengin-Lecreulx, D., van Heijenoort, J. (1996) Characterization of the essential gene *glmM* encoding phosphoglucosamine mutase in *Escherichia coli*. *J. Biol. Chem.* **271**, 32-39.

Merzbacher, M., Detsch, C., Hillen, W., Stülke, J. (2004) *Mycoplasma pneumoniae* HPr kinase/phosphorylase. *Eur. J. Biochem.* **271**, 367-374.

Meury, J., Kohiyama, M. (1992) Potassium ions and changes in bacterial DNA supercoiling under osmotic stress. *FEMS Microbiol. Lett.* **99**, 159-164.

Misra, G., Rojas, E. R., Gopinathan, A., Huang, K. C. (2013) Mechanical consequences of cell-wall turnover in the elongation of a Gram-positive bacterium. *Biophys. J.* **104**, 2342-2352.

Monchois, V., Abergel, C., Sturgis, J., Jeudy, S., Claverie, J. M. (2001) *Escherichia coli ykfE* ORFan gene encodes a potent inhibitor of c-type lysozyme. *J. Biol. Chem.* **276**, 18437–18441.

Monk, I. R., Gahan, C. G., Hill, C. (2008) Tools for functional postgenomic analysis of *Listeria monocytogenes*. *Appl. Environ. Microbiol.* **74**, 3921-3934.

Moscoso, J. A., Schramke, H., Zhang, Y., Tosi, T., Dehbi, A., Jung, K., Gründling, A. (2016) Binding of cyclic di-AMP to the *Staphylococcus aureus* sensor kinase KdpD occurs via the universal stress protein domain and downregulates the expression of the Kdp potassium transporter. *J. Bacteriol.* **198**, 98-110.

Mukherjee, S., Kearns, D. B. (2014) The structure and regulation of flagella in *Bacillus subtilis. Annu. Rev. Genet.* **48**, 319-340.

Müller, M., Deimling, T., Hopfner, K. P., Witte, G. (2015) c-di-AMP recognition by *Staphylococcus aureus* PstA. *FEBS Lett.* **589**, 45-51.

Müller, M., Deimling, T., Hopfner, K. P., Witte, G. (2015) Structural analysis of the diadenylate cyclase reaction of DNA-integrity scanning protein A (DisA) and its inhibition by 3'-dATP. *Biochem. J.* **469**, 367-374.

Munita, J. M., Arias, C. A. (2016) Mechanisms of antibiotic resistance. *Microbiol. Spectr.* **4**, VMBF-0016-2015.

Murray, E. G. D., Webb, R. A., Swann, M. B. R. (1926) A disease of rabbits characterised by a large mononuclear leucocytosis, caused by a hitherto undescribed *Bacillus Bacterium monocytogenes* (n.sp.). *J. Pathol. Bacteriol.* **29**, 407–439.

Nelson, J. W., Sudarsan, N., Furukawa, K., Weinberg, Z., Wang, J. X., Breaker, R. R. (2013) Riboswitches in eubacteria sense the second messenger c-di-AMP. *Nat. Chem. Biol.* **9**, 834-839.

Newton, A. C., Bootman, M. D., Scott, J. D. (2016) Second messengers. *Cold Spring Harb Perspect Biol.* **8**, a005926.

Nicolas, P., Maeder, U., Dervyn, E., Rochat, T., Leduc, A., Pigeonneau, N., Bidnenko, E., Marchadier, E., Hoebeke, M., Aymerich, S., *et al.* (2012) Condition-dependent transcriptome reveals high-level regulatory architecture in *Bacillus subtilis*. *Science.* **335**, 1103–1106.

Nierhaus K. H. (2014) Mg^{2+}, K^{+}, and the ribosome. *J. Bacteriol.* **196**, 3817-3819.

Omasits, U., Ahrens, C. H., Müller, S., Wollscheid, B. (2014) Protter: interactive protein feature visualization and integration with experimental proteomic data. *Bioinformatics*. **30**, 884-886.

Oppenheimer-Shaanan, Y., Wexselblatt, E., Katzhendler, J., Yavin, E., and Ben-Yehuda, S. (2011) c-di-AMP reports DNA integrity during sporulation in *Bacillus subtilis*. *EMBO Rep.* **12**, 594–601.

Pasi, M., Maddocks, J. H., Lavery, R. (2015) Analyzing ion distributions around DNA: sequence-dependence of potassium ion distributions from microsecond molecular dynamics. *Nucleic Acids Res.* **43**, 2412-2423.

Patro, R., Duggal, G., Love, M. I., Irizarry, R. A., Kingsford, C. (2017) Salmon provides fast and bias-aware quantification of transcript expression. *Nat. Methods.* **14**, 417-419.

Peel, M., Donachie, W., Shaw, A. (1988) Temperature-dependent expression of flagella of *Listeria monocytogenes* studied by electron microscopy, SDS-PAGE and western blotting. *J. Gen. Microbiol.* **134**, 2171-2178.

Pesavento, C., Becker, G., Sommerfeldt, N., Possling, A., Tschowri, N., Mehlis, A., Hengge, R. (2008) Inverse regulatory coordination of motility and curli-mediated adhesion in *Escherichia coli*. *Genes Dev.*, **22**, 2434-2446.

Pham, H. T., Nhiep, N. T. H., Vu, T. N. M., Huynh, T. N., Zhu, Y., Huynh, A. L. D., Chakrabortti, A., Marcellin, E., Lo, R., Howard, C. B., *et al.* (2018) Enhanced uptake and potassium or glycine betaine or export of cyclic-di-AMP restores osmoresistance in a high cyclic-di-AMP *Lactococcus lactis* mutant. *PLoS Genet.* **14,** e1007574.

Pirie, J. H. H. (1940) *Listeria*: change of Name for a Genus Bacteria. *Nature.* **145**, 164.

Poolman, B., Spitzer, J. J., Wood, J. M. (2004) Bacterial osmosensing: roles of membrane structure and electrostatics in lipid-protein and protein-protein interactions. *Biochim. Biophys. Acta.* **1666**, 88–104.

Price-Whelan, A., Poon, C. K., Benson, M. A., Eidem, T. T., Roux, C. M., Boyd, J. M., Dunman, P. M., Torres, V. J., Krulwich, T. A. (2013) Transcriptional profiling of *Staphylococcus aureus* during growth in 2 M NaCl leads to clarification of physiological roles for Kdp and Ktr K^+ uptake systems. *mBio*. **4**, e00407-13.

Quintana, I. M., Gibhardt, J., Turdiev, A., Hammer, E., Commichau, F. M., Lee, V. T., Magni, C., Stülke, J. (2019) The KupA and KupB proteins of *Lactococcus lactis* IL1403 are novel c-di-AMP receptor proteins responsible for potassium uptake. *J. Bacteriol.* doi: 10.1128/JB.00028-19.

Radeck, J., Fritz, G., Mascher, T. (2017) The cell envelope stress response of *Bacillus subtilis*: from static signaling devices to dynamic regulatory network. *Curr. Genet.* **65**, 79-90.

Ragland, S. A., Criss, A. K. (2017) From bacterial killing to immune modulation: recent insights into the functions of lysozyme. *PLoS Pathog.* **13**, e1006512.

Raguse, M., Torres, R., Seco E. M., Gándara, C., Ayora, S., Moeller, R., Alonso, J. C. (2017) *Bacillus subtilis* DisA helps to circumvent replicative stress during spore revival. *DNA Repair (Amst.).* **59**, 57-68.

Rall, T. W., Sutherland, E. W. (1958) Formation of a cyclic adenine ribonucleotide by tissue particles. *J. Biol. Chem.* **232**, 1065–1076.

Rall, T. W., Sutherland, E. W., Wosilait, W. D. (1956) The relationship of epinephrine and glucagon to liver phosphorylase. III. Reactivation of liver phosphorylase in slices and in extracts. *J. Biol. Chem.* **218**, 483-495.

Rao, F., Ji, Q., Soehano, I., Liang, Z. X. (2011) Unusual heme-binding PAS domain from YybT family proteins. *J. Bacteriol.* **193**, 1543-1551.

Rao, F., See, R. Y., Zhang, D., Toh, D. C., Ji, Q., Liang, Z. X. (2010) YybT is a signaling protein that contains a cyclic dinucleotide phosphodiesterase domain and a GGDEF domain with ATPase activity. *J. Biol. Chem.* **285**, 473-482.

Reniere, M. L., Whiteley, A. T., Hamilton, K. L., John, S. M., Lauer, P., Brennan, R. G., Portnoy, D. A. (2015) Glutathione activates virulence gene expression of an intracellular pathogen. *Nature.* **517**, 170–173.

Rismondo, J., Gibhardt, J., Rosenberg, J., Kaever, V., Halbedel, S., Commichau, F. M. (2016) Phenotypes associated with the essential diadenylate cyclase CdaA and its potential regulator CdaR in the human pathogen *Listeria monocytogenes*. *J. Bacteriol.* **198**, 416-426.

Rocha, R., Teixeira-Duarte, C. M., Jorge, J. M. P., Morais-Cabral, J. H. (2019) Characterization of the molecular properties of KtrC, a second RCK domain that regulates a Ktr channel in *Bacillus subtilis*. *J. Struct. Biol.* doi: 10.1016/j.jsb.2019.02.002.

Roelofs, K. G., Wang, J., Sintim, H. O., Lee, V. T. (2011) Differential radial capillary action of ligand assay for high-throughput detection of protein-metabolite interactions. *Proc. Natl. Acad. Sci. U.S.A.* **108**, 15528-15533.

Rojas, E. R., Huang, K. C. (2018) Regulation of microbial growth by turgor pressure. *Curr. Opin. Microbiol.* **42**, 62-70.

Rojas, E., Theriot, J. A., Huang, K. C. (2014) Response of *Escherichia coli* growth rate to osmotic shock. *Proc. Natl. Acad. Sci. U.S.A.* **111**, 7807-7812.

Rolhion, N., Cossart, P. (2017) How the study of *Listeria monocytogenes* has led to new concepts in biology. *Future Microbiol.* **12**, 621-638.

Romeo, Y., Bouvier, J., Gutierrez, C. (2007) Osmotic regulation of transcription in *Lactococcus lactis*: ionic strength-dependent binding of the BusR repressor to the *busA* promoter. *FEBS Lett.* **581**, 3387-3390.

Rosenberg, J., Dickmanns, A., Neumann, P., Gunka, K., Arens, J., Kaever, V., Stülke, J., Ficner, R., Commichau, F. M. (2015) Structural and biochemical analysis of the essential diadenylate cyclase CdaA from *Listeria monocytogenes*. *J. Biol. Chem.* **290**, 6596-6606.

Roux, M., Bloom, M. (1990) Ca^{2+}, Mg^{2+}, Li^{+}, Na^{+}, and K^{+} distributions in the headgroup region of binary membranes of phosphatidylcholine and phosphatidylserine as seen by deuterium NMR. *Biochemistry.* **31**, 7077-7089.

Rubin, B. E., Huynh, T. N., Welkie, D. G., Diamond, S., Simkovsky, R., Pierce, E. C., Taton, A., Lowe, L. C., Lee, J. J., Rifkin, S. A., *et al.* (2018) High-throughput interaction screens illuminate the role of c-di-AMP in cyanobacterial nighttime survival. *PLoS Genet.* **14**, e1007301.

Sambrook, J., Maniatis, T., Fritsch, E. F. (1989) *Molecular cloning: a laboratory manual*, 2nd Ed., Cold Spring Harbor Laboratory Press, New York.

Santos, J. S., Asmar-Rovira, G. A., Han, G. W., Liu, W., Syeda, R., Cherezov, V., Baker, K. A., Stevens, R. C., Montal, M. (2012) Crystal structure of a voltage-gated K^{+} channel pore module in a closed state in lipid membranes. *J. Biol. Chem.* **287**, 43063-43070.

Santos, J. S., Grigoriev, S. M., Montal, M. (2008) Molecular template for a voltage sensor in a novel K^{+} channel. III. Functional reconstitution of a sensor-less pore module from a prokaryotic Kv channel. *J. Gen. Physiol.* **132**, 651-666.

Sarenko, O., Klauck, G., Wilke, F. M., Pfiffer, V., Richter, A. M., Herbst, S., Kaever, V., Hengge, R. (2017) More than enzymes that make or break cyclic di-GMP – local signaling in the interactome of GGDEF/EAL domain proteins of *Escherichia coli*. *mBio.* **8**, e01639-17.

Schär, J., Stoll, R., Schauer, K., Loeffler, D. I., Eylert, E., Joseph, B., Eisenreich, W., Fuchs, T. M., Goebel, W. (2010) Pyruvate carboxylase plays a crucial role in carbon metabolism of extra- and intracellularly replicating *Listeria monocytogenes. J. Bacteriol.* **192**, 1774-1784.

Schirmer, F., Ehrt, S., Hillen, W. (1997) Expression, inducer spectrum, domain structure, and function of MopR, the regulator of phenol degradation in *Acinetobacter calcoaceticus* NCIB8250. *J. Bacteriol.* **179**, 1329-1336.

Schneider, C. A., Rasband, W. S., Eliceiri, K. W. (2012) NIH Image to ImageJ: 25 years of image analysis. *Nat. Methods*. **9**, 671-675.

Schuster, C. F., Bellows, L. E., Tosi, T., Campeotto, I., Corrigan, R. M., Freemont, P., Gründling, A. (2016) The second messenger c-di-AMP inhibits the osmolyte uptake system OpuC in *Staphylococcus aureus*. *Sci. Signal.* **9**, ra81.

Scortti, M., Monzó, H. J., Lacharme-Lora, L., Lewis, D. A., Vázquez-Boland, J. A. (2007) The PrfA virulence regulon. *Microbes. Infect.* **9**, 1196–1207.

Sesto, N., Koutero, M., Cossart, P. (2014) Bacterial and cellular RNAs at work during *Listeria* infection. *Future Microbiol.* **9**, 1025-1037.

Sévin, D. C., Sauer, U. (2014) Ubiquinone accumulation improves osmotic-stress tolerance in *Escherichia coli*. *Nat. Chem. Biol.* **10**, 266-272.

Shen, A., Kamp, H. D., Gründling, A., Higgins, D. E. (2006) A bifunctional O-GlcNAc transferase governs flagellar motility through anti-repression. *Genes Dev.* **20**, 3283-8295.

Silhavy, T. J., Kahne, D., Walker, S. (2010) The bacterial cell envelope. *Cold Spring Harb. Perspect. Biol.* **2**, a000414.

Sleator, R. D., Hill, C. (2002) Bacterial osmoadaptation: the role of osmolytes in bacterial stress and virulence. *FEMS Microbiol. Rev.* **26**, 49-71.

Smith L. T. (1996) Role of osmolytes in adaptation of osmotically stressed and chill-stressed *Listeria monocytogenes* grown in liquid media and on processed meat surfaces. *Appl. Environ. Microbiol.* **62**, 3088-3093.

Spiering M. J. (2015) Primer on the Immune System. *Alcohol Res.* **37**, 171-175.

Stannek, L. (2015) Control of glutamate homeostasis in the Gram-positive model organism *Bacillus subtilis*. Dissertation. Georg-August-Universität Göttingen. http://hdl.handle.net/11858/00-1735-0000-0023-9652-B, accessed 04.02.2019.

Stumpe, S., Bakker, E. P. (1997) Requirement of a large K^+-uptake capacity and of extracytoplasmic protease activity for protamine resistance of *Escherichia coli*. *Arch. Microbiol.* **167**, 126-136.

Suomi, T., Corthals, G. L., Nevalainen, O. S., Elo, L. L. (2015) Using peptide-level proteomics data for detecting differentially expressed proteins. *J. Proteome Res.* **14**, 4564–4570.

Suomi, T., Elo, L. L. (2017) Enhanced differential expression statistics for data-independent acquisition proteomics. *Sci. Rep.* **7**, 5869.

Sureka, K., Choi, P. H., Precit, M., Delince, M., Pensinger, D. A., Huynh, T. N., Jurado, A. R., Goo, Y. A., Sadilek, M., Iavarone, A. T., *et al.* (2014) The cyclic dinucleotide c-di-AMP is an allosteric regulator of metabolic enzyme function. *Cell.* **158**, 1389-1401.

Tatusov, R. L., Galperin, M. Y., Natale, D. A., Koonin, E. V. (2000) The COG database: a tool for genome-scale analysis of protein functions and evolution. *Nucleic Acids Res.* **28**, 33-36.

Team, R. D. C. (2014) R: a language and environment for statistical computing. Vienna, Austria: the R Foundation for Statistical Computing. https://www.R-project.org/, accessed 13.02.2019.

Thongsomboon, W., Serra, D. O., Possling, A., Hadjineophytou, C., Hengge, R., Cegelski, L. (2018) Phosphoethanolamine cellulose: a naturally produced chemically modified cellulose. *Science.* **359**, 334-338.

Thorsing, M., Dos Santos, P. T., Kallipolitis, B. H. (2018) Small RNAs in major foodborne pathogens: from novel regulatory activities to future applications. *Curr. Opin. Biotechnol.* **49**, 120-128.

Toledo-Arana, A., Dussurget, O., Nikitas, G., Sesto, N., Guet-Revillet, H., Balestrino, D., Loh, E., Gripenland, J., Tiensuu, T., Vaitkevicius, K., *et al.* (2009) The *Listeria* transcriptional landscape from saprophytism to virulence. *Nature.* **459**, 950-956.

Tosi, T., Hoshiga, F., Millership, C., Singh, R., Eldrid, C., Patin, D., Mengin-Lecreulx, D., Thalassinos, K., Freemont, P., Gründling, A. (2019) Inhibition of the *Staphylococcus aureus* c-di-AMP cyclase DacA by direct interaction with the phosphoglucosamine mutase GlmM. *PLoS Pathog.* **15**, e1007537.

Townsley, L., Yannarell, S. M., Huynh, T. N., Woodward, J. J., Shank, E. A. (2018) Cyclic di-AMP acts as an extracellular signal that impacts *Bacillus subtilis* biofilm formation and plant attachment. *mBio.* **9**, e00341-18.

Valenzuela-García, L. I., Ayala-García, V. M., Regalado-García, A G., Setlow, P., Pedraza-Reyes, M. (2018) Transcriptional coupling (Mfd) and DNA damage scanning (DisA) coordinate excision repair events for efficient *Bacillus subtilis* spore outgrowth. *Microbiologyopen.* **7**, e00593.

van Leeuwenhoek, A. (1677) *Observationes d. Anthonii Lewenhoeck, de natis e semine genitali animalculis. Philos. Trans.* **12**, 1040–1046.

Vázquez-boland, J. A., Kuhn, M., Berche, P., Chakraborty, T., Domi, G., González-Zorn, B., Wehland, J. (2001) *Listeria pathogenesis* and molecular virulence determinants. *Clin. Microbiol. Rev.* **14**, 584–640.

Vienna, H. W. R. C. T., Austria, (2017, n.d.) Tidyverse: easily install and load the "Tidyverse." R package version 1.2. 1. https://CRAN.R-project.org/package=tidyverse, accessed 13.02.2019.

Vlamakis, H., Chai, Y., Beauregard, P., Losick, R., Kolter, R. (2013) Sticking together: building a biofilm the *Bacillus subtilis* way. *Nat. Rev. Microbiol.* **11**, 157-168.

Vollmer, W., Joris, B., Charlier, P., Foster S. (2008). Bacterial peptidoglycan (murein) hydrolases. *FEMS Microbiol. Rev.* **32**, 259-286.

Wach, A. (1996) PCR-synthesis of marker cassettes with long flanking homology regions for gene disruptions in *Saccharomyces cerevisiae*. *Yeast.* **12**, 259-265.

Whatmore, A. M., Reed, R. H. (1990) Determination of turgor pressure in *Bacillus subtilis*: a possible role for K^+ in turgor regulation. *J. Gen. Microbiol.* **136**, 2521-2526.

Whiteley, A. T., Garelis, N. E., Peterson, B. N., Choi, P. H., Tong, L., Woodward, J. J., Portnoy, D. A. (2017) c-di-AMP modulates *Listeria monocytogenes* central metabolism to regulate growth, antibiotic resistance and osmoregulation. *Mol. Microbiol.* **104**, 212-233.

Whiteley, A. T., Pollock, A. J., Portnoy, D. A. (2015) The PAMP c-di-AMP is essential for *Listeria monocytogenes* growth in rich but not minimal media due to a toxic increase in (p)ppGpp. *Cell Host Microbe*. **17**, 788-798.

WHO (2014) *Antimicrobial resistance: global report on surveillance 2014*, World Health Organization (WHO). https://www.who.int/drugresistance/documents/surveillancereport/en/, accessed 22nd January 2019.

Wichgers Schreur, P. J., van Weeghel, C., Rebel, J. M., Smits, M. A., van Putten, J. P., Smith, H. E. (2012) Lysozyme resistance in *Streptococcus suis* is highly variable and multifactorial. *PLoS One.* **7**, e36281.

Witte, C. E., Whiteley, A. T., Burke, T. P., Sauer, J. D., Portnoy, D. A., Woodward, J. J. (2013) Cyclic di-AMP is critical for *Listeria monocytogenes* growth, cell wall homeostasis, and establishment of infection. *mBio.* **4**, e00282-13.

Witte, G., Hartung, S., Büttner, K., Hopfner, K. P. (2008) Structural biochemistry of a bacterial checkpoint protein reveals diadenylate cyclase activity regulated by DNA recombination intermediates. *Mol. Cell*. **30**, 167-178.

Wood, J. M. (1999) Osmosensing by bacteria: signals and membrane-based sensors. *Annu. Rev. Microbiol.* **63**, 230-262.

Wood, J. M. (2011) Bacterial osmoregulation: a paradigm for the study of cellular homeostasis. *Annu. Rev. Microbiol.* **65**, 215-238.

Wood, J. M., Bremer, E., Csonka, L. N., Kraemer, R., Poolman, B., van der Heide, T., Smith, L. T. (2001) Osmosensing and osmoregulatory compatible solute accumulation by bacteria. *Comp. Biochem. Physiol. A.* **130**, 437-460.

Woodward, J. J., Iavarone, A. T., Portnoy, D. A. (2010) c-di-AMP secreted by intracellular *Listeria monocytogenes* activates a host type I interferon response. *Science.* **328**, 1703-1705.

Wu, J., Sun, L., Chen, X., Du, F., Shi, H., Chen, C., Chen, Z. J. (2012) Cyclic GMP-AMP is an endogenous second messenger in innate immune signaling by cytosolic DNA. *Science.* **339**, 826-830.

Wurtzel, O., Sesto, N., Mellin, J. R., Karunker, I., Edelheit, S., Bécavin, C., Archambaud, C., Cossart, P., Sorek, R. (2012) Comparative transcriptomics of pathogenic and non-pathogenic *Listeria* species. *Mol. Sys. Biol.* **8**, 583.

Yan, D., Ikeda, T. P., Shauger, A. E., Kustu, S. (1996) Glutamate is required to maintain the steady-state potassium pool in *Salmonella typhimurium*. *Proc. Natl. Acad. Sci. U.S.A.* **93**, 6527-6531.

Yang, J., Bai, Y., Zhang, Y., Gabrielle, V. D., Jin, L., Bai, G. (2014) Deletion of the cyclic di-AMP phosphodiesterase gene (*cnpB*) in *Mycobacterium tuberculosis* leads to reduced virulence in a mouse model of infection. *Mol. Microbiol.* **93**, 65-79.

Yuan, J., Jin, F., Glatter, T., Sourjik, V. (2017) Osmosensing by the bacterial PhoQ/PhoP two-component system. *Proc. Natl. Acad. Sci. U.S.A.* **114**, E10792-E10798.

Zarrella, T. M., Metzger, D. W., Bai, G. (2018) Stress suppressor screening leads to detection of regulation of cyclic di-AMP homeostasis by a Trk family effector protein in *Streptococcus pneumoniae*. *J. Bacteriol.* **200**, e00045-18.

Zeden, M. S., Schuster, C. F., Bowman, L., Zhong, Q., Williams, H. D., Gründling, A. (2018) Cyclic diadenosine monophosphate (c-di-AMP) is required for osmotic regulation in *Staphylococcus aureus* but dispensable for viability in anaerobic conditions. *J. Biol. Chem.* **293**, 3180-3200.

Zhang, L., He, Z. G. (2013) Radiation-sensitive gene A (RadA) targets DisA, DNA integrity scanning protein A, to negatively affect cyclic Di-AMP synthesis activity in *Mycobacterium smegmatis*. *J. Biol. Chem.* **288**, 22426-22436.

Zhang, L., Li, W., He, Z.-G. (2013) DarR, a TetR-like transcriptional factor, is a cyclic di-AMP-responsive repressor in *Mycobacterium smegmatis*. *J. Biol. Chem.* **288**, 3085-3096.

Zheng, C., Ma, Y., Wang, X., Xie, Y., Ali, M. K., He, J. (2015) Functional analysis of the sporulation-specific diadenylate cyclase CdaS in *Bacillus thuringiensis*. *Front. Microbiol.* **6**, 908.

Zhu, B., Stülke, J. (2017) SubtiWiki in 2018: from genes and proteins to functional network annotation of the model organism *Bacillus subtilis*. *Nucleic Acids Res.* **46**, D743-D748.

Zhu, Y., Pham, T. H., Nhiep, T. H. N., Vu, N. M. T., Marcellin, E., Chakrabortti, A., Wang, Y., Waanders, J., Lo, R., Huston, W. M., *et al.* (2016) Cyclic-di-AMP synthesis by the diadenylate cyclase CdaA is modulated by the peptidoglycan biosynthesis enzyme GlmM in *Lactococcus lactis*. *Mol. Microbiol.* **99**, 1015-1027.

10. Appendix

Used chemical, materials, equipment, commercial systems, enzymes and bioinformatic tools are listed in Tab. **10.1**, **10.2**, **10.3**, **10.4**, **10.5** and **10.6**, respectively.

Tab. 10.1 Used chemicals and manufacturer

Chemicals	Manufacturer
5-bromo-4-chloro-3-indolyl-β-D-galactopyranoside (X-Gal)	Thermo Scientific, USA
Acetonitrile	Roth, Karlsruhe
Agar	Roth, Karlsruhe
Agarose	Peqlab, Erlangen
Amino acids	AppliChem, Darmstadt Roth, Karlsruhe
Ammonium ferric citrate (CAF)	Sigma-Aldrich, München
Ampicillin	AppliChem, Darmstadt
Bradford solution Roti® Quant	Roth, Karlsruhe
Brain heart infusion (BHI) agar	Sigma-Aldrich, München
Brain heart infusion (BHI) broth	Sigma-Aldrich, München
Bromphenol blue	Serva, Heidelberg
Calcium chloride	Roth, Karlsruhe
Casamino acids (CAA)	Sigma-Aldrich, München
Dimethyl sulfoxide (DMSO)	Sigma-Aldrich, München
Disodium phosphate	Roth, Karlsruhe
dNTPs	Thermo Scientific, USA
Erythromycin	Sigma-Aldrich, München
Ethylenediaminetetraacetic acid (EDTA)	Sigma-Aldrich, München
Glucose	Merck, Darmstadt
Glycerol	Merck, Darmstadt
HDGreen™ Plus	Intas, Göttingen
Höchst 33342	Sigma-Aldrich, München
Horse serum	Gibco, Darmstadt
Hydrochloric acid (HCl)	ChemSolute, Renningen
Isopropyl β-D-1-thiogalactopyranoside (IPTG)	Roth, Karlsruhe
Kanamycin	Roth, Karlsruhe
Magnesium chloride	AppliChem, Darmstadt
Magnesium sulfate	Roth, Karlsruhe
Manganese chloride	AppliChem, Darmstadt
Methanol	AppliChem, Darmstadt
Penicillin G	Serva, Heidelberg
Polysorbate 20 (Tween 20)	Sigma-Aldrich, München
Potassium chloride	AppliChem, Darmstadt
Potassium phosphate	Roth, Karlsruhe
Roti®-Chloroform/Isoamyl alcohol (24:1)	Roth, Karlsruhe
Roti®-Phenol/Chloroform/Isoamyl alcohol (25:24:1)	Roth, Karlsruhe
Sodium chloride	Roth, Karlsruhe
Sodium dodecyl sulfate (SDS)	Roth, Karlsruhe

Chemicals	Manufacturer
Sodium hydroxide (NaOH)	Roth, Karlsruhe
Tris(hydroxymethyl)aminomethane	Roth, Karlsruhe
Tryptone	Oxoid, Heidelberg
Yeast extract	Oxoid, Heidelberg
λ phage DNA	Thermo Scientific, USA

Tab. 10.2 Auxiliary materials

Auxiliary materials	Manufacturer
Centrifuge beaker	Beckmann, München
Cuvettes (microliter, plastic)	Sarstedt, Nümbrecht
Erlenmeyer flasks (100 – 2000 ml)	Duran, Wertheim/Main
Falcon® tubes (15 ml, 50 ml)	Sarstedt, Nümbrecht
Gene Amp Reaction Tubes (PCR)	Perkin Elmer, Weiterstadt
Glass beads Ø=0.1 mm	BioSpec Products, USA
Glass pipets	Brand, Wertheim
Inoculation loops	Sarstedt, Nümbrecht
Membrane filter NC45 (0.2 µm pore size)	Schleicher und Schüll, Dassel
Microtest Plate 96-Well,F	Sarstedt, Nümbrecht
Micro tubes (1.5 ml, 2 ml)	Greiner, Nürtingen
Microliter pipets (2 µl, 20 µl, 200 µl, 1000 µl, 5000 µl)	Eppendorf, Hamburg
Micropulser™ electroporation cuvettes (0.1 cm)	Bio-Rad Laboratories, München
Pasteur pipets	VWR International, Darmstadt
Petri dishes	Greiner, Nürtingen
Pipet tips	Greiner, Nürtingen Eppendorf, Hamburg Sarstedt, Nümbrecht
Screw cap micro tubes (1.5 ml, 2 ml)	Sarstedt, Nümbrecht
Single-use syringes (5 ml, 10 ml, 50 ml)	Becton Dickinson Drogheda, Ireland
Tissue flasks (25 cm^2, 75 cm^2,150 cm^2,300 cm^2)	TPP, Switzerland

Tab. 10.3 Equipment

Equipment	Manufacturer
Autoclaves	Zirbus, Bad Grund Thermo Scientific, USA
Centrifuges	Heraeus Christ, Osterode Thermo Scientific, USA
Clean bench HeraSafe	Heraeus Christ, Osterode
Electroporation device Micro Pulser™	Bio-Rad Laboratories, USA
Epoch2 multiwell platereader	BioTek Instruments, USA
Fluorescence microscope Axioskop 40 FL+; Camera AxioCam MRm	Carl Zeiss, Jena
Gel electrophoresis device EasyCast™ Mini gel system	Peqlab, Erlangen
Heating block DB3	Waasetec, Göttingen
High accuracy scale	Sartorius, Göttingen

Equipment	Manufacturer
Horizontal shaker 3006	GFL, Burgwedel
Ice machine	Ziegra, Isernhagen
Incubation water bath 1083	GFL, Burgwedel
Incubator Functionline	Heraeus Christ, Osterode
Incubator shaker Innova® 2300	New Brunswick, Neu-Isenburg
Incubator shaker Innova® 40	New Brunswick, Neu-Isenburg
Magnetic stirrer	JAK Werk, Staufen
Molecular Imager® Gel Doc™ XR+	Bio-Rad Laboratories, USA
Nanodrop® ND-1000	Thermo Scientific, USA
pH-meter Calimatic	Knick, Berlin
Refrigarated centrifuge PrimoR	Heraeus Christ, Osterode
Scale Sartorius universal	Sartorius, Göttingen
Spectral photometer Libra S21	Biochrom, Cambridge
Standard power pac	Bio-Rad Laboratories, USA
Stereo fluorescence microscope Lumar V.12	Carl Zeiss, Jena
Synergy Mx multiwell platereader	BioTek Instruments, USA
Thermoblock TermoStat Plus	Eppendorf, Hamburg
Thermoblock Thermo	Eliwell, Pieve d'Alpago
Thermocycler LabCycler	SensorQuest, Göttingen
Thermocycler Tpersonal	Biometra, Göttingen
Thermomixer compact	Eppendorf, Hamburg
TissueLyser II	Qiagen, Hilden
Vacuum centrifuge SPD111V SpeedVac™ Concentrator	Thermo Scientific, USA
Vacuum pump VacuGene™	GE Healthcare Bio-Sciences AB, Sweden
Vortex Genie 2	Bender & Hobeing AG, Zürich
Water distillation plant	Millipore, Schwalbach

Tab. 10.4 Commercial systems

Commercial systems	Manufacturer
Nucleospin® Plasmid Kit	Macherey-Nagel, Düren
Nucleospin® Microbial DNA Kit	Macherey-Nagel, Düren
QIAquick® PCR-purification kit	Qiagen, Venlo
peqGOLD Gel Extraction Kit	PeqLab, Erlangen

Tab. 10.5 Enzymes

Enzymes	Manufacturer
FastAP™ (alkaline phosphatase)	Thermo Scientific, USA
FastDigest™ restriction endonucleases	Thermo Scientific, USA
Lysozyme from chicken egg white	Serva, Heidelberg
Phusion™ DNA polymerase	Fermentas, St. Leon-Rot
RNaseA	AppliChem, Darmstadt
T4- DNA ligase	Thermo Scientific, USA

Tab. 10.6 Bioinformatic tools, software and web services

Program/Service	Producer	Application
AxioVision Rel 4.8.2	Carl Zeiss	Microscopic analysis of single cells
BLAST http://blast.ncbi.nlm.nih.gov/	National Institutes of Health, USA	BLAST searches
Galaxy S9+	Samsung	Imaging
Gen5 02.09.2001	BioTek Instruments	Incubation and measurement of 96-well plates
Geneious® Prime 2019.0.4	Biomatters Ltd.	Genetic analysis, primer design, analysis of sequence data
Image Lab 3.0.1	GelDoc™ XR+	Imaging and analysis
Image Lab™ software (Gel Doc)	Bio-Rad	Analysis of UV-Vis signals and image processing of agar plates
ImageJ 1.48	National Institutes of Health, USA	Processing of fluorescence microscopy images
KEGG http://www.genome.jp/kegg/	Kanehisa Laboratories	Genome sequence analysis and information about genes
Listeriomics https://listeriomics.pasteur.fr	Institut Pasteur, France	Information about genes and gene expression in *L. monocytogenes*
ListiList http://genolist.pasteur.fr/ListiList/	Institut Pasteur, France	BLAST searches and genome analysis in *Listeria monocytogenes*
ListiWiki http://listiwiki.uni-goettingen.de/	General Microbiology, Georg-August-University, Göttingen	Information about genes and proteins in *L. monocytogenes*
Microsoft® Office 2016	Microsoft® Inc.	Processing of images, text and data
NEBcutter http://tools.neb.com/NEBcutter2/	New England Biolabs, Inc.	Restriction site analysis
OligoCalc http://www.basic.northwestern.edu/biotools/oligocalc.html	Department of Molecular Genetics and Biochemistry, University of Pittsburgh School of Medicine	Oligonucleotide analysis
PubMed http://www.ncbi.nlm.nih.gov/	National Institutes of Health, Bethesda, USA	Literature research
Reverse Complement http://www.bioinformatics.org/sms/rev_comp.html	Bioinformatics Organization, Inc., Massachusetts, USA	Formation of reverse-complement sequences
STRING http://string-db.org	String consortium CRP, EMBL, KU, SIB, TUD and UZH	Information about protein-protein interactions
SubtiWiki http://subtiwiki.uni-goettingen.de/	General Microbiology, Georg-August-University, Göttingen	Information about genes and proteins in *B. subtilis*
UniProt http://www.uniprot.org/	UniProt consortium EMBL-EBI, SIB, PIR	Information about protein functions, sequences and domains

11. Curriculum vitae

Name:	**Johannes Gibhardt**
Date of birth:	**19.01.1991**
Place of birth:	**Kassel, Germany**
Nationality:	**German**

Education

10/2015 – 04/2019	**PhD student in the GGNB Program Microbiology and Biochemistry** Department of General Microbiology Institute of Microbiology and Genetics Georg-August-Universität Göttingen, 37073 Göttingen, Germany Doctoral Thesis Project: "Cyclic di-AMP homeostasis and osmoregulation in *Listeria monocytogenes*"
10/2013 – 08/2015	**Master degree course Microbiology and Biochemistry** Georg-August-Universität Göttingen, 37073 Göttingen, Germany Master thesis: "Cyclic Di-AMP Metabolism and Osmoregulation in *Listeria monocytogenes*" Degree: **M. Sc.** Final grade: 1.1, passed with distinction
10/2010 – 08/2013	**Bachelor degree course Biology** Georg-August-Universität Göttingen, 37073 Göttingen, Germany Major field of study: Molecular Biosciences Bachelor thesis: "Etablierung eines Screening-Systems zur Identifizierung neuer Faktoren, die die Aktivität des Virulenzfaktors PrfA von *Listeria monocytogenes* beeinflussen" Degree: **B. Sc.** Final grade: 1.5, passed with distinction
08/2007 – 06/2010	**Abitur** Georg-Christoph-Lichtenberg-Schule, 34132 Kassel, Germany Abitur certificate grade 2.6

Internships

09/2014 – 11/2014	**Internship at the Institute for Medical Microbiology** Universitätsmedizin Göttingen (UMG), 37099 Göttingen, Germany Topic: Characterization of clinical isolates of *Clostridium difficile* Reference: Dr. Katrin Gunka E-Mail: kgunka@gwdg.de
11/2014 – 12/2014	**Internship at the Robert Koch Institute** Robert Koch-Institut (RKI), 38855 Wernigerode, Germany Topic: Development of a counter selection system for genetic modifications of *Listeria monocytogenes* Reference: Dr. Sven Halbedel E-Mail: halbedels@rki.de

List of publications

Quintana, I. M., **Gibhardt, J.**, Turdiev, A., Hammer, E., Commichau, F. M., Lee, V. T., Magni, C., Stülke, J. (2019) The KupA and KupB proteins of *Lactococcus lactis* IL1403 are novel c-di-AMP receptor proteins responsible for potassium uptake. *J. Bacteriol.* doi: 10.1128/JB.00028-19.

Hauf, S., Herrmann, J., Miethke, M., **Gibhardt, J.**, Commichau, F. M., Müller, R., Fuchs, S., Halbedel, S. (2019) Aurantimycin resistance genes contribute to survival of *Listeria monocytogenes* during life in the environment. *Mol. Microbiol.* doi: 10.1111/mmi.14205.

Wicke, D., Schulz, L. M., Lentes, S., Scholz, P., Poehlein, A., **Gibhardt, J.**, Daniel, R., Ischebeck, T., Commichau, F. M. (2019) Identification of the first glyphosate transporter by genomic adaptation. *Environ. Microbiol.* doi: 10.1111/1462-2920.14534.

Commichau, F. M., **Gibhardt, J.**, Halbedel, S., Gundlach, J., Stülke, J. (2018) A delicate connection: c-di-AMP affects cell Integrity by controlling osmolyte transport. *Trends Microbiol.* **26**, 175-185.

Gundlach, J., Herzberg, C., Kaever, V., Gunka, K., Hoffmann, T., Weiß, M., **Gibhardt, J.**, Thürmer, A., Hertel, D., Daniel, R., Bremer, E., Commichau, F. M., Stülke, J. (2017) Control of potassium homeostasis is an essential function of the second messenger cyclic di-AMP in *Bacillus subtilis*. *Sci. Signal.* **10**, eaal3011.

Großhennig, S., Ischebeck, T., **Gibhardt, J.**, Busse, J., Feussner, I., Stülke, J. (2016) Hydrogen sulfide is a novel potential virulence factor of *Mycoplasma pneumoniae*: characterization of the unusual cysteine desulfurase/desulfhydrase HapE. *Mol. Microbiol.* **100**, 42-54.

Rismondo, J., **Gibhardt, J.**, Rosenberg, J., Kaever, V., Halbedel, S., Commichau, F. M. (2016) Phenotypes associated with the essential diadenylate cyclase CdaA and its potential regulator CdaR in the human pathogen *Listeria monocytogenes*. *J. Bacteriol.* **198**, 416-426.

Johannes Gibhardt Göttingen, 15.02.2019